Developing Cationic Nanoparticles for Gene Delivery

Mahentha Krishnamoorthy

School of **E**ngineering and **M**aterials **S**cience,

Queen **M**ary, **U**niversity of **L**ondon

Submitted in partial fulfilment of the requirements of the Degree of Doctor of Philosophy

July 2015

Statement of Originality

I, Mahentha Krishnamoorthy, confirm that the research included within this thesis is my own work or that where it has been carried out in collaboration with, or supported by others, that this is duly acknowledged below and my contribution indicated. Previously published material is also acknowledged below.

I attest that I have exercised reasonable care to ensure that the work is original, and does not to the best of my knowledge break any UK law, infringe any third party's copyright or other Intellectual Property Right, or contain any confidential material.

I accept that the College has the right to use plagiarism detection software to check the electronic version of the thesis.

I confirm that this thesis has not been previously submitted for the award of a degree by this or any other university.

Mahentha Krishnamoorthy

26th July 2015

Details of collaborations and publications:

Publication -

Krishnamoorthy, M., Hakobyan, S., Ramstedt, M., Gautrot, J. E., 'Surface-Initiated Polymer Brushes in the Biomedical Field: Applications in Membrane Science, Biosensing, Cell Culture, Regenerative Medicine and Antibacterial Coatings, *Chemical Reviews*, 114 (2014), 10976-11026

Acknowledgements

I would like to express my sincerest gratitude to my supervisor, Dr Julien Gautrot, for giving me the opportunity to do this PhD. I appreciate being trained by Julien himself in cell culture, polymerisation and the relevant analytical instruments. Thank you for all the knowledge you imparted and for all the input into making this thesis what it is.

Another admirable individual I would like to acknowledge is my grandfather, Mr Kangatharam Mylvaganam. Thank you for being an inspiration.

I am forever grateful to my parents, Mangai and Krishnamoorthy, for giving me the freedom to do as I choose, for being patient and putting up with me being a student for the last eight years. I would like to also convey my thanks to my brother, Sayanthan, for his support.

I would like to thank my friends, Hari Shanmugarajah, Dr Gowsihan Poologasundarampillai and Pratheepan Subramaniam, for instilling confidence, believing in me and encouraging me to pursue research at the right times.

My sincere thanks to my friend and colleague, Dharmesh Patel, for his continuous backing over the years since working together on our MEng group project in 2010. He has been a pillar of support during this PhD, providing technical and mathematical assistance whenever I required it, including feeding the cells on my behalf when I could not be there to look after them. I would not have enjoyed my PhD journey as much as I did without you.

Many thanks also to the lab technicians, Chris Mole and Shafir Iqbal, and experimental officer, Dr Krystelle Mafina, for all their help with maintaining the Gautrot Lab, and providing the training I needed for various equipment.

I would like to extend my appreciation to the Gautrot Lab for creating a great group spirit and making our group meetings and social events enjoyable. In particular, I would like to thank Burcu Colak for all her help with NMR and free polymer synthesis – I would have been lost with all the chemistry without her and Julien's help, Stefania Di Cio for her help with SEM at late hours, and Dexu Kong for being such a kind and supportive colleague with maintaining the cell culture lab. I wish our new member, Danyang Li, all the best with continuing this work.

Last but not least, my heartfelt thanks to all my friends who have motivated me in various ways at various times, asking after me and giving me the space to focus on my thesis when I needed to.

Thank you.

This work was supported by the Royal Society and the Engineering and Physical Sciences Research Council [Grant EP/J501360/1].

Abstract

Gene delivery can potentially treat acquired and genetic diseases such as cystic fibrosis, haemophilia and cancer. Non-viral gene delivery vectors are attractive candidates over viral vectors such as recombinant viruses, due to their lower cytotoxicity and immunogenicity, despite significantly lower transfection efficiencies. To improve efficiency of non-viral vectors, the investigation of the various parameters influencing DNA transfection is essential. The present study developed a versatile gene delivery system with tailored physicochemical and biological properties. The system used polymer brushes synthesised via atomic transfer radical polymerisation (ATRP), grafted from silica nanoparticles, whose charge density, grafting density, chemistry, length of brush, the size and shape can be altered.

The primary focus of the study was poly(2-dimethylaminoethyl methacrylate) (PDMAEMA), known for its positive charge and DNA condensation. The ability of PDMAEMA to interact with DNA was characterised using dynamic light scattering, electrophoretic light scattering methods, surface plasmon resonance and in situ ellipsometry whilst its interaction with cells was studied via cell viability assays. The brush behaviour in response to pH and ionic strength was also studied. The charge density was altered by copolymerising with poly[oligo(ethylene glycol) methyl ether methacrylate](POEGMA) and the effect of such modification on DNA interaction was studied. PDMAEMA-grafted nanoparticles gave the highest transfection efficiency compared to other synthesised polymer brushes, but still displaying almost 2-fold lower transfection efficiency than the commercially available reagent jetPEI®.

Different brush chemistries were also investigated. Poly(glycidyl methacrylate) (PGMA) decorated with oligoamines: allylamine, diethylenetriamine and pentaethylene hexamine, and PDMAEMA quaternized with alkyl halides: methyl iodide, allyl iodide and ethyl iodoacetate did not show any significant transfection, despite their performance reported in the literature.

The robust system developed is a promising platform for further investigation of parameters influencing cellular uptake and gene expression, and important milestone to develop non-viral gene delivery systems.

Contents

List of Tables

List of Abbreviations and Symbols

*	Significance
Ø	Diameter
ξ	Zeta potential
ϵ	Dielectric constant
η	Solvent viscosity
AA	Allylamine
ACN	Acetonitrile
ATP	Adenosine triphosphate
ATR-FTIR	Attenuated total reflectance – Fourier transform infrared
ATRP	Atomic transfer radical polymerisation
BB	2-bromoisobutyryl bromide
BHK	Baby hamster kidney cells
Bpy	2, 2'-bipyridyl
BSA	Bovine serum albumin
CCC	Cationic comb-type copolymers
CHO	Chinese hamster ovarian cells
COS	African green monkey kidney cells
CLSM	Confocal laser scanning microscopy
CRP	Controlled radical polymerisation
Cu(I)Cl	Copper chloride
Cu(II)Br_2	Copper bromide
D	Translational diffusion coefficient
DAPI	4',6-Diamidino-2-phenylindole dihydrochloride
DCM	Dichloromethane
DEAE	Diethylaminoethyl
DEE	Diethylether
DETA	Diethylenetriamine
DLS	Dynamic light scattering
DMAA	*N,N*-dimethylacrylamide
DMAEMA	2-(Dimethylamino)ethyl methacrylate

DMEM	Dulbecco's modified Eagle medium
DMF	Dimethylformamide
DMRIE	*N*-(2-hydroxyethyl)-*N,N*-dimethyl-2,3-bis(tetradecyloxy)-1-propanaminium bromide
DMSO	Dimethyl sulfoxide
DNA	Deoxyribonucleic acid
DOGS	Dioctadecyl amino glycyl spermine
DOPE	Dioleoylphosphatidyl ethanolamine
DOSPA	2,3 dioleyloxy-*N*-[2(spermine carboxaminino)ethyl]-*N,N*-dimethyl-1-propanaminium trifluoroacetate
DOTAP	1, 2-dioleoyl-3-trimethylammonium propane
DOTMA	2, 3-bis(oleoyl)oxipropyltrimethylammonium chloride
EGF	Epidermal growth factor
EGFP	Enhanced green fluorescent protein
ELS	Electrophoretic light scattering
Et_3N	Triethylamine
f	Particle frictional coefficient
FAD	1:1 mixture of DMEM-F12 and DMEM
FBS	Fetal bovine serum
FITC	Fluorescein isothiocyanate
f-PDMAEMA	Free PDMAEMA
f-PGMA	Free PGMA
f-POEGMA	Free POEGMA
-g-	Graft
GMA	Glycidyl methacrylate
GPC	Gel permeation chromatography
HaCaT	Human adult low calcium temperature keratinocytes
HBS	HEPES-buffered solution
HCA2	Dermal fibroblasts
HEK	Human embryonic kidney cells
HeLa	Human epithelial cells from a fatal cervical carcinoma
HEPES	4-(2-hydroxyethyl)-1-piperazineethanesulfonic acid
hESC	Human embryonic stem cells
IC_{50}	Half maximal inhibitory concentration

k	Boltzmann constant
KSFM	Keratinocyte serum-free medium
LAMA	2-lactobionamidoethyl methacrylate
LCST	Lower critical solution temperature
MC3T3	Mouse osteoblastic cells
MCF	Human mammary carcinoma cells
miRNA	Micro ribonucleic acid
MRI	Magnetic resonance imaging
M_t^n-Y/Ligand	Transitional metal complex
NAAPBA	*N*-acryloyl-*m*-phenylboronic acid
ND	Nanodiamond
NIPAM	*N*-isopropylacrylamide
NMP	Nitroxide mediated polymerisation
NMR	Nuclear magnetic resonance
N/P	Nitrogen to phosphate ratio
NPC	Nuclear pore complex
OEGMA	Oligo (ethylene glycol methyl ether methacrylate)
PAA	Poly (acrylic acid)
PAMAM	Poly (amidoamine)
PFA	Paraformaldehyde
PBMA	poly (*n*-butyl methacrylate)
PBS	Phosphate buffered saline
PDEAEMA	Poly [(diethylamino)ethyl methacrylate)]
PDI	Polydispersity
PDMAEMA	Poly [(2-dimethylamino) ethyl methacrylate]
PEG	Poly ethylene glycol
PEHA	Pentaethylenehexamine
PEI	Poly (ethylene imine)
PGMA	Poly (glycidyl methacrylate)
PHEMA	Poly (2-hydroxyethyl methacrylate)
pI	Isoelectric point
PKC	Protein kinase phosphorylation
PLL	Poly (L-lysine)

PMEDSAH	Poly((2-(methacyloyloxy)ethyl)dimethyl(3-sulfopropyl)ammonium hydroxide)
PMETAC	Poly ([2-(methacryloyloxy)ethyl] trimethyl ammonium chloride)
PMETAI	Poly ([2-(methacryloyloxy)ethyl] trimethyl ammonium iodide)
PMMA	Poly (methyl methacrylate)
PNIPAM	Poly(*N*-isopropylacrylamide)
POEGMA	Poly (oligo (ethylene glycol) methyl ether methacrylate)
PS	Polystyrene
PTMAEMA	Poly (trimethylammonio ethyl methacrylate chloride)
RAFT	Reversible addition fragmentation chain transfer
RI	Refractive index
ROMP	Ring-opening metathesis
SCID	Severe combined immunodeficiency-X1
SE	Standard error
SEM	Scanning electron microscopy
SI-ATRP	Surface-initiated atomic transfer radical polymerisation
siRNA	Small interfering ribonucleic acid
SPR	Surface plasmon resonance
T	Absolute temperature
TGA	Thermogravimetric analysis
THF	Tetrahydrofuran
u	Electrophoretic mobility
UCST	Upper critical solution temperature
QD	Quantum dot
WGA	Wheat germ agglutin
X	Organic halide
X-M_t^{n+1}	Oxidised metal complex
ZP	Zeta potential

Chapter 1 - Introduction[1]

Gene delivery research has expanded significantly over the past few decades to address the growing need for treatments for hereditary and acquired diseases including cancer. Although viral vectors have been extensively studied for clinical application due to their superior transfection properties, their several shortcomings associated with immunogenicity, pathogenicity, loading capacity and so forth have led to the investigation of non-viral vectors in recent times as they overcome these limitations. The transfection efficiency of the non-viral vectors are, however, significantly lower compared to viral vectors and hence require tailoring to improve their gene delivery efficiency. One of the most promising non-viral vectors are cationic polymers.

Polymer brushes have been of interest for almost five decades now as the surface-tethered polymers are functionally versatile, easily accessible, homogenous and provide a defect-free surface compared to other approaches.[1, 2] The rapid growth of interest in polymer brushes is particularly attributed to their flexibility to create defined thin films in which the chemical composition, thickness, grafting density and architecture can be tailored in detail using the surface initiated-atomic transfer radical polymerisation (SI-ATRP) technique.[3] This flexibility makes polymer brushes a valuable platform for the design and development of systems for various useful applications, including therapeutics. One of the many valuable applications is in biofunctional interfaces where polymer brushes of protein resistant properties can be used as antibacterial coating to prevent implant failure whilst cationic brushes can be used in drug and gene delivery amid other applications.

[1] Part of this chapter has been published: Krishnamoorthy, M., Hakobyan, S., Ramstedt, M., Gautrot, J. E., 'Surface-Initiated Polymer Brushes in the Biomedical Field: Applications in Membrane Science, Biosensing, Cell Culture, Regenerative Medicine and Antibacterial Coatings, *Chemical Reviews*, 114 (2014), 10976-11026

1.1 Gene delivery

The process by which exogenous plasmid deoxyribonucleic acid (DNA) or short-interfering ribonucleic acid (siRNA) are introduced into cultured eukaryotic cells to produce genetically modified cells is termed transfection.[4] The ability to transfer genetic material in this way presents a valuable platform via which gene structure, regulation and function, and protein expression can be studied using mammalian cells as the technique eliminates the issue of introducing negatively charged molecules such as phosphate backbones of DNA and RNA into cells with a negatively charged membrane.

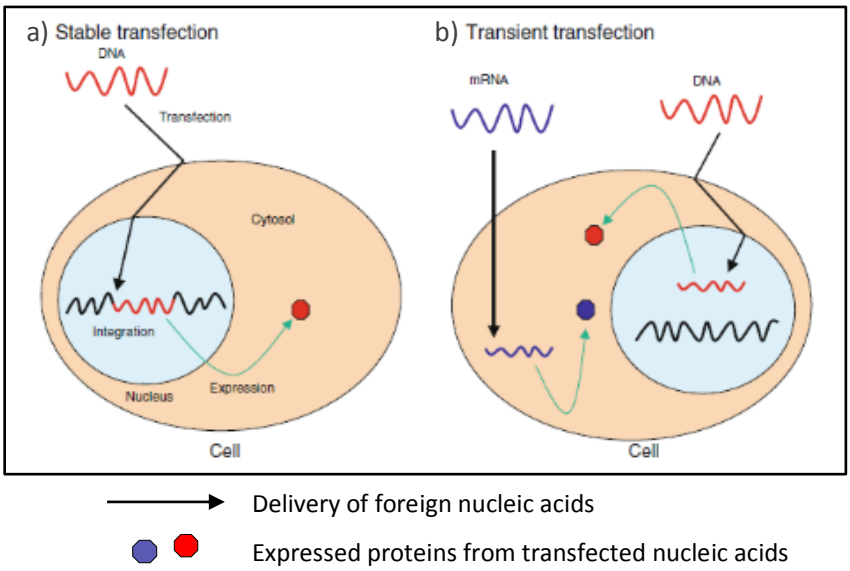

Figure 1: a) Foreign DNA (red wave) delivery occurs by passage through the cell and nuclear membranes, and is integrated into host genome (black wave) and expression is sustained, b) Foreign DNA enters nucleus but is not integrated into the genome. Foreign mRNA (blue wave) is delivered into the cytosol and is translated. Adapted from [4]

Transfection can be described as being either transient or stable in nature depending on the type of nucleic acids and is applied according to the needs of a system (Figure 1). In transient transfection, the genetic material is expressed for a short time and then degraded by environmental factors or diluted by cell division, whilst with stable transfections, marker genes for selection (transgenes) are co-transfected with the foreign gene which can then remain in the genome of the cell and in proliferated cells whilst cells without the marker gene are not sustained.[5, 6]

1.1.1 Applications

The applications using transfection have expanded significantly over the past few decades; in developing gene delivery systems to treat diseases or improving symptoms,[7-11] transfecting transcription factors for induced pluripotent stem cell generation,[12, 13] and siRNA knock-down procedures,[14, 15] DNA vaccination,[16] amongst others.

In particular, gene therapy has shown interesting results over the last 20 years in treating inherited and acquired diseases such as Duchenne muscular dystrophy,[17, 18] cystic fibrosis,[19] haemophilia,[20] wound healing,[21, 22] peripheral vascular,[23, 24] cardiovascular,[25, 26] and neurodegenerative diseases,[27, 28] arthritis,[9, 29] and as an alternative to chemotherapy used for treating cancer.[30, 31] Hence genetic mutation and deletion lead to many genetic disorders which in turn cause severe diseases. Thus transfection has become an indispensable technique in molecular biology and biotechnology research as a foreign gene can be introduced into a patient's cell to produce a specific protein and replace the mutated gene in the affected cells.[32, 33] One of the first successful cases of human gene therapy was carried out by Cavazzana-Calvo *et al.*, who were able to fully correct the phenotype of Severe combined immunodeficiency-X1 (SCID).[34] The inherited disorder presents an early block in T and natural killer lymphocyte differentiation as a result of mutations of the gene encoding specific cytokine receptors of interleukin receptors which are essential in the delivery of growth, survival, and differentiation signals to early lymphoid progenitors.

The efficiency of transfection determines the success of nucleic acid delivery be it in pharmaceutics or as a general research tool. In DNA transfection, this efficiency is dependent on the fraction of DNA entering the nucleus (DNA delivery) as well as the fraction of nuclear DNA that undergo transcription (DNA expression).[35] In addition to DNA delivery, the expression levels, cell survival and viability also plays a significant role in acquiring transfection efficiency suitable for developing therapeutic modalities like gene delivery. It is therefore important to develop a system and method where DNA delivery can occur efficiently and result in high gene expression whilst also being reproducible in the laboratory and in clinical settings in a safe and controllable way.

1.1.2 Transfection methods

Administering naked DNA directly via intravenous injection returns very low levels of gene expressions in major organs therefore an efficient vector is needed for the delivery of the gene. There are several methods by which transfection can be carried out; chemical materials, physical treatment or biological particles, and each method has its own advantages and disadvantages and varies in efficiency depending on cell type and desired effect.

DNA delivery systems are generally classified as either, viral vector-mediated (recombinant viruses) or non-viral vector-mediated (synthetic) systems (Table 1). The former biological method has been the most effective way to deliver DNA and gains high expression (>90%) due to the carrier's highly evolved nature and specific mechanism for transferring their genome into the host cell. Hence recombinant virus-based vectors are widely used in clinical settings. Retrovirus, lentivirus, adenovirus, adeno-associated virus and herpes simplex virus are some of the viruses used as gene delivery vectors where part of the genome of the virus is replaced with a therapeutic gene.[36] The specialised mechanism in infecting cells produces highly efficient gene delivery and expression in the host cell. However, there are many disadvantages to the system, including the inherent immunogenicity, high pathogenicity, high oncogenicity, insertional mutagenesis, restricted targeting of specific cell types, limited DNA loading capacity, limited chemical modification and issues with large-scale vector production.[37-39]

Conversely, non-viral delivery vectors exhibit poor transfection efficiency yet overcome the limitations faced by viral vectors such that the synthetic vectors are non-immunogenic, inexpensive, able to carry higher amount of genetic material and are generally safer thus leading to an increasing number of scientists proposing the non-viral systems, namely cationic lipids, polymers, dendrimers and peptides, as alternatives to viral systems.[35, 40, 41] These vectors are able to electrostatically bind DNA and condense it to form nanometre-sized spherical particles known as lipoplexes or polyplexes (Figure 2) spontaneously when mixing cationic lipids/ polymers with plasmid DNA and facilitate entry into the cell as well as protect the gene from enzymatic degradation during its journey towards the nucleus.

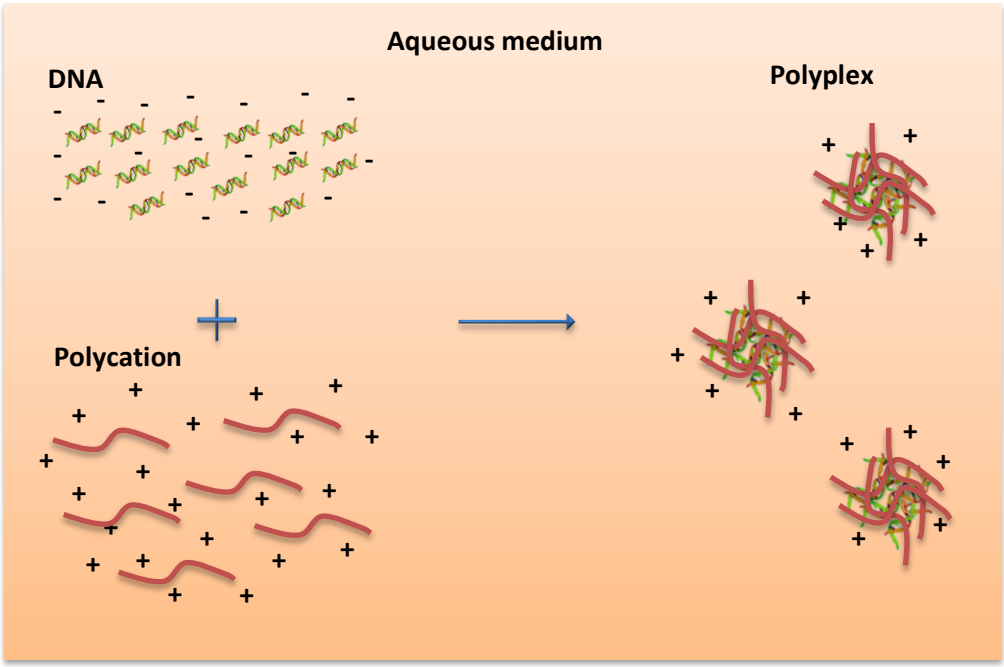

Figure 2: Polyplexes formed from mixing polycations and DNA in an aqueous solution.

In particular, calcium phosphate co-precipitation, originally developed by Graham and van der Eb in 1973[42] has been used for over four decades for the expression of genes in mammalian cells. The method involves combining HEPES-buffered solution (HBS) containing phosphate ions with a calcium chloride solution containing the DNA to be transfected. The resulting precipitate was composed of the positively charged calcium and the negatively charged phosphate, which bind the DNA on its surface. Transferring a suspension of this precipitate to a monolayer of cells results in transfection of some of the DNA. The efficiency of the cellular uptake of the DNA largely depended on the amount of DNA and the type of cell line alongside concentrations of calcium and phosphate, temperature, pH and reaction time.[43] The formation of effective precipitate complexes for efficient transfection can therefore only occur in a limited range of physico-chemical conditions. The calcium phosphate co-precipitation technique was advantageous over DEAE-dextran as the latter was unable to transform cells.

Table 1: Summary of key aspects associated with commonly used gene delivery techniques in mammalian cells.

Type	Class	Vectors	Advantages	Disadvantages	Cell types	Ref.
Viral	Biological	Adenovirus *Transient expression*	*ex/ in vivo* route of gene delivery, targeted expression, effective on dissociated cells and slices and *in vivo*, wide host range, transfect dividing and non-dividing cells with high efficiency, higher viral titre than other viruses and high expression, non-oncogenic, stability of recombinant vectors	Limited insert size compared to non-viral vectors (7-30 kb), short duration of expression *in vivo*, inflammatory response/ toxicity, extensive immunological problems from high vector doses, no integration into host, low level of expression and moderate transfection efficiency in neuronal cells, onset of expression: days	Neuronal cells, HeLa, human epithelial cell lines, haematopoietic cells upon upregulation of α_v-integrin expression, rat 9L gliosarcoma cells	[44-50]
		Adeno-associated virus *Stable expression*	Maintains high level of gene expression for a long duration (years) *in vivo, ex/ in vivo* route of gene delivery, targeted expression, effective on dissociated cells and slices and *in vivo*, potential of targeted integration, infects dividing and non-dividing cells, broad host and cell type tropism range, non-pathogenic, non-immunogenic, lack of cytopathogenicity	Limited insert size (3.5-4 kb), difficult to purify/scale up, difficult generation of high virus titres, slow onset of expression (weeks), low efficiency of integration to genome, requirement of adenovirus or herpesvirus for adeno-associated virus replication	Neuronal/ glial cells, haematopoietic cells, lung epithelial cells, hepatocytes, diploid fibroblasts, ependymal cells	[47, 49-55]
		Herpes simplex virus	Efficient infection, high level of expression in neuronal cells as it is naturally neurotropic– stable viral particles allow generation of high virus titres (10^{12} pfu/mL), targeted expression, onset of expression: hours, infects a wide variety of cells	Limited insert size compared to non-viral vectors but higher than other viral vectors (<50 kb), no integration into host genome, short-term expression, infections spreads to surrounding cells, immunogenic - high toxicity, possible recombination	Neuronal/ glial cells, murine melanoma cells, human embryonic kidney cells (HEK 293), rat 9L gliosarcoma cells	[45, 47, 49, 50, 56-58]
		Retrovirus (Lentivirus) *Stable expression*	High transfection efficiency with numerous cell lines, long duration of expression *in vivo*, *ex/ in vivo* route of gene delivery, allows stable integration into host genome, easy to use, effective on dissociated cells and slices and *in vivo*, targeted expression, infects only once and do not replicate *in vivo,* easy manipulation of viral genome for vector engineering **Lentivirus** – infects dividing and non-dividing terminally differentiated cells, non-pathogenic, lack of expression of viral proteins, stable gene expression	Limited insert size (<7-8 kb), short duration of expression *in vivo*, insertional mutagenesis, *ex vivo* route of gene delivery only, limited scale up, do not infect non-dividing terminally differentiated cells, may be oncogenic hence hazardous to laboratory workers, random integration into host genome, instability of vectors, difficult targeting of viral infection, **Lentivirus** – difficult to produce high titre viruses, potential insertional mutagenesis, presence of protein sequences in the packaging constructs	Neuronal cells, peripheral blood stem cells, human umbilical cord blood cells, rat 9L gliosarcoma cells, rat C6 glioma cells, mouse NIH 3T3 fibroblasts, human embryonic kidney cells	[45, 47, 49, 50, 59-64]
		Poxvirus (Vaccinia virus) *Transient expression*	targeted expression, effective on dissociated cells and slices and *in vivo,* onset of expression: hours	Limited insert size (<30 kb), high toxicity in mammalian tissue	Neuronal cells, guinea pig cochlea cells, Human ovarian cancer cells HeLa S3, monkey kidney cells (CV-1)	[65-67]

Type	Class	Vectors	Advantages	Disadvantages	Cell types	Ref.
		Sindbis and Semliki Forest viruses *Transient expression*	Highest transfection in neuronal cells compared to other viral vectors, targeted expression, effective on dissociated cells and slices and *in vivo,* onset of expression: hours	Limited insert size (<6.5 kb), high toxicity after 24 h (culture), 3-5 days (slices) and 48-72 h (*in vivo*)	Neuronal cells, baby hamster kidney cells (BHK-21), Chinese hamster ovary cells (CHO-K1), African green monkey kidney cells (COS-7)	[68-70]
Non-viral	Chemical	Calcium phosphate *Stable expression*	High efficiency, minimal toxicity	No targeted expression, low transfection efficiency in neuronal cells, not effective on slice cultures and *in vivo*	NIH3T3, BHK, CHO, HeLa, COS-7, murine mammary cells, Jurkat cells, HEK-293, Mouse osteoblastic cells (MC3T3-E1)	[71-74]
		Lipid-based vectors [2,3-bis(oleoyl)oxipropyl trimethyl ammonium chloride (DOTMA)/ dioleoylphosphatidyl ethanolamine (DOPE) - Lipofectin®, 1,2-dioleoyl-3-trimethylammonium propane (DOTAP), *N*-(2-hydroxyethyl)-*N,N*-dimethyl-2,3-bis(tetradecyloxy)-1-propanaminium bromide (DMRIE), dioctadecyl amino glycyl spermine (DOGS), 2,3 dioleyloxy-*N*-[2(spermine carboxaminino)ethyl]-*N,N*-dimethyl-1-propanaminium trifluoroacetate (DOSPA), Lipid 67, Lipofectamine®], Cytofectin® *Transient expression*	Unlimited insert size, no concentration limitation, better stability than viral vectors, easy to scale up, *ex/ in vivo* route of gene delivery, effective on dissociated cells and slices, many commercially available products, low toxicity, effective on dissociated cells and slices and *in vivo*	Short duration of expression *in vivo,* hard to target specific cells, efficiency of delivery falls below *in vivo* levels, preparation of liposomes is a complex procedure	Primary rat hepatocytes, CHO cells, colorectal cancer cells, rat hippocampal and cortical neuronal cells, COS-7 cells, HeLa, porcine intermediate lobe cells	[75, 76] [77-82]
		Polymeric vectors (Poly(ethylene imine) (PEI), poly(L-lysine) (PLL), *β*-Cyclodextrin, chitosan, poly(glycoamidoamine), schizophyllan, DEAE-dextran, linear poly(amido-amine) (PAMAM), poly(4-hydroxyl-L-proline ester), poly[α-(4-aminobutyl)-glycolic acid], poly(amino-ester), phosphorus-containing polymers)	Unlimited insert size, no concentration limitation, no inflammatory response/ toxicity, no insertional mutagenesis, no immunological problems	Chemical toxicity to some cell types, sensitive to serum, antibiotics, limited by overall transfection efficiency	Colorectal cancer cells, human T cell leukaemia cells, NIH-3T3, HeLa	[41, 81, 83-86]
		Dendrimer-based vectors (PAMAM, poly(propylenimine), PLL, phosphorus-containing, carbosilane)	Structurally versatile, low G-PAMAM dendrimers are non-toxic, easy to synthesise High G-PAMAM gives efficient transfection	Small molecular sizes and limited surface charges of the low G-PAMAM prevent efficient DNA complexation, only PAMAM dendrimers of high generation (G>5) efficient in gene transfection – the procedure for which is tedious and low-yield	CHO, HeLa, astrocytes	[41, 87]
		Polypeptide-based vectors (MPG, transportan)	MPG exhibit high affinity for single and double-stranded DNA, oligonucleotides can be delivered	Mechanism underlying cellular translocation of the peptides are poorly understood, minor	COS-7, HeLa, human foreskin fibroblasts, NIH-3T3	[41, 88-91]

Type	Class	Vectors	Advantages	Disadvantages	Cell types	Ref.
			into cultured mammalian cells within 1 h with >90% efficiency, increased stability against nucleases and increased ability to cross plasma membrane, bypasses serum sensitivity, non-cytotoxic	change in the physical state of the peptide by exchange of certain amino acids can significantly alter translocation properties, quantitative comparison of uptaken cargo vs functionally active cargo required, endosomal escape		
Non-viral	Chemical	Nanoparticles (quantum dots (QD), gold, silica (SiO_2), carbon nanotubes, lipid-based nanoparticles)	Easy to fabricate, adds stability to the assembly Gold (mixed monolayer protected clusters, MMPC) –facile post-modification of monolayer – charge and hydrophobicity, interaction with thiols allows effective and selective controlled intracellular release, non-toxic, high surface area - able to maximise payload/carrier ratio with tuning of size, silica- colloidal silica is biologically inert, lower cytotoxicity than PEI, allows post-modification, quantum dots can be modified by multivalent and endosome-disrupting surface coatings	Gold - optimisation needed for non-immunogenicity and bioavailability Silica – optimisation of the buffering capacity of cationically modified silica required for higher transfection efficiency QD – difficult to deliver single QD into cytoplasm of living cells, aggregate inside living cells, usually trapped in vesicles, lysosomes or endosomes	HEK-293, COS-1, neuronal stem/ progenitor cells, HeLa cells	[41, 92-98]
	Mechanical	Microinjection (Micro-needle, atomic force microscopy tip)	High level of expression in neuronal cells, onset of expression: hours, allows targeted expression, no insert limit, accurate transfection of targeted cells	Low transfection efficiency in neuronal cells, damage from cell injection, needs special instruments, hard to transfect cells in suspension	Oocytes	[99, 100]
		Biolistics (Gene gun)	High level of expression in neuronal cells, targeted expression is possible, minimal toxicity with optimisation	Low/medium transfection efficiency, vulnerable nucleic acids	human mammary carcinoma MCF-7 cells, autologous tumour cells; melanoma/renal carcinoma cells, cutaneous dendritic cells	[49, 101-103] [100]
	Physical	Electroporation (Amaxa Nucleofector)	Simple, quick, requires little optimisation, no need for vector, minimal toxicity, high transfection efficiency	-Transfection efficiency restricted by premature termination of voltage pulse, expensive equipment/reagents, requires skilful operator, laborious procedure, no target cell selection	Neuronal cells, HeLa, primary human fetal fibroblasts, NIH 3T3, CV-1	[104, 105]
		Sonoporation	Single-cell transfection, safe, non-invasive, able to reach internal organs without surgical procedure, gene transfer improved by combining ultrasound irradiation with contrast agents and microbubbles	Cavitation initiation and control difficult, especially *in vivo*	Murine fibroblasts, primary fibroblasts from rat hind limb muscles, human chondrocyte cell line, CHO	[100, 106-108]
		Laser-irradiation	Cell type and condition does not impact it, transfects cells in suspension as well as attached cells. No harmful vectors, can select target cells	High cost, large physical size of laser sources, need for appropriate 'know-how'	NIH 3T3, Hepatocarcinoma cell line (HuH-7), murine muscle cells, MCF-7 cells	[109-112]
		Magnetic nanoparticle (Magnetofection)	With polycation coating - Increases efficacy of vectors several 100-fold, duration of gene delivery - minutes, high transfection efficiency reproduced *in vivo,* lower vector dose, gene delivery to otherwise non-permissive cells	The pH of the water solution of the polycation e.g PEI must be in the alkaline range for pronounced gene expression, transfection levels need optimising	NIH 3T3, CHO-K1 cells, murine melanoma cell line, glial cells, human lung epithelial cells	[113-116]

1.1.3 Mechanism of transfection

The way in which nucleic acids, such as DNA, interact with the cell membrane and navigate from the cell surface to the nucleus is crucial to successful delivery and expression of the gene. The large hydrodynamic volume and the anionic charge of the DNA, however, restricts entry through the negatively charged cell membrane.

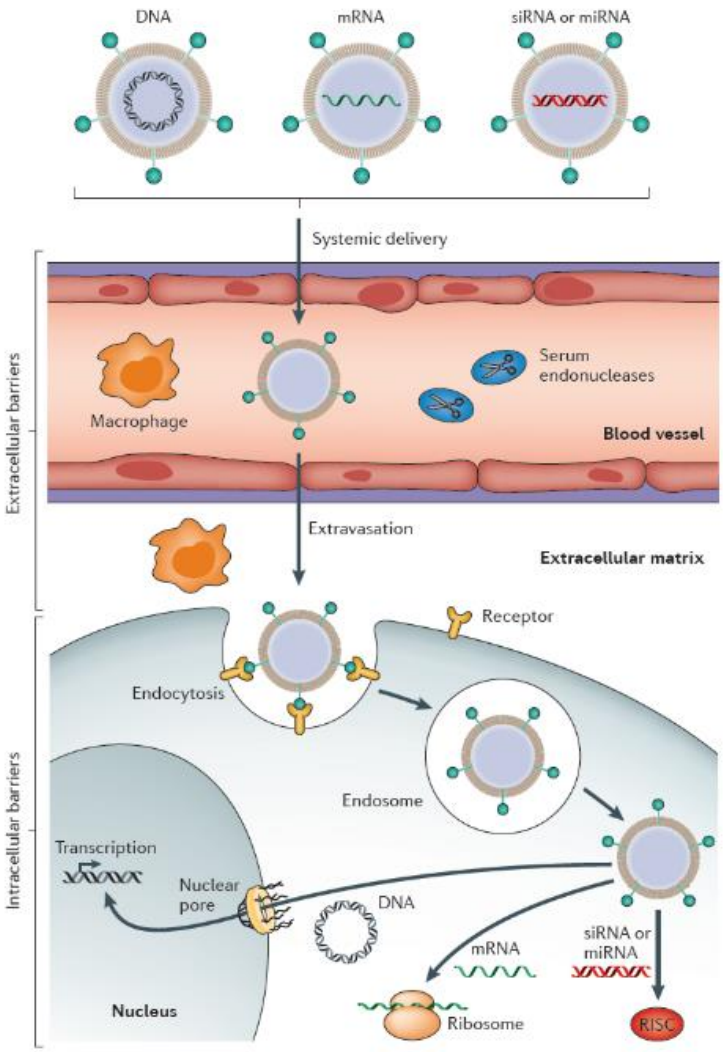

Figure 3: Extracellular and intracellular barriers to successful in vivo *delivery of nucleic acids such as DNA, mRNA and short double-stranded RNA, including siRNA and microRNA (miRNA) mimics, via non-viral vectors. Extracellularly, the carriers must resist degradation by serum endonucleases, evade immune detection, avoid renal clearance from the blood and prevent non-specific interactions. They then need to extravasate from the bloodstream to reach target tissues and mediate cell entry and endosomal escape in the intracellular region so that siRNA and miRNA mimics can be loaded into the RNA-induced silencing complex, mRNA can bind to the translational machinery and DNA to the transcriptional machinery.*[117]

Once the DNA enters the cell, it must be transported through the endosomes and lysosomes towards the nucleus. DNA degradation occurs extensively when nucleases are present in the extracellular compartment. Further DNA fragmentation can also ensue during the passage through the cytoplasm which contains cytosolic endonucleases. Once the DNA survives this, it must traverse the nuclear envelope in order to be transcribed. Nuclease degradation impacts systemic circulation of free DNA hence transfection methods such as electroporation, biolistics and direct injection into target tissue are rendered ineffective in clinical applications. The size of the plasmid DNA also affects diffusion across the cytoplasm and nucleus; the large size causes restricted diffusion in the former due to extensive binding with immobile obstacles, whilst the large DNA is almost immobile in the latter, the reason for which is attributed to molecular crowding in the cytoplasm.[118] Such barriers (Figure 3) encountered by DNA can be overcome upon developing a vector with specialised features which can also subsequently deliver DNA to the nucleus.[39]

In this regard, non-viral vectors such as cationic polymers have very useful physico-chemical properties as they interact strongly with the anionic phosphates of the DNA and condense the DNA fragment into a compact particle via an entropically-driven process.[119] The resulting cationic complexes, ranging from 30 nm to some hundred nanometres, gives rise to charge neutralisation and provides a protective shell for the DNA during nuclear transport by sterically hindering the access of nucleolytic enzymes. Free plasmid DNA can be degraded within minutes whilst DNA/vector complex remains stable for hours.[120] The structure and morphology of the cationic polymer influence DNA binding and condensation; the number of cationic groups strongly impacts the polymer-DNA interaction. The same physical features are kinetically controlled for the resulting complex and are dependent on the order in which the counterparts (DNA or cationic polymer) are mixed together. The structure of the polymer and the DNA/polymer charge ratio also effect the stability of the complexes in serum; large aggregates are usually formed when complexes possess a neutral charge and are considered to be inefficient gene delivery vectors that are toxic due to the particulates forming embolus in the lung, whilst complexes with a positive charge remain stable in solution, though time-dependent.[121]

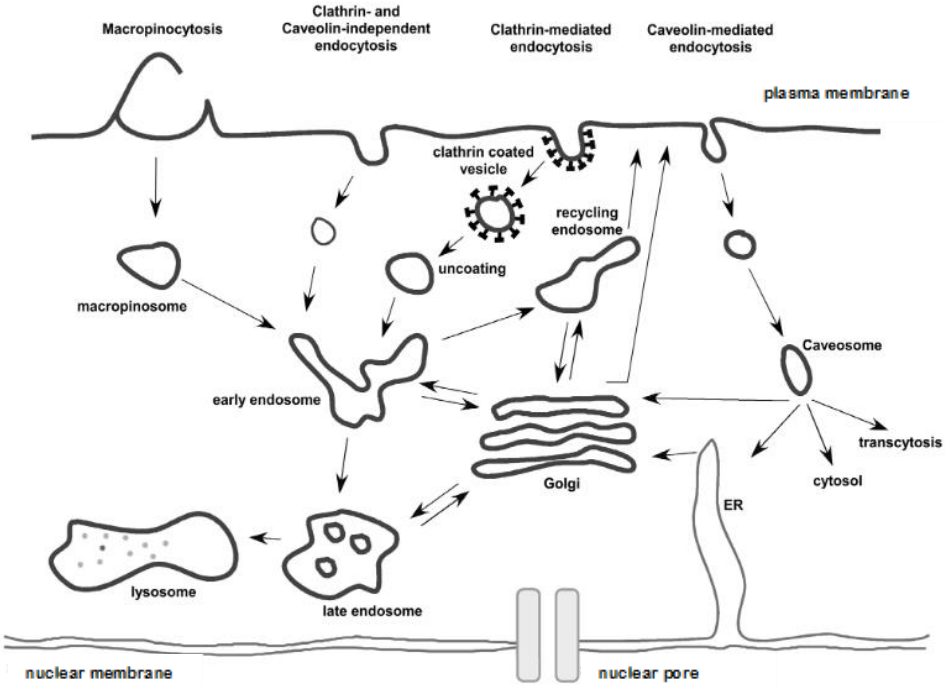

Figure 4: Entry routes into the mammalian cell varies with the size of the endocytic vesicle, the nature of the cargo (ligands, receptors and lipids) and the mechanism of vesicle formation.[90, 122]

The resulting complexes can be routed to the nucleus via conjugation with targeting ligands or without such targeting. At the cellular uptake stage, the non-targeting complexes associate with the plasma membrane via electrostatic interactions with the anionic cell surface proteoglycans. Absence of the proteoglycans have been shown to inhibit cellular uptake dramatically though it is very much dependent on the type of carrier, type of cells and amount of glycosaminoglycans on the cell surface.[123-125] The complexes are believed to be uptaken by various routes of endocytosis (Figure 4); following the binding of complex with heparin sulfate proteoglycans, the resulting complexes gather to form cholesterol-rich rafts on the cell surface and trigger protein kinase phosphorylation (PKC). Subsequently, linker proteins allow the attachment of the proteoglycan-bound complexes to the actin skeleton which enables adsorptive phagocytosis.[126] Other uptake routes include clathrin-mediated endocytosis and macropinocytosis and is controlled by inhibitors and promoters for PKC and Na^+/H^+ antiport.[127, 128] Untargeted polyplexes are believed to bind electrostatically to the cell surface and internalised via adsorptive pinocytosis.[38, 123] Targeting complexes, however, bind with specific cell-surface receptor proteins and are internalised by receptor-mediated endocytosis as shown in Figure 3.

Efficiency of the cellular uptake is further influenced by the size of the complex which in turn is dependent on the concentration of the DNA, type of aqueous medium, the ratio of the nitrogen residues of the polymer to the anionic phosphates of the DNA (N/P ratio) and pH, as well as the type of cell. As cellular uptake takes place, the complexes are enveloped by the endocytic vesicles which are an unfavourable environment; the initial vesicle known as the early endosome fuses with sorting membranes and can eventually lead to the expulsion of the complexes by exocytosis, whilst in the late endosome, large amount of the complexes are trafficked. The endosomal and lysosomal compartments become more acidic (pH 5.0 – 6.2 and pH ≈4.5, respectively) than the cytosol or the intracellular space, upon accumulation of adenosine triphosphate (ATP)-mediated protons from the cytosol into the vesicles. If the vector becomes trapped in the endosomal compartment and is unable to escape then DNA degradation occurs by lysosomal degradative enzymes. The highly evolved viral vectors are able to utilise the lower pH and proceed towards the nucleus.[129] In the case of non-viral vectors, amine group-containing polymeric carriers such as poly (ethylene imine) (PEI)[84] and polyamidoamine (PAMAM) dendrimers[130] which are largely composed of secondary and tertiary amines, with low pK_a values between the physiological and lysosomal pH, have been shown to display a 'proton sponge' effect.[131] These polymers, as a result, are subjected to great changes in protonation during endocytic trafficking. Such proton-sponge polymers resist acidification of endocytic vesicles by encouraging the ATPase to transport more protons to reach the pH required. An influx of counterions occurs in the vesicle in order to balance the accumulation of the protons. The amine group-containing polymer, thus, buffers the endosomal vesicle, subsequently leading to endosomal swelling followed by rupture of the endosomal membrane which results in the release of the complex into the cytoplasm as shown in Figure 5.[132]

Other ways in which the endolysosomal compartments are tackled include the use of chloroquine[133] to treat cells during transfection; thus allowing its accumulation in acidic vesicles and thereby buffering their pH consequently leading to improved gene delivery albeit only in vitro. Another way is the conjugation of inactivated adenovirus to poly (L-lysine) (PLL) which has been found to enhance gene transfer by 2000-fold.[134] Synthetic peptides can also facilitate the endosomal escape as the peptides are pH-sensitive amphiphiles which change in structure in acidic pH and rupture the vesicle membrane thus further enhancing gene transfer.[135] The non-viral vectors which survive the acidic nature of the intracellular compartments, escape degradation but must overcome further barriers in order for DNA/carrier complexes to be delivered into the nucleus of another cell.[41]

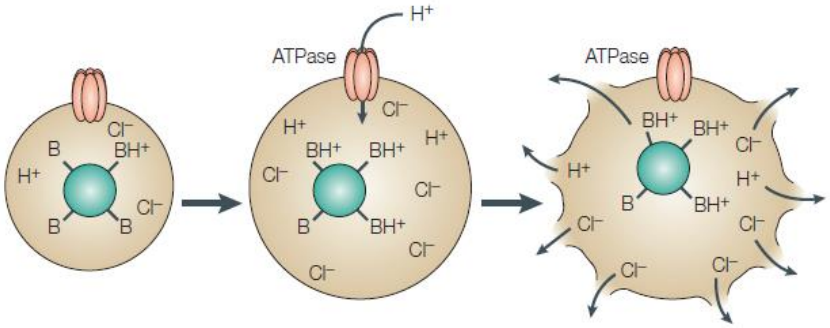

Figure 5: The proton sponge mechanism - when the proton-sponge polymer (green) is protonated, there is an influx of protons and counterions into the endocytic vesicles leading to increase in osmotic pressure and subsequent swelling rupture.[38]

In the cytosol, cytoskeletal elements such as protein, microtubules and other organelles prevent diffusion of large molecules by acting as molecular sieves thus sequestering and restricting the mobility of free plasmid DNA as DNA larger than 3,000 base pairs in length is usually immobile.[118] Viral vectors have the advantage of a microtubule-mediated transport which enable their transport through the cytoplasm. Cationic vectors, however, do not have such assisted transport but they could move along microtubules by non-specifically interacting with anionic microtubules or motor proteins, or they could rely on the natural transport of endolysosomes along the microtubules. Their ability to compact DNA into small particles may also help the movement of DNA towards the nucleus. Relatively large complexes, however, can be expected to remain immobile.[38]

The plasmid DNA must then cross the nuclear membrane in order to reach the transcriptional machinery of the nucleus. Pore complexes within the nuclear envelope (nuclear pore complex, NPC, a 10^7-Da assembly of at least 30 specific proteins) allow the passive diffusion of plasmid DNA from the cytoplasm into the nucleus, provided the compounds are between 9 – 11 nm in diameter.[136] Gene transfer across the nuclear membrane occurs in a similar way to proteins; wheat germ agglutinin (WGA) alongside specific antinucleoporin antibodies inhibit reorganisation of short peptide sequences which trigger an ATP-dependent process via which protein structures with molecular weights above 20 kDa are actively transported through specific nuclear import proteins (importins) and trafficked into the nucleus. WGA can also inhibit the expression of foreign plasmid DNA.[137] Furthermore, the transfected DNA is prevented from accumulating in the nucleus by the elimination of endosome-lysosome fusion with microfilament or translocation with microtubule toxins. Disruption of lysosomal function with protease inhibitors, however, promotes it.[138]

The highly evolved viruses can enter the nucleus by utilising the nuclear import machinery whilst polymers are not able to do this and depend on nuclear membrane breakdown during mitosis in order to enter the nucleus.[139] Mitotic cells usually display higher transfection than non-mitotic cells which indicates that plasmid DNA can reach the nucleus during nuclear envelope disassembly as cell mitosis occurs. Brunner *et al*. have reported that transfection just before mitosis is 30- to 500-fold more efficient than transfection of cells during the beginning of their cell cycle.[140] Hence one of the barriers for non-viral vectors is the transport of gene across the nuclear membrane in non-mitotic cells. However, higher levels of gene expression can be observed when DNA is complexed with a cationic carrier compared to free plasmid DNA. This suggests that the positively charged vector may have a nuclear-localising effect[141] which is recognised by importins. Nuclear localisation sequences have been utilised to promote cellular uptake. Hence gene sequences bound to cationic vectors exhibit better in vitro transfection than free plasmid DNA. This is however not always reproducible in in vivo transfection and is still inefficient with in vitro transfection as seen by the limited number of vectors reaching the nucleus. Further nuclear targeting could be achieved by the use of nucleotide sequences on the gene.[142] However, in depth characterisation is needed to gain an understanding of the nuclear import of complexes.

The vector must release the genes at some point during its journey through the cytoplasm. It is therefore important that polymer/DNA binding strength is tailored by either reducing the cationic charge,[143] reducing the molecular mass[144] or conjugating with poly ethylene glycol (PEG)[145, 146] so that the complex can dissociate, preferably in the nucleus, upon a responsive trigger in order to attain higher gene expression. The efficiency of the expression is measured through reporter gene systems which are usually bound to the inserted gene. The reporter protein can be easily detected by observing the protein itself such as with green fluorescent protein or by measuring its enzymatic activity using a colorimetric assay as with luciferase enzyme reporter, whilst stable transfection can be measured by reverse transcript polymerase chain reaction (RT-PCR).[147]

Although it has been reported that over 95% of cells in culture uptake vectors, less than 50% express the gene.[148] Efficient gene delivery to the nucleus is restricted in non-viral vectors mostly due to the number of extracellular and intracellular barriers that need to be overcome. The amount of DNA being transported through the cell decreases with each step and in turn results in substantially lower gene expression. Initially, cellular internalisation is limited as a result of aggregation from colloidal instability of the non-viral vectors. Charged vectors delivered systemically interact with blood components leading to opsonisation by the reticulo-

endothelial system.[39] Various parameters affecting the vector such as the size, shape and surface characteristics impact its pharmacokinetic properties and hence delivery efficiency. Shielding of the vector's surface charge has improved issues of steric instability and rapid blood clearance.

The design and development of non-viral vectors must therefore take into consideration all the criteria necessary for efficient gene transfection and expression. These include; the ability to protect DNA, ability to pack large DNA plasmids, easy administration, stability in serum, targetable to specific cell types, easy to produce, inexpensive to synthesise, easy to purify, robust/stable, ability to be internalised, suitable for endosomal escape, allows nuclear transport, efficient unpacking, able to infect non-mitotic cells, safe, non-cytotoxic, non-immunogenic and non-pathogenic.[38]

1.1.4 Polymeric vectors

Amongst chemical-based transfection methods, polymeric vectors are attractive due to their versatility in structural modification to package and deliver cargoes to a site of interest, and their ability to respond to specific physiological or external stimuli. The chemistry of the polymers and their payloads determine their stability, biodegradability, biocompatibility, biodistribution and cellular and subcellular fate.[149] Free polymers or polymer brushes can be in the form of linear, branched or dendritic structures or a mixture depending on their application (Figure 6).

A variety of polymers have been investigated on their own or in combination with other polymers to develop potential non-viral vectors (Table 2). Cationic polymers, in particular, hold great promise as non-viral vectors due to their facile synthesis, robustness, chemical diversity and their potential for functionalisation which, with the advances of controlled polymerisation, allows the formation of precisely controlled architectures which can direct their assembly and successive transformations into vectors of specific shapes, sizes, internal morphologies and external surface charges to facilitate biological transport processes at the cellular and sub-cellular levels. The design of the vectors is, however, dependent on the therapeutic application, target site and the route of administration.[149]

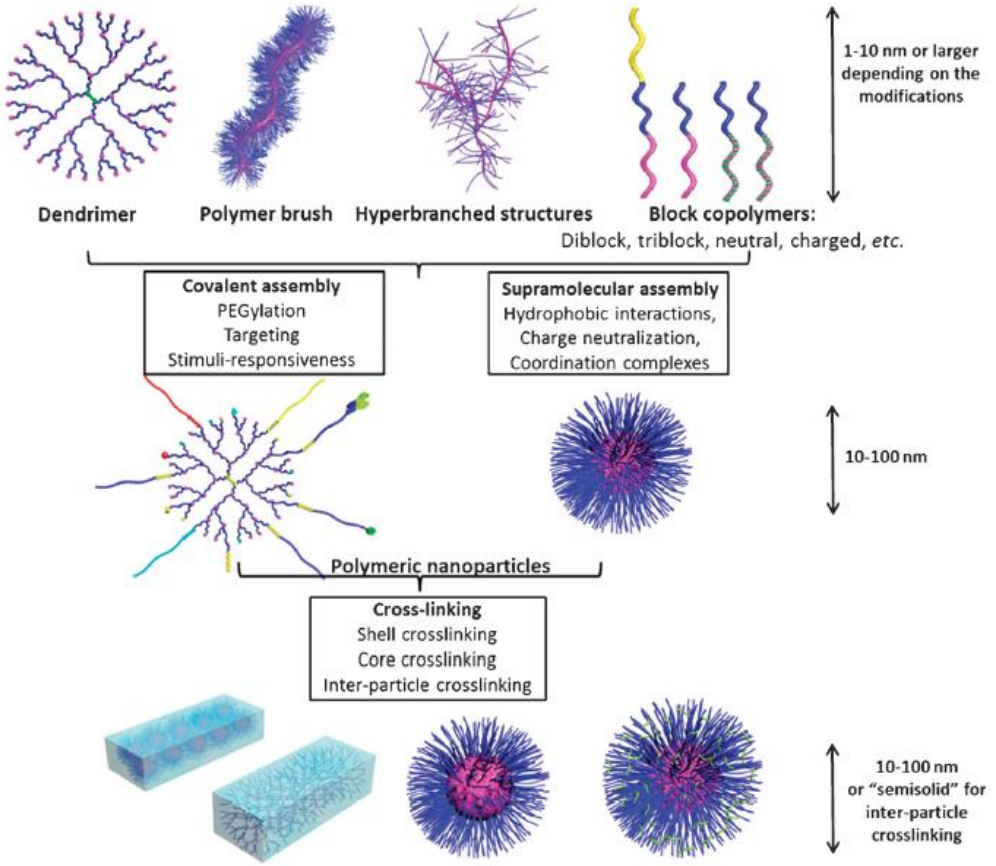

Figure 6: Types of polymeric nanoparticles and potential chemical modifications.[149]

Table 2: Common polymers used in gene delivery.[150]

Polymer	Abbreviation	Unique feature
Poly(ethylene)glycol	PEG	Inert
Polyethylenimine	PEI	Cationic
Dithiobis(succinimidylpropionate)	DSP	Biodegradable PEI
Dimethyl-3,3′-dithiobispropionimidate	DTBP	Biodegradable PEI
Poly(ethylene imine) biscarbamate	PEIC	Biodegradable PEI
Poly(L-lysine)	PLL	Cationic
Histidine modified PLL		Biodegradable
Poly(*N*-vinylpyrrolidone)	PVP	Neutral
Poly(propylenimine)	PPI	Dendromer
Poly(amidoamine)	PAMAM	Dendromer
Poly(amido ethylenimine)	SS-PAEI	Biodegradable
Triethylenetetramine	TETA	Cationic
Poly(β-aminoester)		Biodegradable
Poly(4-hydroxy-L-proline ester)	PHP	Biodegradable
Poly(allylamine)		Cationic
Poly(α-[4-aminobutyl]-L-glycolic acid)	PAGA	Biodegradable
Poly(D,L-lactic-co-glycolic acid)	PLGA	Biodegradable
Poly(*N*-ethyl-4-vinylpyridinium bromide)		Cationic
Poly(phosphazene)s	PPZ	Biodegradable
Poly(phosphoester)s	PPE	Biodegradable
Poly(phosphoramidate)s	PPA	Biodegradable
Poly(*N*-2-hydroxypropylmethacrylamide)	pHPMA	Cationic
Poly (2-(dimethylamino)ethyl methacrylate)	pDMAEMA	Cationic
Poly(2-aminoethyl propylene phosphate)	PPE-EA	Biodegradable
Chitosan		Polysaccharide
Galactosylated chitosan		Synthetic chitosan
N-Dodecylated chitosan		Synthetic chitosan
Histone		Natural
Collagen		Natural
Dextran–spermine	D-SPM	Polysaccharide

A few of the early cationic polymers that were able to electrostatically interact with negatively charged nucleic acids and used for gene delivery research were PLL and PEI. PLL is a homopolypeptide of the basic amino acid lysine and was widely investigated for its ability to condense DNA since the 1960s.[151] The transfection efficiency, however, was poor on its own as at physiological pH, its amine groups are usually positively charged thus gives rise to lower endosomal buffering capacity and lysis. Lysosome disrupting agents such as chloroquine increased the transfection efficiency of PLL (Figure 7).[41] The *in vitro* cytotoxicity exhibited by unmodified PLL was overcome by modifying PLL with, for example, a hydrophilic polymer, PEG, which reduced non-specific interaction with serum proteins thus increasing circulation time and improved the potential of PLL as a gene delivery vector, with the addition of targeting ligands further enhancing its *in vitro* and *in vivo* delivery efficiency.[152-154] One of the first studies on PLL-mediated gene delivery utilised the asialoorosomucoid glycoprotein conjugate to target the asialoglycoprotein receptor for non-viral liver-targeted delivery.[155] Subsequent studies formed the foundation for better understanding the behaviour of PLL in polyplex formation and in endolysosomal escape.[156, 157] The modified variants of PLL have also been investigated for their clinical potential for the treatment of cystic fibrosis,[158, 159] however the relatively low transfection efficiency of PLL-based polyplexes, due to poor escape from the endocytic pathway, has limited the possibility of finding clinical applications.

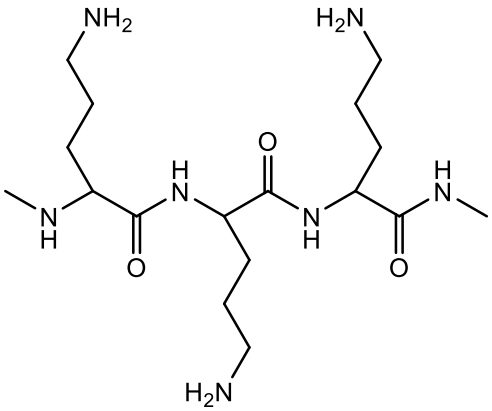

Figure 7: Chemical structure of PLL, pK_a between 9 and 10.[160]

PEI (Figure 8) is one of the most studied cationic polymers for gene delivery due to the high charge density at reduced pH values arising from the presence of a nitrogen atom at every third position along the polymer that can be protonated. This unique property facilitates PEI

as a gene delivery vector in both DNA condensation and endosomal escape (without the need for any exogenous endosomolytic agent, via the proton sponge mechanism) and has been shown to promote gene transfection *in vitro* and *in vivo* for the first time in 1995.[84] Further *in vivo* delivery successes include studies on the central nervous system,[161] kidney,[162] lung[163] and tumours[164, 165].

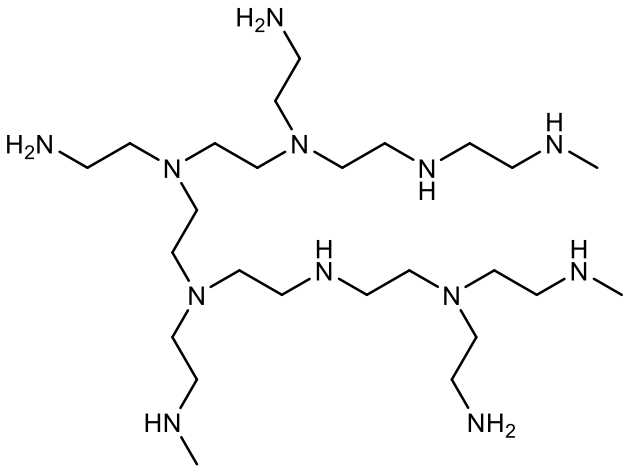

Figure 8: Chemical structure of branched PEI, pK_a of the primary amines is ≈5.5.[160]

Conjugation with ligands such as galactose and transferrin amongst others allowed targeted delivery of PEI-based vectors to specific cell types.[165, 166] It was, however, later found that the molecular weight of PEI alongside other structural properties such as linear form against branched form, strongly influence the transfection efficiency and cytotoxicity of PEI.[167, 168] Despite the usefulness of the large positive charge of PEI in DNA condensation and efficient transfection with a wide range of cell lines, this property of PEI also makes it highly cytotoxic as it destabilises the cellular membrane and initiates apoptosis.[169-171] Due to the substantial cytotoxicity of PEI,[172] variants have been developed; block copolymers of PEG and PEI for enhancing biocompatibility and stability, degradable disulphide-cross-linked PEIs for lowering cytotoxicity, and alkylated PEI for increasing the polymer's effectiveness.[173-178] Full deacylation of linear PEI[179] and partial acetylation of the branched PEI[180] have been shown to improve the transfection efficiency. The results reported for modified PEI indicated the need for balancing the buffering capacity of PEI with other properties of the polymers such that the improved transfection efficiency can be attributed to weaker polyplex formation

resulting in more efficient unpackaging in addition to the endolysomal escape mediated by the proton sponge mechanism.

In order to overcome the issues of transfection efficiency and cytotoxicity related to PLL and PEI, various other polymers such as poly[(2-dimethylamino) ethyl methacrylate], PDMAEMA, poly(β-amino ester)s and carbohydrate-based polymers and dendrimers, are being increasingly investigated[38, 41] with consideration for delivery and safety challenges arising from the large molecular size of DNA, difficulties in crossing the nuclear membrane and potential risk of mutagenesis.

Amongst polymethacrylates, PDMAEMA plays a significant role as a gene delivery vector as it is inherently positively charged, able to destabilise the endosome and dissociate easily from the complex once uptaken into the cytosol. One of the first studies to show high transfection efficiency with moderate cytotoxicity was by Cherng and co-workers who reported an optimum PDMAEMA/DNA (N/P) ratio of 6/1 (w/w), for polymers with molecular weights above 300 kDa.[181, 182] Despite the in vitro success, PDMAEMA has not been able to demonstrate its suitability for *in vivo* gene delivery for a number of reasons including aggregation resulting from the type of application.[183, 184] Modifications to the structure of PDMAEMA have been investigated to promote transfection efficiency. Addition of a tertiary amino group to improve the proton sponge mechanism[185] did not return favourable results as the gene delivery efficiency was found to be lower than that of unmodified PDMAEMA although cytotoxicity was reduced. Other studies attempted derivatisation of PDMAEMA using pyridine, imidazole and carboxylic acid functionalities to improve endosomal escape, but this also did not give desirable results as the first largely reduced transfection efficiency whilst the others eliminated transfection altogether. This indicated that the 'proton sponge' effect is not applicable to all cationic polymers with endosomal buffering capacity.[186] However, PDMAEMA-based star-shaped nanoparticles were also designed which were shown to be efficient vectors in hard-to-transfect and clinically relevant Jurkat T cells and primary T lymphocytes.[187] Copolymerisation of PDMAEMA with other hydrophobic and hydrophilic polymers have also been studied in order to improve the cytotoxicity of the polymer which returned some positive results due to the synergistic effect of the DNA condensing PDMAEMA and the prevention of complex aggregation by the other polymer, for example, *N*-vinyl methacrylate[188, 189] or to enhance cellular uptake by poly(2-hydroxyethyl methacrylate) (PHEMA).[190] Aggregation was also reduced by grafting PEG chains.[191, 192] Targeting of PDMAEMA-based vectors have been investigated by Hennink *et al*. who used Fab' fragment of mAB 323/A3 on a lipid-coated PDMAEMA polyplex to target human ovarian carcinoma cell

line and the results indicated improved gene delivery efficiency when compared to unconjugated PDMAEMA polyplex[193] as did conjugation with folate, in the same cell line.[194]

In this way, minor modifications of the cationic polymers via end group functionalisation or alkylation of the cationic moieties have been studied and have resulted in large differences in the gene delivery activity. Significant variations were observed with changes in the number of cationic groups in each DNA-binding moiety,[195] and hydrophobic modifications of the polymer backbone due to the hydrophobic interaction given to the resulting amphiphilic polycation derivatives and by the enhanced cellular uptake by the hydrophobic chains via the lipophilic membrane.[196-198] It is therefore evident that each type of polymer behaves differently with each modification, and low transfection efficiency and undesirable cytotoxicity continue to be a challenge hence further research is required to fully understand the basic structural requirements such as the size, shape, geometry, charge, structure and composition, for the optimisation of polymeric vectors for efficient gene delivery.

1.2 Polymer brushes for drug and gene delivery

Polymer brushes allow the design and coating of a variety of nanoparticles such as nanodiamond, gold, magnetic and silica nanoparticles, with well-defined core-shell architecture and chemistry and hence are of high interest as vectors and carriers for gene (in detail in section 1.2.2) and drug delivery.[38, 41, 95, 199]

Gold nanoparticles have been functionalised with PEG to allow reversible drug adsorption and photodynamic therapy of cancer.[200] They displayed good biocompatibility *in vitro* and *in vivo,* and their cellular internalisation correlated well with their surface chemistry and size.[201] The integration of receptor-specific targeting ligand to the design of such carriers could further improve their potential. Thermo- and pH-sensitive polymer brush coatings are also used for delivery of drugs as they allow reversible entrapment and release, and consequently enable on-demand delivery.[202-205] The excellent protein resistance of polymer brushes may also be used to control the pharmacokinetics of particles[206] in drug delivery, in particular if combined with targeting strategies.

Although the potential of polymer brushes has not been extensively investigated in drug delivery, perhaps due to the fact that thin brushes do not allow high density of drug immobilisation or controlled long term release, these coatings may still find application in this field. Potentially, brushes could be combined with hollow cores such as carbon nanotubes[207, 208] or other porous structures used for drug delivery applications, to modify their surface properties and drug release profile. Polymer brush decorated nanocapsules, for example, have been shown to alter the release kinetic of doxorubicin.[209]

1.2.1 Brush-protein/ macromolecules interaction

In order to efficiently use polymer brushes in drug and gene delivery, it is important that their interaction with proteins/macromolecules is understood.

Protein adsorption to the surface of materials is the result of a combination of hydrophobic and electrostatic interactions as well as hydrogen bonding.[210-213] Adsorption can be multi-stage, involving primary interactions, sometimes followed by conformational changes in the protein structure and possible denaturation that can reinforce the adsorption to the surface. Such behaviour is also observed in polymer brushes.

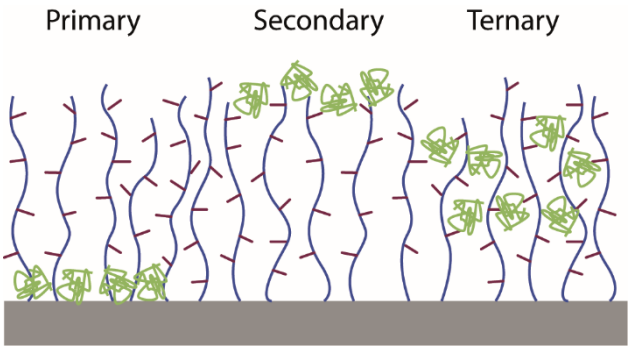

Figure 9: Modes of protein adsorption to polymer brushes.

Three different scenarios have been proposed for describing the interaction of proteins with polymer brush interfaces (Figure 9).[214] Primary adsorption arises from interactions with the underlying substrate, providing the brush height, swelling and grafting densities allows sufficient diffusion. Secondary adsorption is restricted to the outer part of the brush, directly exposed to the bulk solution, and can be expected to dominate in the case of large proteins and very dense and homogenous polymer brushes. Ternary adsorption occurs when the free energy of adsorption to the underlying surface is low and the attraction energy to the brush is sufficiently high. The main forces that proteins have to overcome in primary and ternary adsorption are the brush solvation energy and the penalty in osmotic pressure of the brush, whereas the latter can be ignored in secondary adsorptions. Adsorption is also modulated by the conformation, length and grafting density of the brush as well as the protein size.

Interactions with charged brushes occur for proteins bearing a global opposite charge and adsorption is strongest near the isoelectric point (pI) of the protein. High protein adsorption, however, is not restricted to oppositely charged brushes and proteins: proteins adsorb strongly to polymer brushes on the "wrong side" of their pI (at a pH for which the brush and the protein bear the same net total charge).[215-217] In order to account for these observations, two mechanisms have been explored.[218, 219] The first, based on charge reversal, proposes that a local variation in the pH close to the brush results in electrostatic attraction of proteins.[215, 220] In the second, the localisation of counterions close to the brush leads to a strong osmotic pressure, which can be reduced upon interaction with protein pockets bearing opposite charges to that of the brush. Hence, in this second model, protein adsorption is entropically driven and strongly depends on the buffer ionic strength. Evidence for this latter mechanism was recently provided by isothermal titration calorimetry.[217, 221, 222] In both mechanisms, it would be expected that the strong underlying interactions with the brush and the size of the proteins result in ternary adsorption. Indeed, neutron reflectometry and small angle X-ray

scattering revealed that proteins were able to penetrate and diffuse throughout the brush [223, 224] and could even accumulate close to the core, giving rise to protein aggregation.[225, 226] This behaviour was observed despite slower protein diffusion within brushes compared to free proteins in solution.[227] Local changes in pH and interaction with the underlying substrate may contribute to shaping such protein distribution. In comparison, proteins located in the outer part of the brush are less tightly bound and easier to displace.[226] Not surprisingly, protein adsorption from more complex protein solutions, such as blood or cell culture medium, give rise to high protein adsorption to charged polymer brushes,[228, 229] which could be an important parameter determining cell behaviour at these interfaces.[230] For example, poly((diethylamino)ethyl methacrylate) (PDEAEMA) brushes were shown to respond to changes in pH induced by exposure to CO_2 gases, which in turn promoted protein adsorption in a reversible manner.[231] Similarly, lysozyme adsorption to polyampholyte brushes was found to be pH- and thickness-dependent.[232]

In addition, Halperin described that upon collapse, the brush osmotic pressure decreases, and with it the penalty of insertion of a protein within the brush.[233] This results in increased protein adsorption, as observed experimentally.[234-237]

The interaction between the net negatively charged bovine serum albumin (BSA) and cationic PDMAEMA brush of varying grafting density and degrees of polymerization grafted from gold surfaces, characterized via surface plasmon resonance (SPR), exhibited a high capacity for electrostatically selective uptake as expected.[238] The uptake of BSA increased linearly with the surface mass concentration of grafted PDMAEMA regardless of the grafting density, at a constant ratio of 120 DMAEMA monomer units per bound BSA molecule. Compared to the time necessary for BSA adsorption saturation to a solid surface, the kinetics of BSA uptake in the charged brush was described to be very rapid. Furthermore, the lack of desorption when rinsing BSA adsorbed brush with dilute NaCl solutions displayed the brush's high affinity for BSA, whilst changing the pH/ionic strength hindered the electrostatic attraction for BSA and resulted in desorption. The same study examined PDMAEMA's binding ability with a net positively charged protein; lysozyme and found that PDMAEMA did not have any affinity for the protein molecule thus confirming the cationic brush's charge selectivity and high capacity ion exchange medium for protein binding.

The same polymer brush can be of use in drug and gene delivery as its responsive nature allows controlled release of drug/gene upon a trigger. PDMAEMA-grafted on hollow mesoporous silica nanoparticles were shown to be able to control access to the pores through a pH-

dependent open-close mechanism thus allowing drugs such as doxorubicin hydrochloride to be released from the mesopores via tuning of the solution pH. This method has been proposed to have applications in site-selected drug release and gene delivery.[239]

With DNA, the anionic phosphates can electrostatically interact with the cationic moieties of the polymer brushes, thereby condensing the DNA into compact (where the volume fraction of solvent and DNA are comparable), positively-charged nanoparticle complexes.[35, 119, 240] The genetic information is as a result packaged and protected from extracellular and intracellular degradation during gene delivery. The smaller size also facilitates a more efficient cellular uptake whilst the cationic polymer brush coating on the DNA increases its permeability through the anionic cell membrane. The process of condensation is dependent upon the ratio of polymer to DNA, alongside the hydration forces and correlated counterion fluctuations. As per Manning's counterion condensation theory, approximately 90% of the DNA charge must be neutralised for condensation to occur.[119] Hence polymer brushes with sufficient positive charges such as PDMAEMA are able to successfully bind and condense DNA as shown by Zhang *et al.* who investigated the gene delivery capacity of PDMAEMA grafted from nanodiamond (ND) at various polymer brush/DNA (N/P) ratios.[241] Agarose gel electrophoresis characterisation confirmed that the ND-brushes condensed plasmid DNA into stable nanoparticles which could effectively deliver both luciferase reporter and enhanced green fluorescent protein (EGFP) plasmids into COS-7 cells with higher expression and lower cytotoxicity than PEI25k (polyethylenimine with a molecular weight of 25 kDa). The stability of the complexes is an important factor affecting the transfection efficiency. To test this, the same authors added heparin, a strong anion, previously shown to displace DNA from a cationic vector/DNA complex. The result indicated that the ND-brushes were more stable than the complex made from linear PDMAEMA. The strongest condensation ability against plasmid DNA is attributed to the higher positive surface charge of the ND-brushes which results in tighter packing of DNA. This can be observed by zeta potential and hydrodynamic size measurements.

Although PDMAEMA is one of the most extensively studied polymer brushes for nucleic acid delivery, others include cationic comb-type copolymers (CCC) with PLL and PEG of different weight percentage for siRNA delivery.[242] A lower polycationic backbone and higher water-soluble side chains exhibited stronger interaction with siRNA as the dense PEG brush reinforced the interpolyelectrolyte complex between the PLL backbone and siRNA. Poly(*D,L*-lactic acid) and PLL-graft (g)-polysaccharide copolymers have also been suggested to be

potentially good as DNA carrier *in vivo* as the nanoparticle from the graft copolymer resisted self-aggregation and nonspecific adsorption of serum proteins as a result of the 'polymer brush' effect of the polysaccharide graft chains.[243] Cylindrical brush polymers, quaternized poly(vinyl pyridine) or PEI, of different side chain lengths and charge densities, and a fifth generation PAMAM dendrimer[244] have been reported to form complexes with supercoiled DNA and showed a large cationic excess charge that could not be compensated by extensive back-folding of the same DNA molecule interacting with a cylindrical brush. The complex formation was observed to be kinetically controlled and depended on parameters like the concentration, speed and sequence of mixing. With increasing number of DNA molecules interacting with one complex, the cationic core became surrounded by a corona of anionically charged DNA loops as a result protecting the cationic core against further complexation. Here, the initial formation of complexes was diffusion-controlled until a certain net charge of the complexes was reached. These primary complexes appeared to be stabilised electrostatically and/or sterically when a slight excess of anionic charges of the whole complex was reached. Hence, the interaction of the anionic charge of the DNA with the varying positive charge density is significant in the formation of an efficient complex that can then dissociate for gene expression to occur.

1.2.2 Application of brushes for gene delivery

The delivery of plasmids into various types of cells can be achieved, whilst ensuring low cytotoxicity, using cationic polymeric vectors such as the gold standard PEI or those obtained by controlled radical polymerizations. Such cationic materials constitute interesting alternatives to viral vectors.[190, 245, 246]

Cationic polymer brushes such as PDMAEMA have the ability to condense DNA and enable cell uptake of ND-PDMAEMA vectors, whilst protecting DNA from enzyme degradation.[241] Hence nanoparticles decorated with PDMAEMA brushes have been used for plasmid DNA and siRNA delivery.[187, 241, 247]

Compared to branched PEI, these vectors were reported to perform better and to be less toxic to cells (Figure 10). The transfection of hard-to-transfect cells, including differentiated cells and human primary T lymphocytes was also reported and it was proposed that the core shell architecture was key to such performance.[248] In addition, the core-shell approach allows the use of cores with diagnostic ability (e.g. magnetic resonance imaging, MRI, or fluorescence),

making brush-decorated particles useful to the field of theranostics. Protein resistant brushes have also been used as protective coatings for the stabilisation of superparamagnetic particles for MRI imaging.[249] An interesting feature of polymer brush-functionalised nanoparticles is that the chemistry of the core and its shape can be varied independently from the chemistry of the brush. Hence gold nanorods decorated with PDMAEMA brushes were also reported to give rise to high transfection efficiencies in COS-7 and human liver carcinoma cells.[250]

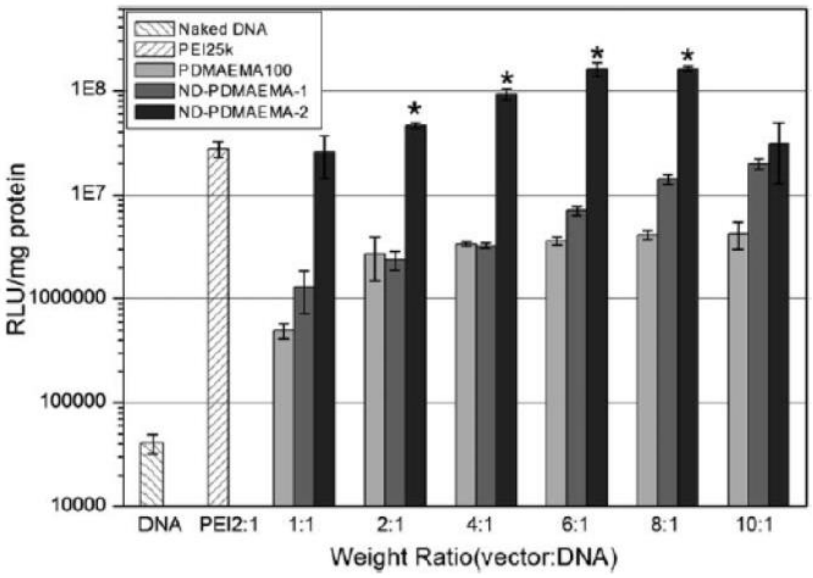

Figure 10: Evaluation of the transfection efficiency of PDMAEMA-coated nanodiamond. Results are presented as the mean ± SD in triplicate.[241]

The issue of serum stability of polyplexes can be overcome by grafting hydrophilic polymer brushes such as PEG and *N*-(2-hydroxypropyl)methacrylamide)[153] though PEGylation reduces internalisation of non-targeted polyplexes and alters intracellular trafficking as shown by Davis and co-workers.[251] Such modification methods prevent salt-, protein- and complement-induced inactivation. The increased serum stability can be accounted for by the steric effects which result in decreased particle-particle and particle-protein interactions. This can be further influenced by grafting density, molecular mass and grafting method of the hydrophilic polymer to the polycation.

Targeting moieties required for cell-specific gene delivery varies greatly with each gene therapy. In the case of cancer therapies, where the aim is to kill target cells, gene delivery is required in a very specific set of cells whilst in the case of diseases such as haemophilia, all that is necessary is that the transfected cells, regardless of their identity, produce adequate

amounts of the secreted therapeutic protein. The cell-specific targeting with polymer brushes is possible due to their flexible chemistry via which targeting moieties could be attached. The resulting complexes exhibit increased cellular uptake and cell specificity. In addition to receptor-mediated endocytosis, epidermal growth factors (EGF),[252] antibodies/ antibody fragments[253] and integrin-binding sequence also facilitate cell-specific targeting.[254] The efficiency of the targeting, however, is dependent upon the conjugation chemistry, spacer length between the ligand and polyplex, strength of the ligand-receptor binding and the number of targeting ligands per polyplex.[38]

The ability of cationic polymeric vectors, obtained by controlled radical polymerizations, to efficiently deliver plasmids into various types of cells as well as exhibiting comparable expression levels to the gold standard PEI25k, whilst ensuring low cytotoxicity, is promising for the use of cationic brush coatings as alternatives to viral vectors.[190, 241, 246]

1.3 Polymer brush synthesis

Polymer brushes are end-tethered polymer chains bound to and stretched away from a solid substrate/interface. End-grafted polymer chains can adopt three regimes: the mushroom regime - if the interaction between the polymer and the surface is weak or repulsive, the chains form a typical random coil that is linked to the surface through a "stem" of varying size, the pancake regime - if the segments of the surface attached chains adsorb strongly to the underlying surface, the polymer molecules obtain a flat, "pancake"-like conformation, and the brush regime – the segments of the chains try to avoid each other as much as possible and minimize segment–segment interactions by stretching away from the surface, as illustrated in Figure 11.[255]

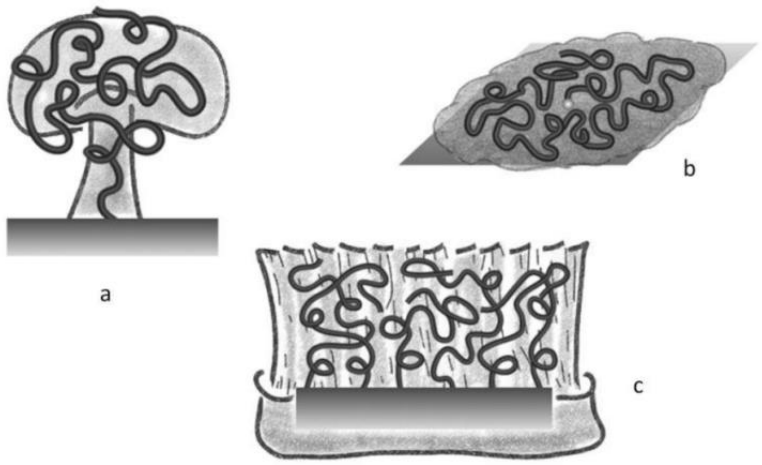

Figure 11: a) 'mushroom', b) 'pancake', c) 'brush' used for the different possible conformations of surface-attached polymers.[255]

The assembly of polymer brushes allows for tailor-made surfaces for various applications. Responsiveness of polymer brushes to external stimuli refers to changes of polymer molecule conformations (correlated to changes of free energy of the brush in its environment due to the change of grafting density, solvent quality or pH of solution). The swelling of polymer chains is sensitive to its environment.

1.3.1 Synthesis

Polymer brushes can be synthesised using various living polymerisation techniques; cationic, anionic, free radical, ring-opening metathesis (ROMP),[256, 257] chain-growth polycondensations and group-transfer polymerisation. This method allows control over the polymer architecture; molecular weight, molecular weight distribution/ polydispersity (PDI), functionality and composition, and limits premature termination of the reaction as it facilitates the continuation of the polymerisation reaction until all monomer is consumed or provides the option of controlled termination. Recent advances use three fundamental controlled radical polymerisation (CRP)/ reversible-deactivation radical polymerisation techniques; atom transfer radical polymerisation (ATRP),[258-260] reversible addition fragmentation chain transfer (RAFT),[261, 262] and nitroxide mediated polymerisation (NMP).[263, 264] CRP can be utilised with a wide variety of monomers for a broad number of applications due to the robustness of the polymerisation conditions. ATRP, with its ability to tailor the catalyst to meet specific requirements, is used in surface modification applications that require tailoring hydrophilicity, adhesive properties or nanoparticle functionalisation. Both, ATRP and RAFT are versatile methods used to synthesise block copolymers for bio-applications in drug and gene delivery and bio-mineralisation, whilst block copolymers obtained via NMP, a least versatile method, are used in composite manufacturing, memory devices and so forth.

Earlier works to form polymer brushes involved physisorption where selective adsorption of a block polymer from a diblock polymer to a surface occurred. The surface and solvent were chosen to maximise preferential adsorption of one block to a solid surface while the solvent was chosen to preferentially interact with the other block. The disadvantage of this method was that the physisorbed blocks can be unstable when subjected to certain conditions of solvent, temperature and can also be displaced by other adsorbents.

Presently, however, polymer synthesis strategy is mainly outlined around the ‘grafting to’ and ‘grafting from’ approaches (Figure 12) which entail covalent binding of polymer chains at the interface (chemisorption) resulting in enhanced stability of the bound chains. An attractive quality of both methods is that they are both compatible with a wide range of technologically relevant substrates other than gold and silicon.

One of the methods in polymer brush synthesis is the ‘grafting to’ approach which involves the chemical reaction of pre-synthesised, functionalised polymers with a surface containing complementary functional groups such as thiols, silanes, amino or carboxylic groups. The advantage of this approach is that it is a technically simple method and it allows a more

accurate characterisation of the pre-synthesised polymers. Though it is generally said that higher concentrations of polymer lead to higher grafting densities via this method, it has been argued that the disadvantage of the grafting to approach is that achieving high density polymer grafting becomes more difficult with increasing size of polymer chains (limits their protein and cell resistance) because of steric crowding of reactive surface sites by already adsorbed polymers.[265] Polymer tends to no longer remain linear with increasing size, and aggregation of polymers near the polymer backbone blocks other potential sites for polymerisation. This difficulty is further enhanced by when synthesising high molecular weight polymers. Brittain and Minko report that grafting density can be regulated by grafting time and that the residual ungrafted polymer can be removed by solvent extraction immediately after the grafting process is terminated.[266]

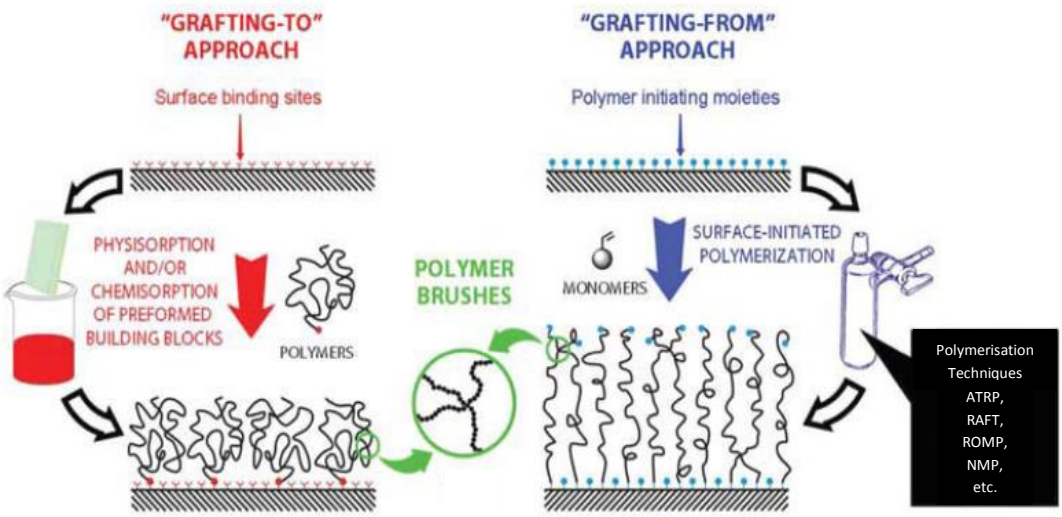

Figure 12: Chemical strategies used to tether polymer brushes on a range of substrates.[3]

Conversely, 'grafting from' approach involves the in situ polymerisation of an initiator-functionalised surface with monomer thus allowing the growth of a polymer chain hence is also termed surface-initiated polymerisation. The advantages of the 'grafting from' approach are that the functionality, density and thickness of polymer brushes can be controlled with molecular precision and can be executed with almost all available polymerisation techniques.[265] The substrate needs to be functionalised with a radical initiator site to supply the radical necessary for free radical or CRP. The latter gives every radical site on the polymer

backbone an equal chance for polymerisation therefore much longer chains can be polymerised into backbone. The 'grafting from' approach can form polymer brushes of higher grafting density than the 'grafting to' approach as the grafted layer is swollen by the monomer solution such that the monomer units migrate to the growing polymer chains and feeds it. Here, the growth of chains isn't limited by the diffusion of monomer until a very high grafting density is approximated hence the 'grafting from' approach has become the preferred option for polymer brush synthesis with chain thickness reaching between 10 and 100 nm.[267] The disadvantage of this technique however, is that the limitation of initiator surface coverage, initiator efficiency and the rate of diffusion of monomer to active polymerisation sites can lead to some problems. The effect of side reactions could be considered more important than the bulk polymerisation due to the high local concentration of polymer chains in the grafted layers; e.g. bimolecular termination in RP. This form of polymerisation may lead to a broader molecular mass distribution.[266] Controlled surface-initiated polymerisation has been shown to be possible on a range of substrates including silicon and glass,[268-271] various metals (gold)/ alloys/ metal oxides,[272-274] hydroxyapatite,[275] graphene,[276, 277] cellulose,[278] fluorinated polymers,[279, 280] electrospun fibres,[281] polystyrene,[282, 283] poly(methyl methacrylate) (PMMA),[282] poly(dimethylsiloxane),[284] poly (2-hydroxyethyl methacrylate-*co*-methyl methacrylate) hydrogels[285] amongst many others.

The hybrid or the 'multi-step grafting' approach combines and creates surface-grafted hyper branched polymer chains. It allows increased density of polymer attachment in 'grafting to' where synthesis can be switched to a 'grafting from' to increase branching of the previously attached polymer chains.[286]

1.3.1.1 Atom Transfer Radical Polymerisation (ATRP)

ATRP is the most extensively used living polymerisation which has tolerance to a wide range of functional monomers and allows the precise control of polymer architecture. The living/controlled character of the ATRP process yields polymers with a low PDI that are end functionalised and so can be used as macroinitiators for the synthesis of di- and triblock copolymers.[265, 287] This can be used for the surface-initiated synthesis of block copolymers in relatively benign solvents under ambient conditions. The advantages are that it requires less stringent experimental conditions and provides control over the chain length and surface density of the polymer graft.[288]

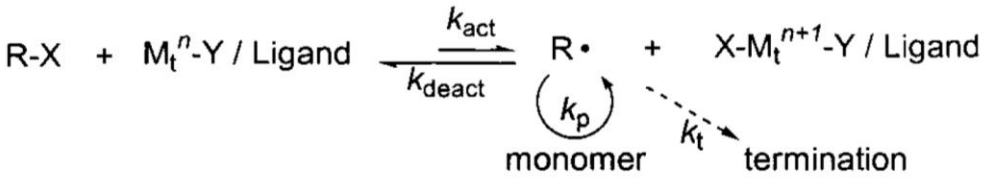

Figure 13: Basic mechanism of ATRP.[289]

The basic mechanism of ATRP involves a reversible switching between two oxidation states of a transition metal complex. The radicals are generated through a reversible redox process which is catalysed by a transitional metal complex (M_t^n-Y/Ligand) which undergoes one-electron oxidation with simultaneous removal of a transferable organic halide, X, from a dormant species, R-X (Figure 13).[289]

Polymer chains are grown by the addition of the intermediate radicals to monomers in a manner similar to conventional radical polymerisation. The equilibrium is mainly shifted to the left (dormant) side to suppress termination and transfer reactions. Termination does occur as a result of radical coupling and disproportionation but, in a well-controlled system, it is limited to a fraction of the polymer chains. The generation of oxidised metal complexes, X-M_t^{n+1}, that behave as persistent radicals, reduce the stationary concentration of growing radicals and thereby minimise the contribution of termination. A successful ATRP requires fast and quantitative initiation and rapid reversible deactivation to obtain a uniform growth of all the chains which results in a narrow molecular weight distribution.[288] The rapid reversible deactivation of propagating radicals is required to maintain low radical concentrations and minimise normal termination of living polymers.[258]

1.3.2 Types of brushes and biomedical applications

Polymer brushes can be homopolymer, polyelectrolyte, block copolymer, molecular, or reversible self-assembled. Architectural modulation of the brushes diversifies their applications in biotechnology and nanotechnology, with it becoming increasingly valuable at the interface of materials science and biology. Understanding and controlling such interfaces has proven to be key in the application of polymer brushes in biosensing,[290, 291] cell culture and regenerative medicine,[292, 293] and antibacterial coatings.[294, 295]

The interfacial properties including hydrophilicity and surface energy, rheological and tribological behaviour, electron and energy transfer, binding and adsorption of molecules and proteins, catalytic activity, diffusion of molecules and particles and, cell adhesion can be tailored by exploiting the flexibility of polymer brushes. The responsive nature of the brushes to environmental triggers like pH, temperature, solvent quality, ionic strength and counterions determine their suitability for each of these applications and is therefore largely dependent on the chemistry of the repeat monomer unit (Figure 14).

Systems sensitive to pH are based on polyacids or polybases (further discussed in Chapter 2.1.1.1) such as poly(acrylic acid) (PAA),[296] poly(methacrylic acid),[297] (PDMAEMA),[298] PDEAEMA,[299, 300] and poly(4-vinylpyridine).[301] These brushes achieve a high degree of swelling reaching from 400% to 700% in their fully charged state, due to the strong intra- and interchain repulsive forces arising from the charged monomers and associated osmotic pressure, whilst also being influenced by the ionic strength.[296, 298] Similarly, zwitterionic brushes such as poly(carboxybetaine methacrylate) (PCBMA)[302] and random copolymers of oppositely charged monomers[303] can display responsive properties due to a change in electrostatic interactions and osmotic pressure upon deprotonation of the brush.

Furthermore, temperature-sensitive brushes are based on polymers displaying a lower critical solution temperature (LCST)[304, 305] or an upper critical solution temperature (UCST)[306] in aqueous solutions. Poly(*N*-isopropylacrylamide) (PNIPAM) is one of the most popular polymers displaying LCST properties, with a sharp transition at 32°C for free polymers in solution, and has been employed to generate brushes with thermally responsive properties. Researchers have developed other systems that would either allow precise control of the position of the LCST in a wider range of temperatures or avoid the large hysteresis observed for PNIPAM. POEGMA and poly(bis(ethylene glycol) methyl ether methacrylate) copolymers display little hysteresis during the cooling process.[307] The copolymer's LCST linearly increases with increasing OEGMA monomer ratio.[304] Poly((2-(methacyloyloxy)ethyl)dimethyl(3-sulfopropyl)ammonium hydroxide) (PMEDSAH) is an example of a zwitterionic polymer which displays UCST properties.[306, 308] In such cases, the strong dipoles arising from the zwitterionic repeat units associate at low temperature, resulting in brush collapse and surface hydrophobicity, whereas they dissociate above the UCST, inducing brush swelling and surface hydrophilicity, depending on the brush thickness and grafting density; UCST occurs near 52°C for thick dense brushes.

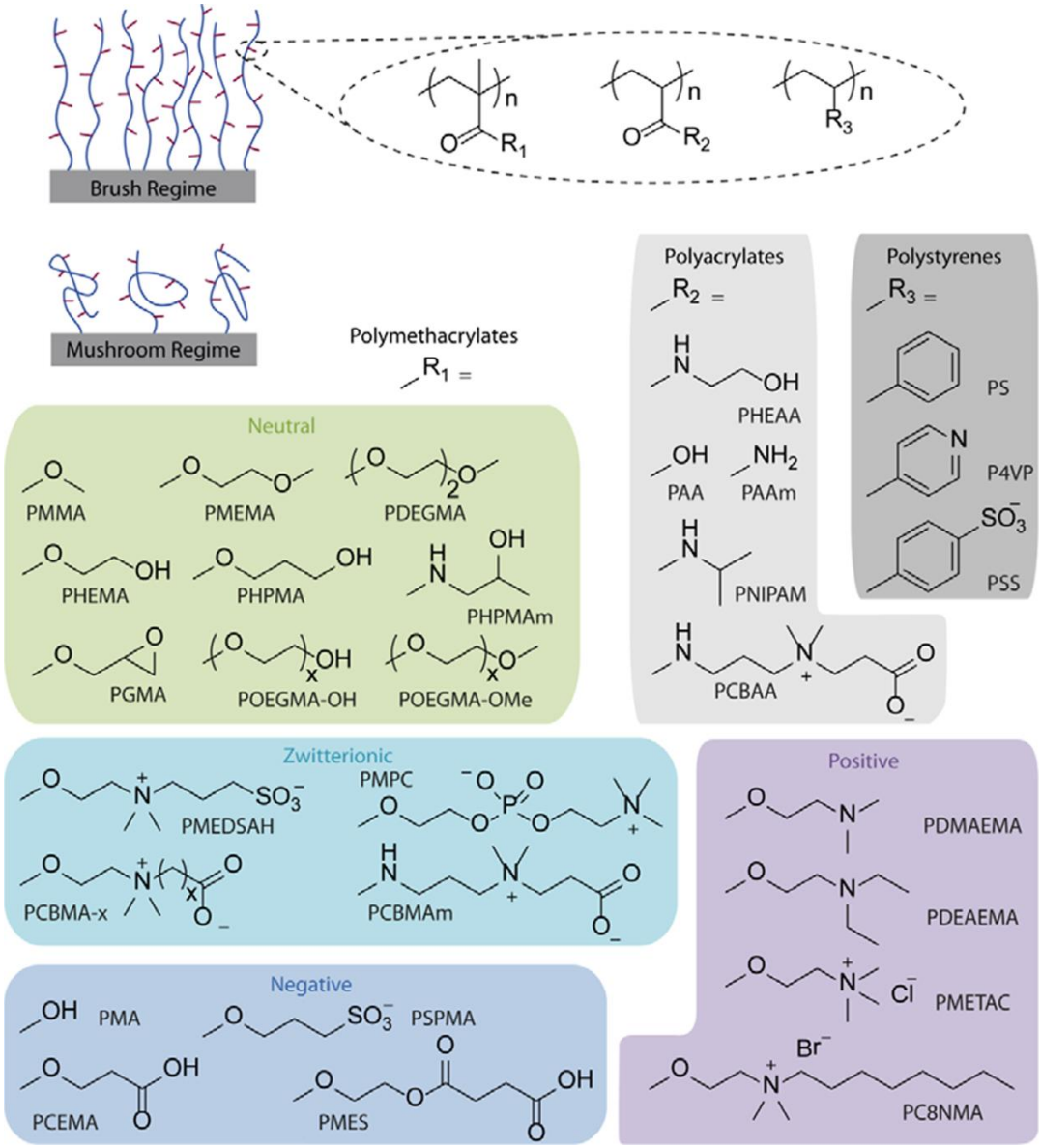

Figure 14: Chemical structure of polymer brushes commonly used in biomedical applications. Abbreviations: poly(methyl methacrylate)(PMMA), poly(methoxyethyl methacrylate)(PMEMA), poly(bis(ethylene glycol) methyl ether methacrylate)(PDEGMA), poly(hydroxyethyl methacrylate)(PHEMA), poly(hydroxypropyl methacrylate)(PHPMA), poly(hydroxypropyl methacrylamide)(PHPMAm), poly(glycidyl methacrylate)(PGMA), hydroxyl-terminated poly(oligo (ethylene glycol) methacrylate)(POEGMA-OH), methoxy capped POEGMA (POEGMA-OMe), poly((2-(methacryloyloxy)ethyl)dimethyl(3-sulfopropyl)ammonium hydroxide)(PMEDSAH), poly((methacryloyloxy)ethyl phosphorylcholine)(PMPC), poly(carboxybetaine methacrylate)(PCBMA), poly(carboxybetaine methacrylamide (PCBMAm), poly(methyl acrylate)(PMA), poly(3-sulfopropyl methacrylate)(PSPMA), poly(2-cinnamoyloxyethyl methacrylate)(PCEMA), poly(2-(methacryloyloxy)ethyl succinate)(PMES), poly(N-hydroxyethyl acrylamide)(PHEAA), poly(N-isopropylacrylamide)(PNIPAM), poly(carbocybetaine acrylamide)(PCBAA), polystyrene (PS), poly(4-vinylpyridine)(P4VP), poly(styrenesulfonate)(PSS), poly((dimethylamino) ethyl methacrylate)(PDMAEMA), poly((diethylamino) ethyl methacrylate)(PDEAEMA), poly((2-(methacryloyloxy)ethyl)-trimethylammonium chloride)(PMETAC), poly(methacryloyloxy ethyl-dimethyloctyl ammonium bromide)(PC8NMA).[309]

Amongst biomedical applications, cell culture platforms based on polymer brushes is a vast area of research. The biofunctionalisation of implant and devices to alter interfaces between a material and surrounding cells or a tissue is an important element of design in bioengineering. Such biointerface should allow the control of behaviours such as cell recruitment, adhesion, spreading, motility, matrix deposition, proliferation and differentiation. The biofunctionalisation of materials with extra-cellular matrix molecules or fragments, growth factors and drugs is essential and polymer brushes are particularly well suited to do so without altering the bulk properties of such materials. Similar strategies are also employed to design new generations of cell culture systems and cell-based assays.

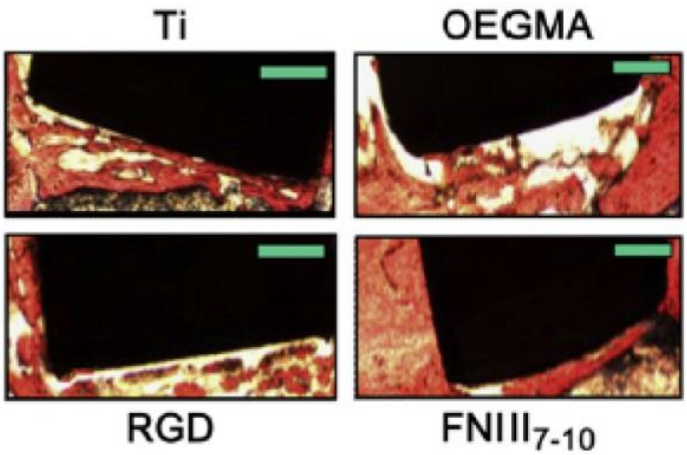

Figure 15: Osseointegration of titanium implants coated with POEGMA brushes and POEGMA brushes functionalised with RGD peptide or a FNIII$_{7-10}$ fibronectin fragment.[310]

POEGMA brushes, which are typically protein- and cell-resistant, have been biofunctionalised to be used to coat titanium substrates (Figure 15) for applications in implants such as hip and knee joint replacements, dental implants, and cardiac pacemakers, as these require some level of integration with the surrounding bone to avoid implant failure.[311] Shorter oligo(ethylene glycol) in POEGMA brushes were found to allow partial anti-fouling properties for only short periods of time but were still able to sustain cell spreading for longer term cultures.[312] Similarly, sparse brushes allowed non-specific adsorption of fibronectin which resulted in cell spreading,[313, 314] and gradient PHEMA brushes allowed the control of cell spreading. More generally, peptide or protein adsorption and cell attachment occurs preferentially at low grafting density, in the mushroom regime, whilst slight or no peptide attachment and cell adhesion were observed for denser brushes.[315, 316] Other low fouling brushes such as poly(glycerol monomethacrylate) similarly displayed cell resistance,[317] but allowed cell

spreading when copolymerized with PDMAEMA. The protein and cell antifouling properties of polymer brushes such as PMEDSAH can be useful for coating poly(caprolactone) to improve hemocompatibility[318] and metal stents to avoid restenosis and thrombosis.[319] Platelet adhesion and hemolysis were also decreased on PMEDSAH-coated stents.

The brush chemistry itself has been shown to impact cell behaviour. In such systems, deposition of biomolecules from the medium is thought to be important to bioactive properties. Non-functionalised PMEDSAH was shown to promote attachment and proliferation of undifferentiated human embryonic stem cells (hESC),[320] despite its reported protein and cell resistance in other systems.[321] It was reported that this coating was not fully resistant, which could perhaps account for the observed behaviour of stem cells.[228] The absence of strong cell adhesion and spreading may be beneficial. In particular, ultraviolet exposure used for sterilisation of substrates may lead to the deterioration of anti-fouling properties, thus enabling sufficient adhesion of hESCs. The chirality of polymer brushes was also shown to trigger differential cell behaviours. This was illustrated by enantiomorphic surfaces that modulated cell spreading. Cells adhering at high densities formed cell-cell adhesions and generated large interconnected clusters on the L-films whilst nearly rounded cells in segregated stacks were observed on D-films.[322] Topography was also shown to alter cell behaviour and had an impact on the cell resistance of POEGMA brushes. The long term adhesion of human hepatocyte and human carcinoma cells was improved when the roughness of surfaces was modified using gold nanoparticles, compared to smooth controls.[323] Moderately specific interactions, as for boronate-containing brushes which can bind to glycoproteins on the surface of cell membranes,[324] were used for selective cell adhesion. Cells were shown to detach from these surfaces on demand, when treated with fructose solutions. In addition, copolymers of *N,N*-dimethylacrylamide (DMAA) and *N*-acryloyl-*m*-phenylboronic acid (NAAPBA) were shown to distinguish between different cell lines,[324, 325] where complex formation between boronates and glycoproteins and glycolipids at the cell surface gave rise to stronger binding between the murine hybridoma cells (M2139) and poly(DMAA-co-NAAPBA) brushes compared to human myeloid leukaemia cells.

Another useful application of polymer brushes such as PNIPAM is cell and cell-sheet harvesting, made possible by the thermoresponsive nature of the brushes. PNIPAM has been the most extensively studied brush for thermally controlled cell detachment and cell sheet generation (Figure 16),[326-329] and it has been applied to a wide range of cell types, including fibroblasts, epidermal cells, chondrocytes, aortic endothelial cells, muscle cells, kidney cells, cardiac myocytes and hepatocytes.

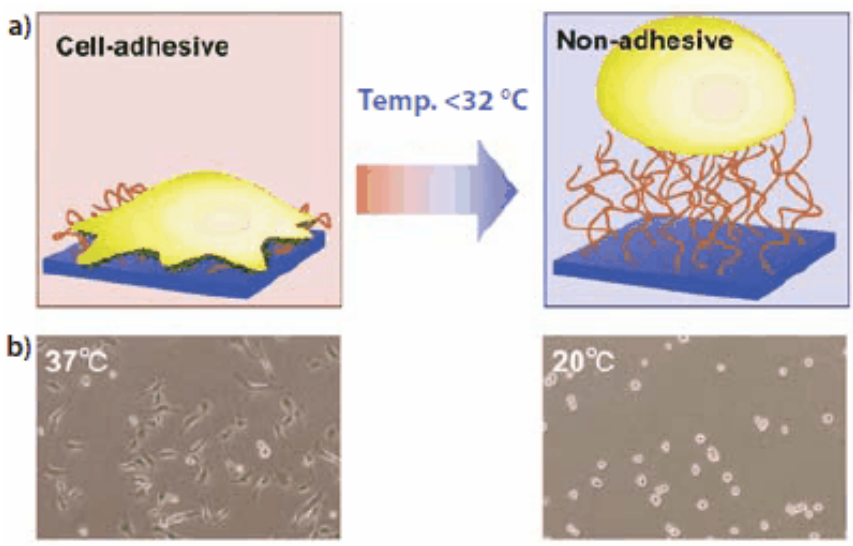

Figure 16: a) Schematic representation of the adhesion (37 °C) and detachment (20 °C) of a cell on a PNIPAM brush-grafted surface hence lowering the temperature allows cell harvesting, (b) Micrographs of endothelial cells on PNIPAM brush-coated dishes at 37°C and 20°C.[330]

PNIPAM has been shown to display some protein resistance below its LCST, especially at high grafting densities. Above this transition protein adsorption and cell adhesions are promoted,[236, 237] hence enabling the use of PNIPAM brushes as thermoresponsive tissue culture substrates, especially considering their good bio-compatibility and apparent lack of toxicity (some reports of cytotoxicity exist, perhaps due to the presence of unreacted monomers).[331] A variety of copolymers of PNIPAM have also been generated, with controlled LCST between 20°C and 42°C[332-336] and found application for selective cell detachment.[337, 338] Copolymers of PNIPAM with 2-lactobionamidoethyl methacrylate (LAMA) were able to bind hepatocytes above the LCST and released them only on brushes where LAMA monomers were presented as a top layer of the co-polymer.[339, 340] Oligo(ethylene glycol)-based copolymer brushes have also attracted some attention for controlling cell adhesion as they are biocompatible and their LCST can be controlled over a relatively wide range of temperatures.[304, 307, 341-343]

The use of polymer brushes as antibacterial coatings is another rapidly increasing area of research. Bacterial biofilms on surfaces can for example cause problems in healthcare by medical device associated infections. Polymer brushes have been presented as possible candidates for antibacterial coatings, and have been reported to reduce the overall adhesion of bacteria both for hydrophobic and hydrophilic brushes.[229, 344] It has also been described that bacterial adhesion on “switchable” polymer brushes, such as PNIPAM, differs above and

below the LCST. Below the LCST the brush is extended, which reduces the amount of adherent bacteria on the surface.[332, 345] In the literature, three main approaches are reported for constructing antibacterial brush coatings (Figure 17): 1) polymer brushes composed of a bactericidal polymer, 2) polymer brushes functionalised with a bactericidal or bacteriostatic compound, either covalently linked to the brush or embedded in the brush film to allow subsequent diffusion, and 3) non-fouling polymer brushes that aim to repel bacterial adhesion and subsequent biofilm formation.

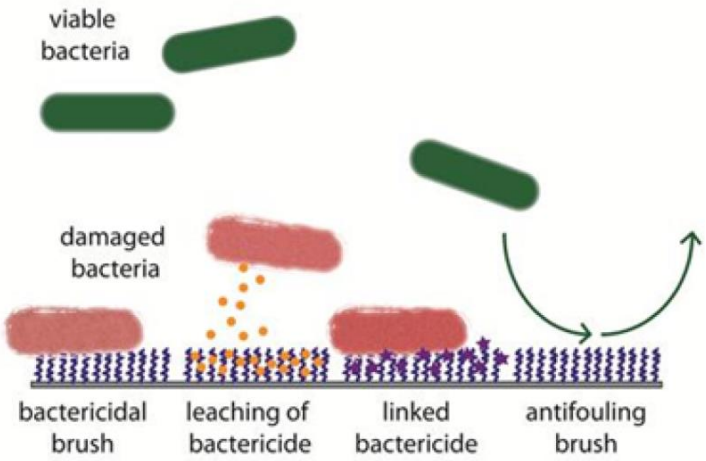

Figure 17: Schematic of the approaches used for creating polymer brush surfaces that inhibit bacterial adhesion and biofilm formation.[309]

1.4 Aims & Objectives

1.4.1 Aim

To develop a novel and versatile cationic system using surface-initiated polymerisation, to control and understand the physicochemical properties (chemistry, charge, architecture, size and shape) as illustrated in Figure 18, as well as the biopharmaceutical behaviour of the non-viral gene delivery agent.

1.4.2 Objectives

- To characterise the behaviour of cationic PDMAEMA brush grafted from flat surfaces and silica nanoparticles, in the presence of different solvent systems and their interaction with DNA.

- To determine the DNA/polymer complex's interaction with cells via cell cytotoxicity studies and ultimately their gene transfection efficiency using the novel cationic nanoparticle system.

- To tailor the chemistry of the system to improve the transfection efficiency.

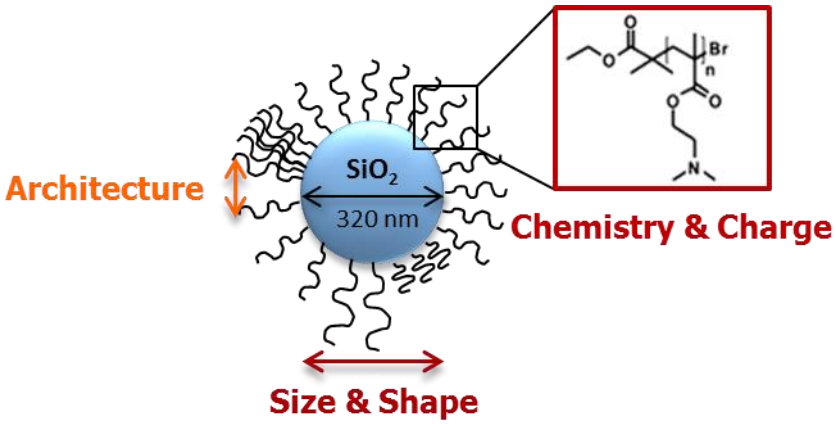

Figure 18: Nanoparticle coated with polymer brush exhibiting various physicochemical properties

Chapter 2 - Behaviour of PDMAEMA, copolymers and their interaction with DNA

2.1 Introduction

Controlling the way in which charged polymer brushes interact with DNA is important for a number of applications, especially in the development of an efficient gene delivery system. There are various ways in which the interaction can be tailored. The balance of charge density and hydrophobicity has been reported to control this interaction and consequently govern the compaction of DNA as well as the stability and dissociation behaviour of the polymer/DNA complex. These factors together with the proton sponge effect (as discussed in Chapter 1.1.3) of cationic polymers, which facilitate lysosomal escape, also impact the transfection efficiency against cytotoxicity.[198, 346-349] At high cationic charge density, although the polymeric vectors give tight DNA condensation resulting in small and positively charged complexes that generally exhibit high cellular uptake, the responsive polymers also become hydrophilic to hydrophobic as they are protonated in acidic environment, thus disrupting the cell membrane leading to high cytotoxicity. At moderate charge density and hydrophobicity, favourable levels of cytotoxicity and transfection can be achieved.

Introducing hydrophilic units such as PEG have been shown to give higher transfection efficiency as they reduce the interaction of the polymer/DNA complex with serum proteins and prevent colloidal aggregation.[145, 347, 350-352] The PEG chains are proposed to be able to resist protein adsorption via steric repulsion as a result of chain compression, and via a 'barrier' formed by the structured water associated with the PEG.[353] The critical water contact angle separating hydrophobic and hydrophilic surfaces is ≈65°; modification of smooth gold and rough gold nanoparticle layer with POEGMA, a PEG derivative, was shown to reduce the water contact angle from 66.6° and 115.5° to 31.5° and 54.7°, respectively, which conforms to the critical water contact angle.[323] Li *et al.* have also shown the water contact angle being reduced from 73° on the unmodified surface to 40° on the POEGMA-modified surface thus confirming the formation of the POEGMA layer.[354] Such reduction in non-specific interaction by POEGMA-like polymers is a desirable property for DNA delivery systems for *in vivo*

applications.[145, 346] Moreover, PEG-conjugated polymers exhibit low cytotoxicity to cells both *in vitro* and *in vivo,* increases water-solubility of the polymer/DNA complex and increases *in vivo* biodistribution of the complex. PEG can also be used as a spacer between a targeting ligand and a cationic polymer.[355] Hence PEG derivatives are useful for preparing non-fouling coatings by allowing control of charge density and providing some level of hydrophobicity.[356, 357]

This method of preventing non-specific binding of proteins also finds use in biosensing applications as membrane biofouling is a major problem affecting the detection of analytes.[358-360] POEGMA copolymerised with glycidyl methacrylate (GMA) brush has been used as a supporting matrix for SPR arrays to efficiently load probe proteins for high sensitivity whilst reducing non-specific adsorption for good selectivity.[361]

The present study focuses on varying the charge density of the PDMAEMA brush through copolymerisation with OEGMA to control the brush-DNA interactions and cell toxicity. These combination of monomers have been used previously.[357, 362-364] PDMAEMA homopolymer was shown to give larger polymer/DNA complexes and aggregate with plasma proteins whilst copolymerising with hydrophilic PEG derivatives that are generally inert, produced compact stable DNA complexes with minimised interaction ability with blood components thus prolonging blood-circulation time as mentioned earlier, and in turn allowing preferential accumulation of the complexes in the affected areas of the body.[365] Lutz and co-workers showed that PDMAEMA-*co*-POEGMA not only prevented gene vector aggregation but also kept cytotoxicity low even at high concentrations. Although gene vector binding with the cell surface was limited, the cellular internalisation of the bound complexes was not affected. In addition, a 7-fold greater gene expression was also achieved in the lungs compared with PEI, a highly efficient polymeric transfection agent. PEGylated cationic polymers are thus considered to be promising non-viral delivery agents to achieve systemic gene delivery.[363]

This chapter, therefore, focuses on studying the ability of cationic PDMAEMA polymer brushes to condense DNA efficiently in order to allow the transfection of plasmid DNA to cultured cells.

PDMAEMA has been extensively investigated for its potential as a drug/ gene delivery vector since its discovery as a suitable vector for transfection in 1996 by Hennink and co-workers.[181, 182, 190, 245, 247, 366-371] PDMAEMA can be synthesised simply by controlled radical polymerisation of its monomer to obtain regulated molecular weights, well-defined chain ends and different macromolecular architectures; block, star or graft. It contains only tertiary amine groups; around 50% of which is positively charged at physiological pH hence it has a lower charge

density than the well-established PEI thus making it less toxic and is adequately protonated for the formation of polyanion complexes. PDMAEMA has also been reported to have a higher proton buffering capacity than poly(ethylenimine-*ran*-2-ethyl-2-oxazoline) (9:1) in both water and 150 mM NaCl.[372]

The disadvantage of the polymer, however, is its toxicity and non-biodegradability, although it exhibits less cytotoxicity (half maximal inhibitory concentration (IC_{50}) ≈ 40 µg/mL) than other comparable polymers like PEI (25 kDa, IC_{50} ≈ 30 µg/mL).[373] As toxicity is influenced by charge density amongst other factors, polycations like PDMAEMA with broadly spread charge distribution along the polymer chain are useful in controlling toxicity. Various approaches have been taken to reduce the toxicity whilst maintaining high transfection efficiency, including copolymerisation.[188, 365, 374] Degradable PDMAEMA has also been investigated through the use of cleavable disulphide bonds in the repeating units or labile functionalities like ester linkages.[241, 375]

Transfection efficacy of PDMAEMA has been shown to be dependent on the polymer's molecular weight, the complex size, pH, ionic strength, polymer/plasmid DNA ratio, temperature and viscosity.[181, 366, 376] An appealing property of PDMAEMA is its pH responsiveness as it provides great scope in biomedical applications. The charge density of such weak polybases is dependent on the pH of the solution and can in turn influence the composition of the resultant polyanion complex and subsequent cellular uptake, endosomal escape and DNA release.[346] Tuning these parameters can lead to obtaining better transfection efficiency with reduced cytotoxicity.

2.1.1 PDMAEMA and responsive brushes

The responsiveness of a polymer brush is dependent on the chemical composition of the brush. The structure and conformation of polymer brushes can be altered through external stimuli such as changes in pH, counterions, solvent or temperature. PDMAEMA contains a basic 2-(dimethylamino) ethyl group with pK_a reported near 7.5 – 8 in aqueous solution.[183, 373, 377-379] At pH above this pK_a, PDMAEMA is neutral and hydrophobic, and becomes positively charged and hydrophilic at lower pH. Therefore, a hydrophobic-to-hydrophilic equilibrium exists and is controlled by the exposure of PDMAEMA to external properties of the aqueous environment such as pH and ionic strength. The ability to tune these external triggers are crucial for developing 'smart' surfaces.[379-381] For example, PDMAEMA was employed for its

temperature responsive behaviour in a smart hybrid system with gold and silica nanoparticles, for thermally adjustable catalysis such as in the reduction of 4-nitrophenol.[382]

2.1.1.1 *Effect of pH*

Weak polyelectrolyte brushes contain a number of charged groups. The solvation state of the groups can be influenced through changing the pH and ionic strength. Strong polyelectrolytes, however, are charged at all pH in aqueous solutions whilst its physico-chemical properties can be influenced by ionic strength. PDMAEMA falls in the category of weak polyelectrolytes and is inherently responsive to pH. As it is a polybase, the addition of acid results in protonation of the charged side groups (tertiary amine moieties). Swelling is therefore dependent on pH and is controlled by the osmotic effect of the counterions confined in the brush, which causes the polymer chains to stretch outward from the surface, thus resulting in high swelling and associated increase in the wet thickness of the brush (Figure 19a). Conversely, when the pH of the solution becomes increasingly basic, the brush becomes deprotonated and hydrophobic, and the wet thickness decreases (Figure 19b).[298, 380, 383, 384]

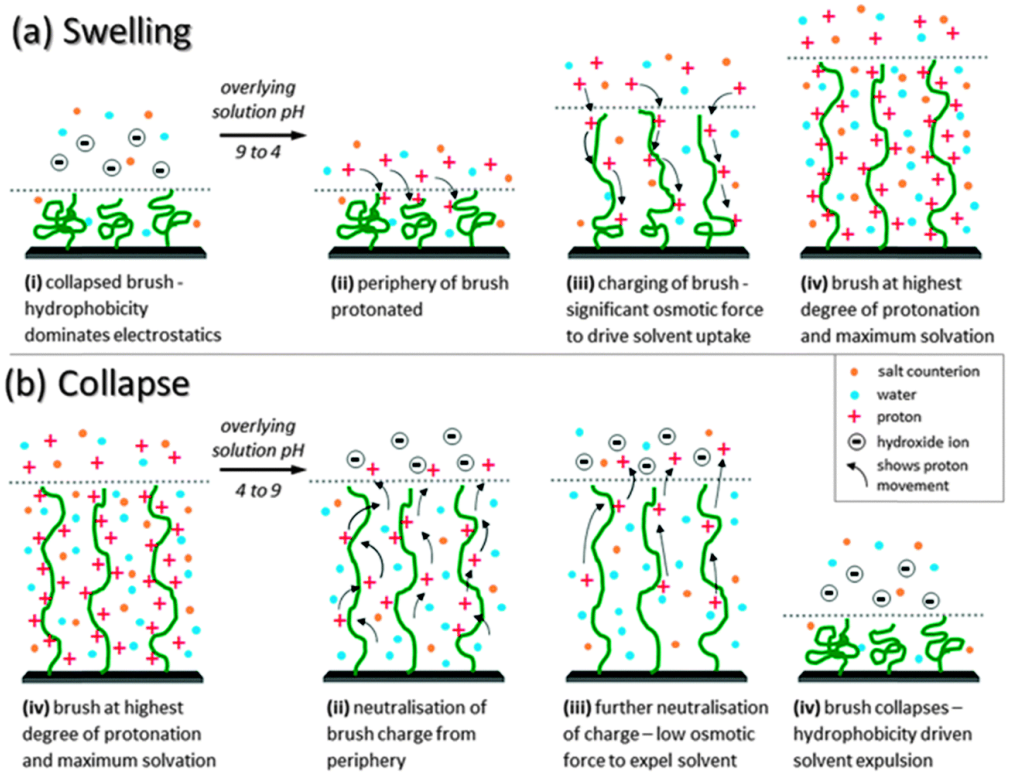

Figure 19: Schematic representation of the possible mechanisms that are accountable for a) the brush swelling and b) brush collapse transitions.[385]

The pH responsive behaviour can be suppressed with the quaternization of PDMAEMA which produces a strong polyelectrolyte brush; poly [2-(methacryloyloxy) ethyl] trimethylammonium iodide) (PMETAI) which has a permanent charge regardless of the pH.[386] Similar behaviours were reported with other tertiary amine moieties-containing polymer brushes such as PDEAEMA and poly[2-diisopropylamino)ethyl methacrylate] with pK_a values of pH 7.4 and pH 6.5, respectively.[299]

The pH-responsive behaviour of polyacid brushes such as PAA is opposite to that of PDMAEMA; their wet thickness increases with the addition of base as it deprotonates the pendant acidic groups along the polymer brush backbone, thus introducing charges within the layer. The resulting osmotic pressure and coulombic repulsions between the brush chains causes the brush to swell.[286, 296, 387]

This pH responsive nature of weak polyelectrolyte brushes have been used for various applications. PDMAEMA has been employed in nanosensor platforms in combination with gold nanoparticle composite films, by utilising the swelling-shrinking transition of the brush which enables the transduction of changes in the solution pH into an optical signal. Minko and co-workers reported that as the solution pH could be measured within pH 5 and pH 9, which is near physiological range, it creates more opportunities for the use of their pH-responsive polymer brush/gold nanoparticle composite film system such as for the development of sensors for biochemical/ biomedical analytes and plasmon coupling to enzymatic reactions which produce or use up protons.[388] PDMAEMA brushes tethered on silicon surfaces have been used as ‘smart’ interfaces to help diagnose breast cancer recurrence after surgery; genomic DNAs were captured and released from tethered PDMAEMA via tuning the pH, which allowed the detection of specific DNA molecules from one droplet of human blood. Such results pave way for the development of lab-on-a-chip cartridges for quick diagnosis.[389] Polyelectrolyte brushes such as poly (2-methacryloyloxyethyl phosphate) have also been utilised for their pH responsiveness as their swelling associated osmotic pressure is able to actuate the displacement of atomic force microscopy cantilevers.[390] Compressive stresses produced by the collapse of the brush below pH 2 and swelling at high pH result in the deflection of the cantilever.

2.1.1.2 *Effect of counterion*

Ionic strength, alongside pH, also contributes to the responsive behaviour of polymer brushes. However, this parameter affects equally strong and weak polyelectrolytes. The electrostatic interactions of polyelectrolyte brushes are screened upon addition of salt to the solution, alongside the reduction in osmotic pressure; at high salt concentrations, where the neutral/collapsed regime, also known as the salted out regime, occur, polyelectrolyte brushes almost reach a balance in the salt concentrations inside and outside the brush. Slightly decreasing the salt concentration creates an imbalance which leads to electrostatic interactions which cause swelling of the brush. However, in the osmotic regime, where the salt concentration is much lower, the electrostatic conditions become unfavourable such that a large difference in electric potential arises between the brush and the bulk solution – the salt concentration inside the brush is much greater. This results in the expulsion of the counterions and associated swelling of the brush. Plamper *et al.* demonstrated that strong polyelectrolyte brushes like the quaternized derivatives of star-shaped PDMAEMA, PMETAI, result in decreased hydrodynamic diameter with increasing ionic strength.[378] The drop is attributed to collapse of the polyelectrolyte arms as a result of the electrostatic screening, which reduces the high net osmotic pressure within the star polymer.[386]

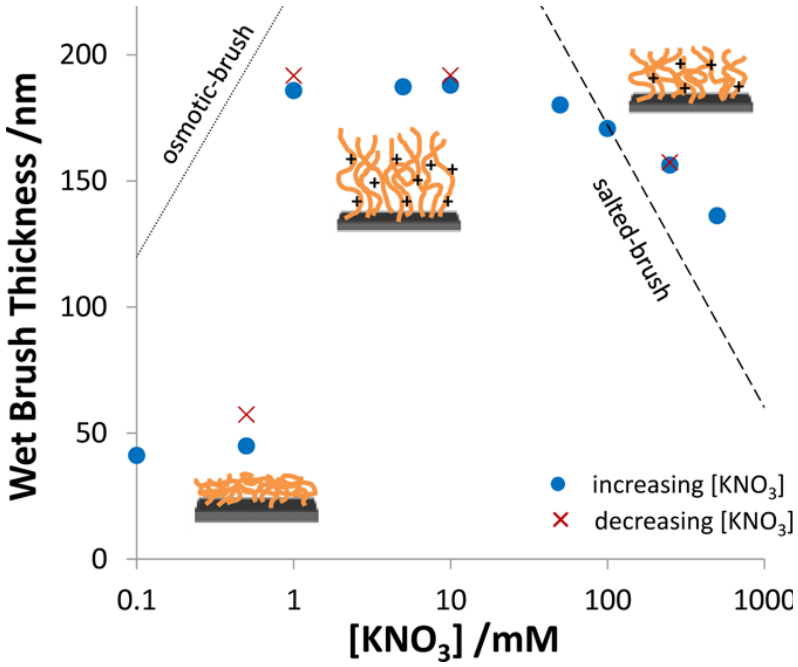

Figure 20: Equilibrium brush swelling ratio with increasing solution ionic strength, at pH 5.5. Dotted line and dashed line at the low and high ionic strengths, respectively, represent the predicted scaling behaviour.[300]

Measuring the solvated brush thickness of polybasic PDEAEMA brush over a range of KNO_3 concentrations, at a constant pH below the pK_a, exhibited typical swelling behaviour such that the swollen brush starts to collapse at higher ionic strength. It displayed a significant change in the brush conformation in the range of 0.5-1 mM electrolyte, where there was rapid swelling when ionic strength was increased from low to high, and a sharp decline in swelling ratio as ionic strength was decreased from high to low; the hydrophobicity of the brush is thought to be responsible (Figure 20). This low ionic strength range is reported to be much narrower than predicted by the theory of the osmotic brush regime.

The kinetics of the electrolyte-induced brush swelling and collapse transitions occur at the same rate. The same study also examined the swelling behaviour of PDEAEMA in response to changes in the solution pH. It was found that the salt-induced swelling was slower than pH-induced swelling thus suggesting a different mechanism for the two processes depending on the manner of the environmental trigger. For pH-induced swelling, the ions must both enter and leave in order to replace the hydroxide ions with nitrate ions but the salt-induced collapse was faster than pH-induced collapse which could be due to neutralisation of the brush without the initial formation of the hydrophobic periphery.[300]

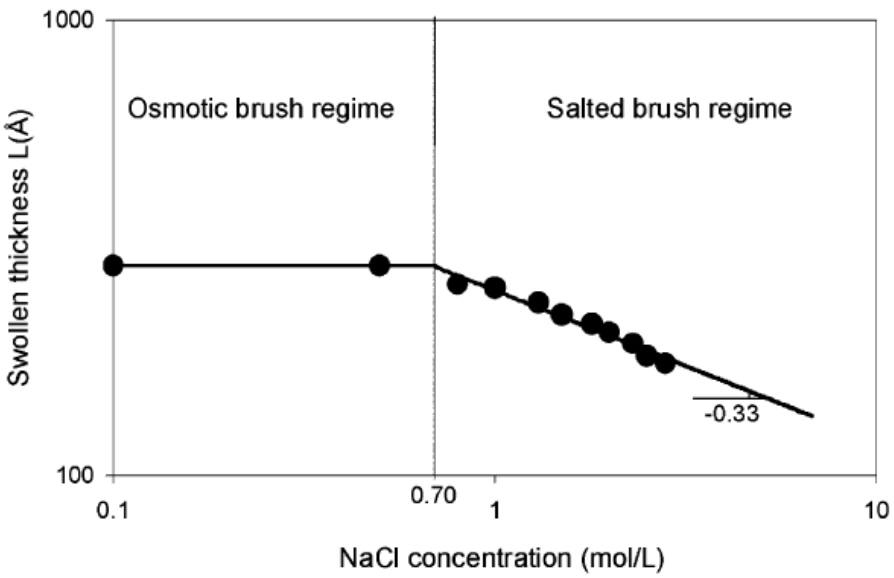

Figure 21: Swollen thickness of PTMAEMA brush with changing NaCl concentration.[298]

Sanjuan *et al.* also showed that subjecting poly (trimethylammonio ethyl methacrylate chloride) (PTMAEMA) brush to changes in NaCl concentration resulted in contraction of the

brush at higher NaCl concentrations.[298] The swelling thickness, measured via dynamic light scattering (DLS), was not influenced at lower concentrations. Two distinct regimes were observed as expected; the osmotic and salted regimes. In the former regime, the quenched PTMAEMA was not sensitive to the added electrolytes and the brush is seen to stretch solely due to the osmotic pressure of the counterions trapped inside the brush whilst in the latter regime, the brush thickness was seen to follow a power law dependence with salt concentration (Figure 21).

Tan *et al.* have similarly reported on the ion-specific collapse of poly([2-methacryloyloxy)ethyl]trimethyl ammonium chloride) (PMETAC) brush grafted from silica nanoparticles at higher concentrations of percholate ion (ClO_4^-) (≥ 5 Mm $NaClO_4$).[2] The hydrodynamic diameter of the particles remained constant at concentrations between 5-25 mM $NaClO_4$ which confirmed the colloidal stability of the particles. Beyond 25 mM $NaClO_4$, aggregation and sedimentation of the particles were observed. Furthermore, as per the Hofmeister series, the salting out of cationic brushes is dependent on the type of counterion. This study showed that increasing the concentration of percholate ions (an earlier member of the series) gave rise to rapid collapse of PMETAC brush, even at relatively low concentrations, whilst increasing the concentration of chloride ions (a later member of the series) resulted in gradual decrease in the hydrodynamic diameter of the PMETAC-coated silica nanoparticles. The surface wettability was affected in such a way that the water contact angle of PMETAC-coated silicon wafers in $NaClO_4$ increased to 59° whilst it was reported to be 19° when in NaCl, which is consistent with the series. As the Hofmeister series indicates the ability of the counterions to salt in or salt out proteins, charged brushes respond differently to the presence of various types of ion, their concentration and their subsequent effect on protein or biomolecule adsorption via changes in the charge distribution, pK_a, hydration and ion adsorption.[391]

Cationic brushes such as PDMAEMA, have high adsorption capacity for negatively charged BSA. The adsorption and desorption of the proteins could be tailored by varying the ionic strength and pH as the electrostatic interactions between the proteins and the brush can be screened; decreasing the degree of ionisation of the PDMAEMA chains and screening the electrostatic attraction allowed BSA desorption. This is because the interaction of the ion pairs between acidic amino acid residues and the amine groups of PDMAEMA were disrupted by competitive binding by Na^+ and Cl^-.[238] This is useful in the application of such materials in ion exchange chromatography.

2.1.1.3 *Effect of solvent*

Solvent quality is another important aspect governing the conformation of polymer brushes. Polymer chains stretch in a good solvent as a result of the favourable interaction between the solvent molecules and the polymer segment. Equally, in a poor solvent, the polymer chains collapse due to the stronger interactions between the chains themselves. The surface wettability is directly correlated to the quality of the solvent to which the brush is being exposed.

The solvent response of polymer brushes can also be affected by the density of the brush. In a good solvent, a low density PMMA brush swells fast whilst there is not marked swelling in higher density brushes, even in good solvents, as the polymer chains are already stretched due to the dense packing.[392]

Diblock polymers such as PDMAEMA-*b*-MMA decorating the surface of a particle, when exposed to various alcohols such as 1-butanol caused the overall particle diameter to increase by 1.42 µm from its size in methanol whilst 1-octanol caused a decrease by 2.1 µm.[393] The effect of relative block length on solvent response was investigated via water contact angle by Xu *et al.* using PDMAEMA as top block and poly(*n*-butyl methacrylate) (PBMA) brush as the bottom block.[394] On separate exposure to hexane and water, where the former is a good solvent for PBMA and latter a good solvent for PDMAEMA, the longer PDMAEMA block resulted in the reduction of the water contact angle of the block copolymer to that of a PDMAEMA homopolymer.

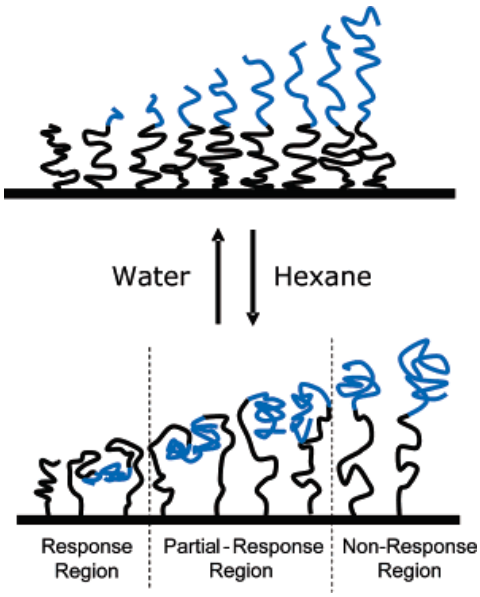

Figure 22: Schematic illustration of three regions of the block copolymer brushes after hexane treatment. Black segments represent PBMA Blue segments represent PDMAEMA.[394]

As illustrated in Figure 22, in the presence of hexane, PBMA governed the surface of the response region when PDMAEMA block length was short. Thick PDMAEMA block suppressed the surface responsive properties of PBMA in the non-responsive region, whilst PDMAEMA and PBMA coexisted in the partial response region, at the air interface. Overall, PBMA was shown to have a better ability to swell from the surface to occupy the air interface whilst covering the collapsed chains of PDMAEMA when the bottom block length is longer thus enhancing the surface properties which is otherwise suppressed by a long top block.

2.1.1.4 Effect of temperature

Temperature is another external trigger which effects polymer brush responsiveness. It does not affect the physicochemical properties of PDMAEMA brushes significantly within a reasonable range, but becomes an important parameter when DMAEMA is copolymerised with temperature responsive monomers such as NIPAM. Typically, polymers displaying a LCST or an UCST exhibit a thermoresponsive behaviour and polymer brushes constituted from the same monomers display temperature-modulated swelling.

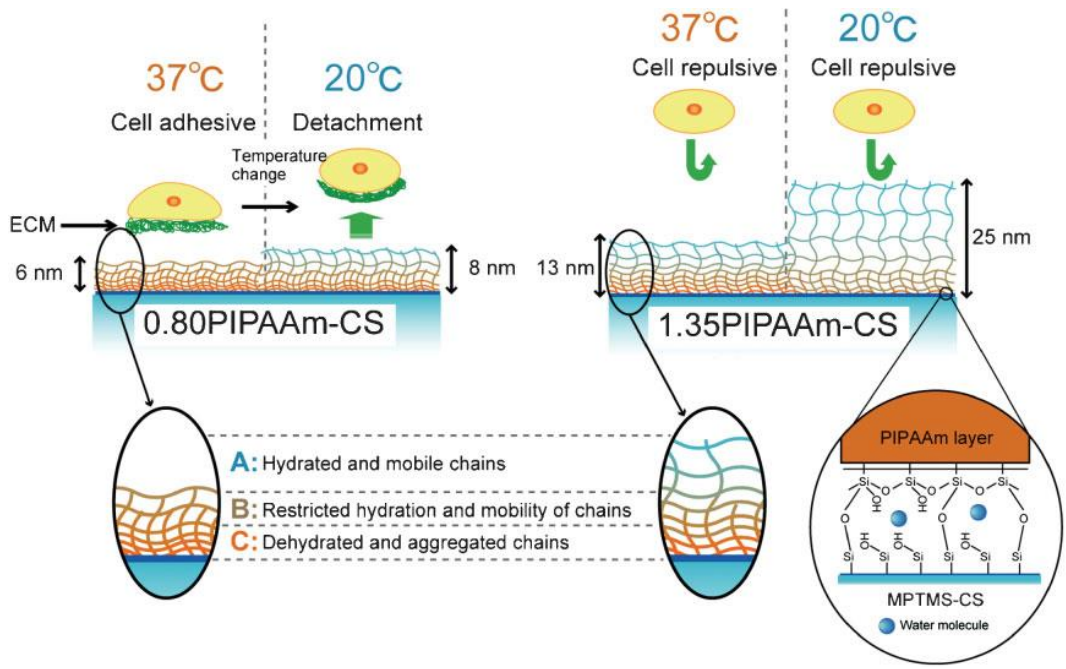

Figure 23: Schematic representation of the effect of temperature and thickness of PNIPAM (PIPAAm), on cell attachment/detachment.[395]

PNIPAM is a typical thermoresponsive brush which displays an LCST behaviour. Below its LCST of 37°C, the hydrogen bonding between the polymer units and the surrounding water molecules causes the polymer chains to extend thus reaching a hydrophilic state. Above the LCST, the polymer brush collapses due to the disruption of these interactions hence giving rise to the hydrophobic state (Figure 23); this behaviour is widely used for cell sheet engineering[395, 396] and chromatography. Various other factors such as the molecular weight of the polymer[397] and grafting density[398, 399] also impact the conformation of the brushes and the position of the LCST.[400]

PDMAEMA brushes are also inherently thermoresponsive with an LCST of around 46°C in pure water at pH 7.[401, 402] Their temperature-responsive behaviour is dependent on the pH of the buffer solution; when both, the temperature and the pH, are low, hydrogen-bonding interactions and electrostatic repulsive forces dominate, whilst when they are both high, intra- and interchain hydrophobic interactions control the brush swelling behaviour.

PDMAEMA has been reported to have an LCST of 31°C under pH 10 and 33°C under pH 8 – the shift in the LCST to a higher value is due to the fact that PDMAEMEA is more hydrophilic at pH 8.[380] In addition, the hydrodynamic diameter increases with decreasing pH as PDMAEMA becomes more charged with strong electrostatic repulsive and hydrogen bonding interactions (Figure 24b). Consequently, LCST shifts to a higher temperature (Figure 24c). However, with increasing pH, these very interactions become weakened whilst powerful hydrophobic interactions govern the brush causing it to collapse and leading to flocculation of nanoparticles. As a result, the LCST shifts to a lower temperature as less thermal energy is required for the phase transitions (Figure 24a).[383] Generally, as the temperature increases, the hydrogen bonds between hydrophilic groups and water become destroyed, and hydration of the grafted polymer are weakened, resulting in collapse of the brush.[403]

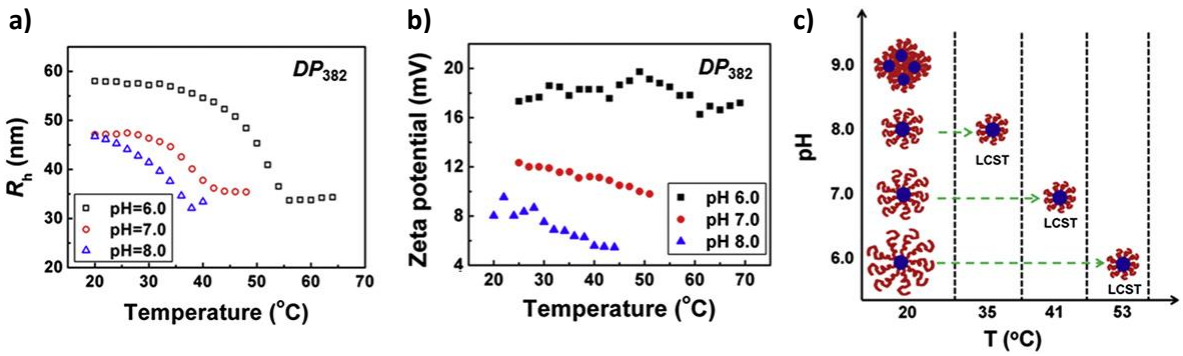

Figure 24: Temperature and pH responsive behaviour of SiO_2-g-PDMAEMA, a) change in the hydrodynamic diameter as a function of temperature at pH 6.0, 7.0 and 8.0, b) changes in the surface charge as a function of temperature for pH 6.0, 7.0 and 8.0, and c) the effect of pH on LCST of the cationic polymer brush.[383]

Han *et al.* have also studied the effect of pH and temperature, on PDMAEMA-*b*-PAA diblock copolymers of different compositions and observed a significant difference in the stimuli responsive behaviour of the two polymers.[404] The PDMAEMA-rich compositions exhibited dominant pH-responsive behaviour and thermoresponsive behaviour over a broad range of temperature (40-60°C) whilst the PAA-rich copolymers only displayed a weak thermoresponsive behaviour around the specific isoelectric point.

Such thermoresponsive cationic polymer brushes have been used in separation of biomolecules. Nagase and co-workers copolymerised NIPAM with DMAEMA on silica bead surfaces using ATRP and characterised them via chromatographic analysis to find that the chromatographic retention times for adenosine nucleotides decreased with increasing column temperature as a result of the rapid changes in the copolymer brush's electrostatic properties and the decrease in the basicity of the copolymer brush at neutral pH.[405]

PDMAEMA can therefore be tailored for use in many applications hence this project focuses on its potential as a non-viral gene delivery vector and how modifying the surface of silica nanoparticles with the cationic brush could allow optimisation of the gene delivery efficiency. Surface functionalisation of nanoparticles using polymer brushes is a useful way to produce an effective system where the physicochemical properties such as the chemistry, charge, architecture, size and shape could be tuned easily and independently of each other, thus providing a greater degree of control for studying particle-cell interactions. Spherical silica nanoparticles were chosen for the gene delivery system as they are biologically inert, can be tailored with a variety of surface modifiers which allow the adjustments of properties like zeta potential and surface reactivity, and has the capability to be internalised by cells irrespective of their surface charge.[406] The large surface area, improved binding kinetics over flat surfaces, low non-specific binding of a variety of biomolecules, hydrophilicity, unique refractive index (RI) and density all make silica nanoparticles a valuable nanomaterial. Thus a responsive colloidal system can be created by functionalising the surface with polymer brushes.[92] [2]

2.2 Experimental methods

It is important to be able to synthesise and characterise the standard free polymer and polymer brush of interest in a controlled manner before utilising it in any new system. In this regard, a series of experiments were carried out to determine brush thickness of PDMAEMA on flat substrates and spherical silica nanoparticles, charge density variation through copolymerisation with POEGMA, the brush's behaviour in different solvents and finally its ability to interact with DNA when grafted from nanoparticles.

2.2.1 Materials

2-(Dimethylamino)ethyl methacrylate (DMAEMA, M_n = 157.21), Oligo(ethylene glycol methyl ether methacrylate) (OEGMA, M_n = 300), copper chloride (Cu(I)Cl), copper bromide (Cu(II)Br_2), 2, 2'-bipyridyl (bpy), anhydrous toluene and triethylamine (Et_3N) were purchased from Sigma-Aldrich and used as received. All chemicals and solvents were analytical grades unless otherwise stated. Cu(I)Cl was kept under vacuum until used. Deionised water, with resistivity of 18.2 MΩ·cm was obtained using Milli-Q Integral 3 System from Millipore. Silicon wafers (100 mm diameter, ⟨100⟩ orientation, polished on one side/reverse etched) were purchased from Compart Technology Ltd and cleaned in Plasma System Zepto from Diener Electronic, for 10 min in air plasma. Gold-coated silicon wafers were obtained through the evaporation of a chromium layer (20 nm followed by the evaporation of a gold layer (200 nm) using an Edwards Auto 500 evaporator. Silica particles (unfunctionalised) were purchased from Bangs Laboratories (supplied as powder, mean diameters of 310 nm). The thiol ester initiator, ω-Mercaptoundecylbromoisobutyrate (**1**) was synthesised from mono-methoxy capped PEG[407] of 550 g/mol from Sigma, and the ester silane initiator, 2-bromo-2-methyl propionic acid 3-trichlorosilanyl-propyl ester (**2**) was synthesised according to Jonas *et al.*[304] and Husseman *et al.*[263], by Dr Julien Gautrot (Figure 25).

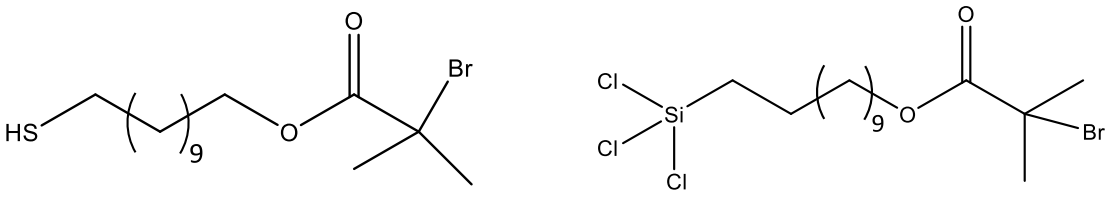

1 **2**

Figure 25: Chemical structure of initiator 1, ω-Mercaptoundecylbromoisobutyrate, and initiator 2, 2-bromo-2-methyl propionic acid 3-trichlorosilanyl-propyl ester.

2.2.2 Growth of PDMAEMA/POEGMA on flat surfaces

The weak polyelectrolyte of interest; PDMAEMA homopolymer, the complementary POEGMA homopolymer, and amphiphilic PDMAEMA-co-POEGMA brushes as utilised by Lutz and co-workers,[363] were grown on initiator-coated gold wafers via surface-initiated ATRP as shown in (Figure 26).

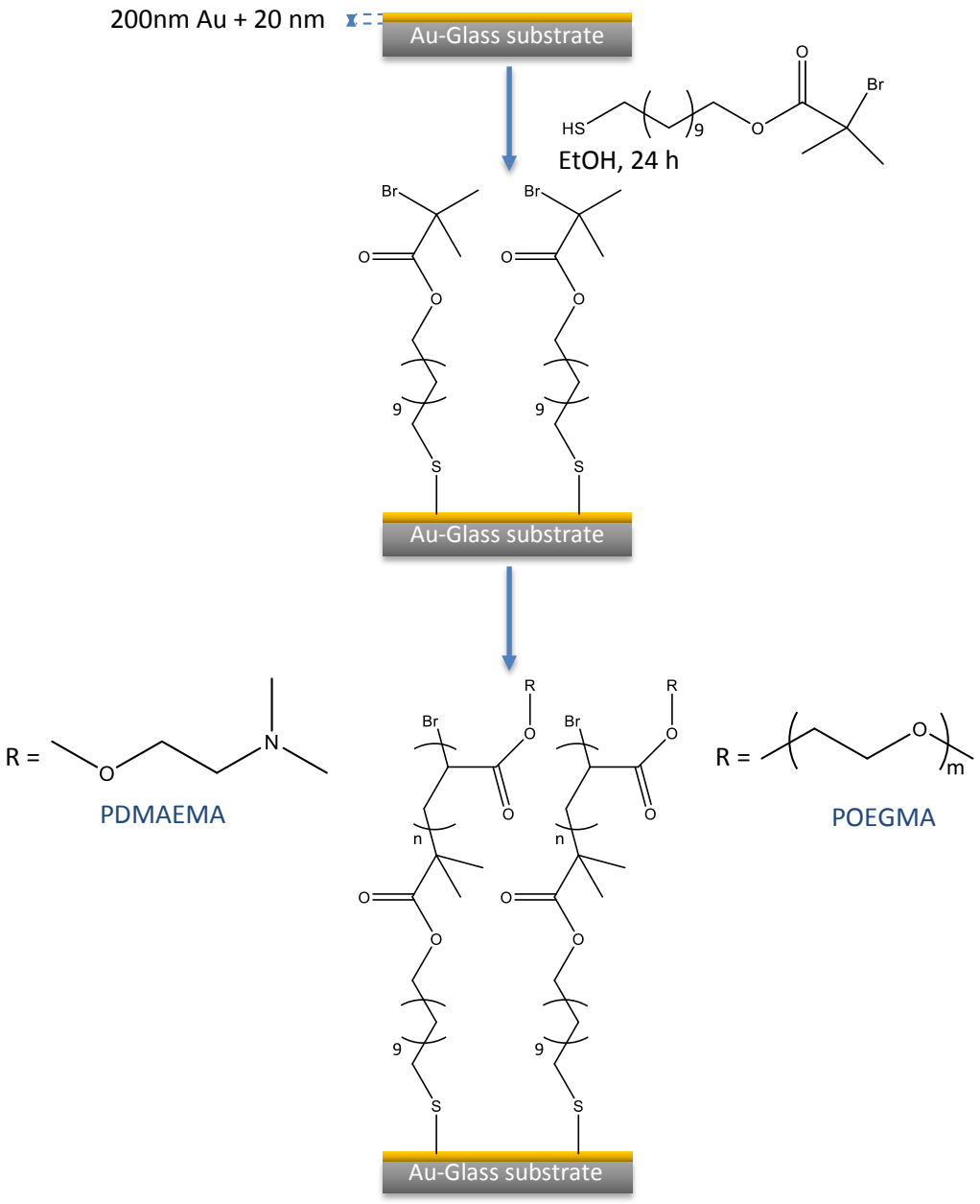

Figure 26: Schematic representation of the immobilisation of thiol ester initiator onto the gold-coated glass substrate and of the surface-initiated ATRP of DMAEMA/OEGMA monomers.

2.2.2.1 Deposition of thiol initiator on gold-coated silicon wafers

The gold-coated silicon substrates were immersed in 5 mM ethanolic solution of the thiol initiator, and left at room temperature overnight. The substrates were then washed in copious amounts of ethanol and dried under stream of nitrogen.

2.2.2.2 Deposition of ester silane initiator on silicon wafers

The plasma-oxidised silicon wafer was immersed in a recrystallisation dish containing dry toluene (30 mL), Et_3N (50 µL) and silane initiator (10 µL), and covered with aluminium foil and left at room temperature overnight. The wafer was washed with ethanol and dried under a stream of nitrogen. The initiator functionalised wafer was kept under nitrogen until use.

2.2.2.3 Polymer brush growth on silicon/gold-coated silicon wafers

Kinetics study

To study the PDMAEMA brush growth and the evolution of its thickness as a function of time, a solution of $CuBr_2$ (18 mg, 80 µmol), bpy (320 mg, 2.05 mmol), and DMAEMA (6.6 g, 42 mmol) in water/ethanol (4/1 v/v, 30 mL) was degassed using nitrogen bubbling for 20 min. CuCl (82 mg, 828 µmol) was added to this solution and the resulting mixture was further degassed for 20 min before transferring to tubes containing the initiator-coated surfaces under inert atmosphere. The polymerisation was stopped at different polymerisation times by immersing the coated substrates in deionised water, followed by washing with copious amounts of ethanol and drying in a nitrogen stream.

Copolymer brush synthesis

To prepare the POEGMA polymerisation mixture, a solution of $CuBr_2$ (18 mg, 80 µmol), bpy (320 mg, 2.05 mmol), and OEGMA (12.6 g, 42 mmol) in water/ethanol (4/1 v/v, 30 mL) was degassed using nitrogen bubbling for 30 min. CuCl (82 mg, 828 µmol) were added to this solution and the resulting mixture was further degassed for 20 min.

0 mL (0%) 0.04 mL (2%), 0.1 mL (5%), 0.2 mL (10%), 0.5 mL (25%), 1 mL (50%), 1.5 mL (75%) and 2 mL (100%) of the PDMAEMA polymerisation solution and 2 mL, 1.96 mL, 1.9 mL, 1.8 mL, 1.5 mL, 1 mL, and 0.5 mL of the POEGMA polymerisation solution, respectively, were taken in a syringe and mixed before transferring to tubes containing the initiator-coated substrates under inert atmosphere. The polymerisation was stopped after 20 min by immersing the coated substrates in deionised water, followed by washing with copious amounts of ethanol and drying in a nitrogen stream.

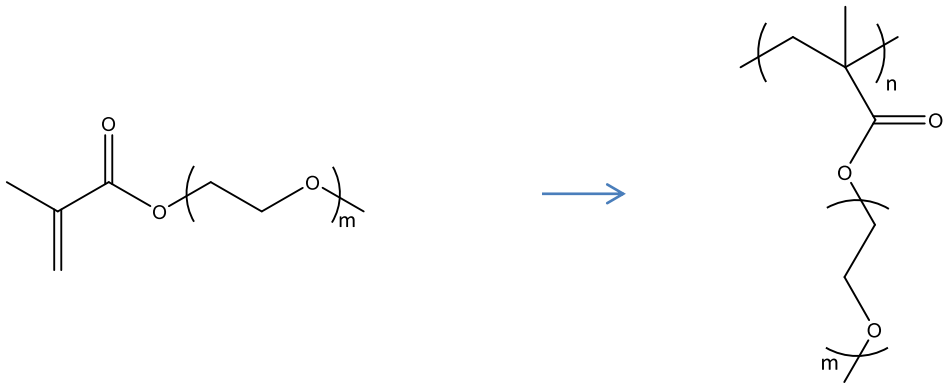

Scheme 27: Chemical structure of OEGMA and POEGMA

The PDMAEMA polymerisation mixture was prepared as described in the kinetics study.

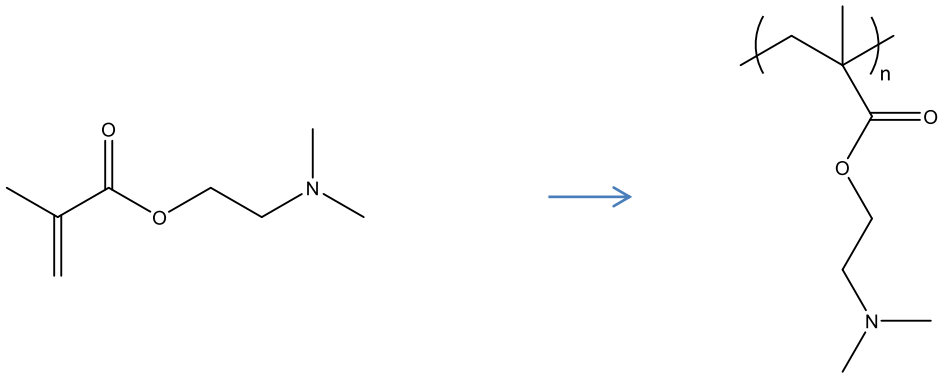

Scheme 28: Chemical structure of DMAEMA and PDMAEMA

Pure PDMAEMA synthesis

To grow 30 nm-thick PDMAEMA brushes, the polymerisation solution was prepared as detailed previously and 2 mL of the polymerisation mixture was transferred to tubes containing the initiator-coated surfaces under inert atmosphere. The polymerisation was stopped after 20 min using the method described previously.

2.2.3 Free PDMAEMA/POEGMA synthesis

For the synthesis of free polymers, separate solutions (water/ethanol, 4/1 v/v, 30 mL) of DMAEMA (6.6 g, 42 mmol) and OEGMA (12.6 g, 42 mmol) each also containing $CuBr_2$ (0.018 g, 81 µmol) and bpy (320mg, 2.05 mmol) were degassed via bubbling of nitrogen gas. CuCl (0.082 g, 828 µmol) was added after 20 min to both solutions. 12 mL of monomer solutions were transferred to polymerisation tubes under nitrogen in 0%, 25%, 50%, 75% and 100% ratios of PDMAEMA: POEGMA. An initiator solution containing 2.5 mL water and 84 mg of oligo ethylene glycol ATRP initiator was also degassed in a vial for 20 min. 500 µL of the solution were added to each polymerisation tube and left to polymerise for 4 h. The polymer solution was then transferred to dialysis bags (Spectra/Por® Biotech Cellulose Ester (CE) Dialysis Membranes, MWCO: 3000-5000 D, Spectrum Laboratories) and purified through extensive dialysis against deionised water over 3 days, replacing with deionised water twice per day. 100% f-PDMAEMA with relatively low molecular weights were prepared by Dr Julien Gautrot.

2.2.4 Growth of PDMAEMA/POEGMA on silica particles

Silica nanoparticles were coated with PDMAEMA/ POEGMA brushes or a copolymer of these generated through surface-initiated ATRP (Figure 29).

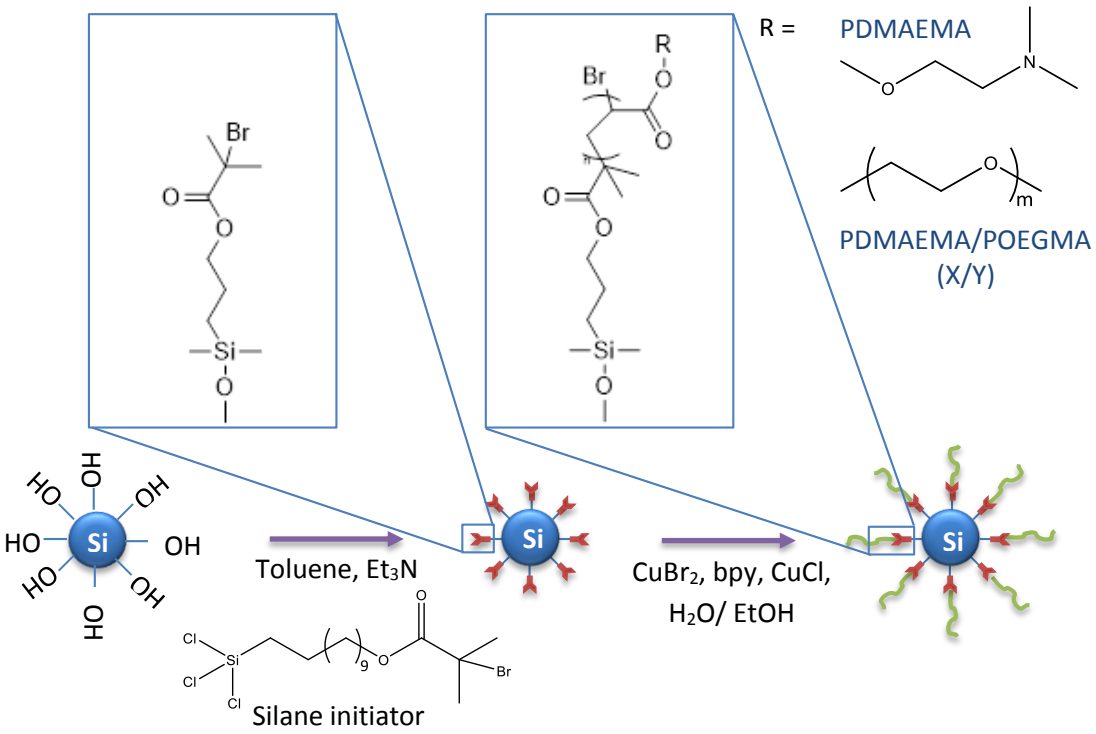

Figure 29: Schematic representation of the surface functionalisation of silica nanoparticle with silane initiator, and subsequent synthesis of SiO_2-g-polymer brush via SI-ATRP.

2.2.4.1 Deposition of ester silane initiator on silica nanoparticles

Silica nanoparticles (Ø ≈ 310 nm, 200 mg) were dispersed in dry toluene by sonication (Ultrawave IND7800D Ultrasonic Cleaning Tank), washed in dry toluene via three centrifugation (4000 rpm for 1 minute)/ redispersion cycles, and finally dispersed in dry toluene (4 mL). Triethylamine (200 µL) and silane initiator **2** (40 µL) were added to this dispersion and the suspension was left on a 3D lab application shaker (Gyro Twister GX-1000 3-D Shaker from Labnet) overnight for thorough mixing. The resulting particles were collected by centrifugation, washed three times with dry toluene, and finally redispersed in 4 mL ethanol as stock solution for storage (50 mg/mL).

2.2.4.2 Polymer brush synthesis on silica nanoparticles

Polymerisation solutions were prepared as described previously by dissolving DMAEMA (6.6g, 42 mmol) and/or OEGMA (12.6 g, 42 mmol), bpy (320 mg, 2.05mmol), $CuBr_2$ (80 mmol) and CuCl (0.082 g, 828 µmol) in half of the total polymerisation solvent (water/ethanol 4/1 v/v, 15 mL). Initiator-coated silica nanoparticles (1/10 v/v, 100 µL, 5 mg/mL stock solution) were dispersed in ethanol (1/10 v/v, 100 µL) and water (8/10 v/v, 800 µL) in a tube and degassed in nitrogen/argon for 15 min. The polymerisation solution was then injected into the initiator-coated silica nanoparticles and left at room temperature whilst under inert gas, for 20 min. To terminate the polymerisation, the dispersion was diluted with water, and compressed air was bubbled through the mixture until a colour change of dark brown to blue-green was observed. The nanoparticles were recovered by centrifugation, washed three times with water and finally dispersed in water.

2.2.5 Characterisation

2.2.5.1 Ellipsometry

Ellipsometry was chosen to determine the polymer film thicknesses on silicon and gold-coated silicon substrates as the sensitivity of the technique allows measurements of nanometer-scale layers in a precise and accurate manner. This optical measurement technique is both non-invasive and non-destructive, and only requires a low-power light source. [408] The thickness measurements were obtained via an α-SE spectroscopic ellipsometer (J. A. Woollam) at an

incident angle of 70°. Bare substrates of silicon or gold were used to build the model using a cauchy layer to measure the brush thickness. Measurements were taken at least three different points per sample and average values are reported ± standard deviations.

The method measures the change in polarisation caused by the presence of the material which reflects or transmits the light as per the material structure. The material thickness as well as optical constants of the material determine the measured response. The change in the polarisation is represented as an amplitude ratio (Ψ) and phase difference (Δ) between p- and s-polarised light waves. The changes measured are then compared to mathematical models (using the software from J. A. Woollam) to extract the coating's thickness and optical constants.

2.2.5.2 Fourier transform infrared: Attenuated total reflectance (FTIR-ATR)

FTIR was used to characterise the free polymer/polymer brushes to confirm the distribution and concentration of the different chemical species expected within the respective polymers through obtaining an infrared spectrum (a plot of measured infrared light intensity versus a property of light) of absorption of the samples. The method is efficient as it allows the collection of high spectral resolution data over a wide spectral range. This technique uses interferometry to give details of a material placed in the IR beam. Attenuated total reflectance, in particular, is a simple sampling technique in FTIR which allows the measurement of solid or liquid samples directly without requiring further sample preparation.

The method utilises total internal reflection to produce an evanescent wave. When a beam of infrared light passes through the ATR crystal, it reflects at least once via the internal surface in contact with the sample thus forming the evanescent wave which penetrates the sample. A detector collects this beam as it exits the crystal. The fourier transform converts the output from the detector to a spectrum that can be interpreted where a molecular 'fingerprint' of the sample is produced. Thus a specific chemical functional group in the molecule is presented by spectral features in a certain region of the spectrum.[409]

ATR-FTIR spectroscopy in this study was carried out using Bruker Tensor 27 with an MCT detector (liquid N_2 cooled). Spectra were taken at a resolution of 4 cm^{-1} with a total of 16 scans per run.

Free polymers were measured by dissolving the sample in methanol, placing a drop on the ATR crystal and allowing it to dry.

ATR-FTIR spectroscopy was also carried out on PDMAEMA-g-SiO_2 nanoparticles and copolymer-grafted nanoparticles. Background subtraction was automatically achieved by taking background scan with the bare silica particles prior to performing measurements with the sample.

2.2.5.3 Proton nuclear magnetic resonance (^{1}H NMR)

NMR is an essential analytical chemistry technique which determines the content and purity of a sample alongside its molecular structure. Majority of the nuclei of atoms have spin and all nuclei are electrically charged. When an external magnetic field is applied, a magnetic moment, arising from nuclei having an odd number of protons/neutrons, experiences an interaction that results in a parallel or opposite alignment to the direction of the applied field. An energy transfer, which happens at wavelengths matching radio frequencies, occurs between the base energy to a higher energy level, usually referred to as the energy gap. As the spin returns to the base, an energy from the same radio frequency is emitted. The signal matching such transfer is measured and processed to give a NMR spectrum for the relevant nucleus. The environment of different protons will shift their signals. The intensity of the peaks observed in NMR correlate with the abundance of the corresponding protons and this can be used to characterise the relative ratio of these protons.[410]

The conversions of the free polymers in the current study were analysed through ^{1}H NMR. The data was acquired using Bruker AV 400 and AVIII 400, for the f-PDMAEMA and PDMAEMA: POEGMA copolymers, dissolved in deuterium oxide (D_2O, 99.0 % atomD).

The copolymer composition was determined by calculating the ratio of the two peaks at 3.35 ppm and 2.70 ppm which represent the methoxy peak in POEGMA and methylene peak in PDMAEMA, respectively. The integration area values obtained from Mnova software were corrected for the number of protons involved in the signal (3 for methoxy and 2 for methylene). This allowed the determination of the ratio of the monomers and hence actual percentage of the monomer in the copolymer (See Appendix 1 for sample calculation).

2.2.5.4 Gel permeation chromatography (GPC)

GPC is a type of size exclusion, elution chromatography in which the separation occurs in accordance with the size of the solute molecules. The technique allows the acquiring of molecular-weight distributions of polymers.[411] Liquid chromatography uses columns which are packed with porous particles within which the solvent of interest is flown. Molecules dissolved within the solvent are separated based on their size.

Molecular weight distribution of the f-PDMAEMA and copolymers was obtained via GPC, using Agilent 1260 Infinity System operating in THF with 5mM NH_4BF_4 and equipped with RI detector and variable wavelength detector, 2 PLgel 5 µm mixed-C columns (300×7.5 mm), a PLgel 5 mm guard column (50x7.5mm) and an autosampler. The instrument was calibrated with linear narrow poly(methyl methacrylate) standards in range of 550 to 46890 g/mol (Agilent Technologies UK). All samples were passed through neutral aluminium oxide and 0.2 µm PTFE filter before analysis. The division of weight-average molecular weight (M_w) by number-average molecular weight (M_n) provided the polydispersity of the molecular weights.

2.2.5.5 Scanning Electron Microscope (SEM)

SEM is a useful, high-resolution imaging technique that can be used to qualitatively assess the surface morphology of any sample. The method involves the scanning of the surface of the sample using a beam of electrons which are then reflected to form an image. The beam of electrons interact with the sample to produce various signals which offer details of the surface topography and composition of the sample.[412]

SEM images for this study were acquired on Inspect F (FEI Company) to visualise silica nanoparticles. The samples were prepared by adding a few drops of dilute particle suspension onto a clean silicon wafer and allowing the solvent to evaporate in air. The samples were then mounted on an aluminium stub using double-sided tape before coating with a 10 nm thick palladium/gold (60:40) film (Desk II, Denton Vacuum Sputter Coater). The coated samples were then analysed using an electron acceleration voltage of 5-10keV.

2.2.5.6 Thermogravimetric analysis (TGA)

TGA is another essential analytical technique which can show the change in mass of a substance loaded on a pan via a microgram balance, as a function of temperature where a constant heating rate is used through a programmable furnace. The basic principle is that there is a mass change upon heating the sample, as a result of the decomposition, reduction or evaporation, in the case of mass loss, and oxidation or absorption, in mass gain. This change can give an indication of the thermal stability or the composition of the sample, up to 1000 °C.[413] Thus it is very useful for the determination of the organic content in a sample via the weight percentage change reading obtained from the resulting mass change.

The analysis for this study was performed in nitrogen[383, 414] using TA Instruments Q500 Analyser. Samples were heated from room temperature to up to 1000 °C at a heating rate of 10 °C/min. TGA was used to determine the decomposition temperature (at the onset of weight loss) and the percentage of polymer brush grafted on the silica nanoparticle (taken from 150 °C until full degradation). It was assumed that the weight change was due to the burning of the organic coatings and the remainder was non-combustible silica particles. All samples were dried under vacuum at room temperature prior to TGA runs.

2.2.5.7 Zetasizer Nano ZS

In order to gain a better understanding of the changes in surface charges of the nanoparticle in different conditions and coatings, the nanoparticle system was characterised by Zetasizer. The brush thickness via the hydrodynamic diameter and the surface charge of the nanoparticles via the zeta potential were determined by DLS and ELS by using the Malvern Zetasizer Nano ZS fitted with a 633 nm red laser. For DLS, a scattering angle of 173° was used to measure the scattered light intensity. The hydrodynamic particle was determined according to the Stokes-Einstein equation[415]:

$$D_H = \frac{kT}{f} = \frac{kT}{3\pi\eta D}$$

Where k is the Boltzmann constant, f is the particle frictional coefficient, η is the solvent viscosity, T is the absolute temperature, and D is the translational diffusion coefficient. The nanoparticles were assumed to be spherical, monodisperse, non-interacting.

The zeta potential (ξ) of the particles were estimated from the electrophoretic mobility (u) as according to the Helmholtz-Smoluchowski equation:

$$u = \epsilon \frac{\xi}{\eta}$$

Where η is the viscosity, and ϵ is the dielectric constant.

For DLS measurement, samples were passed through 0.45 µm syringe filters to remove any large contaminant particles prior to analysis. Samples were prepared by dispersing particles in deionised water/ 150mM NaCl/ PBS, to obtain a slightly cloudy solution, which was then sonicated for 5 min. Each measurement was repeated at least three times at 25°C, over 5 – 15 min, and the average result was taken as the final hydrodynamic diameter. The PDI index of the readings were below 0.5 suggesting a homogenous size distribution.

2.2.5.8 Charge titration and swelling behaviour (Ellipsometry/Zetasizer)

The PDMAEMA-grafted silica particles were dispersed in 6mL of 150 mM NaCl solution and the pH was varied with the addition of HCL/NaOH. The zeta potential and the hydrodynamic diameter of the particles were recorded at the respective pH values, measured using a SevenGo Duo™ pH meter (Mettler Toledo).

To measure the thickness of polymer brushes grown from flat silicon substrates and their swelling in liquids, samples were placed in a liquid cell (500 µL LiquidCell™) fitted with quartz windows normal to the laser beam path of the ellipsometer, and deionised water or salt solutions (150 mM NaCl at different pH between 4 and 12) were injected using a syringe. The data was fitted by using a Cauchy model, with a medium that had a RI > 1 (determined by fitting the optical constants of the medium for a standard silicon substrate with a known layer of silicon oxide of 25 nm).

The pH was adjusted by using small volumes (10 µL) of concentrated 0.01-0.5 M HCl or 0.01-0.1 M NaOH, as required. The wet ellipsometric thickness/swelling was measured at each pH. A reverse titration was also performed by changing pH from 12 to 4.

2.2.6 Interaction with DNA

2.2.6.1 Materials

NaCl (150 mM, PolyPlus), PBS (tablets, Sigma-Aldrich), keratinocyte serum-free medium (KSFM, Gibco), HBS (1 M, Gibco), 10 x 12 mm SPR-Au chips purchased from Senss bv, and stored under nitrogen, at room temperature). 10 mM HBS contained 1mL of 1 M HEPES and 100 mL of 150 mM NaCl. EGFP was prepared by Dr Julien Gautrot and Dr Amir Sharili.

2.2.6.2 Methods

SPR measurements were performed with Biacore X. The 15 nm-thick PDMAEMA was grown on the SPR chips (functionalised with the thiol initiator **1**) using the method described in section 2.2 but with the polymerisation terminated at 5 min. 30 nm-thick PDMAEMA was also used for comparison and study of the effect of brush thickness on DNA binding. The resulting brush-coated SPR chips were mounted upon the lens. Plasmid DNA (EGFP) dissolved in the concentration of 1 µg/mL in 150 mM NaCl or 10 mM HBS buffer, pH 7.4, was allowed to interact with the immobilised polymer brush. Saline solution (150 mM NaCl) at pH 9 and pH 5 were also injected to study binding stability at different pH.

Ellipsometry measurements were carried out on silicon wafers (1 cm x 3 cm) grafted with PDMAEMA. The wafers were mounted on the liquid cell, and injected with 10 mM HBS/ 150 mM NaCl buffer and allowed to reach its swelling equilibrium. This was then followed by injection of plasmid DNA dissolved in the respective buffer, and the wet thickness was measured at regular intervals.

DNA interaction studies with the SiO_2-g-PDMAEMA and copolymer brush were carried out via Zetasizer Nano ZS. Plasmid DNA was dissolved in the concentration of 10 µg/mL and diluted in 1 mL of 150 mM NaCl. Brush-coated nanoparticles were also diluted in 1 mL of 150 mM NaCl for the N/P ratios 1:1, 5:1 and 20:1, where N/P ratio is the ratios of moles of the amine groups of cationic polymers to those of the phosphate ones of DNA. The amount of DNA used was kept constant here whilst the amount of the polymer brush-coated nanoparticles was varied. 1 mL of the polymer brush-grafted nanoparticles solution was added to 1 mL of the DNA solution and allowed to complex for 15 - 30 min. The particle hydrodynamic diameter and the zeta potential were then measured for each N/P ratio before and after complexation. Pre-binding values were obtained with same particle concentration as N/P 5:1 but without DNA.

2.3 Results and discussion

2.3.1 Control of PDMAEMA brush growth

In order to determine the control of the brush chemistry and structure, brush thickness measurements were carried out. Figure 30 represents the kinetics study performed with PDMAEMA where the brush growth with respect to time was investigated. The targeted brush thickness was 30 nm, based on the good protein resistance achieved for many polymer brushes of similar thickness.[309] This thickness was achieved at a polymerisation time of approximately 20 min. Copolymer brushes consisting PDMAEMA and POEGMA at different ratios were then grown at a constant polymerisation time of 20 min, using similar conditions, but changing the molar ratio of the two monomers. Figure 31 demonstrates a relatively constant thickness of around 30 nm for the various copolymer brushes. This confirms that the brush growth is controlled, and the growth profile confirms a high grafting density.

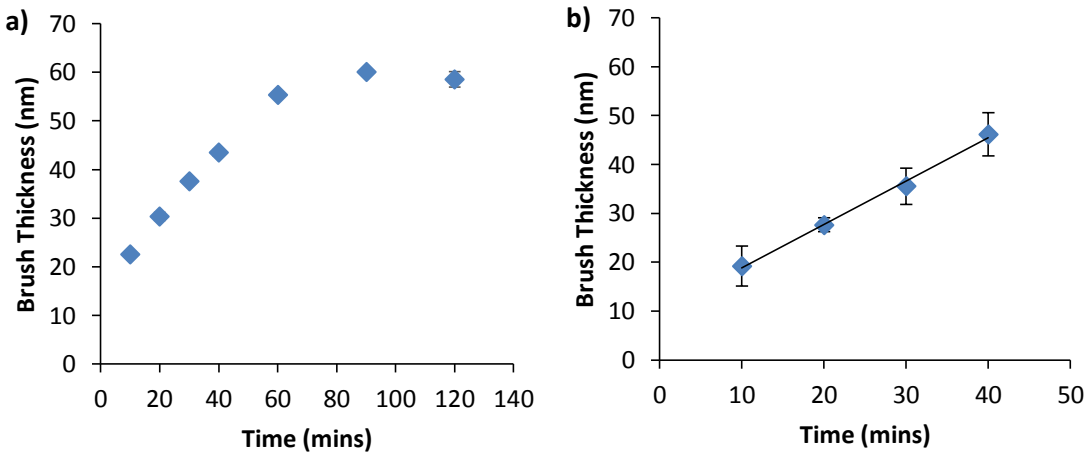

Figure 30: Pure PDMAEMA brush thickness with time via a) microcontact printing of the initiator on gold-coated silicon substrates and via b) solution deposition of the initiator. Brush thickness as by ellipsometry and results are expressed as mean values ± SE, n=6.

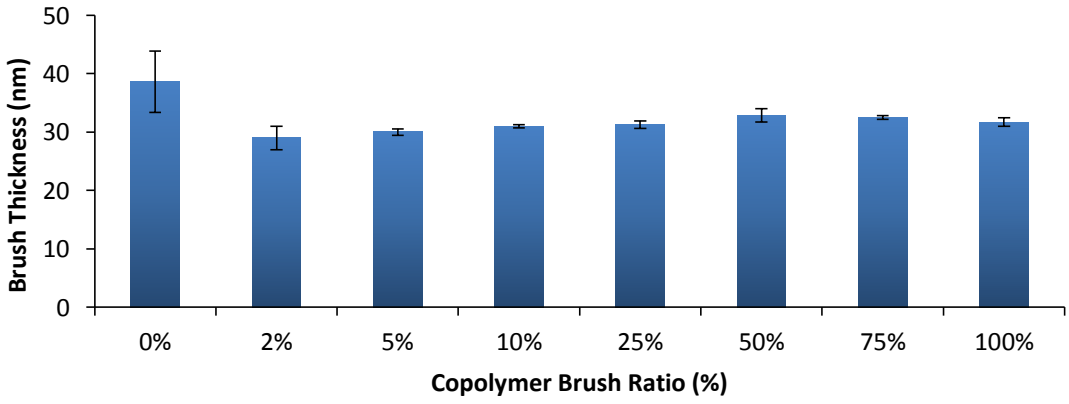

Figure 31: PDMAEMA-co-POEGMA brush grown via solution deposition of the initiator, at a polymerisation time of 20 minutes. Values are expressed as mean values ± SE, n=6.

2.3.2 Structural characterisation of polymers

Proton nuclear magnetic resonance (^{1}H NMR) was utilised to analyse the structure of free copolymers generated in solution (Figure 32) and confirm the control of the mole ratio of comonomer actually incorporated in the polymer backbone. The signals at 2.3 and 2.7 ppm are attributed to the methyl (N-CH_3) and methylene groups (N-CH_2-) on the tertiary amine of the PDMAEMA side chain, respectively. The chemical shift at 4.1 ppm corresponds to the methylene group adjacent to the carboxylate group (–O-CH_2-) of PDMAEMA.[368, 380] The curve displays the expected protons of methyl in the main polymer chain at 0.8 - 1.0 ppm. No peaks of protons in C=C double bond around 5.8-6.5 ppm was observed which indicates the absence of any residual monomers in free PDMAEMA (f-PDMAEMA).[403]

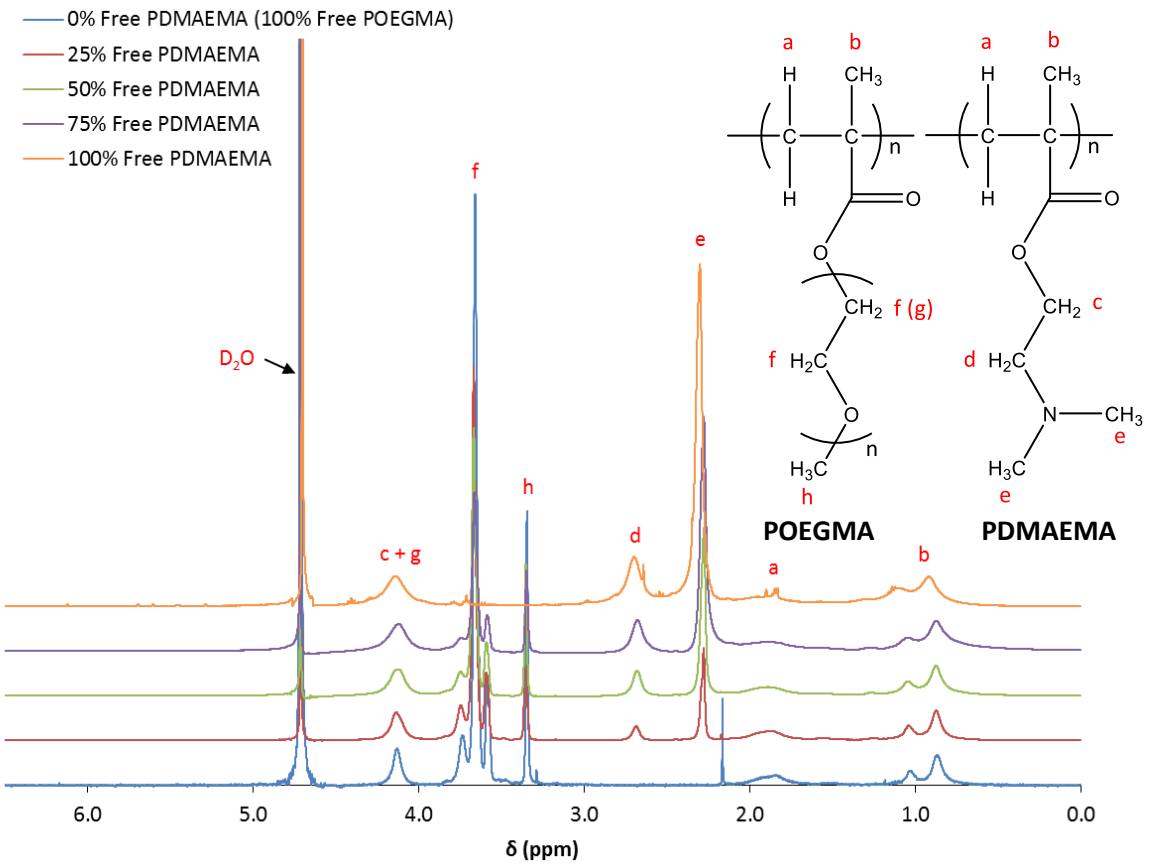

Figure 32: ^{1}H NMR spectra of f-PDMAEMA/ f-POEGMA copolymers in D_2O.

For pure free POEGMA (f-POEGMA), the presence of the methoxy group (-O-CH_3) is evidenced by the peak at 3.35 ppm whilst it is absent in the pure f-PDMAEMA. Signals at 3.6 – 3.7 ppm is assigned to the methylene group adjacent to the methoxy group (-CH_2-O-CH_3). The signals at 4.1 ppm is ascribed to the methylene group beside the carboxylate group (-O-CH_2-). The

protons of the methyl and methylene in the main polymer chain also appear between 0.8 – 1.0 ppm and 1.7 – 2.1 ppm, respectively.[416]

With an increase in the PDMAEMA content, the peak areas belonging to PDMAEMA and common to POEGMA increased in parallel.[417] The decrease in the signals at 3.6 – 3.7 ppm, with no signal on pure PDMAEMA indicates a decrease in the POEGMA content and the eventual absence of it.

The integration area ratio of the peaks at 3.35 and 2.70 ppm (the two signals which represents change in PDMAEMA content where the former indicates increasing PDMAEMA in copolymer with decreasing peak strength whilst the latter displays an increase in PDMAEMA content with increasing peak strength) in Figure 32 was used to determine the actual ratio of monomers in the copolymers at 25%, 50% and 75% PDMAEMA expected. The ratio of these two peaks once corrected for the number of protons in the signal allow the determination of the ratio of the monomers and hence actual percentage of the monomer in the copolymer as shown below in Figure 33 (See Appendix 1).

The graph exhibits a moderate ideal behaviour with slightly more DMAEMA achieved in the copolymer than expected. This can be attributed to the higher reactivity of DMAEMA compared to OEGMA toward both propagating species, as the latter has a higher molecular weight.[288]

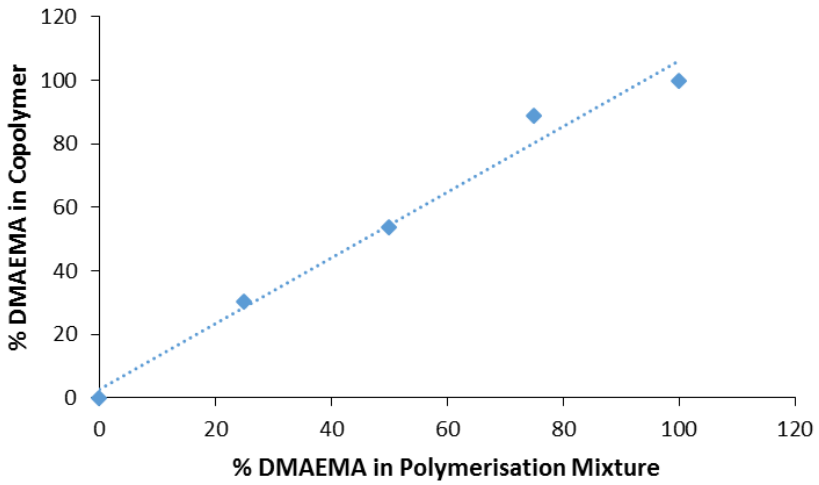

Figure 33: Copolymer composition as determined by the ratio of the integration areas of the NMR peaks.

Together these results confirm the good control of polymer brush growth and the thickness of the resulting coating, but also the composition of the copolymers generated.

The attenuated total reflectance – Fourier transform infrared (ATR-FTIR) spectra acquired for the free polymers; POEGMA, PDMAEMA, and their copolymers confirmed successful (co)polymerisations (Figure 34).

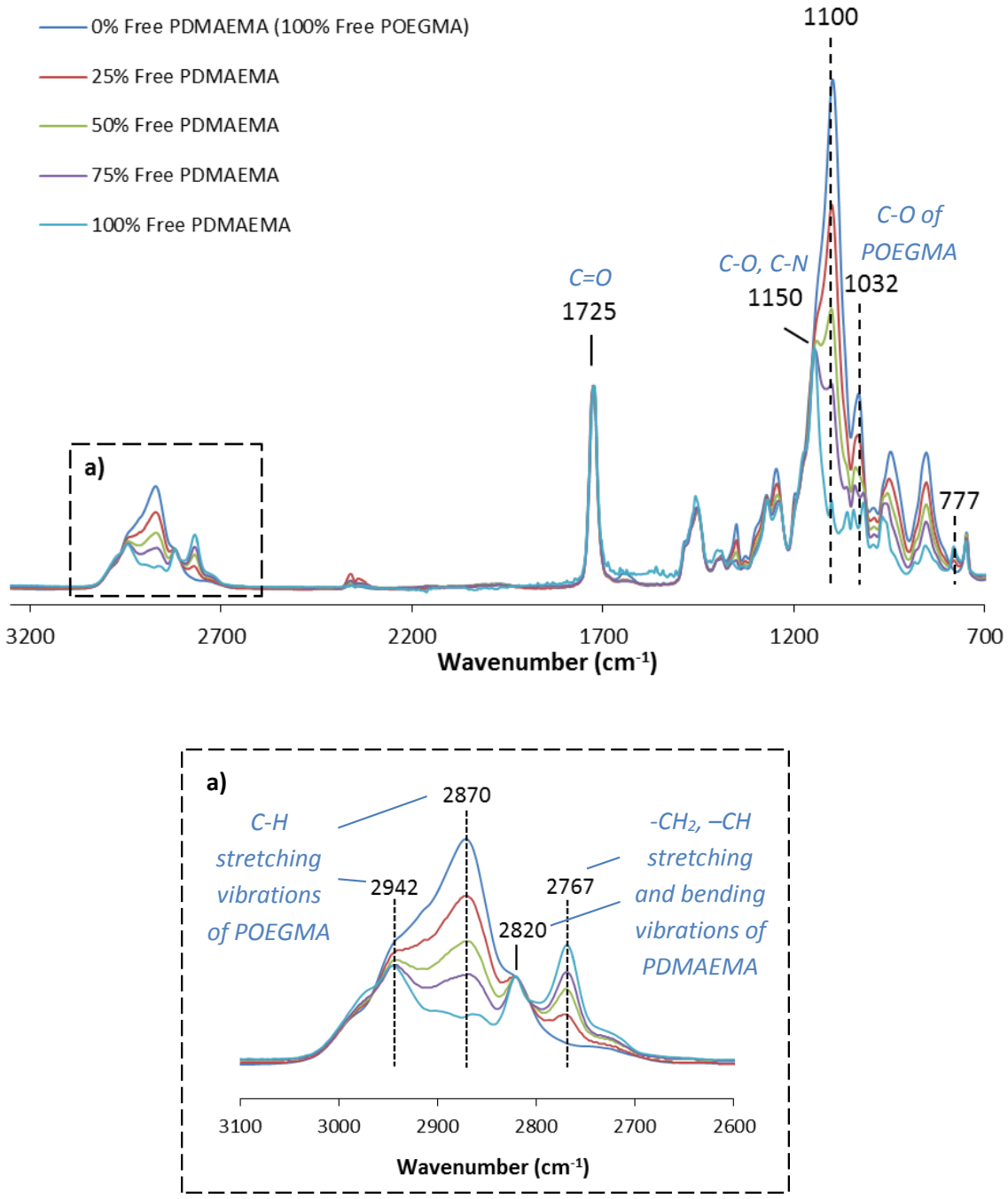

Figure 34: ATR-FTIR spectra of f-PDMAEMA-co-POEGMA copolymers.

The sharp absorption at 1725 cm^{-1} was ascribed to the stretching vibration typically associated with the ester group of PDMAEMA (C=O). The stretching vibration of C-N bonds from $–N(CH_3)_2$ groups or C-O in the polymer was also observed at 1150 cm^{-1}. The peak of wave vibrations occurring at 777 cm^{-1} belong to the alkyl group of the polymers. The absorption bands at 2767 cm^{-1} and 2820 cm^{-1} are the stretching and bending vibrations of $–CH_2$, -CH groups of the $–N(CH_3)_2$.[418]

The characteristic C-O stretching of POEGMA appeared at 1032 cm^{-1} whilst the absorption band for the –C=O stretching (also present in PDMAEMA) occurred at 1725 cm^{-1} as shown in Figure 34. The absorption band at 2870 cm^{-1} and 2942 cm^{-1} is ascribed to C-H asymmetric stretching vibrations.

It is notable that both characteristic peaks of PDMAEMA at 2767 cm^{-1} and 2820 cm^{-1} become much stronger with increasing PDMAEMA content while the intensity of the C-H stretching vibrations at 2870 cm^{-1} and 2942 cm^{-1} (characteristic of POEGMA) decreased, which is in agreement with reports in the literature.[384, 416, 417, 419, 420]

No absorption was detected for C=C double bonds at 1640 cm^{-1} which could have indicated the presence of free DMAEMA, therefore confirming the NMR results with regards to the lack of unreacted monomer.[419]

2.3.3 Characterisation of free polymer molecular weights

The molecular weight and PDI (M_w/M_n) of two samples of f-PDMAEMA were determined by gel permeation chromatography (GPC), using tetrahydrofuran (THF) as eluent.

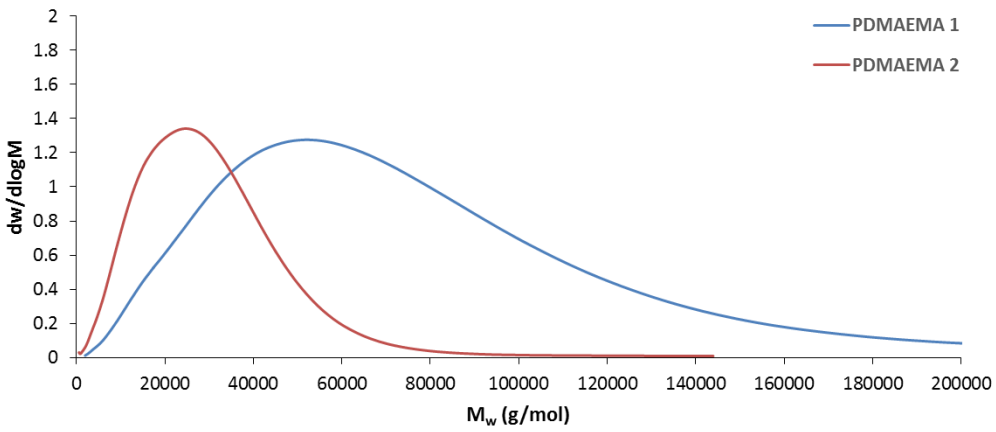

Figure 35: Overlaid multidetector molecular weight distributions of the free polymers synthesised, via GPC.

Figure 35 shows an overlay of the accurate molecular weight distributions of the samples. The positions of the peaks and the width of its distribution gives an indication of whether the molecular weight has been controlled under the conditions used for the polymerisation.

The results showed that PDMAEMA 1 and 2 had molecular weights in two different ranges (M_n =11,000 Da/M_w = 22,000 Da, and M_n = 28,000 Da/ M_w = 52,000 Da, respectively. They both exhibited relatively high PDIs (1.96-1.9). This could be an indication of an uncontrolled polymerisation caused through a complex formation between the growing polymer chains and the copper catalyst. The higher PDIs could also be due to interaction of the free polymers with the column material thus leading to incomplete elution.[190] As these samples were only required to test the transfection efficiency with PDMAEMA free polymers, this lack of control was not investigated further.

The molecular weight of interest was 25,000 Da as this has been reported to be suitable for gene transfections with PEI, a transfection reagent similar to that of PDMAEMA in structure and charge.[363] PDMAEMA 1 was successfully polymerised in reaching this value. This also confirms that the molecular weight was controlled.

2.3.4 Structural characterisation of polymer brush-functionalised nanoparticles

ATR-FTIR was used to confirm the structure of the brushes generated on particles, using spectra recorded for free polymers as a comparison (Figure 36).

The intensity of the absorbance for the bands of interest were found to be lower than that for the free copolymers due to the lower polymer brush content grafted from the surface of the silica nanoparticle compared to the size of the silica nanoparticle. The strong absorbance peak of C=O ester occurred at 1730 cm^{-1} in the spectrum of both, SiO_2-g-PDMAEMA and SiO_2-g-POEGMA. [403, 420] The absorption band at 1458 cm^{-1} is characteristic of PDMAEMA units and can be ascribed to the CH_2 bending. The absorbance peaks appearing at 2815 cm^{-1} and 2765 cm^{-1} belong to C-H stretching of the $–N(CH_3)_2$ groups.[421]. These peaks become stronger with increasing content of PDMAEMA.[417] The peak at 2980 cm^{-1} is attributed to the –C-H symmetric and asymmetric stretching of CH_3- and $–CH_2$- groups in the main chain of the grafted PDMAEMA.[422] It is also noticeable that with decreasing PDMAEMA content, the characteristic peak of POEGMA at 2870 cm^{-1} assigned to $–CH_2$ stretching vibration increases.[420] The absorption band at 2942 cm^{-1} also belongs to the C-H asymmetric stretching vibration but the intensity of the bands are not as distinct as those for 2870 cm^{-1} however the trend is still clear.

Below 1200 cm^{-1}, the large vibrational bands arising from the silica core preclude any analysis of the spectra. Hence, these observations of the evolution of vibrational bands as function of composition of the brushes match observations that were made for free copolymers and confirm that PDMAEMA-*co*-POEGMA copolymer brushes have been successfully synthesised on the surface of silica nanoparticles via SI-ATRP.

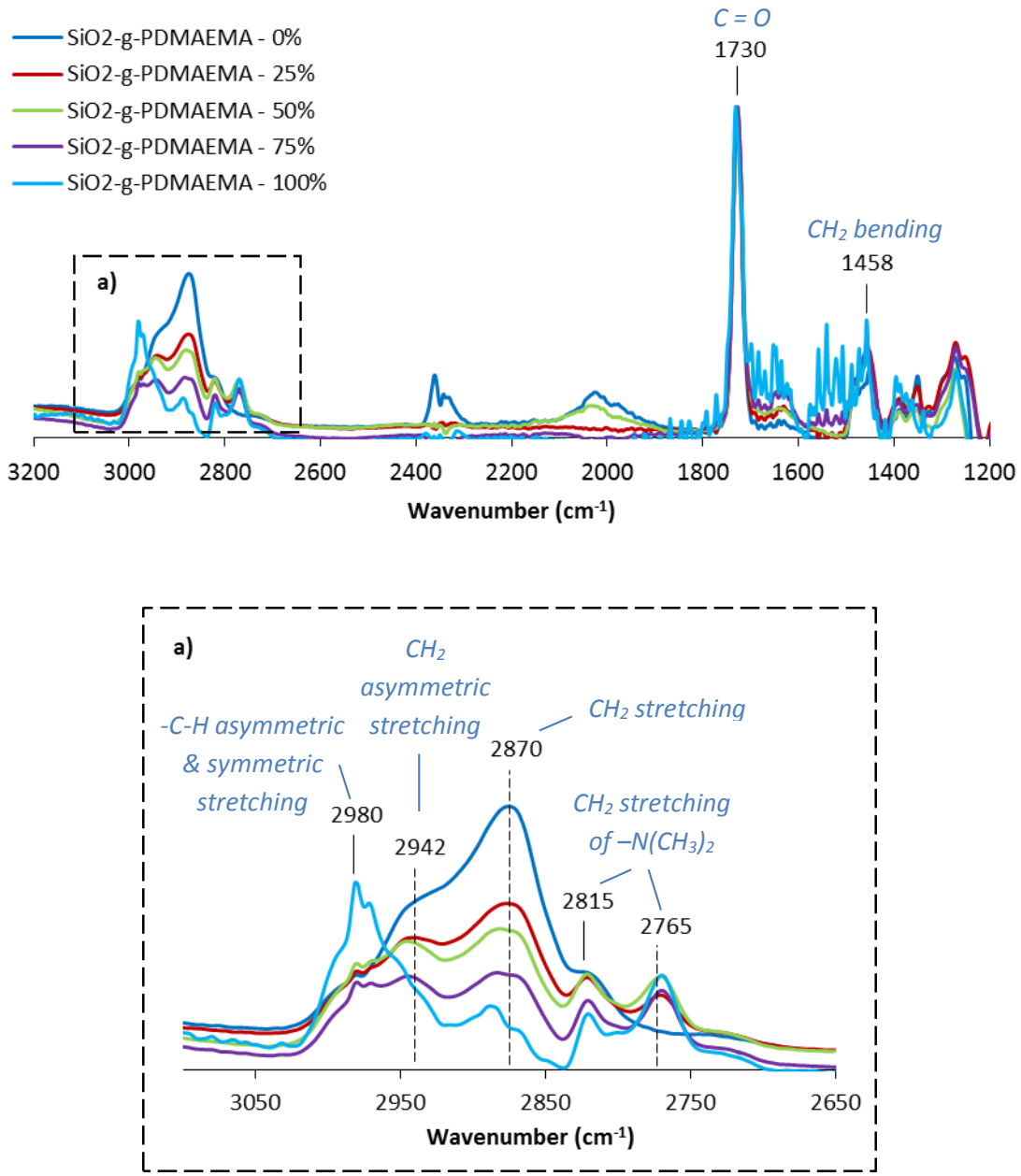

Figure 36: ATR-FTIR spectra for (co)polymer brush grafted from SiO_2 nanoparticles.

2.3.5 Characterisation of the surface morphology of particles

The morphology (size, shape and surface morphology) of the nanoparticles were observed by scanning electron microscopy (SEM). The SEM images of the bare silica nanoparticles and cationic brush-grafted silica nanoparticles qualitatively show that they remained spherical, near-monodisperse with a smooth, featureless surface morphology and no apparent sign of aggregation (Figure 37).

The average size of the nanoparticles was estimated by measuring the diameter of each particle using the SEM software. The mean particle diameter observed on SEM micrographs was 333 nm (standard error, SE = 9 nm) for 15 bare silica nanoparticles. Silica particles surface-grafted with brushes were aggregated at lower magnification. The mean diameter of 15 nanoparticles with brush as measured on SEM micrograph was 357 nm (SE = 7 nm). This suggests a dry brush thickness of approximately 24 nm. The dry brush thickness for brush grown on flat substrates as measured by ellipsometry was ≈ 30 nm hence both measurement are comparable to an extent and confirm the presence of brush on the surface of the silica nanoparticles.

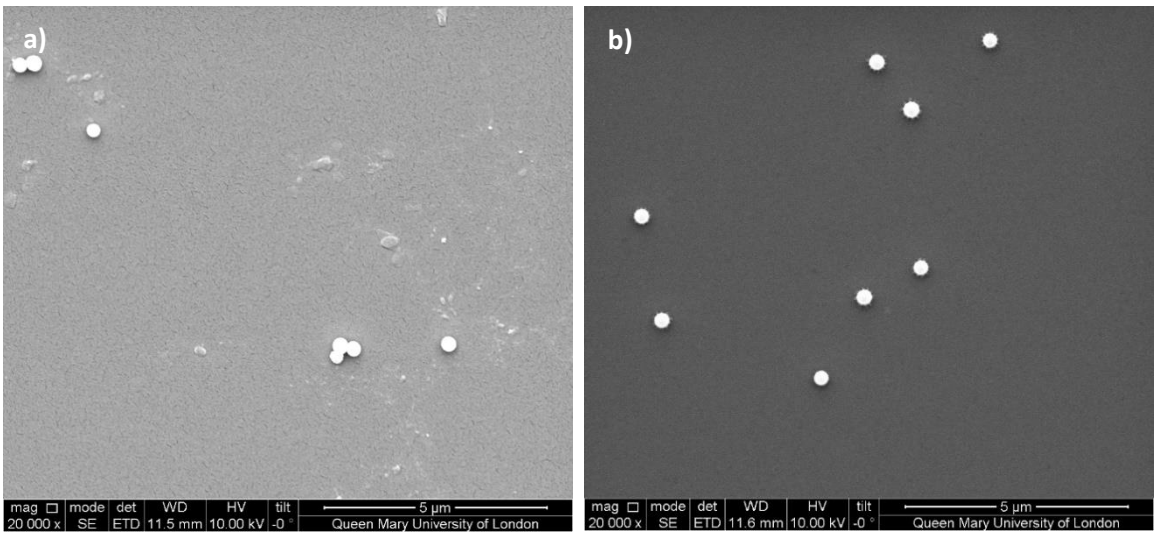

Figure 37: SEM micrographs of a) Bare 310 nm silica nanoparticles and b) 310 nm silica nanoparticles coated with brush, at magnification 20,000 x.

2.3.6 Determination of the weight fraction of polymer brush

In order to determine the weight fraction of polymer forming the grafted particles prepared, thermogravimetric analysis (TGA) was carried out where the particles were heated from room temperature up to a temperature at which their respective curves plateaued. From the thermal degradation profile, the weight fraction of polymer brushes grafted from silica nanoparticles was determined, in order to calculate the weight of particles required to achieve the different N/P ratios required for the DNA interaction and transfection studies. The percentage of the grafted polymer was attained through calculating the change in weight percentage from 150 °C until full degradation had occurred (where the trace levelled off) via the TA Instruments Q500 Analyser software.

As can be seen from Figure 38, all sample traces start at 100% and it is clear that the weight loss occurs in two stages. The first weight loss is from RT to approximately 250 °C, with a more pronounced decrease below 100 °C, caused by the desorption of physically adsorbed water. The second stage, which takes place above 280 °C, with two main decomposition peaks, is due to the decomposition of the grafted polymer brush. From these traces, the average weight percentage of PDMAEMA grafted on silica particles was found to be close to 27 % whilst POEGMA-grafted nanoparticles gave 29%.

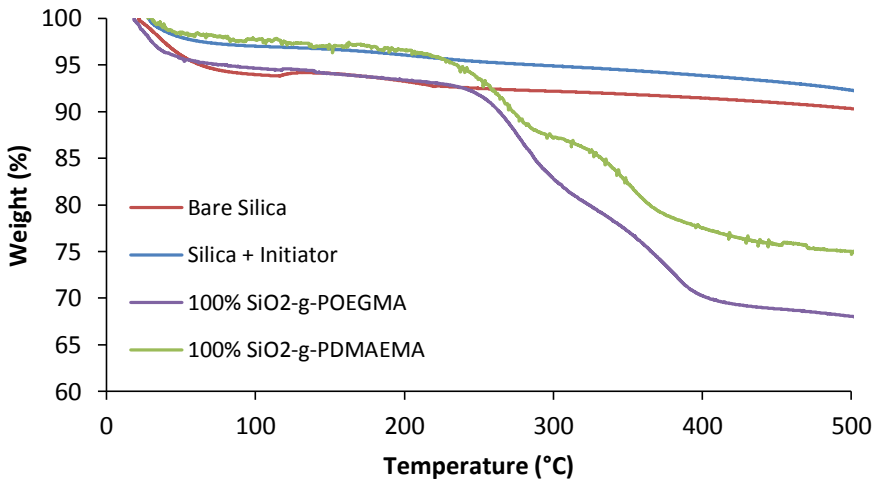

Figure 38: TGA of SiO_2, SiO_2-Initiator, SiO_2-g-POEGMA and SiO_2-g-PDMAEMA. Traces start at room temperatures.

Moreover, the trace for silica deposited with initiator indicates higher percentage weight compared to bare silica over the same temperatures, this is possibly due to bare silica absorbing more water than silica with initiator hence as the water is burnt off, the trace the change in the weight percentage is greater.

2.3.7 Determination of particle size and zeta potential

In order to confirm the swelling behaviour of brush-grafted particles, DLS studies were conducted at 25°C. These measurements were carried out on silica nanoparticles decorated with (co)polymer brushes that had been grown for the same amount of time as brushes grown from silicon substrates and for which a dry thickness of 30 nm was measured by ellipsometry. Dynamic light scattering was used to determine the size of the nanoparticles in deionised water and study the impact of the brush composition on its swelling.

Generally, the hydrodynamic diameter of the SiO_2-g-PDMAEMA-co-POEGMA in deionised water, increased with increasing content of PDMAEMA as the relative hydrophobicity arising from the OEGMA repeat units decreased and the relative ratio of charged repeat units increased (Figure 39).

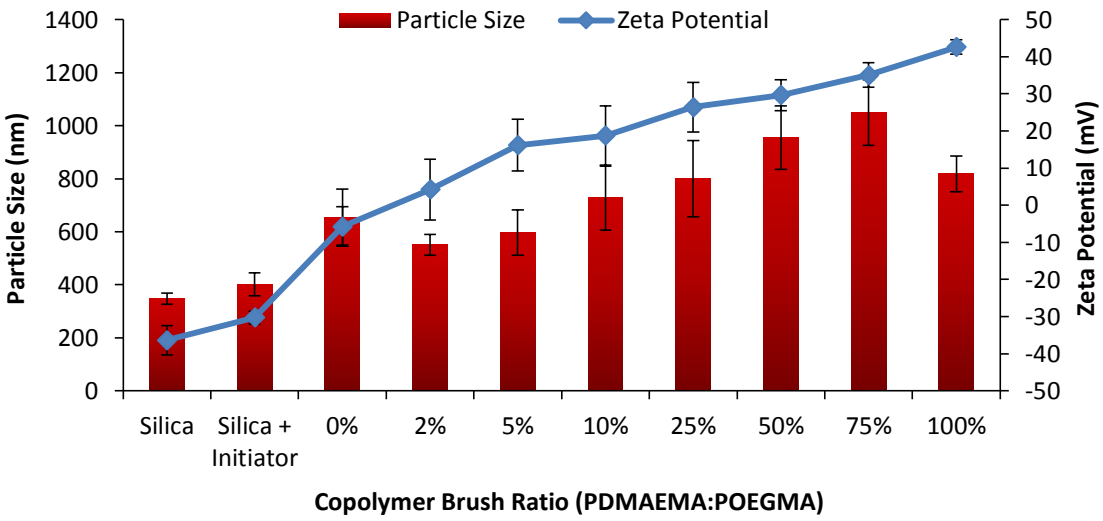

Figure 39: Effect of varying charge density on the particle size and zeta potential of the polymer brush-coated nanoparticles, in deionised water (pH ≈7). Values represent mean ± SE, n ≥ 9.

The surface charge properties of the silica nanoparticles coated with polymer brushes were determined in terms of the zeta potential via electrophoretic light scattering (ELS). Variation in the charge density with the different % copolymerisations were evident through the zeta potential measurements. The zeta potential of POEGMA (0% PDMAEMA) was observed to be -5.7 mV (SE = 5.3 mV) which is in agreement with what is reported in literature.[228] The zeta potential became increasingly positive with the rise in the percentage of cationic PDMAEMA as expected. The highest zeta potential of 42.6 mV (SE = 1.9 mV) was recorded for 100%

PDMAEMA on particles which also aligns with literature values.[423, 424] The large zeta potentials signify high electrostatic repulsive forces between the particles and therefore stable dispersions, where the existence of an energy barrier prevents the proximity of the particles.[425, 426] The zeta potential was controlled reasonably well with the range of copolymers.

The brush swelling was also seen to increase with increasing content of PDMAEMA in the copolymer brush as the charge of the brush also increased. Charged polymer brushes swell more due to the higher degree of protonation and solvation which results in the polymer chains stretching away from the silica surface. Maximum brush swelling occurred at 1050 nm (SE = 123 nm) for 75% PDMAEMA, with a slight decrease at 100%. The slight decrease in swelling measured in the 100% PDMAEMA-coated particles, compared to 75% PDMAEMA could be due to the basicity of the DMAEMA repeat units, contributing to increase the pH further than in the 75% PDMAEMA brushes and resulting in a partial collapse of the brush (see discussion of the pH responsive behaviour below).

2.3.8 Charge titration

The pH dependence of the hydrodynamic diameter and net surface charge of SiO_2 coated with copolymer brushes was studied by light scattering and zeta potential measurements (Figure 40). The polymer brush-coated nanoparticles were dispersed in 150 mM NaCl and their pH was adjusted as required using NaOH or HCl. This study used 150 mM NaCl as the medium for the characterisation of PDMAEMA brushes as the physiological concentration of 150 mM has a notable effect on the way in which NaCl weakens the electrostatic repulsion between charged amine groups in the polymer chain which consequently enhances the protonation of the chain.[427]

The SiO_2-g-brush particle system is governed by the coexisting electrostatic repulsive, hydrophobic and hydrogen bonding interactions. As discussed in section 2.1.1.1, PDMAEMA displays a marked pH-responsive behaviour. In the acidic region, at pH 4, SiO_2-g-PDMAEMA nanoparticles (Ø320 nm), coated with 30 nm-thick PDMAEMA brush, containing the tertiary amine group, is fully protonated to the corresponding quaternary ammonium thus creating a hydrophilic surface. The polymer chains are highly stretched along the radial direction due to the geometrical constraint, electrostatic repulsions, strong chain-solvent interactions and osmotic pressure.[380, 422] This gives rise to a larger hydrodynamic diameter for 100%

PDMAEMA and 75% PDMAEMA at pH 4 as PDMAEMA is more charged with strong electrostatic repulsive and hydrogen bonding interactions. A hydrodynamic diameter of above 650 nm is observed for 100% PDMAEMA, which is expected to reduce with increasing pH however as the pH approached the pK_a of PDMAEMA (≈ 8),[183, 379] the colloidal stability is reduced hence a slight increase in the swelling to a maximum hydrodynamic diameter of 701 nm is reached.

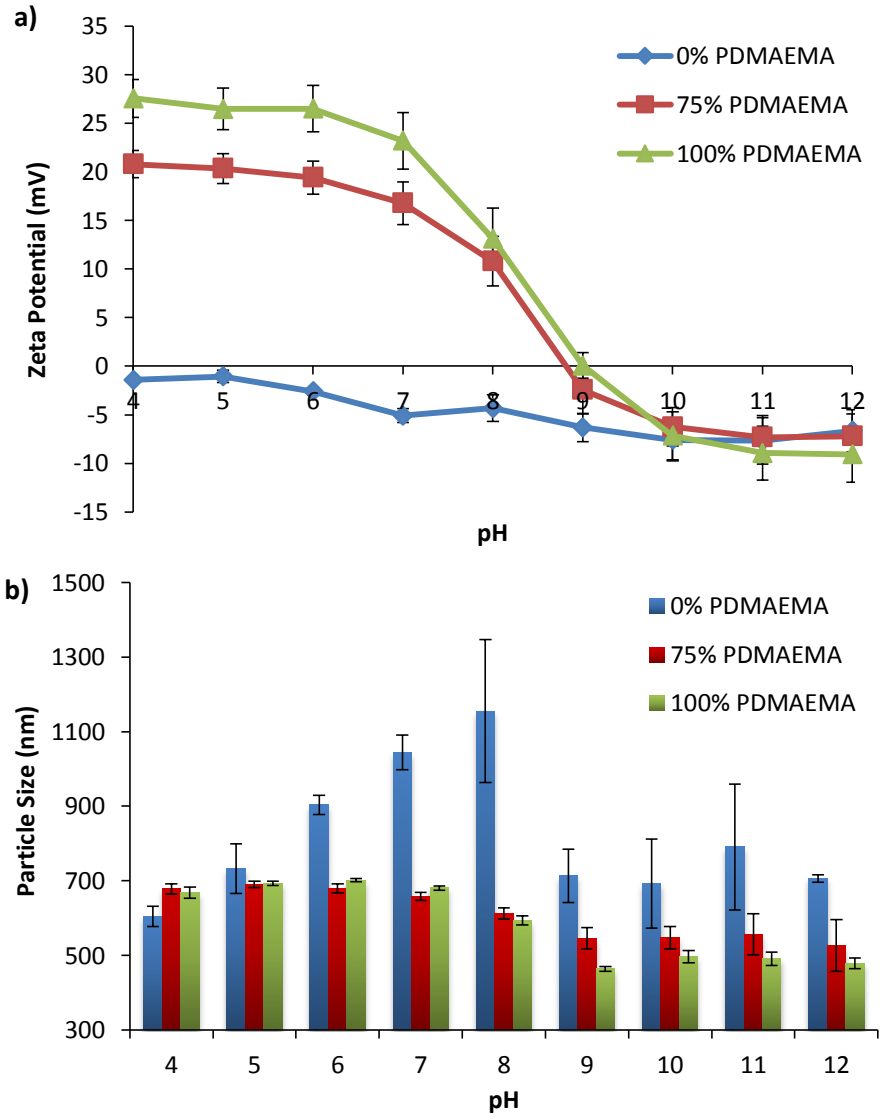

Figure 40: Effect of pH on a) the zeta potential and b) the hydrodynamic diameter, of 0% PDMAEMA (100% POEGMA), 75% (25% POEGMA) and 100% PDMAEMA, grafted on SiO_2 nanoparticles, in 150 mM NaCl, measured by DLS and ELS. Values represent mean ± SE, n ≥ 9.

Raising the pH results in gradual deprotonation of the PDMAEMA brush until the brush becomes neutral above the pK_a of DMAEMA. The brush becomes hydrophobic and there is

limited space available for the polymer chains to occupy due to the high grafting density. Polymer chain-chain interactions dominate chain-solvent interactions which leads to the polymer chains collapsing abruptly between pH 7 and pH 9, in the range of the pK_a of PDMAEMA and, as a result, smaller hydrodynamic diameters are observed by DLS.[383, 422] As mentioned previously, the hydrophobic-to-hydrophilic equilibrium in PDMAEMA contributes in a way such that as the pH changes, the phase state of the macromolecule changes accordingly.

With pure PDMAEMA, aggregation is also expected in neutral/alkaline aqueous environment as a result of the decreasing positive charge as the brush is subjected to increasingly basic pH which leads to increased hydrophobicity of the brush and eventual aggregation.[199] This was not observed in this charge titration study, possibly due to the concentration of the suspension being too dilute for aggregation to occur.

The zeta potential is notably lower for 100% PDMAEMA compared to the value in Figure 39 (a decrease of 15 mV) due to a change in the ionic strength as the charge titration was carried out in 150 mM NaCl as opposed to deionised water. A sharp decrease in zeta potential also occurred near the pK_a of PDMAEMA ≈ 8,[183] between pH 7 and pH 9 for 100% PDMAEMA grafted on silica nanoparticles, with a more gradual drop for 75% PDMAEMA and with little effect on POEGMA. This was also reflected to an extent in the hydrodynamic diameter where the brush swelling was reduced from 636 to 409 nm for 100% PDMAEMA brushes and 678 to 526 nm for 75% PDMAEMA brushes.

Nanoparticles functionalised with POEGMA brushes did not show any clear trend regarding the evolution of their hydrodynamic diameter. The gradual increase in particle size near pH 8 is not expected theoretically as the brush is not responsive and its charge is near 0 mV. The large swelling thicknesses seen could therefore be due to some level of aggregation of these particles at neutral pH, followed by dissociation at slightly higher pH. This is indicated by their zeta potential which seems to decrease slightly and could therefore overcome the weak hydrophobic forces causing aggregation. The presence of salt in the buffer solution may also contribute to the intermolecular aggregation. Such interactions between the SiO_2-g-PDMAEMA and SiO_2-g-POEGMA nanoparticles are captured by the Derjaguin-Landau-Verwey-Overbeek (DLVO) theory, predicting stability of colloids.[428-430] According to the DLVO theory, two opposing forces, namely, the van der Waals attractive (hydrophobic) forces and the electrostatic repulsive forces, govern the stability of charged colloidal particles in aqueous solutions. The electrical double layer forces give rise to an energy barrier – the extent of which

is depicted by the magnitude of the zeta potential. This energy barrier repels particles from each other, however, when this energy is overcome, the attractive van der Waals forces dominate as particles collide and result in aggregation and destabilisation of the nanoparticles. Hence colloidal stability is reduced around the isoelectric point of a particle.

The responsiveness of increasingly cationic PDMAEMA-co-POEGMA brushes in deionised water, phosphate buffered saline (PBS) and 150 mM NaCl was studied via DLS and ELS. The responsive behaviour was followed via changes in the particle size and surface charge in the different solvents, as shown in Figure 41.

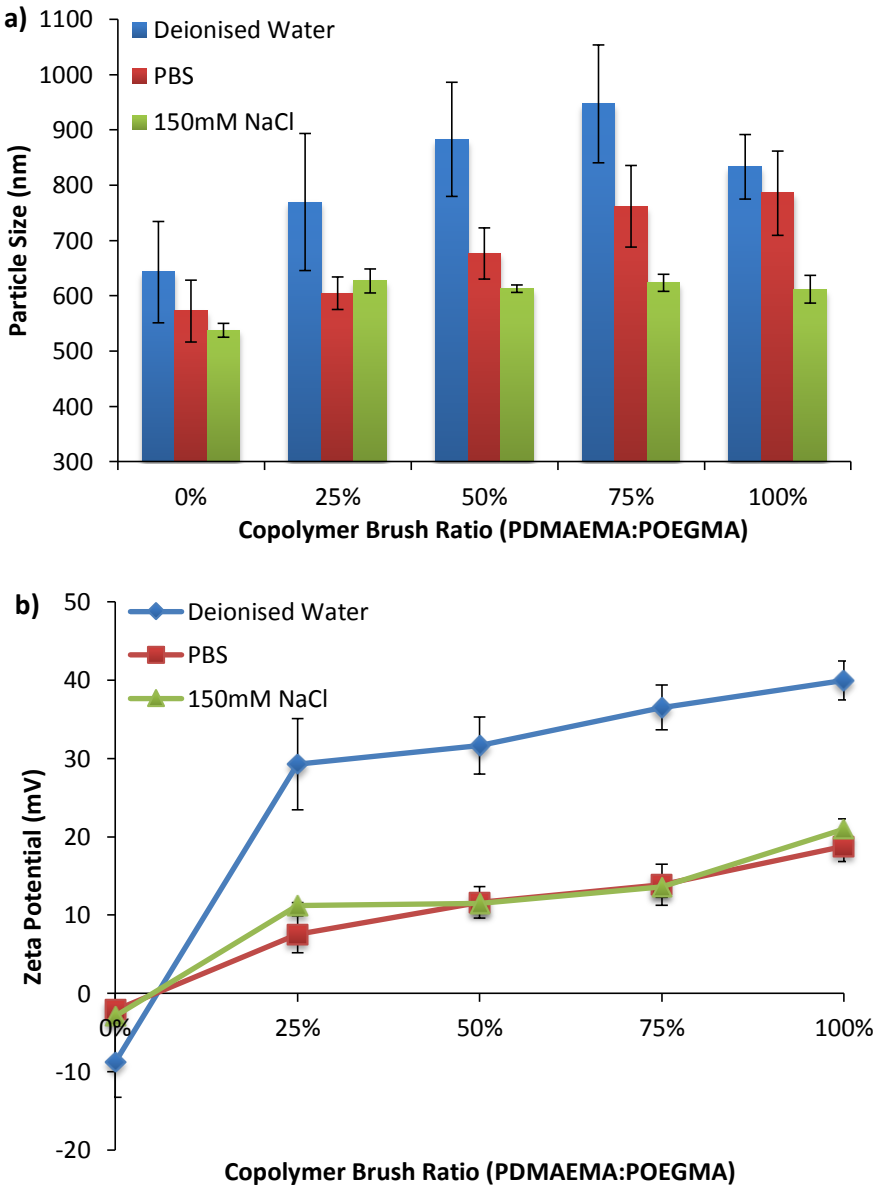

Figure 41: Effect of solvent on a) the hydrodynamic diameter and b) zeta potential of varying PDMAEMA: POEGMA copolymer brush on silica nanoparticles. Values represent mean ± SE, n ≥ 9.

Compared to deionised water, the particle size decreased in PBS and 150 mM NaCl with an average reduction in hydrodynamic diameter of 16% and 25%, respectively (Figure 41a). This collapse is attributed to the decrease in osmotic pressure at high ionic strength, the salting out effect, and therefore the decrease in the stretching of the polymer chains. Interestingly, although the ionic strength of PBS solutions is higher than that of 150 mM NaCl solutions (PBS contains 137 mM NaCl and 10 mM phosphate), the swelling of PDMAEMA brushes was higher in the case of PBS. This could indicate a level of salting in effect of phosphate ions. The measured zeta potential is also reduced but the general trend remains (Figure 41b).

2.3.9 Responsive behaviour of polymer brushes grown from flat silicon surfaces

2.3.9.1 Ellipsometry

In situ ellipsometry was carried out, using the Liquid Cell system, to characterise the swelling behaviour of PDMAEMA brushes grafted from silicon substrates. The dry ellipsometric thickness of the brushes studied were 11.2 nm (SE = 0.5 nm) and 32.4 nm (SE = 0.8 nm), corresponding to polymerisation times of 8 min and 20 min, respectively. The pH response of these brushes was investigated by measuring the swollen brush thickness in 150 mM NaCl as the pH was lowered from pH 9 to pH 4 and then returning to pH 9 with the same sample (Figure 42). The range of pH was chosen so that the lowest is well below the pK_a of PDMAEMA but would not cause significant hydrolysis of the brush at room temperature, during the course of this experiment.

At the highest pH, which is well above the pK_a of PDMAEMA, the brush is collapsed, owing to its neutral charge, consistent with DLS and zeta potential measurements carried out with brush-coated particles. The pH-swelling data clearly shows a hysteresis phenomenon with a retarded swelling as the pH decreased (Figure 42b). A similar phenomenon was reported by Willott *et al*. and was ascribed to the formation of a dense, hydrophobic outer region during collapse that retards solvent egress (Figure 42a).[300]

Tertiary amine groups of PDMAEMA becomes protonated under acidic conditions thus bringing solvent and counterions into the brush. A maximum swelling thickness of 49.7 nm at pH 5 and 98.7 nm at pH 5.5 was reached for brushes with dry thickness of 14.4 nm and 34.3 nm, respectively, corresponding presumably to a maximum charging of tertiary amine groups. The higher swelling measured for thin (10 nm) brushes indicate that these brushes may be more polydisperse than the 30 nm brushes. On the other hand, increasing the pH led to

deprotonation of tertiary amine groups, consequently neutralising the brush layer and decreasing the brush thickness as a result of solvent and counterion expulsion. Interestingly, at such high pH, brushes did not collapse to their dry thickness, but only relatively modestly (swellings of 24.4 nm for the 10 nm-thick brushes and 63.2 nm for the 30 nm-thick brushes), perhaps reflecting the fact that these measurements were carried out below the reported LCST of this polymer (Section 2.1.1.4).[401] The hysteresis in the swelling behaviour could be attributed to the disentanglement of the polymer brush chains which then allows higher retention of solvent after being protonated for the first time, as proposed by Cheesman and co-workers.[431] This phenomenon is thought to be due to the hydrophobic interactions arising from aliphatic backbones and nonpolar moieties in pendant groups of the brush. Protonation of the amino groups of PDMAEMA is impeded by such interactions which results in a decrease of the pH at which swelling occurs.[388]

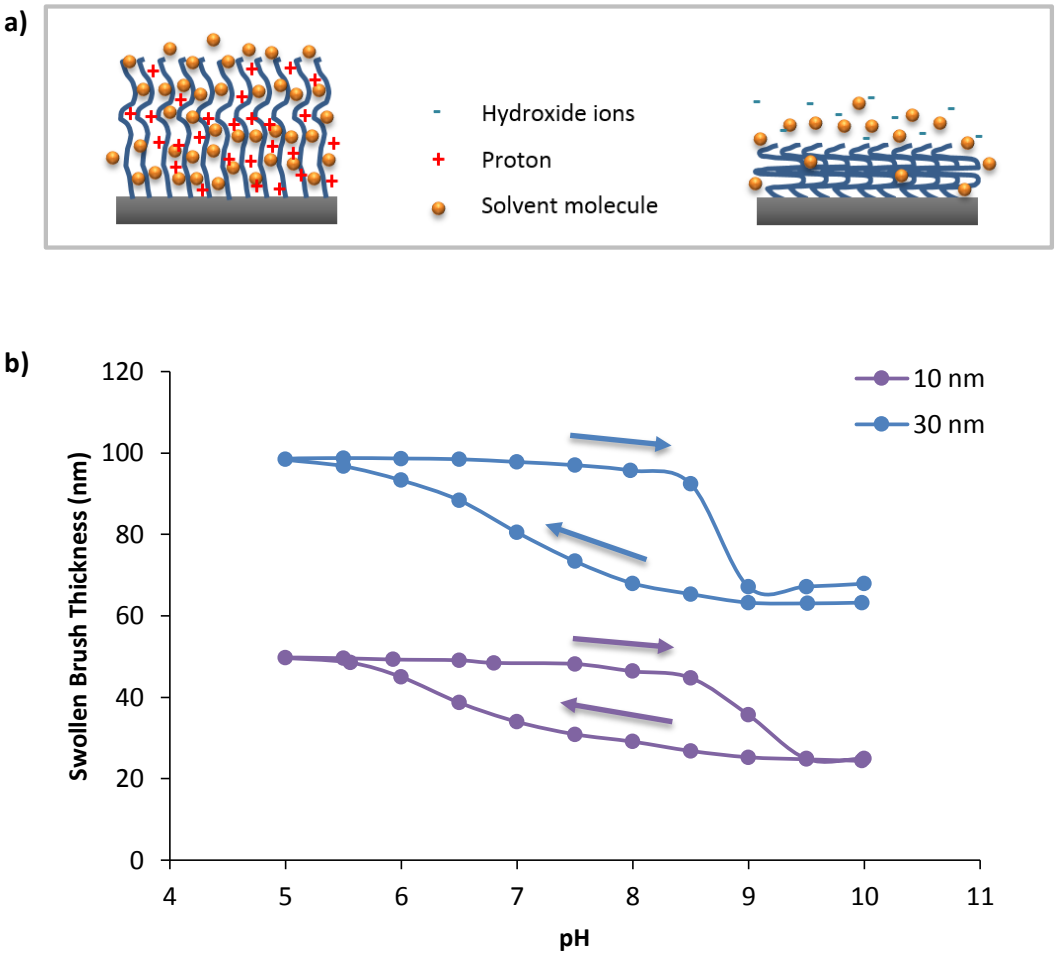

Figure 42: a) Schematic reflecting the effect of pH on brush swelling b) in situ ellipsometry data on the swelling behaviour of 10 nm and 30 nm-thick PDMAEMA brushes on silicon substrates as a function of pH, in 150 mM NaCl, via reverse titration.

2.3.10 Interaction of DNA with polymer brushes

It is widely reported that cationic polymers brushes can condense DNA efficiently; this has led to their application as non-viral gene delivery vectors.[35, 160, 432] Polymer-DNA interactions are important to control at different stages of the transfection process; at the complexation stage and for initial uptake of complexes, to ensure reliable entry of the complexes in the cytoplasm, for the protection of DNA towards enzymatic degradation and during the release of the DNA material within the cell cytoplasm or the nucleus. In addition, proton uptake may play an important role for endosomal escape, in cases involving such an uptake pathway.[347, 367, 433-436] Hence, investigating DNA interaction with brushes is important for our understanding of parameters impacting plasmid transfection. In the case of PDMAEMA brushes (rather than f-PDMAEMA polymers), such interactions have not been systematically examined. The quaternary ammonium groups of PDMAEMA interact electrostatically with the anionic phosphate moieties of DNA to form polyplexes, driven by the increase of entropy associated with the release of counterions. Detailed knowledge of these interactions can give an insight into the polymer brush's transfection performance.

The strength and reversibility of the cationic brush/DNA association and dissociation characteristics, and the structure of the resulting brush-DNA complexes was studied by SPR and *in situ* ellipsometry.

2.3.10.1 Surface plasmon resonance

SPR technique can be used to characterise and quantify biomolecular interactions. This optical method measures the RI of thin layers of material adsorbed on a metal (typically gold), within 300 nm of the sensor surface, in real time.[437] The excitation of surface plasmons in a thin gold layer at the boundary between the sensor chip and the flow cell, allows the absorption of p-polarised light when it is reflected from the boundary. The angle at which absorption is maximal is directly proportional to the RI within 300 nm of the surface. The sensor surface is usually immobilised with a biomolecular recognition element which interacts with analytes in solution injected via the flow cell. As binding occurs to the immobilised target the local RI increases, leading to a change in SPR angle, which is measured in real time by detecting changes in the intensity of the reflected light, thus producing a sensorgram.[438] SPR is routinely used to investigate protein-protein or protein-small molecule interactions, as well as the protein resistance of coatings.[238, 356, 430, 439, 440]

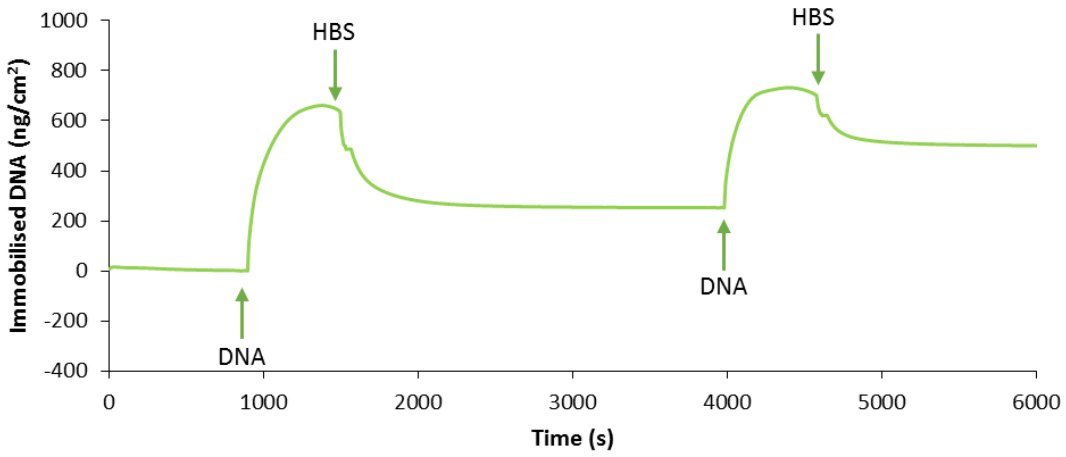

Figure 43: Functionalisation of 10 nm-thick PDMAEMA brush with plasmid DNA (10 µg/mL), monitored by SPR.

Interaction of DNA with PDMAEMA-coated on SPR gold chips was monitored via changes in the RU response of the SPR, which translates as 10 RU for 1 ng/cm^2 of adsorbed material[441] as represented in Figure 43. A fixed plasmid concentration of 10 µg/ mL was used. After equilibration of the brush in the relevant medium, this DNA solution was injected onto the brush for 10 min, at a flow rate of 10 µL/min, and the sensor surface was washed with fresh medium.

The media used in this study were 150 mM NaCl and 10 mM HBS. 150 mM NaCl was used to evaluate the interaction as it is a standard solvent in transfection.[84] The latter buffer, HBS, contained 1 M 4-(2-hydroxyethyl)-1-piperazineethanesulfonic acid (HEPES) and 150 mM NaCl (1:100). This buffer was chosen as it is a standard biological buffer used in cell culture as well as a common running buffer used for most type of interaction studies in SPR; it has been used in the past to study polymer-DNA interactions.[439] The pH of the buffer solutions were also adjusted to a value below the pK_a of PDMAEMA hence kept between pH 6.5 and 7. The results from the present study confirmed the stable binding of DNA to PDMAEMA brush as DNA remained bound to the surface following the washing step.

DNA prepared in 150 mM NaCl gave the highest bound DNA for both 10nm, and 30 nm surfaces. The 10-nm thick PDMAEMA brushes were able to bind the highest level of DNA with 405 ng/cm^2 of bound DNA in the brush layers (Figure 44). This large uptake of DNA is possibly due to the electrostatically driven penetration of the positively charged PDMAEMA layer. However, a slight decrease in the quantity of DNA can be seen for 30 nm brush; though it is expected that the thicker brush should bind more DNA, it is possible that this wasn't the case

due to the loss of sensitivity in the SPR. DNA may have bound near the surface of the brush but as the SPR sensor is distance sensitive, it was not able to quantify the DNA on the surface accurately. Alternatively, this could be a sign that large plasmid DNA molecules cannot infiltrate dense PDMAEMA brushes in these conditions. There are also clear differences between the first and the second injections. The amount of DNA bound to the brush is lower after a second injection as some of the available quaternary ammonium groups are already bound from the first incubation.

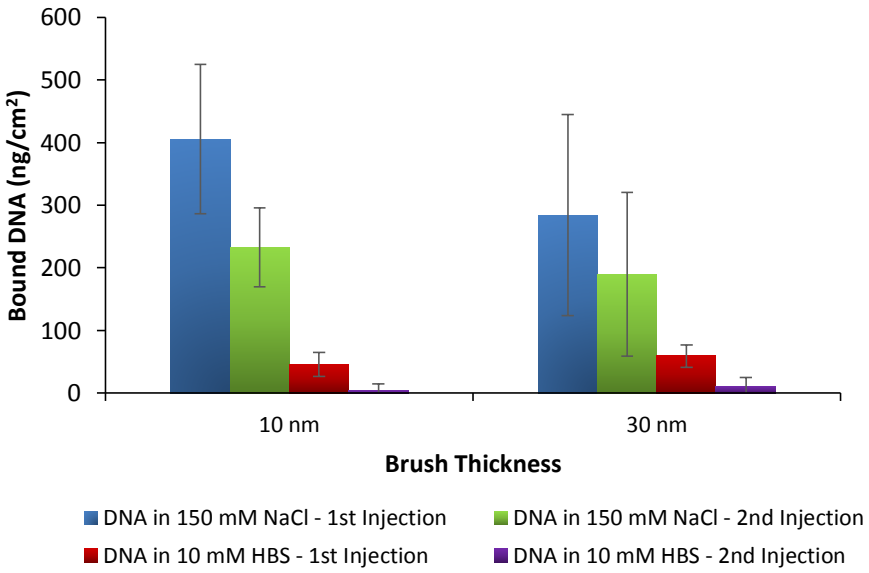

Figure 44: Effect of DNA solvent on the binding between DNA and PDMAEMA brushes of 2 different thicknesses; 10 nm and 30nm, during a 2-step injection. Values represent mean ± SE, n ≥ 3.

It was also noted that upon subjecting the brush to more than two DNA injections, it was still possible to bind further DNA molecules to the brush after each injection, although the amount retained decreased with the number of injections (Figure 45a). These results show that the PDMAEMA brush is not saturated with DNA after a single injection and that DNA infiltration through dense PDMAEMA brushes is a slow process (Figure 45b). Alternatively, such behaviour could result from remaining exposed patches of PDMAEMA brushes to which DNA may not have bound, perhaps due to the size of plasmid DNA. Upon maturation of the surface and further exposure to plasmid DNA, these sites could become more available for further DNA binding.

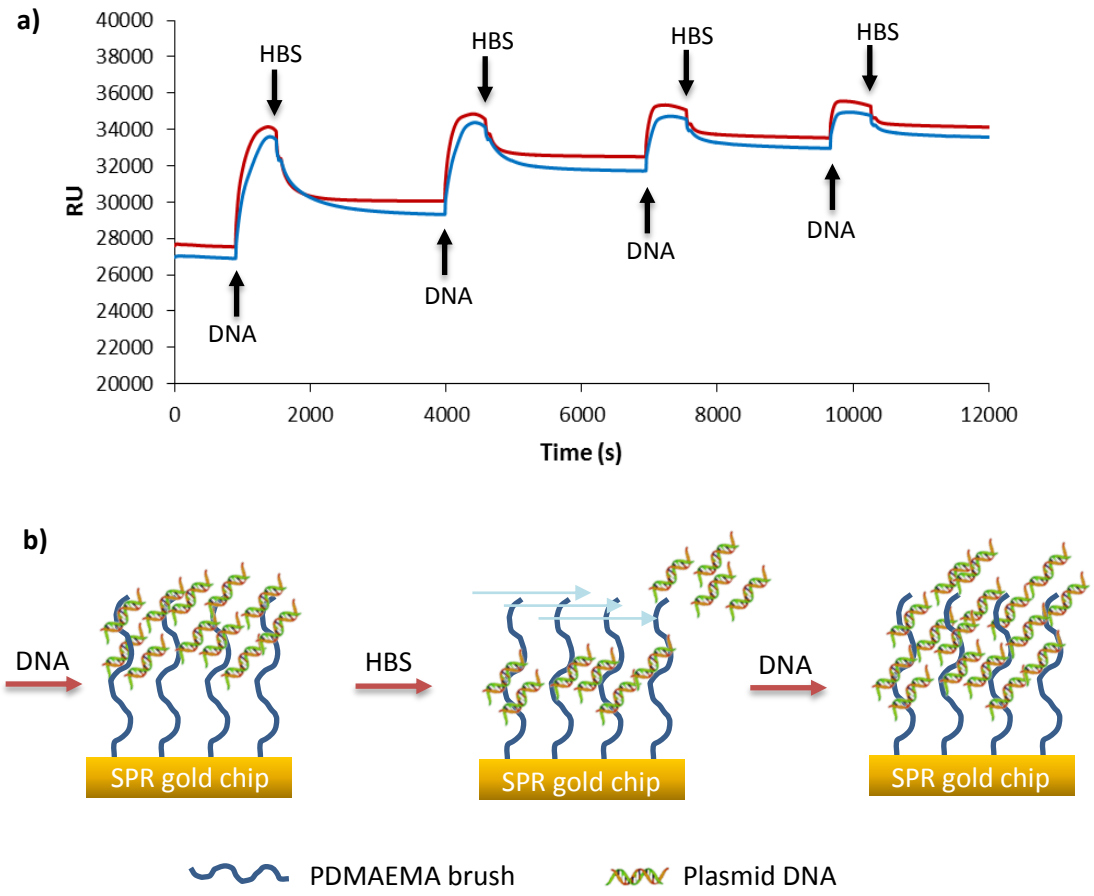

Figure 45: a) SPR sensorgram trace of channels Fc 1(red) and Fc 2 (blue) during functionalisation of 10 nm-thick PDMAEMA with DNA (10 µg/ mL), during four subsequent injections, b) schematic of the DNA-brush interaction with repeated functionalisation with DNA and washing with HBS.

In contrast, DNA prepared in 10 mM HBS did not have any significant effect on the quantity of DNA bound to the brush surface following the washing step with 10 mM HBS (Figure 46). This could be attributed to the presence of small molecules in the buffer which prevent DNA association. This was, however, not the case with 150 mM NaCl, where the amount of bound DNA exceeded that of 10 mM HBS by almost eight-fold solely with the first injection of DNA.

However, increasing the pH to 9 significantly affected the formed polyplex brushes and resulted in the release of some of the DNA material. Using 10 mM HBS of pH 6.5 as eluent, at pH 9, there was almost no binding of the DNA with PDMAEMA. This may be explained by the neutral nature of the polymer brush at this particular pH which consequently contributed a lack of significant Coulombic or electrostatic interaction with the DNA, despite the gain in osmotic pressure as a result of the partial brush collapse. Lowering the pH to 5, however, presented increased interaction forces and therefore association with DNA remained stable as is evident from Figure 46. This is in agreement with existing literature data. Wink *et al.*

studied the interaction of plasmid DNA with overnight-immobilised, 5%-thiolated PDMAEMA polymer at different pH values (pH 8.8 and pH 5.4) of the running buffer (HBS) and determined the resulting association and dissociation reaction rate constants. Interaction between plasmid DNA and PDMAEMA showed a regular binding pattern and bound DNA remained stable in HBS at pH 5.4 and 7.4. However, at pH 8.8, the DNA dissociated from the complex.[439]

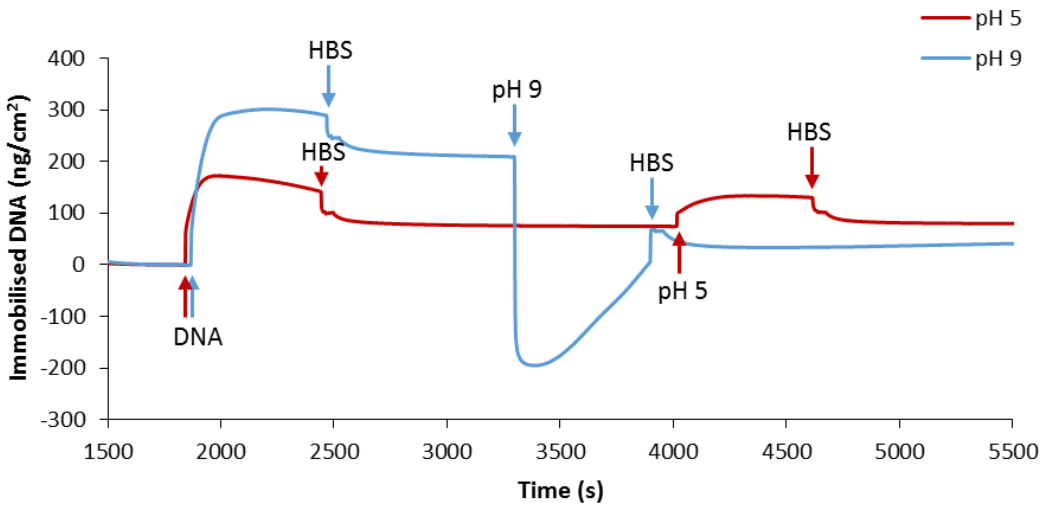

Figure 46: Functionalisation 10 nm-thick PDMAEMA with plasmid DNA (10 µg/mL) followed by association/dissociation of brush-DNA when injected with pH 9 (blue) and pH 5(red) 10 mM HBS buffer.

2.3.10.2 Ellipsometry

DNA binding was also studied via *in situ* ellipsometry to confirm the interactions between PDMAEMA and DNA in 150 mM NaCl (Figure 47a) and 10 mM HBS (Figure 47b) observed via SPR. As for SPR results, ellipsometry seems to indicate that DNA interact at the brush surface with little infiltration as the increase in swollen thickness is only moderate. The difference in swollen thickness upon addition of DNA was found to be 9 nm (SE = 3.2 nm) and 1.1 nm (SE = 3.5 nm) for 10- and 30 nm-thick PDMAEMA brushes in 150 mM NaCl, respectively. In alignment with the SPR data, injecting DNA in 10 mM HBS had little effect on the swollen thickness with 4.4 nm (SE = 2.2 nm) difference for 10 nm-brush and 0.9 nm (SE = 0.5 nm) for 30 nm-brush.

The difference in swelling following the injections of DNA was greater for studies carried out in 150 mM NaCl than 10 mM HBS. Swollen thickness of the PDMAEMA brushes equilibrated in the buffers, however, were larger in 10 mM HBS than 150 mM NaCl by 6 nm and 15.7 nm for 10- and 30 nm-thick brushes, respectively. This is perhaps due to salting out at higher ionic

strength. Hence the reduced DNA adsorption in HBS may be a result of the greater osmotic pressure experienced by the brush in these conditions.

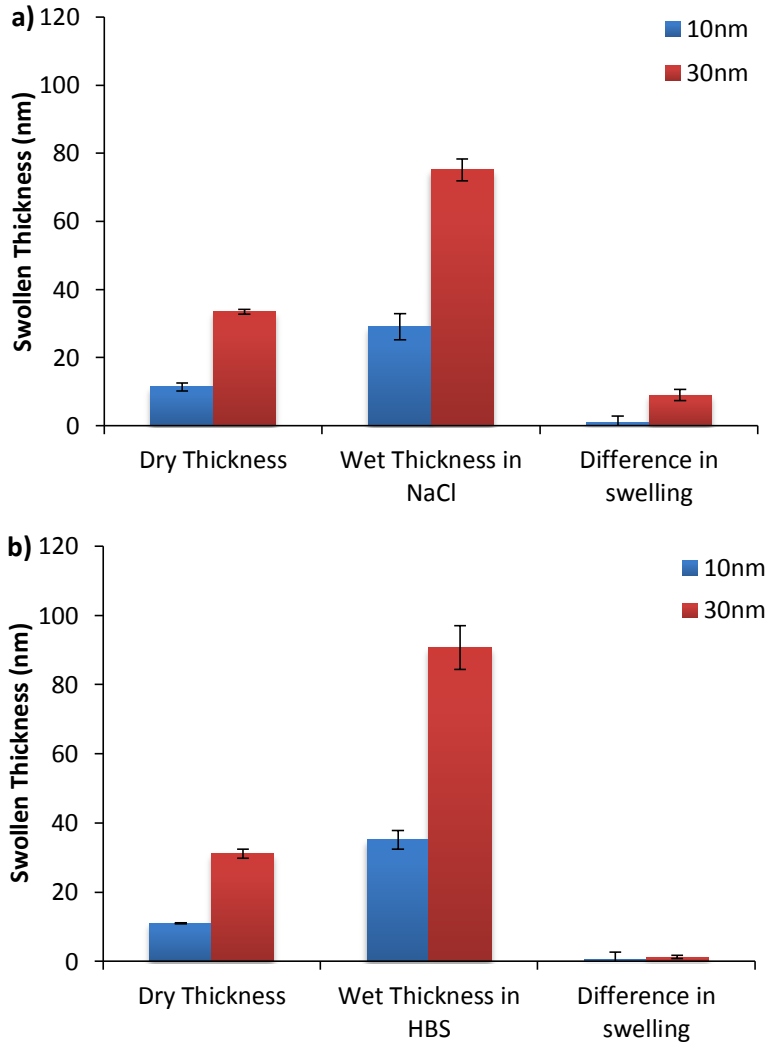

Figure 47: Changes in swelling behaviour of PDMAEMA, grafted on silicon substrates, after adding DNA in a) 150 mM NaCl or b) 10 mM HBS. Results are expressed as mean ± SE, n ≥ 3.

Several processes could have opposite effects on the evolution of the measured ellipsometric thickness as increase in bound material should result in an increase in thickness, whereas the complexation of cationically charged brushes by negatively charged DNA could result in the expulsion of some solvent present in the brush and, as a result, a decrease in the swollen thickness. The latter phenomenon is not supported by an increase in RI of the coating, or an improvement of the fits with a bilayer model. For both brush thicknesses in 150 mM NaCl, the RI decreased from 1.4 to 1.39 indicating the addition of highly hydrated DNA molecules rather than the collapse of the brush-DNA construct whilst in 10 mM HBS, there was no change in

the RI. The quality of the fit, defined by the Mean Squared Error (MSE), also did not change with the addition of DNA and confirms that the brush is not collapsing when binding with DNA. In any case, the stronger DNA adsorption observed by ellipsometry on 30 nm brushes, as opposed to 10 nm brushes, indicates that SPR was underestimating DNA binding.

Hence, the picture emerging from the combined SPR and ellipsometry data is that DNA adsorption occurs only at the surface of the brush, with a slow infiltration process, leading to further DNA being immobilised after repeated injection. In addition, immobilisation in HBS systematically showed lower binding levels, highlighting the importance of the choice of buffer to stabilise brush-DNA complexes and potentially optimised the transfection process.

2.3.10.3 Particle size and zeta potential

The DNA binding to polymer-brush coated nanoparticles was studied next via DLS and ELS and compared to results obtained via SPR and ellipsometry for brushes grown from flat surfaces.

The principal factor involved in condensation of DNA is the electrostatic interaction between the positively charged groups of the cationic polymer and the negatively charged phosphate groups of DNA, resulting in the release of counterions and gain in entropy.[432, 442] The persistence length of DNA and the distance between its ends alongside the excluded volume also determines its ability to be compacted.[443] Large electrostatic repulsion between the two strands and the inherent stiffness of the uncharged helix maintains the elongated coil state of DNA. These electrostatic interactions and the persistence length are, however, reduced as a result of shielding in high salt conditions.[444] This illustrates the importance of the solvent strength and the cationic charges of the counterions in DNA condensation.

The DNA-brush interactions of the range of brush-decorated particles, was examined via dynamic light scattering, using similar conditions as for the preparation of complexes for transfection, but with a fixed plasmid concentration of 10 µg/mL (compared to 1 µg/mL for transfections experiments). This is due to the detection limits of the DLS. The N/P ratio of the polymeric nanoparticles/DNA complexes were varied from N/P 1:1 to N/P 20:1 and the study was performed in 150 mM NaCl. The N/P ratio strongly affected the charge and size of the complexed system.

At equal ratio, DNA was condensed efficiently with PDMAEMA-coated particles displaying a reversal in their zeta potential and a decrease of their size (Figure 48). Naked plasmid

possessed a negative zeta potential of -20 mV and a hydrodynamic diameter of around 200 nm (PDI ≈ 0.5), under the same conditions (pH, ionic strength) as used for the preparation of the polymer-DNA nanoparticles. Hence, at an N/P ratio 1:1, although 0 mV is expected due to the compensation of every positive charge with a negative charge, a charge reversal occurs post-binding as the particles become saturated with DNA. This suggests a partial insertion of plasmid DNA molecules into the polymer brush resulting in the complete saturation of the surface of the brush and thus forming a negative shell around the particles. Therefore the charge reversal indicates a complete coating of the particles, with negatively charged phosphate groups now presented on the surface. The collapse of the brush-DNA complexes, as evidenced by the reduction in the size of particles suggest that complexation results in the neutralisation of the brush and expulsion of solvent molecules. This behaviour contrasts with ellipsometry results, which showed a slight increase in swollen thickness upon DNA binding. This is perhaps the result of lower N/P charge ratios in ellipsometry experiments, as the DNA concentrations used are expected to be in excess of the total density of DMAEMA molecules present in the brush.

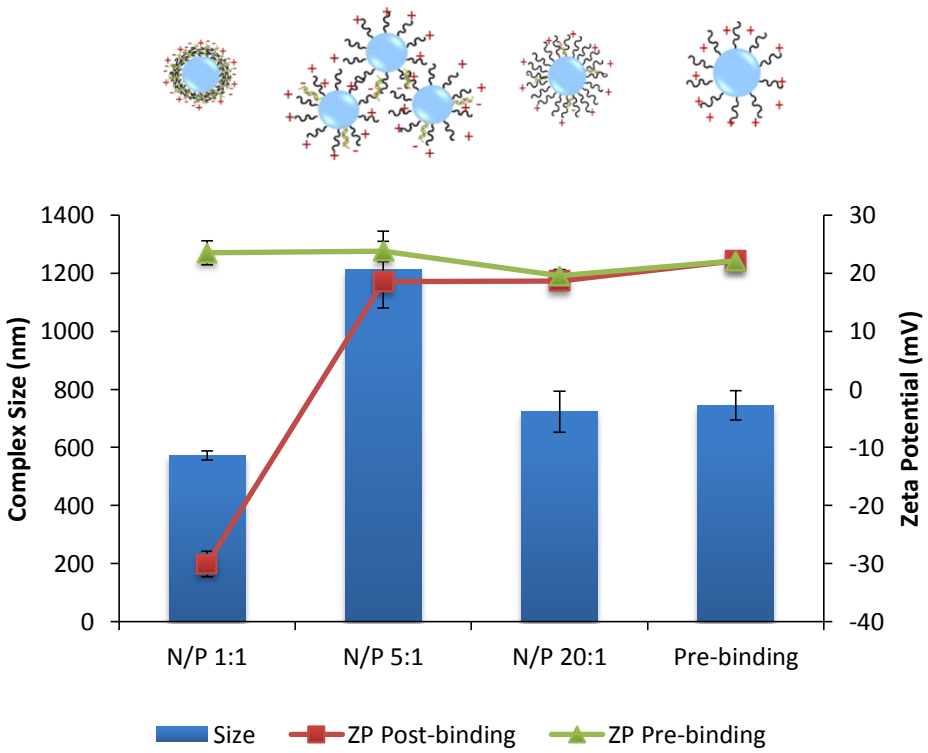

Figure 48: Changes in complex size and zeta potential (ZP) before and after DNA binding with PDMAEMA-grafted silica nanoparticles at varying N/P ratios in 150mM NaCl buffer. Values represent mean ± SE, n = 3.

At N/P ratio of 5:1 or above, positively charged complexes were formed. With increasing N/P ratios, large excess of positive charges are present therefore DNA molecules are not able to fully neutralise the surface of brushes. This implies also perhaps some level of infiltration, so that segments of PDMAEMA brushes are exposed at the surface of particles.

Particle size also increase significantly at higher N/P ratios, due to aggregation caused by partial insertion of DNA which then allows interaction of one plasmid DNA molecule with more than one particles. This phenomenon seems especially marked at a moderate N/P ratio of 5:1, compared to 10:1 and 20:1. This is presumably a result of the higher concentration of DNA per particles at a 5:1 charge ratio, which may allow several particles to quickly interact with one DNA molecule, before it fully complexes with the brush coating as a single particle. In addition, at higher N/P ratios, the PDI index showed a tendency to increase, at times reaching 1, thus indicating that the particle distribution widened hence readings were taken such that any hydrodynamic diameter with a PDI of above 0.5 were excluded. Hence, potentially larger aggregates can be expected.

The DNA binding behaviour of particles decorated with copolymers showed important differences compared to 100% PDMAEMA brush-coated particles. For these experiments, the amount of polymer (calculated from TGA) and DNA was kept constant. Hence the N/P ratio (which corresponded to 5:1 for 100% PDMAEMA brushes) gradually increased as the density of positively charged ammonium groups decreased.

Hence, varying the copolymer ratio changed the charge density and resulted in lower excess of positive charges as the ratio of DMAEMA/OEGMA decreased. This phenomenon explains the observation that 50-100% DMAEMA copolymers displayed positive zeta potentials and increased sizes after DNA binding (presumably due to aggregation), whereas 25% DMAEMA brushes displayed a negative zeta potential indicating a full coverage of the particle surface with DNA molecules and a lack of complete infiltration within the brush (Figure 49a and Figure 49b). The lack of collapse of 25% PDMAEMA brushes post-binding still indicates some level of aggregation, and potentially a poorer condensation of the copolymer brush, due to the presence of OEGMA repeat units. For 0% PDMAEMA, the lack of positive charges on the POEGMA structure resulted in almost no interaction with DNA as evident from the unaffected zeta potential.

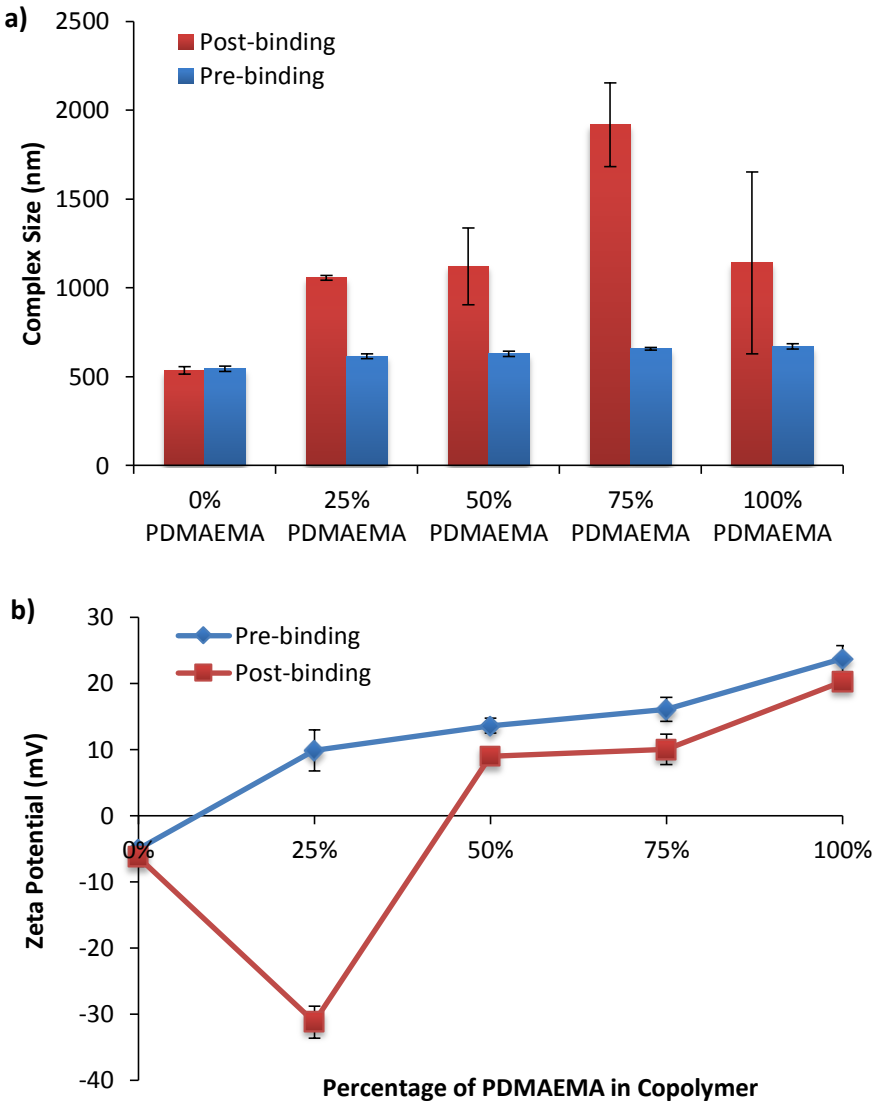

Figure 49: Effect of charge density on the interaction of polymer brush-coated SiO_2 nanoparticles with DNA at N/P ratio 5:1, in 150 mM NaCl, in terms of a) the complex size and b) the zeta potential. Values represent mean ± SE, n ≥ 15.

It is evident from the DNA interaction data obtained from DLS and ELS measurements that DNA-particle interactions are generally likely to form aggregates at N/P ratios typically used for DNA transfection experiments (N/P 1:1 to N/P 20:1). Furthermore, the slight reductions in zeta potential of the resulting complexes will also have an impact on their interaction with the cell membrane.

2.4 Summary

Controlled brush growth was achieved with PDMAEMA and the copolymer brushes, as confirmed by ellipsometry, NMR, FTIR, GPC and Zetasizer. Both PDMAEMA and PDMAEMA-*co*-POEGMA brushes was synthesised to give a thickness of 30 nm. A molecular weight of approximately 25,000 Da was also obtained in line with the molecular weights of existing non-viral vectors presented in literature. Polymer brushes were introduced onto a silica core as it allows easy modification of the surface, has controlled morphologies and is biocompatible. Moreover, the size and shape of nanoparticles are known to have a considerable impact on their interaction with cells. PDMAEMA brush grafted from silica nanoparticles gave an average hydrodynamic diameter of approximately 820 nm and a zeta potential of 43 mV, in deionised water. It was clear that the charge density, pH, ionic strength, N/P ratio and complex size all have a significant impact on the polymer brush's behaviour in the respective testing systems. With increasing incorporation of the neutral POEGMA brush in the copolymer system, the zeta potential was seen to decrease rapidly whilst also displaying a decrease in the hydrodynamic diameter. The charge titration study demonstrated a decrease in the zeta potential with increasing pH with a dramatic drop between pH 7-9, in the range of the pK_a of PDMAEMA. In 150 mM NaCl and PBS buffers, both the hydrodynamic diameter and the surface charge of the brush-grafted nanoparticles were noticeably lower compared to that in deionised water, owing to the different ionic strength which in turn alter the osmotic pressure surrounding the brush system. It was evident from the DNA interaction study that the cationic charge of the brush enables electrostatic interaction and a useful N/P ratio range of 3:1 to 20:1 were established for later use in transfection. The complex size was also dependent on the N/P ratio – with increasing N/P ratio and hence increasing cationic charge, the complex sizes were observed to be fluctuating due to partial insertion of DNA and aggregation.

The responsive nature of PDMAEMA confirmed through these series of characterisations indicates a great scope for it to be tailored for its efficient use in gene transfection.

Chapter 3 - Polymer brush interaction with cells and transfection efficiency

3.1 Introduction

The way in which cells interact with charged surfaces is important as knowledge of this can be useful for the development of valuable biomaterials for tissue engineering and regenerative medicine, particularly in antimicrobial coatings,[445, 446] improving implant biocompatibility,[447, 448] and facilitating gene/drug delivery.[172, 449, 450] The bulk of the literature on brush interactions with cells focused on the study of bacterial cells exposed to polymer brush functionalised nanoparticles or surfaces. Polymer brushes are a good model system for studying cell-brush interactions as they allow to control surface chemistry independently of other physical and geometrical parameters.[267, 309] Cheng *et al.* have shown that switchable polymer brushes, poly (*N, N*-dimethyl-*N*-(ethoxycarbonylmethyl)-*N*-[2'-(methacryloyloxy) ethyl]-ammonium bromide) (PCBMA-1 C2, cationic precursor), can kill bacterial cells effectively in its cationic form and also switch to a zwitterionic non-fouling surface which releases the dead bacterial cells upon hydrolysis.[451] The latter surface also prevents any further adsorption of proteins/micro-organisms thus reducing biofilm formation on surfaces. These novel switchable properties of the polymer brush make it a promising coating for medical implants to prevent implant failure caused by microbial adhesion and the subsequent biofilm formation. Other brushes which have been investigated with potential for use with implantable devices include cationic poly(2-vinyl pyridine) (P2VP), quaternized P2VP, and PEG mixed with P2VP and quaternized P2VP. Altering the polymer brush composition allowed regulation of bacterial cell adhesion.[452] Other functionalised polycationic brushes investigated for their antibacterial effects include chitosan,[453] poly (glycidyl methacrylate) (PGMA),[454] PHEMA[455] and poly (ionic liquid),[456] alongside unfunctionalised PMETAC.[229]

Polymer brushes also have great potential in siRNA therapeutic application. CCC with highly dense PEG brush has been shown to reinforce interpolyelectrolyte complex between PLL backbone and siRNA. It displayed higher selectivity in its ionic interaction with siRNA than other anionic substances in the blood stream. The study showed that this polyplex carrier was the first example amongst other carriers in prolonging blood circulation time of unmodified

siRNA.[242] Another example in which cationic polymer brushes have been used at the cell interface is the use of strong, cationic PMETAC brush for the directed growth of rat hippocampal neurons with the capacity to be used in the coating of neural devices or in cell-based nanosensors.[403, 457]

The cationic polymer brush of interest in the present study, PDMAEMA, is, in addition to being useful in antibacterial coatings,[287, 458, 459] also suitable for use as a non-viral gene delivery vector[241, 245, 247, 250] as it is safer and easier to fabricate than viral vectors. However, their comparatively low transfection efficiency alongside the polymer brush's cytotoxicity has limited its applications and has prompted further investigations into improving efficiency. Consequently, a versatile non-viral gene delivery system was developed for this study; a tailorable system where the charge, grafting density and chemistry of the polymer brush as well as the size and shape of the nanoparticle could be altered (See Chapter 1.4, Figure 18). Having studied the DNA condensation and complexation via changes in the hydrodynamic diameter and zeta potential in the previous chapter, the effectiveness of this process together with endocytosis and nuclear entry can be confirmed by determining the gene transfection efficiency. Whilst the cytotoxicity was investigated through live/dead assay using human primary keratinocytes and human adult low calcium temperature keratinocytes (HaCaT), the gene delivery efficiency of f-PDMAEMA and its copolymer, and SiO_2-g-PDMAEMA nanoparticles were evaluated through conducting *in vitro* transfection assays on HaCaT, dermal fibroblasts (HCA2)[460] and HeLa cell lines, using the EGFP reporter gene. The positive control used in the experiments was jetPEI®, a commercially available transfection reagent, described as a 'linear polyethylenimine derivative, free of components of animal origin' by PolyPlus Transfection. Human keratinocytes were initially used as these cells are relevant in skin biology, especially in regenerative medicine strategies and wound healing. Some diseases pertaining to the skin such as epidermolysis bullosa can potentially be tackled by gene delivery. As primary human keratinocytes were discovered to be hard-to-transfect cells, HaCaTs, a keratinocyte cell line, was used instead. It was important to determine whether transfection efficiency was cell line-dependent hence the HeLa cells which have been shown to easily transfect were compared with HaCaTs and HCA2 cell as the latter are another type of cells with a different phenotype and therefore aided in the understanding of whether the transfection efficiency is specific to one cell line investigated or whether it could be generalised. As transfection efficiency is ultimately dependent on the amount of DNA molecules delivered to the nucleus, and the amount of nuclear DNA molecules that undergo transcription, the cellular uptake of the SiO_2-g-nanoparticles was also probed.

3.2 Experimental methods

3.2.1 Materials for cell culture and immuno-staining

Versene (Gibco), Trypsin (0.25%, Gibco), Dulbecco's Modified Eagle Medium (DMEM, Gibco), DMEM-F12 (Gibco), L-Glutamine (200 mM, Gibco), Penicillin Streptomycin (PS, 5000 U/mL, Gibco), KSFM (Gibco) were purchased from Life Technologies. Collagen (rat, type I, BD Sciences, San Jose, CA), foetal bovine serum (FBS, LabTech) and sterile Dulbecco's Phosphate Buffered Solution (DPBS, PAA Laboratories/ Sigma-Aldrich) were also used. KSFM supplemented with 1 mL pituitary extract (Gibco), 3 µL EGF human recombinant (Gibco) and 5 mL PS, FAD medium prepared with 100 mL DMEM, 100 mL DMEM-F12, 20 mL FBS, 2.2 mL PS, hydrocortisone (0.5 µg/mL) containing 10^{-10} M cholera toxin, 10 ng/mL EGF and insulin (5 mg/mL), and DMEM medium supplemented with 50 mL bovine serum, 5 mL L-glutamine and 5 mL PS were used for the culture of primary keratinocytes and fibroblasts, respectively. 4',6-Diamidino-2-phenylindole dihydrochloride (DAPI, Sigma), 4% paraformaldehyde (PFA) prepared from 16g PFA (Sigma Aldrich) and PBS (Sigma-Aldrich) dissolved in deionised water, 0.2% Triton X-100 prepared from Triton X-100 (Sigma Aldrich) and PBS were used for immunostaining. EGFP was used for cell transfection. LIVE/DEAD® Viability/Cytotoxicity Kit containing 4 mM calcein AM in anhydrous dimethyl sulfoxide (DMSO) and 2 mM ethidium homodimer in DMSO/H_2O 1:4 (v/v), for mammalian cells was purchased from Life Technologies.

3.2.2 Toxicity studies

3.2.2.1 Cell interaction with brush-functionalised nanoparticles

Cell culture

HaCaT cells were cultured in DMEM medium supplemented with 10% FBS, 1% L-glutamine and 1% PS. Cells cultured in a T75 flask, incubated at 37°C were washed with 10 mL DPBS, then dissociated with Versene/trypsin (4/1 v/v, 5 mL) for 15 min. The trypsin was quenched with 15 mL DMEM medium, transferred to a centrifuge tube and centrifuged at 1200 rpm for 5 min. The supernatant was aspirated and the cells were resuspended in 10 mL DMEM medium before determining the number of cells using an haematocytometer. The well-plates were coated with 20 µg/mL collagen diluted in DPBS per well, for 30 min at RT, and washed with

DPBS. The cells were then seeded at a density of 25k cells per well (500 µL) in two separate 24-well plates and live/dead assay was carried out at 4 h and 24 h time points.

The medium was replaced from each well with 500 µL KSFM without supplements on the following day. Cells were either incubated with particle suspensions only or particle suspensions with DNA in the N/P ratios 1:1, 3:1, 5:1, 7:1, 10:1 and 20:1. A set of 3 wells per well plate, containing cells, were also incubated with jetPEI and DNA (positive control).

DNA complexation was first carried out by adding 50 µL of 150 mM NaCl containing 1 µg of EGFP plasmid (i.e 2.8 µL of 0.358 µg/µL EGFP stock solution) to 50 µL of 150 mM NaCl containing PDMAEMA-coated particles (3.8 mg/mL stock solution concentration) of the required N/P ratios (N/P 1:1 = 1.3 µL, 3:1= 3.9 µL, 5:1=6.5 µL, 7:1=9.1 µL, 10:1=13 µL, 20:1=26 µL). These were incubated for 15 min at room temperature. 100 µL of each complex was then added dropwise into a row of wells (24-well plate) containing the cells as prepared above. In addition, 100 µL of 150 mM NaCl containing PDMAEMA-coated particles (3.8 mg/mL) were then added dropwise into another row of the 24-well plate in which cells had been seeded as above. After 4 h or 24 h, the medium in the well was replaced with 1 mL DMEM containing 4 mM calcein AM (0.5 µL) and 2 mM ethidium homodimer (2 µL). The well-plates were incubated for 30 min at 37°C, and imaged using a Leica DMI4000B Epifluorescent Microscope after their respective time-points. Images were taken at three different points per well and cell counts were obtained via ImageJ analysis to determine % live cells and total number of cells per mm^2.

3.2.2.2 Cell-brush interaction on flat substrates

Cell culture

Primary human epidermal keratinocytes (isolated from neonatal foreskin) were maintained with feeders; J2 3T3 fibroblasts. FAD medium was used to culture keratinocytes on feeders whilst DMEM was used for the culture of feeder cells. To harvest keratinocytes (T75), the feeder cells were removed by incubating with versene (5 mL, 37°C) only for 5-10 min and gently shaking and tapping the side of the flask. Then, the keratinocytes were dissociated from the flask via trypsinisation (versene/trypsin, 4/1 v/v, 5 mL, 37°C) for an extra 5 min. 15 mL of FAD medium was then added to the flask to quench the trypsin, transferred to a 50 mL centrifuge tube and centrifuged at 1,200 rpm for 5 min. After discarding the supernatant solution, the pellet was resuspended in 10 mL FAD medium and the concentration of cells was measured with a haematocytometer. Cells were re-seeded onto polymer brush-coated

substrates, which were sterilised using 70% ethanol and washed with DPBS, at a density of 75k cells per well (in 500 µL of KSFM medium) in 24-well plates. Quantification of cell viability was carried out via a live/dead assay, by incubating cells in 1 mL FAD medium containing 0.5 µL of 4 mM calcein AM and 2 µL of 2 mM ethidium homodimer, for 30 min prior to imaging. Time points at which the cell viability and the total number of cells were measured at were 5 min, 15 min, 30 min, 1 h, 2 h and 4 h, for PDMAEMA homopolymer brushes, and 2 h for copolymer brush-coated substrates (0%, 10%, 25%, 50% and 100% PDMAEMA: POEGMA). Fluorescence imaging was used to capture the live-dead cells and these were counted via ImageJ to obtain % live cells and total no. of cells per mm^2.

3.2.3 Transfection assay

3.2.3.1 Materials

7.5 mM solution of JetPEI® (Polyplus), 150 mM NaCl (Polyplus), EGFP, mTEAL, KSFM (without supplements, Gibco), Opti-MEM® (Gibco), DMEM (Gibco, with 10% FBS, and without supplements) were used.

3.2.3.2 Optimisation of parameters

The protocol for the transfections with PDMAEMA (free polymer and particles) was adapted from jetPEI® *in vitro* DNA Transfection Protocol from PolyPlus transfection™.

2 µL of jetPEI® per µg of DNA was used as a control, following a protocol recommended by the manufacturer and after testing of a restricted number of conditions (jetPEI® and DNA concentration, cell density, time of incubation) in our cell culture system. For transfection with polymer brushes and free polymers, 1 µg of DNA, 2 µL of jetPEI® reagent and PDMAEMA-g-SiO_2 at N/P ratios 1:1, 5:1 and 20:1 were diluted in 50 µL of 150 mM NaCl solution separately. 50 µL of the resulting cationic polymer solution was then added to the 50 µL DNA solution (adding in the reversed order can reduce transfection efficiency), the resulting solution mixed gently and then incubated for 15 to 30 min at room temperature. 100 µL of the cationic polymer/DNA mix was then added dropwise to each well containing the cells seeded on the previous day (density: 50k or 75k) in 1 mL of KSFM and gently mixed by moving the plate side-to-side. The complexes were incubated with the cells for 4 hours then the medium was

replaced with KSFM with supplements. The cells were incubated for a further 24 h to allow sufficient expression of the plasmid DNA before performing reporter gene assay.

Variation of cell density and medium type

The transfection experiments thereafter were altered by initially changing the density of the cells seeded per well to 5k, 10k, 20k and 40k. Seeding densities of 20k and 40k were used in the subsequent experiment. Incubation with complexes was carried out with FAD or KSFM for 4 h before replacing with KSFM.

Variation of cell type and plasmid type

Another series of experiments were conducted using different types of cells and different types of plasmids. HaCaTs were seeded initially at 20,000 cells/well and HCA2 were seeded at 40,000 cells/well. Transfection efficiency was tested with mTEAL and EGFP plasmids, using different batches of EGFP, in DMEM medium with and without serum or KSFM.

Transfection with free polymers

In order to explore the role of the brush architecture on transfection, f-PDMAEMA at N/P ratios of 1:1 and 5:1 were also tested. N/P ratios 3:1, 5:1, 7:1 and 10:1 were subsequently selected for transfection studies based on the charge distribution and toxicity of the cationic polymer/DNA complexes. HaCaT cells were seeded at 30k for these experiments. F-PDMAEMA of different molecular weights ($M_n \approx$ 11,000 and 27,000 g/mol described as low and high molecular weight PDMAEMA were also examined at N/P 3:1, 5:1, 7:1 and 10:1, using KSFM without supplements during complex incubation and replaced with KSFM with supplements after 4 h. As a comparison, HeLa cells, seeded at 20,000 cells/well, were also transfected with jetPEI®, free PEI (Sigma Aldrich, M_w = 25,000 g/mol) and f-PDMAEMA, using KSFM without supplements for complex incubation for 4 h and KSFM with supplements for 24 h prior to performing reporter gene assay. Lipofectamine® 2000 (Life Technologies) was also used in the same cell line but with Opti-MEM medium for both complex incubation and plasmid expression.

The different parameters tested during the optimisation phase are summarised in Figure 50 and following this optimisation process, a cell seeding density of 25k, KSFM without supplements for the complex incubation for 4 h, KSFM with supplements for plasmid expression for 24 h and N/P ratios of 3:1, 5:1, 7:1, and 10:1 were chosen for further testing with SiO2-g-PDMAEMA nanoparticles.

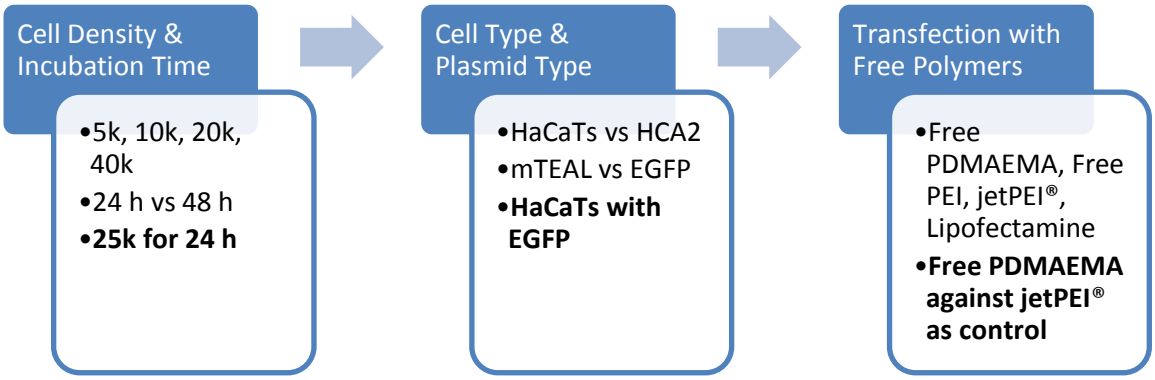

Figure 50: Summary of parameters optimised during assay development.

3.2.4 Cellular uptake

3.2.4.1 Materials

FITC-300 nm mesoporous silica nanoparticles were provided by Tina Gulin, Åbo Akademi University. Dil stain (Molecular Probes) and Hoescht 33342 (Molecular Probes), 2-bromoisobutyryl bromide (BB, Sigma-Aldrich), Et_3N (Sigma-Aldrich), (3-Aminopropyl)triethoxysilane (APTS, Sigma-Aldrich), anhydrous toluene (Sigma-Aldrich), deionised water with resistivity of 18.2 MΩ·cm (Millipore) and ethanol (absolute) (VWR Chemicals) were used as received.

3.2.4.2 Deposition of BB initiator on labelled particles

100 mg FITC-300 nm mesoporous silica nanoparticles were redispersed in 20 mL anhydrous toluene and stirred. 1032 µL (3.7 mmol) Et_3N was added and the dispersion was placed in an ice bath for 30 min to cool to 0°C. 0.5 mL (2 mmol) BB was added to the dispersion, drop-wise,

under vigorous stirring and the reaction was allowed to proceed at 0°C for 1 h and then at room temperature overnight. The BB-coated nanoparticles dispersion was centrifuged at 4000 rpm for 10 min and redispersed in toluene via two centrifugation/washing cycles, followed by washing with ethanol twice before finally redispersing in 2 mL ethanol.

3.2.4.3 Growth of PDMAEMA on labelled particles

PDMAEMA brush was synthesised on BB-functionalised silica by preparing the monomer/catalyst solution as in section 2.2.4.2. 400 µL BB-functionalised silica nanoparticles (50 mg/ mL), 400 µL ethanol and 3.2 mL deionised water were degassed with argon bubbling for 15 min, followed by polymerisation for 20 min after adding 4 mL of monomer/catalyst solution. PDMAEMA-coated nanoparticles were washed and collected as described previously, and were finally redispersed in 4 mL deionised water.

3.2.4.4 Cellular uptake study

24-well plates, containing Ø12mm coverslips were washed three times each with ethanol and PBS, and coated with 10 µg/mL collagen Type 1 (BD Biosciences). HaCaTs were seeded in the well-plates as described previously.

Fluorescently labelled silica nanoparticles grafted with PDMAEMA were used to obtain complexes with DNA at the previously mentioned N/P ratios and added drop-wise into wells seeded with cells.

After 4 h and 24 h, the well medium was replaced with DMEM medium containing Hoescht 33342 (1 µg/mL), and incubated for 20 min at 37 °C. The cells were then fixed with 4% PFA for 10 min and washed with PBS twice before the coverslips were removed from the well-plate, washed with medium, dried and mounted on glass slides with mowiol, and studied under Leica Epifluorescent Microscope.

3.2.5 Characterisation

Fluorescence images were acquired using Leica Epifluorescent Microscope DMI4000B for the transfection assays and cellular uptake assays. Zetasizer Nano ZS was used to measure the

hydrodynamic diameters of the PDMAEMA-g-labelled SiO_2 nanoparticles, following the protocol described in section 2.2.5.6. SEM was used to study qualitatively the homogeneity of the size of the mesoporous silica nanoparticles and solid silica nanoparticles, with and without PDMAEMA brush.

3.2.6 Statistical Analysis

The statistical analysis was performed for the cell viability and transfection results via either one-way ANOVA followed by Tukey's test using OriginPro 9.0 or pairwise Student's T-test for post hoc analysis where p values < 0.05 were considered significant (* = $p<0.05$, ** = $p < 0.01$ and *** = $p < 0.001$).

All data values are expressed as mean ± standard error (SE) where $n \geq 3$.

3.3 Results and discussion

3.3.1 Adhesion and Toxicity studies

The interaction of PDMAEMA with cells is of significance for effective gene delivery, hence the cytotoxicity of PDMAEMA was studied through the exposure of cells to silica nanoparticles coated with the brush, and through depositing cells on a flat, gold substrate coated with brush. The former gave useful information about the toxicity of the cells when they are in contact with the brush-coated nanoparticles or when cellular uptake of the particles occurs, whilst the latter presented information on whether contact itself was sufficient to induce cell death.

3.3.1.1 Particles

As the extent of cytotoxicity of all polymers is concentration- and time-dependent, the cell viability of HaCaT (seeding density: 25,000 cells/well) on interaction with SiO_2-g-PDMAEMA nanoparticles was studied at a fixed plasmid concentration of 1 µg/ mL with six different PDMAEMA/plasmid ratios – N/P 1:1, 3:1, 5:1, 7:1, 10:1 and 20:1, and at two different time points; 4 h and 24 h (Figure 51). The cell viability was calculated as a percentage of total number of cells; acquired by counting the number of live and the number of dead cells in each fluorescent image (n = 3 per well).

The colloidal silica core used in this study is bioinert[92, 461] hence does not influence cytotoxicity greatly whilst its cationic coating largely contributes to the toxicity depending on the concentration of the polymer. At N/P 1:1 (1.5 µg/ mL polymer concentration), the cell viability did not change considerably in comparison with the control of cells alone. The cytotoxicity around N/P 5:1 and below was marginal with the lowest viability at 42 % (SE = 8 %) whilst N/P ratio nearing 20:1 exhibited substantial toxicity with a decrease in the cell viability by 69-81 % depending on the exposure time and presence of DNA, compared to the control (untreated cells). At 24 h, cells have been able to divide and proliferate to some extent and hence higher cell viability is generally observed than at the 4 h time points. However, prolonged exposure would be normally expected to result in increased cytotoxicity as indicated by the results reported by Kean *et al.* who investigated the cytotoxicity of trimethylated oligomeric and polymeric chitosan at 6 h and 24 h time points, against COS-7 and MCF-7 cells using an MTT assay.[462] The results showed that increasing the exposure time decreased the viability in both

cell lines. The time-dependent nature of cytotoxicity was also seen with a number of polycations in L929 mouse fibroblasts.[348] Longer incubation times resulted in more pronounced cell debris and changes in cell morphology.

The general trend also indicates that the polymer brush coated nanoparticles displayed increased viability upon complexation with DNA than those without DNA, especially in the intermediate range of concentrations of polymer particles (N/P 3:1 – 7:1). This is likely to be an outcome of the shielding of positive charges on the surface of the brush by DNA molecules, which in turn protects the cells by limiting membrane disruption, as has been observed in the literature.[84, 181] At the higher N/P ratios, the positive charges dominate due to higher polymer concentration as evident from the DNA interaction study in Chapter 2.3.10.3 (Figure 48), hence increased cell death is seen as a result of the strong electrostatic interactions with negatively charged phospholipids forming the cell membrane[348] leading to permeabilisation of the cell membrane, loss of proteins in the cytoplasm and collapse of the membrane potentials. The dead cells will burst or undergo apoptosis.

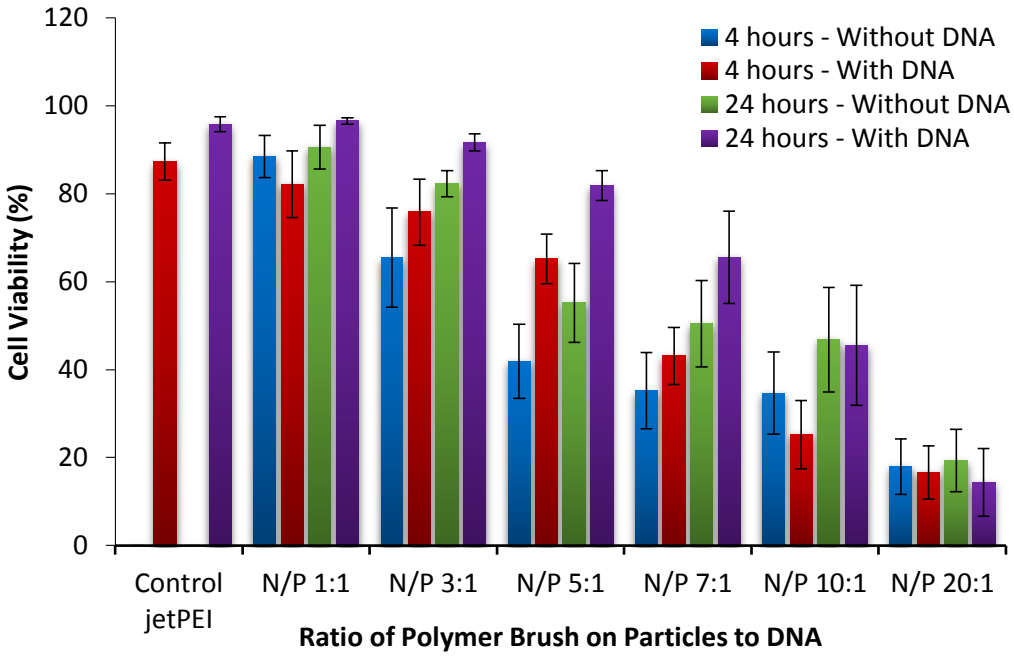

Figure 51: Cell viability assay based on interaction between HaCaTs and SiO_2-g-PDMAEMA nanoparticles (3.8 mg/mL stock solution concentration), at 4 h and 24 h time points, with and without DNA (1 µg/mL), where N/P 1:1=1.5 µg/mL, N/P 3:1=4.5 µg/mL, N/P 5:1=7.4 µg/mL, N/P 7:1=10.4 µg/mL, N/P 10:1=14.8 µg/mL, N/P 20:1=29.6 µg/mL. Control is jetPEI with DNA at 4 h and 24 h. Values represent mean ± SE, n = 12.

The charge density arising from the number and three-dimensional arrangement of the cationic residues of the polymer brush is a crucial factor for cytotoxicity. According to Ferruti and co-workers, tertiary amine groups display lower toxicity than those with primary and secondary residues and this was confirmed by Fischer *et al*.[348, 463] Therefore PDMAEMA, with its tertiary amines, would be expected to display lower cytotoxicity than other coatings with primary or secondary amines and this may be reflected in the relatively low toxicity observed at moderate N/P ratios.

Understanding the relationship between the structure of the SiO_2-g-PDMAEMA nanoparticles and toxicity is useful for lowering the cytotoxicity and optimising the biocompatibility of the non-viral gene delivery system. In addition to the cationic charge density, the type of cationic functionalities, the molecular weight, structure and sequence as well as the conformational flexibility of the polymer can be critical parameters affecting interaction with the cell membrane and so can be tuned to optimise biocompatibility. However, prior to investigating these factors, it is important to determine whether the toxicity is caused by direct contact of the cell with the polymer brush on the nanoparticles or as a result of an interaction process occurring after initial contact. Hence interaction of cells with flat surfaces would be a sufficient model to identify the possibility of cytotoxicity occurring upon immediate contact.

3.3.1.2 Flat substrate

The mechanism of cytotoxicity is yet to be fully understood; it is unclear whether the toxicity is a result of the interaction of the polymeric particles with the cell membranes or caused by cellular uptake and subsequent activation of intracellular signal transduction pathways or toxicity to organelles, hence a cytotoxicity assay was conducted with flat surfaces coated with PDMAEMA brush. These flat substrates cannot be endocytosed and therefore any toxicity arises from direct disruption of the cell membrane.

3.3.1.2.1 Kinetics

This primary interaction study between cells and PDMAEMA-coated gold substrates provided an insight into the number of cells that are able to adhere as well as how many remain alive as a function of contact time with the charged surface and variations in the charge density of

the surface. Unlike adhesion to extracellular matrix, cells that are adhering here are adhering to a toxic surface.

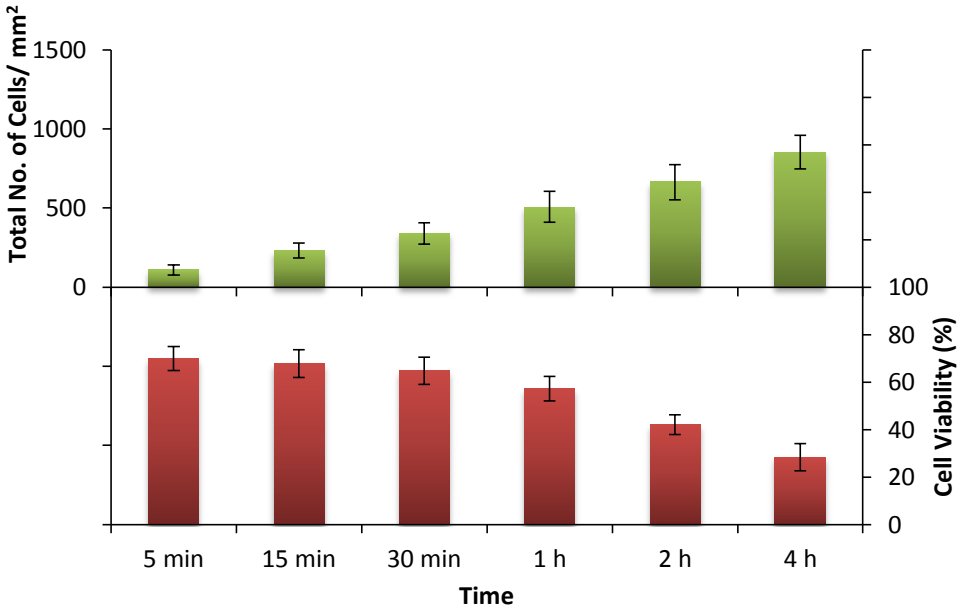

Figure 52: Total number of cells (top), and % live cells (bottom) with increasing time when keratinocytes are cultured in FAD and seeded onto PDMAEMA brush-coated substrate. Values represent mean ± SE, n = 32.

Figure 52 shows the long-term effect of contact between cells and the brush on the density of cells adhered and their viability. Results showed that non-specific cell adhesion to the PDMAEMA brush takes time. Cells that adhered in the first 5 min to 1 h remained mostly alive with the viability above 50%. The number of cells per mm^2 increased consistently with time, from 108 (SE = 31) cells per mm^2 to 853 (SE = 107) cells per mm^2, approximately an eight-fold increase.

The decrease in the number of viable cells with time is understood to be due to the positive charge of PDMAEMA brushes, which can disrupt the cell membrane. Strong electrostatic interactions between the brush and the negatively charged membrane perturbs the phospholipid bilayer and alters the osmotic pressure causing cell death.[246, 348, 464] The number of cells dying increases with prolonged exposure to the brush (Figure 53). This suggests that direct contact with the substrate is not sufficient to instantaneously cause cell death and that membrane disruption takes time. Alternatively, membrane damage may initiate stress signals resulting in delayed cell death.

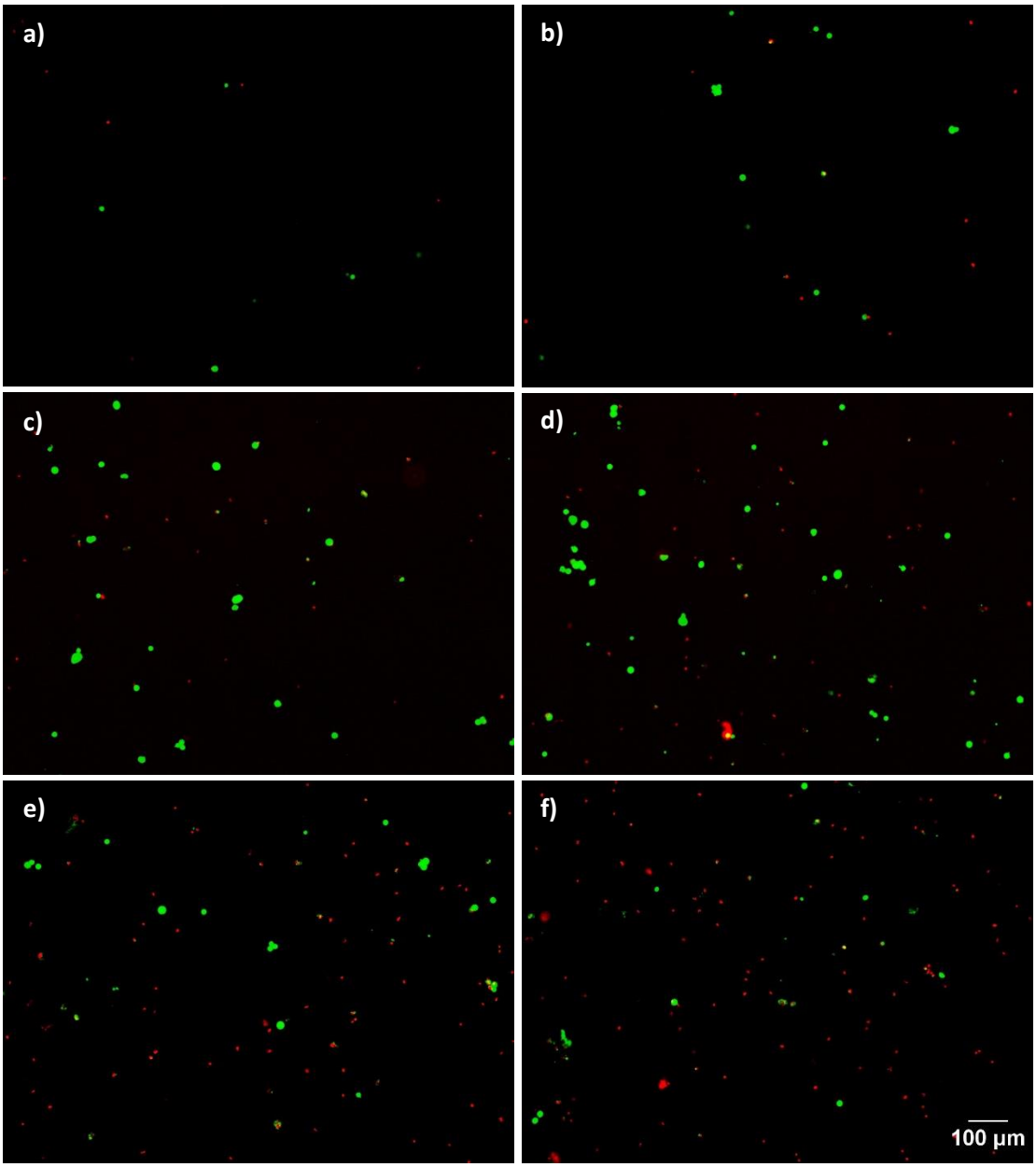

Figure 53: Fluorescence microscopy images (magnification 10x) representing the change in cell viability of keratinocytes with increasing exposure time to PDMAEMA brush coated Au substrate, a) 5 min, b) 15 min, c) 30 min, d) 1 h, e) 2 h and f) 4 h. Live cells (green) and dead cells (red).

3.3.1.2.2 Copolymer brush

As charge density is known to be an important factor affecting cytotoxicity, the impact of changing surface charge density on the cell viability via copolymer brushes on keratinocytes was studied. The cell viability after a contact time of 2 h is presented in Figure 54.

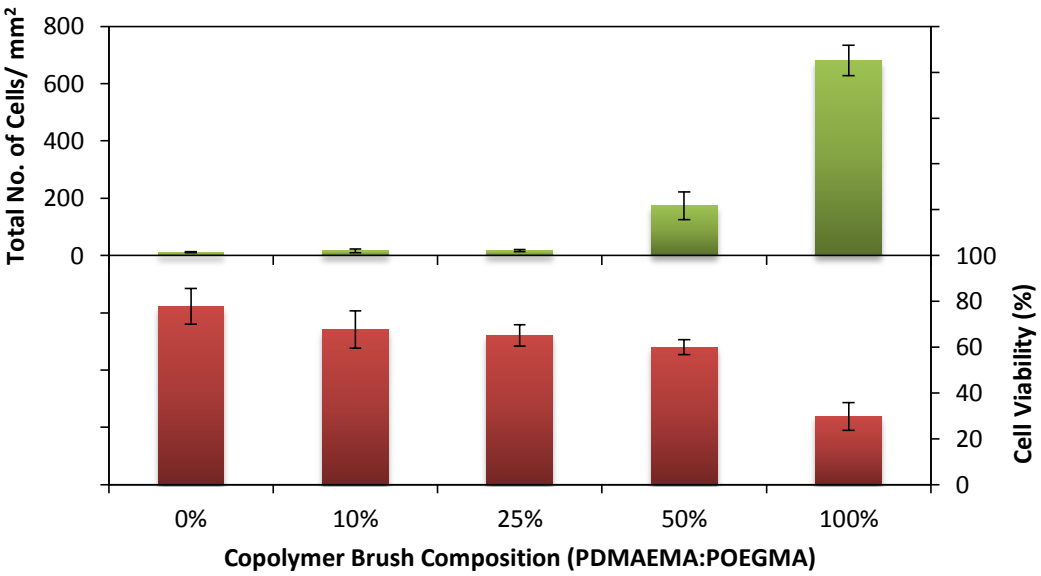

Figure 54: Total number of cells (green), and % live cells (red) with varying copolymer brush ratio when keratinocytes are cultured in FAD and seeded onto PDMAEMA-co-POEGMA brush-coated substrates, for 2 h. Values represent mean ± SE, n ≥ 24.

As expected, the protein-resistant nature of POEGMA resulted in low cell adhesion such that there were only 12 (SE = 2) cells per mm^2 at 0% PDMAEMA compared to 681 (SE = 52) cell per mm^2 for 100% PDMAEMA. This is due to the lack of favourable interaction between the cell and the POEGMA brush as is evident in Figure 55. A low number of cells are seen to adhere for the lower percentages of PDMAEMA in the copolymer brush as the residual charge of the copolymer is too low for cells to adhere. Although cell interaction with the surface of the copolymer brush is not promoted, cell viability remained relatively high. However, with 100% PDMAEMA, although there is positive interaction with cells as evident from the almost seven-fold increase in total number of cells on the surface, there is also a clear decrease in cell viability, by 48 %, as a result of the highly positively charged surface and associated disruption of the cell membrane. However, the trends obtained are not closely matching the trend of the surface charge of these copolymers (Figure 40, Chapter 2.3.8). Indeed, although total cell numbers and decrease in viability seem to peak for 100% PDMAEMA copolymer brushes, the zeta potential of the copolymer brushes prepared was gradually increasing as a function of

cationic monomer density. This suggests a charge density threshold above which cell adhesion and death were both significantly increased, further suggesting an impact via the destabilisation of the cell membrane.

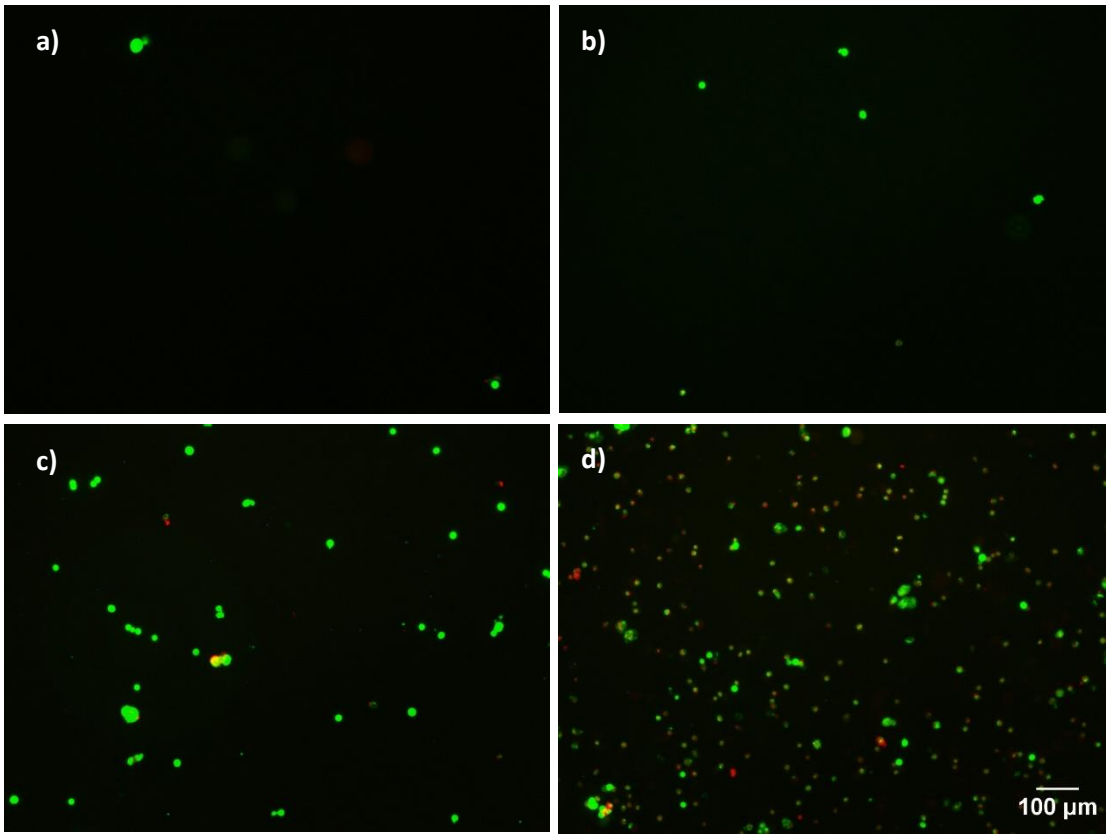

Figure 55: Fluorescence microscopy images (magnification 10x) of copolymer brush on Au-coated substrate, cultured with keratinocytes for 2 hours where a) 0% PDMAEMA: POEGMA, b) 25% PDMAEMA: POEGMA, c) 50% PDMAEMA: POEGMA and d) 100% PDMAEMA: POEGMA.

Following the study of time of incubation and the role of the composition of copolymer brush on cell adhesion and viability, the impact of the type of medium (KSFM or a 1:1 mixture of Dulbecco's Modified Eagle Medium (DMEM)-F12 with DMEM, FAD) used during the cell-brush interaction was next examined (Figure 56). Human keratinocytes were seeded on PDMAEMA brushes, with collagen as control, as keratinocytes express suitable integrins (α3β1) to adhere quickly to this matrix and remain viable for long term culture. The type of medium used during the expansion of these cells and during the cell-brush interaction experiment were both varied independently, leading to 4 different combinations of culture media. Hence, in Figure 56, FAD to KSFM describes that cells were cultured in FAD medium (on feeder cells) and were seeded on PDMAEMA brushes in KSFM medium. Cells were cultured in these conditions for 24 h.

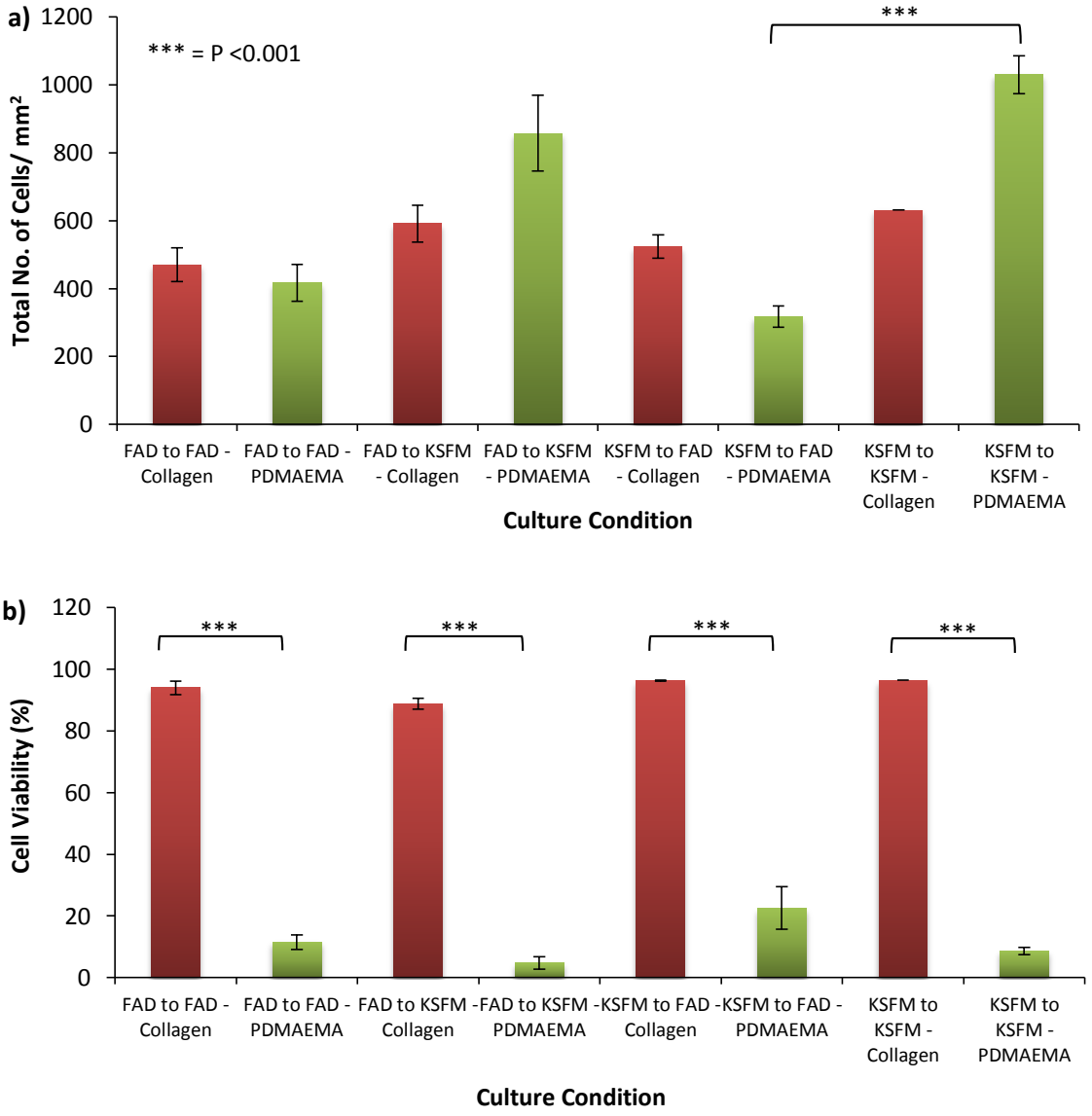

Figure 56: a) Total number of adhered keratinocytes and b) the number of live keratinocytes per culture condition on collagen (red) versus on PDMAEMA (green). Values represent mean ± SE, n ≥ 4. One-way ANOVA with Tukey's Test, p < 0.001 statistically significant.

As shown in Figure 56a, the total numbers of cells on the collagen-coated substrates, in the different culture conditions, are comparable. However, when the final condition was KSFM, there were slightly more cells adhering on the collagen-coated substrates. Slightly more cells died when the final condition was KSFM, and this was more pronounced when cells were expanded in FAD but this was not very significant ($p = 0.99$ when comparing FAD to KSFM with KSFM to KSFM, and $p = 0.21$ when comparing FAD to FAD with KSFM to FAD for incubations on PDMAEMA brushes, Figure 56b). These differences in cell viability are thought to arise from the strong adsorption of serum proteins from the FAD medium, which decrease the zeta

potential of PDMAEMA brushes[228] and therefore their cytotoxicity. This may also explain the higher cell densities observed for cells adhering to PDMAEMA in KSFM.

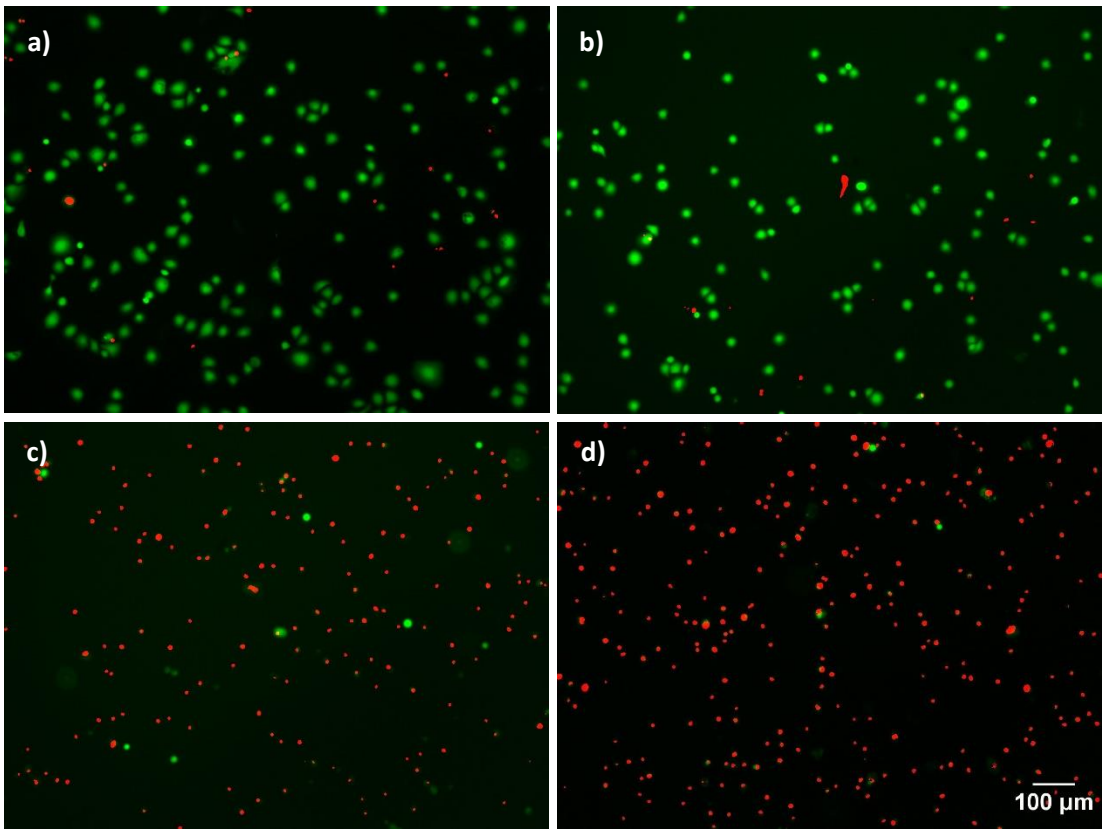

Figure 57: Representative fluorescence microscopy images (magnification 10x) of the keratinocytes cell viability for control: a) Au-Collagen cultured in FAD to final condition of FAD and b) Au-collagen from KSFM to KSFM in comparison with c) Au-PDMAEMA from FAD to FAD and d) Au-PDMAEMA from KSFM to KSFM, as acquired by live/dead assay kit, where green denotes live cells and red is dead cells.

Figure 57 displays typical images of the live/dead stains obtained for collagen-coated substrates and PDMAEMA-coated substrates when the cells were expanded in FAD or KSFM and the final condition was FAD or KSFM, respectively. Differences in cell adhesion and viability between cells exposed to brushes in the same medium but expanded in different conditions (e.g. KSFM, feeder-free vs FAD with feeders) may arise from differences in protein expression, proteins glycosylation and phospholipid composition of the cell membrane.

3.3.2 Transfection assay

Efficiencies of synthetic transfection reagents have been shown to have improved over the past years as a result of increased understanding of the biological processes which occur during transfection and the manipulation of these using a rational approach. In an effort to provide alternative DNA carriers for the assembly of gene delivery systems, this study evaluates the potential of cationic polymer-brush coated silica nanoparticles as a transfection reagent.

The efficiency of DNA delivery and expression via cationic PDMAEMA brushes grafted on silica nanoparticles was determined through the development and optimisation of a transfection assay based on the expression of EGFP.

3.3.2.1 Optimisation of parameters

Considering the relatively low transfection levels obtained even in the case of the jetPEI® control, the effect of some of the large number of parameters potentially associated with transfection efficiency[149, 160, 465] were investigated (see Figure 58). This was essential to optimise the efficiency of the non-viral gene delivery system of interest in this study.

The first part of the optimisation studies focused on the type of media used during the 4-hour transfection. Results indicate that serum did not have a strong effect on efficiencies with jetPEI®, both for HaCaTs and HCA2 cells. However, KSFM showed slightly higher transfection levels for both cell lines, although not statistically significant ($p = 0.08$ when comparing KSFM to DMEM without serum and $p = 0.3$ for KSFM to DMEM with serum, Figure 58).

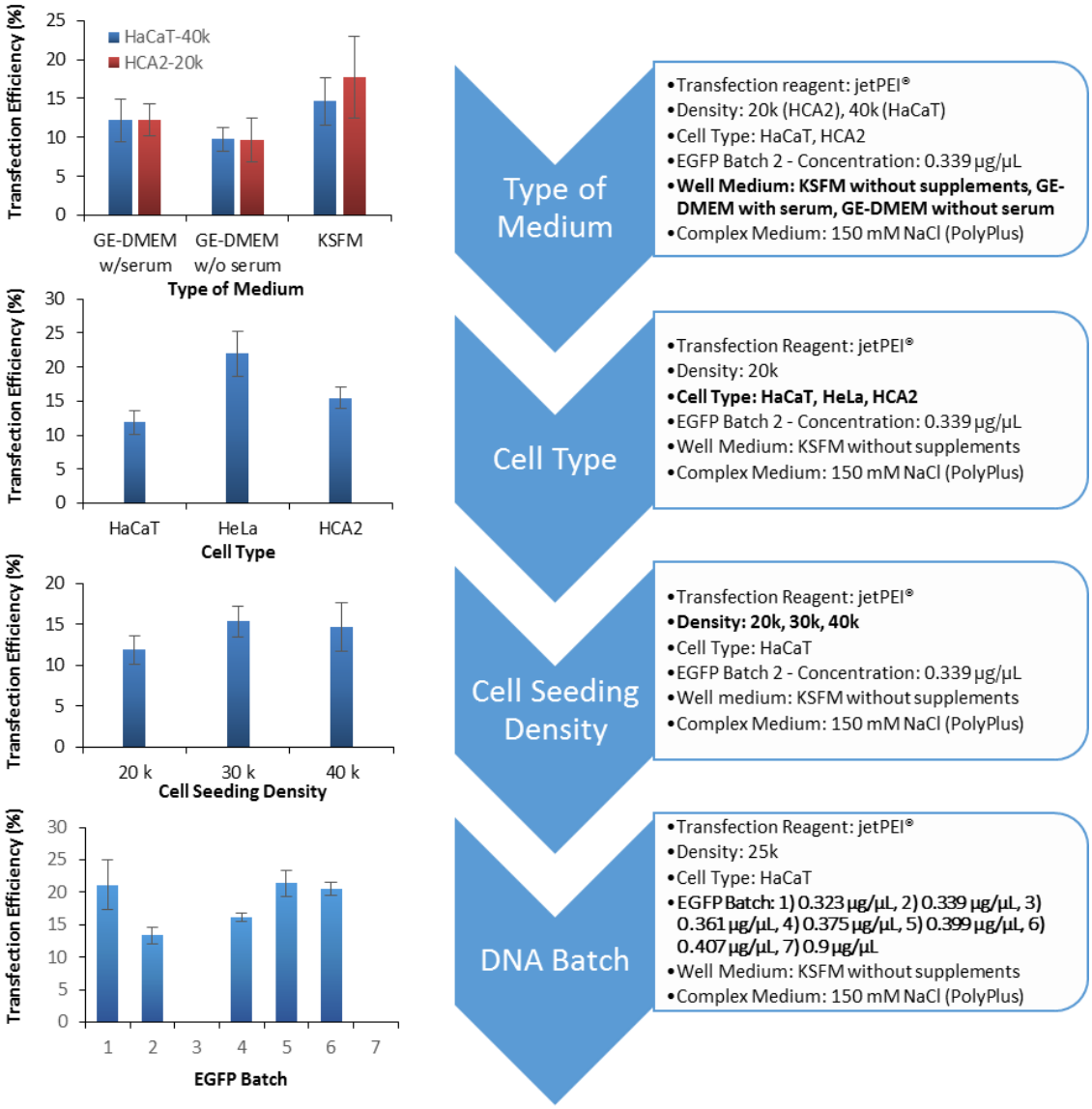

Figure 58: Schematic representation of the parameters investigated, inclusive of results, for the development of an optimised transfection assay.

Further tests were carried out with f-PDMAEMA polymer which did not display any significant transfection level whilst the control displayed over 15% transfection efficiency although total number of cells for both were similar (Figure 59). The performance of f-PDMAEMA here is in contrast to what is reported in the literature.[187, 373, 466] The low transfection efficiency may be due to residual catalyst which is possibly inducing toxicity. With the little transfection seen, it was noted that the presence of serum totally suppressed transfection. The transfection noticed for KSFM and the lack of any transfection for DMEM with serum is possibly because the overall positive charge of the polymer/plasmid complex when in KSFM was not neutralised

by serum proteins, nor did they bind to and increase the particle size of the complexes which could have facilitated some cellular uptake and succeeding transfection.[172]

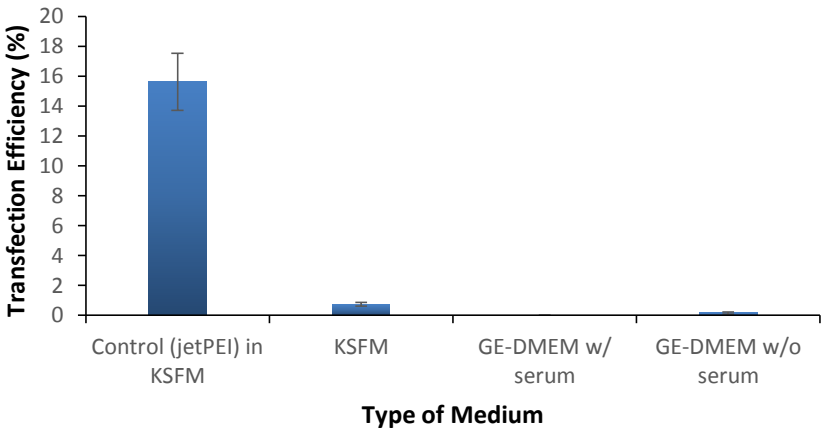

Figure 59: Transfection efficiency of f-PDMAEMA with KSFM without supplements, GE-DMEM with and without serum, against control: jetPEI® in KSFM, with HaCaT cells, using a cell seeding density of 30k and EGFP-0.339 µg/µl. Values represent mean ± SE, n = 9.

Different cell types can also display different transfection efficiencies hence the extent to which this was altering the performance of the positive control was investigated. Three cell types were tested with the positive control jetPEI® and showed comparable transfection levels although transfection with HeLa cells was slightly higher. However, even for this cell line, transfection levels were substantially lower than those reported (80% reported by PolyPlus with jetPEI® as found in the Cell Transfection Database, www.polyplus-transfection.com) in the literature.[467] These differences between cell types and with the literature may highlight the importance of optimisation of transfection assays (including the type of plasmid and read out) in achieving high efficiencies.

It was also important that cells were seeded on collagen-coated wells prior to transfection study in order to obtain a well with suitably spread cells as without collagen HaCaT had the tendency to form colonies of cells which would not facilitate transfection efficiency nor quantification of the transfected cells (Figure 60).

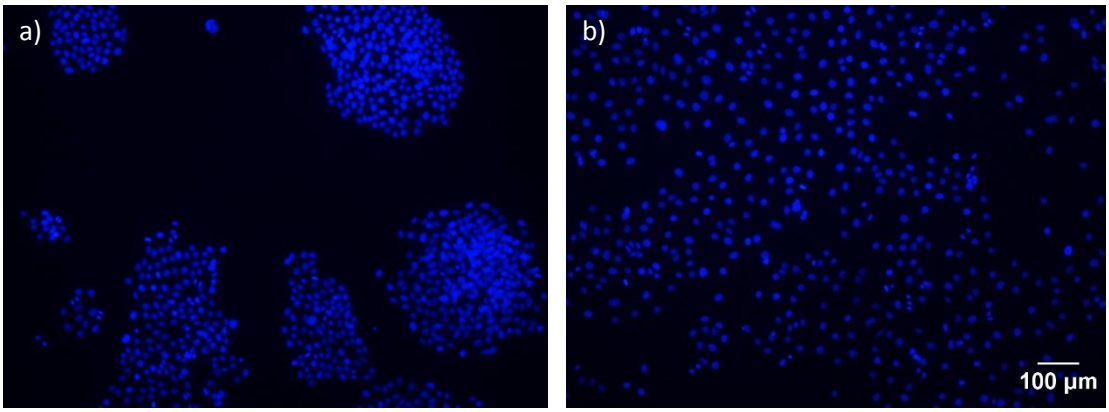

Figure 60: Fluorescence microscopy images (magnification 10x) of HaCaT (20k) adhered to a) uncoated wells and b) collagen-coated wells of a 24-well plate, using DAPI.

Controlling the cell seeding density allowed more reliable quantification of the transfection efficiency. Although the obtained results showed higher transfection with 30,000 cells per well of a 24-well plate, overcrowding of cells were noticed near the centre of the well thus 25,000 cells per well was used for future studies to obtain evenly spread cells.

Batch-to-batch variation in the quality of EGFP stock solutions also had an impact on the transfection efficiency. Whilst some batches displayed moderate efficiencies with the control (jetPEI®), reaching above 20%, others showed no transfection. This resulted in the testing of each new DNA batch prior to transfection studies. Those displaying an efficiency of over 10% were further considered. The effect of total quantity of DNA incubated was also examined for jetPEI® transfections but no significant difference was observed.

A constant EGFP concentration of 1 µg/ mL was used for all transfections whilst the polymer concentration was altered. N/P ratios 1:1, 5:1 and 20:1 were initially trialled and N/P 20:1 was discarded from further transfection studies as this polymer concentration was highly toxic as is evident from the toxicity studies (Figure 51). N/P 1:1 did not lead to any significant transfection level, presumably because of charge reversal (Figure 48 in Chapter 2.3.10.3) of the resulting construct and therefore the final N/P ratios further considered were N/P 3:1, 5:1, 7:1 and 10:1.

Further studies to test the suitability of the control transfection reagent, jetPEI® against Lipofectamine® 2000 also did not display any notable improvement in transfection. However, it was found that the most efficient transfections, in the case of for Lipofectamine® 2000, occurred with the Opti-MEM medium, whilst it performed poorly with KSFM without

supplements. However, Opti-MEM did not improve the transfection efficiency compared to KSFM in the case of PDMAEMA brush-nanoparticles.

To summarise the optimisation of transfections in various conditions, it was highlighted that gene transfection efficiency depended strongly on the cell type, DNA batch quality and N/P ratio of the nanoparticles amongst the parameters tested.

3.3.2.2 Assay quantification

The quantitative determination of the transfection efficiency of this specific gene delivery system varies from some of those reported in the literature. Whilst most studies use the luciferase assay and flow cytometry, a simple yet accurate approach to quantifying the transfection efficiency was employed using an EGFP assay in this study. The percentage efficiency was acquired from counting each transfected cells through the EGFP reporter gene and the total number of cells via 4',6-Diamidino-2-phenylindole dihydrochloride (DAPI) fluorescence (quantification was carried out using ImageJ).

The blue (DAPI-fluorescent) and green (EGFP-fluorescent) channels were opened in ImageJ and split such that only the green and blue channels were kept. In Set measurements, the mean grey value measurement was checked and redirected to the green channel. Following adjusting the threshold of the blue channel, the nuclei of the cells are displayed as spread as possible whilst excluding any debris. Any overlap of nuclei was separated by the 'watershed' tool. The 'Analyze Particles' option was then chosen with the size defined between 50 and infinity in pixel units which further ensures that only the nuclei of cells are counted; choosing to show 'masks' confirms this. The results window then displays the total number of nuclei and their corresponding mean grey value in the EGFP channel. EGFP positive cells were defined with a threshold two-fold higher than the basal fluorescence level (defined as the fluorescence level of the lowest 5% cells). The number of transfected cells as a percentage of the total number of cells was then presented in all studies involving transfection efficiency. Data sets were only considered if the transfection efficiency of the control, jetPEI®, was above 8%.

3.3.2.3 Free PDMAEMA

The performance of f-PDMAEMA as a transfection reagent was evaluated through its comparison with the positive control, jetPEI® (Polyplus), a commercially available transfection reagent. Figure 61 shows the transfection efficiencies with HaCaT cells, performed with a fixed plasmid concentration of 1 µg/ mL and a varying concentration of f-PDMAEMA of different molecular weights.

Transfection efficiency of both f-PDMAEMA were found to be below 1.5% whilst jetPEI® reached 15% (SE = 2%). For both molecular weights of f-PDMAEMA, slightly higher transfection levels were observed at higher polymer/plasmid ratios, but these results were not statistically significant ($p = 0.27$). As discussed in section 3.3.2.1, the low levels of transfection are likely due to the residual copper catalyst in the sample generating toxicity.

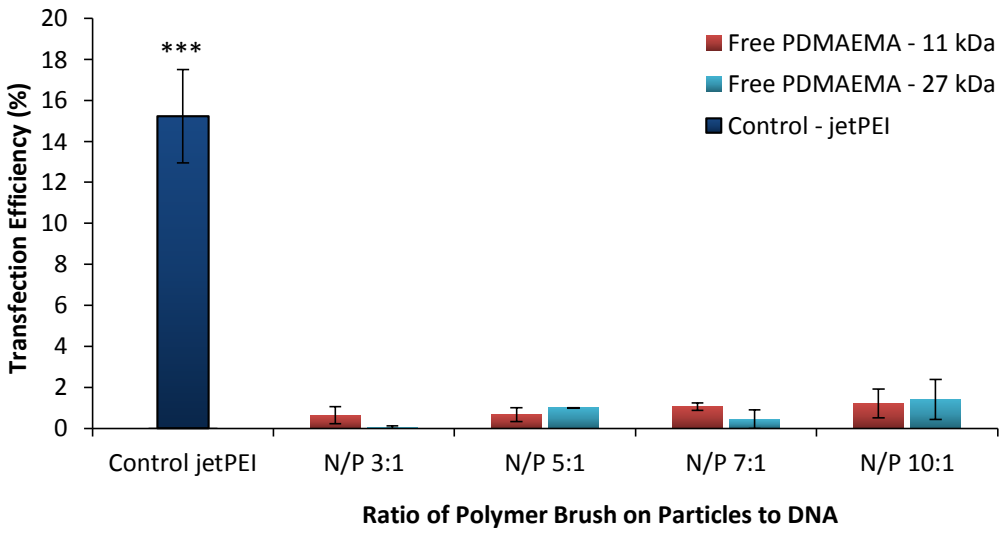

*Figure 61: Transfection efficiency of synthesised free polymers of varying Mw, with HaCaT (25k per 24-well plate). Transfections levels for f-PDMAEMA, for each molecular weight, at all N/P ratios, were significantly lower than the control (jetPEI®). Values represent mean ± SE, n ≥ 6, *** = p < 0.001.*

High molecular weight PDMAEMA with longer chains condenses plasmid into smaller particles than low molecular weight PDMAEMA and these smaller particles can penetrate more easily through the formed pores resulting in a higher number of transfected cells. [468, 469]However, the transfection efficiency of f-PDMAEMA polyplexes is not comparable to jetPEI® despite their similar chemical structure and molecular weight (PEI believed to produce high transfection efficiency amongst non-viral cationic polymers, is reported to have a molecular

weight of 25 kDa) which makes the cause of lower transfection efficiencies with PDMAEMA – 27 kDa unclear. It is possible that other compounds in the composition of jetPEI® contribute significantly to improving efficiencies although the details of the modification of PEI is not accessible. Free PEI of the same molecular weight was also employed in a transfection study using the same conditions yet yielded similar if not lower levels of transfection as f-PDMAEMA. This could be the consequence of using the EGFP assay which determines the exact number of transfected cells hence is more representative of the true transfection efficiency and therefore more reliable than luciferase assays often used in the literature. However, such low transfection levels are surprising.

In addition, the pH of the complexation and transfection medium, 150 mM NaCl and KSFM without supplements respectively, were confirmed to be between 6.8 and 7.4, below the pK_a of PDMAEMA. The complex size only increases marginally with increasing pH of the complex medium but this is reported to be not pronounced below pH 7 due to the protonation of the amino groups below this pH.[465] The tendency of the cationic particles to aggregate would have only been possible at higher solution pH therefore this factor is unlikely to have affected the transfection efficiency. It is possible that the large fraction of the polyplexes may be routed to lysosomes following endocytosis.[468] If this occurs, the acidic nature of the lysosome and the enzymes could degrade the DNA. Furthermore, it is known that the strong complexation between the polycation and DNA and subsequent decomplexation and release within the cytoplasm for efficient transfection is a challenge. In addition, the intrinsic proton sponge nature of PDMAEMA is expected to assist endosomal escape,[376] but perhaps its buffering capacity needs to be further increased to improve its potential as an efficient transfection reagent.

Free PDMAEMA was not studied further as the focus of this study was brush-grafted nanoparticles.

3.3.2.4 PDMAEMA-g-particles

Examining the transfection efficiency of SiO_2-g-PDMAEMA nanoparticles at N/P ratios 3:1, 5:1, 7:1 and 10:1 (Figure 62) showed how vectors attached to particles performed better than their respective free polymers. These polymeric nanoparticles are advantageous over other systems such as liposomes as they are easier to produce and readily allow modulation of their size and extent of positive charge.

With this particular system, the highest transfection efficiency was achieved at N/P 5:1 with 9% (SE = 3%), notably higher transfection level than N/P 10:1 ($p = 0.11$), whilst jetPEI® averaged at 23% (SE = 5%). The transfection efficiency of PDMAEMA-grafted particles at N/P 5:1 was not significantly lower than the transfection efficiency of the control. Meanwhile the efficiency for N/P 3:1 and N/P 10:1 were significantly lower than the control. The results also exhibited a clear correlation between transfection efficiency of the nanoparticle complexes and their cytotoxicity, caused by the cationic polymer. Maximum transfection occurred when cell viability was 65.2–81.9% for N/P 5:1 between 4 h and 24 h. As the relative cell viability decreased below 40%, with increasing N/P ratio, there was also a large decrease in the number of transfected cells as shown in Figure 51 and Figure 62, respectively. The lower efficiency measured at N/P of 3:1 could be due to the zeta potential of the complexes being too low, resulting in weaker interaction with the cell membrane.

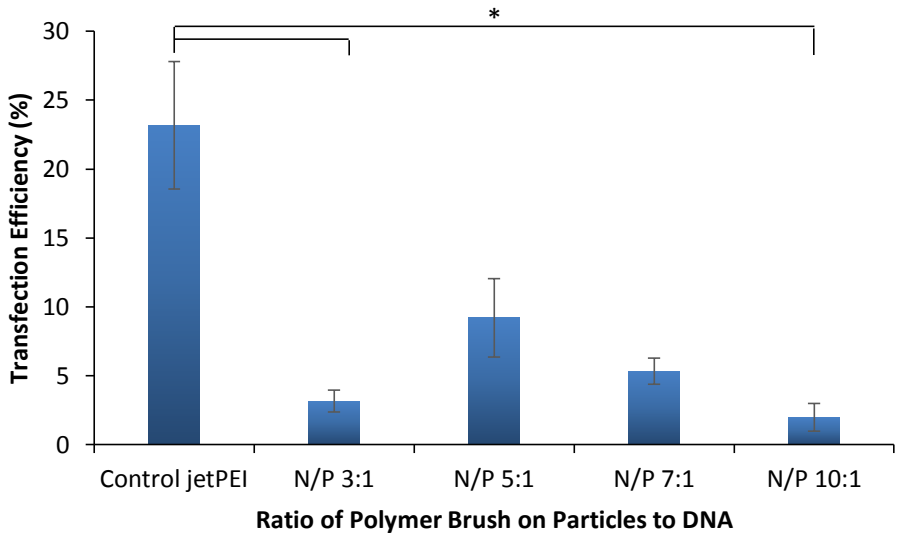

*Figure 62: Transfection efficiency of SiO_2-g-PDMAEMA nanoparticles with HaCaTs (25k per 24 well-plate). The transfection efficiencies for PDMAEMA coated nanoparticles at N/P 3:1 and N/P 10:1 were signifcantly lower than the control. Values represent mean ± SE, n = 9, * = P < 0.05.*

In addition to toxicity, the lower transfection efficiency of PDMAEMA particles compared to the control may also be attributed to the poor intracellular delivery of DNA by the PDMAEMA-coated nanoparticles. Although the presence of the cationic PDMAEMA brush protects the DNA during diffusion through the cytosol towards the nucleus by preventing degradation of the DNA by nucleases in the environment and maintains its stability, the transfection efficacy is still low.

Potential pathways utilised by nanoparticles include endocytosis via clathrin-coated pits (receptor-mediated endocytosis) or uncoated pits through fluid phase.[469, 470] Both of which transport the particles to the lysosomal degradative compartment. Caveolar endocytosis, on the other hand, results in the particles being transferred to the endoplasmic reticulum or Golgi or through the cell via transcytosis (Figure 63).[367, 471] With this study, non-specific adsorptive endocytosis is believed to occur; once the particles are wrapped around the cell membrane to form endosomes, they are transported to lysosomes; those which survive the low pH and enzymes then travel on to other intracellular compartments including the nuclei.[468, 472] Endosomal escape may be limited despite PDMAEMA's buffering capacity. The DNA must also dissociate from the condensed complexes either before or after entering the nucleus via nuclear pores (≈Ø10 nm) or during cell division.[35, 41] The complexes in the present system are too large in size for nuclear entry therefore DNA dissociation should occur outside the nucleus. At this stage, the cationic particles/DNA complex may also not be sufficiently near the nucleus for transcription and translation of the transferred DNA to ensue, in addition to the lack of nuclear targeting. Following the DNA delivery near the nucleus, the transfection efficiency is also then dependent on the composition of the gene expression system.[35]

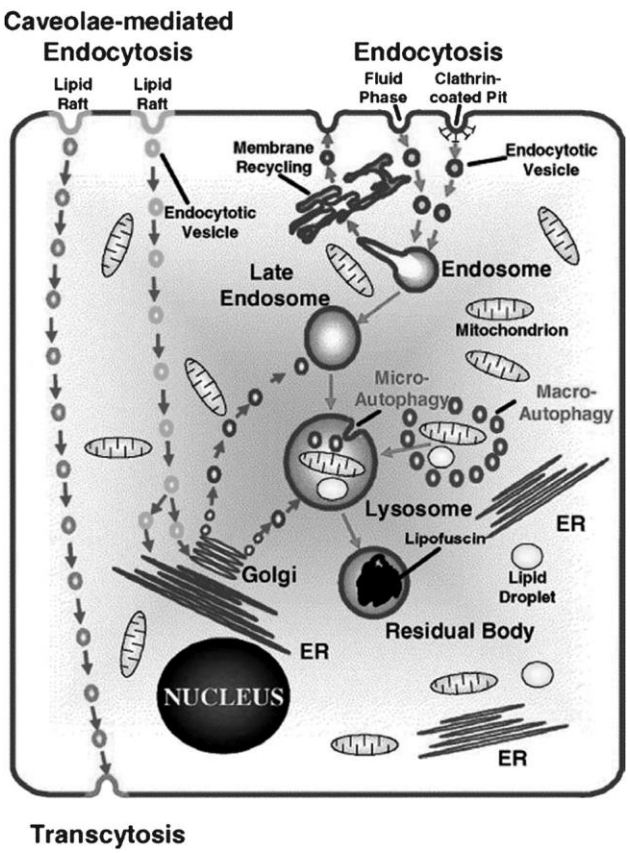

Figure 63: Potential endocytotic pathways for nanoparticle entry into cells.[473]

It is also possible that other molecules may be dissociating the DNA from the complex. KSFM may contain small molecules which may be preventing DNA from binding, or displacing DNA. DNA release from the macromolecular assembly might not occur in time for transcription to proceed. The stability of the complex formation and hence the rate of DNA unpackaging could influence gene expression efficiency as an intermediate stability is required since stable complexes restrict transcription whilst unstable complexes allow DNA degradation.[433, 474] Although these considerations are speculative, the collection of factors that may impact transfection and that are not addressed by simple PDMAEMA systems seems compatible with the moderate transfection levels measured.

The complexes between genetic material and polymeric nanoparticles should be small and tightly formed to facilitate endocytosis. DNA interaction studies from Chapter 2 show that at the optimum ratio of N/P 5:1, the complexes reach a hydrodynamic diameter of 1210 nm (SE = 130 nm) and a zeta potential of 18.5 mV (SE = 1.2 mV). Though the intermediate positive zeta potential offers complex stability suitable for allowing transcription, the large average hydrodynamic diameter could possibly be limiting cellular uptake and subsequent motion through the cytosol to the nucleus. It is worth noting that the size of jetPEI®-based complexes was measured to be around 1000 nm yet gives higher transfection which could mean that the observed difference in transfection efficiency are not solely due to differences in physicochemical properties of the complexes but perhaps to do with the properties of the carrier itself.

Finally, the lower transfection efficiencies for the f-PDMAEMA (11 kDa and 27 kDa) compared to PDMAEMA grafted from silica nanoparticles is not in agreement with existing reports.[181]ch[188, 363, 365, 433]u[369] As the free polymer is not restricted by the size unlike SiO_2-g-PDMAEMA, cellular uptake and hence the gene transcription efficiency should be higher. The observed low transfection efficiency compared to SiO_2-g-PDMAEMA could be due to the presence of residual copper catalyst in the free polymer as it is not possible to purify the free polymer as extensively as with SiO_2-g-PDMAEMA nanoparticles, and possibly higher cytotoxicity arising from the free polymer present following complexation.

3.3.3 Cellular Uptake

As the efficiency of gene expression is controlled by processes involving the intracellular uptake and release of DNA, stability of DNA in the cytoplasm, unpackaging of the DNA-vector complex and the transfer of DNA to the nucleus,[35] particular focus was placed on the cellular uptake of the SiO_2-g-PDMAEMA nanoparticles to further understand the poor transfection with PDMAEMA compared to what is reported in the literature.[245, 247, 250, 363]

It is known that the size, shape, charge and surface chemistry of colloidal particles play an active role in governing cellular uptake and subsequent delivery.[95, 96, 475] The internalisation rate alongside cytotoxicity are also critical factors influencing transfection, however the relationship between these factors combined with particle size is yet to be understood. The influence of the particle size is also thought to be dependent on the chemical structure of the particles and the cell types. Although some studies have shown that 100-200 nm DNA/vector particles of N/P ratio 10-20 [476] and silica nanoparticles averaging 200 nm[477] improve transfection efficiency, this is not the case for all systems since cellular uptake, endosomal escape and toxicity of the carriers amongst other factors also impact this efficiency. Moreover poly (lactic-co-glycolic acid) particles of 375 nm and 600 nm were shown to be better uptaken than those below 200 nm.[478] Spherical nanoparticles such as those utilised in this transfection efficiency study should potentially be easily endocytosed as shown by Chithrani *et al.* who compared the cellular uptake of spherical (14 nm and 74 nm) and rod-like (14 X 40 nm and 14 x 74 nm) Au particles to find that spherical particles displayed higher uptake.[96] Although the shape of the nanoparticles in the current study are suitable for uptake, the size of the nanoparticle may not be facilitating the process. Uptake of such nanoparticles may therefore occur through different mechanisms for each cell type depending on the particle size, shape and their ability to aggregate.

Surface chemistry of the particles is also an essential parameter controlling cellular uptake. In that respect, the structure and morphology of PDMAEMA brushes as well as the hydrophilicity of the surface coating of nanoparticles are of particular importance. Extracellular (and potentially intracellular) enzymatic degradation of DNA may contribute to low transfection efficiency, however complexation with a cationic polymer brush such as PDMAEMA, with its strong positive charges and endosomal buffering capacity, should lower such degradation. [35] Generally, it is expected that the cationic polymeric particles would be taken up more efficiently than neutral or anionic particles as the cell membrane is negatively charged though neutral nanoparticles have been reported to have higher cellular uptake than anticipated.[201,

[479] However, high positive charges may be causing aggregation of particles in the medium thus hindering cellular uptake. Silica nanoparticles utilised in this study are also believed to enhance uptake by sedimentation to the cell surface[480] but the number of DNA molecules carried by these polymeric nanoparticles decrease during their journey through the intracellular compartments which could be contributing to the lower gene expression efficiency.

To clarify where the complexes accumulate following transfection, qualitative epifluorescent microscopy studies were performed at 4 h (Figure 64) and 24 h (Figure 65), using N/P ratios 1, 5 and 10, with fluorescein isothiocyanate (FITC)-labelled SiO_2-g-PDMAEMA nanoparticles. It was not possible to quantitatively study the cellular uptake due to lack of fluorescence of the batch of particles available for this study, so images were qualitatively analysed.

At N/P 1:1, very few particles complexed with DNA were distributed around the nuclei and this number multiplied with an increase in the N/P ratio. Comparing the 4 h and 24 h time points, an increase in the number of particles surrounding the nuclei at longer incubation times was observed, especially at lower N/P ratios (Figure 65). Both, particles with and without DNA aggregate and accumulate near the nuclei at N/P 10:1.

The localisation of FITC-SiO_2-g-PDMAEMA-DNA complexes near the nuclei suggests that particles have bound to the cell surface and internalised. As expected, particles were unable to enter the nucleus due to their size, but this assay did not allow us to establish whether DNA was released and able to localise at the nucleus. Future assays developed with this system should address this issue.

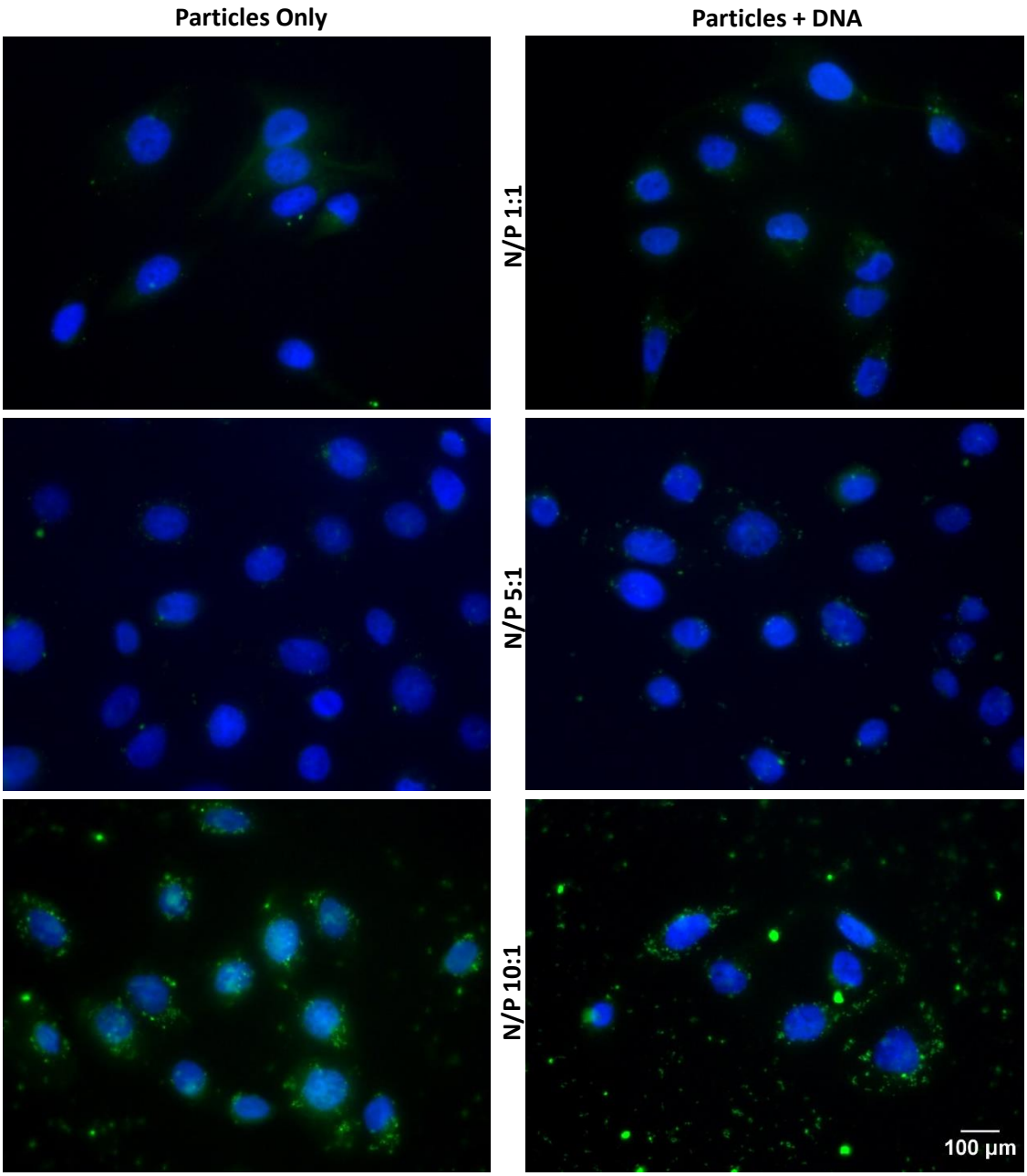

Figure 64: Fluorescence microscopy images, at magnification 63x, cellular uptake of FITC-labelled SiO_2-g-PDMAEMA nanoparticles (green) at 4 hours, Hoescht 33342 stained nuclei (blue).

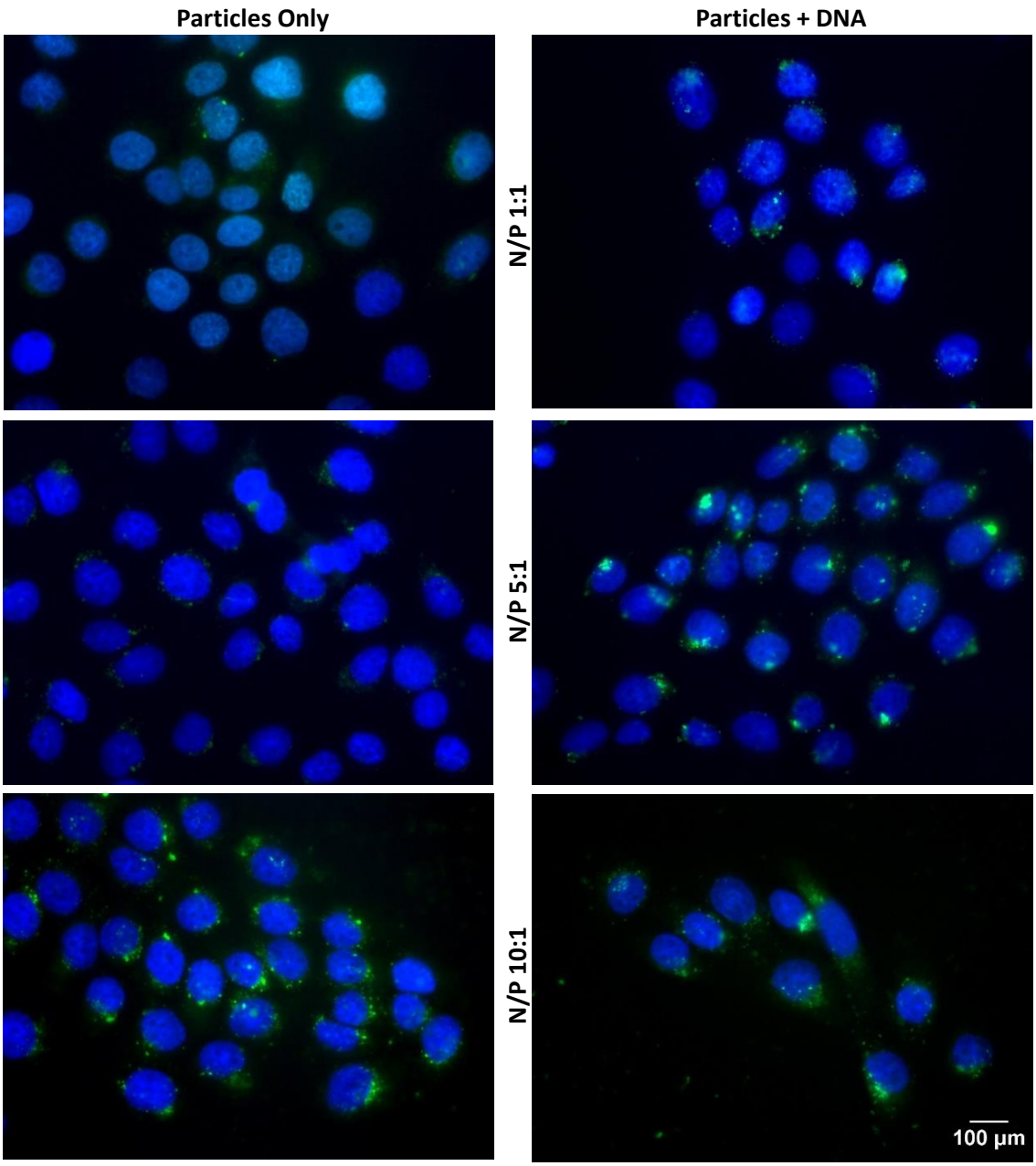

Figure 65: Fluorescence microscopy images, at magnification 63x, cellular uptake of FITC-labelled SiO_2-g-PDMAEMA nanoparticles (green) at 24 hours, Hoescht 33342 stained nuclei (blue).

Confocal laser scanning microscopy (CLSM) was used to observe the subcellular distribution of the particles. Figure 66 shows three-dimensional images of HaCaT cells from the coverslip to the top of the cell at a series of depths along the z-axis, with Δz = 300 nm. The main panel shows the fluorescent image in the x-y cross-section at a given z-location whilst the 2 smaller panels show the structure along the x-z (bottom) and y-z (right side panel) at the position

indicated by the yellow lines in the main panel. The images show cell nuclei in blue (Hoescht 33342), particles in green (FITC) and the cell membrane in red (D282 Dil). The lower intensity of the FITC-labelled polymeric nanoparticles makes it difficult to see the position of the complexes on the 3-D image but they were indeed internalised by the cell though not in large amounts, consistent with the moderate transfection efficiencies observed.

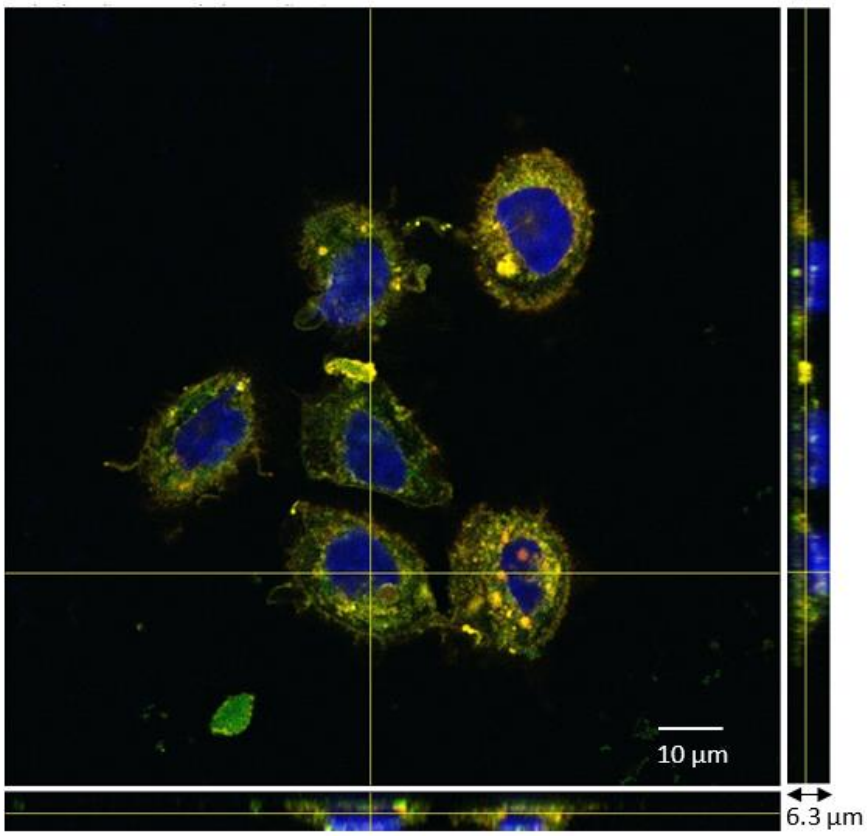

Figure 66: Three-dimensional confocal images of HaCaTs with FITC-labelled particles with DNA at N/P 10:1. The main panel shows the enface image at a given z depth whilst the bottom and side panels show the x-z and y-z cross-sectional images, respectively.

As discussed in Chapter 1, both endosomal escape and destabilisation of the complexes impact DNA delivery thus strategies aiming to release DNA earlier from the endosome could improve transfection efficiencies. Developing targeted systems in which the vectors can be uptaken via receptor-mediated endocytosis could be another approach to improve cellular uptake and gene expression. Conjugating ligands such as antibodies, peptides, proteins, growth factors and other small molecules to these nanoparticles can give direct, targeted delivery to cancer

cells or intracellular organelles including the nucleus (using nuclear localisation factors), whilst avoiding any undesirable side effects. Particle size is another pivotal factor that could influence cellular uptake. Further studies must be performed using smaller nanoparticles and hence smaller complexes to determine the effect of size on the transfection efficiency. It would also be interesting to monitor the transportation process of particles via live CLSM to understand in detail the process of endocytosis and nuclear targeting/entry. In order to solve the issue of quantifying cellular uptake, the current system could employ quantum dots or labelled particles with more robustly fluorescent particles as they can be more easily detected, thus allowing quantification of the uptake. Simultaneous labelling of DNA would also allow to determine DNA-brush dynamics in the cytosol.

3.4 Summary

The succession of experiments in Chapter 3 elucidated details of the way in which the charged surface, cationic PDMAEMA, interacts with mammalian cells. The adhesion and cytotoxicity studies of PDMAEMA and its copolymer grafted from flat substrates confirmed that both the adhesion and the cell viability were time- and charge density-dependent; more cells adhered with increasing time, higher number of cells adhered with increasing composition of PDMAEMA in the copolymer brush however, the converse was true for the cell viability with both time and composition of PDMAEMA.

Cell viability of PDMAEMA-grafted from silica nanoparticles with and without DNA, at 4 hours and 24 hours, over a range of N/P ratios; 1:1 to 20:1, generated interesting data which indicated that the presence of DNA shields the positive charges of the brush thus allowing a higher cell viability than those without DNA. Cell viability increases following one proliferation cycle at the 24-hour time-point and is over 60% below N/P ratio 5:1 in the presence of DNA. After establishing the system's cytotoxic behaviour, the ability of the cationic nanoparticles to be endocytosed and be successful in entering the nucleus was assessed through a number of transfection assays at N/P ratios 3:1, 5:1, 7:1 and 10:1. As the amount of molecules entering the nucleus and getting transcribed determines the efficiency, cellular uptake studies were carried out to ascertain the localisation of the cationic nanoparticles. It was evident that the nanoparticles were indeed endocytosed however the level of nuclear entry and thus gene expression was not to a favourable extent hence further tuning of the system is required.

Chapter 4 - Functionalisation of PGMA and PDMAEMA brushes for DNA interaction and gene delivery

4.1 Introduction

Considering the moderate transfection efficiencies achieved with PDMAEMA brushes, the possibility to control the chemistry of brushes to design novel cationic systems was explored. Investigating the chemistry of polymer brushes and tuning the charge in this way is an essential approach to understand the physico-chemical parameters controlling DNA-brush interactions, the interaction of complexes with cell membranes, DNA release in the cytosol, cytotoxicity and therefore potentially improve the efficiency of gene delivery systems. As with PDMAEMA, poly(glycidyl methacrylate) (PGMA) is an attractive polymer due to the ease with which PGMA brushes can be grown efficiently from a variety of surfaces and its reactiveness in mild conditions.[481-483]

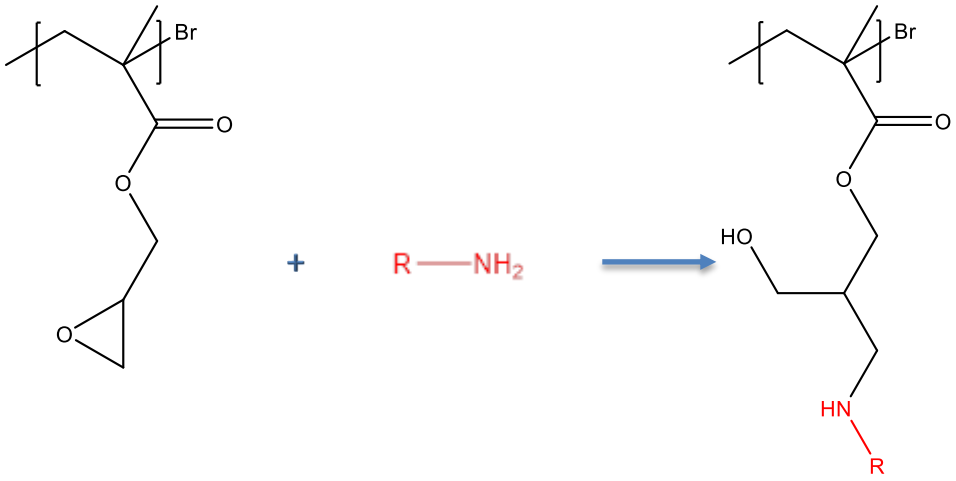

Figure 67: Ring opening reaction with the pendant epoxide group of PGMA via amination

The pendant epoxide groups of the PGMA can be opened with different functional groups to produce poly (glycerol methacrylate) derivatives (Figure 67). The possibility of such post-polymerisation modification has generated great interest due to the potential for preparing

many functional polymers of interest for various uses which may not be accessible by direct polymerisation of the functional monomer. Some of these uses include the preparation of functionalised magnetic microspheres with hydrophilic properties for molecular diagnostic applications[484] and the generation of biofunctionalised sensors.[361, 485]

In addition, free PGMA (f-PGMA) has found application for the delivery of drugs and nucleic acids. Aminated poly(glycidyl methacrylate) (PGMA) has been reported to be a safe and efficient gene delivery vector[486-489] as the cationic amine species can also condense DNA through electrostatic interactions. Their interaction with DNA was reported to be stronger than PEI whilst the cytotoxicity of the aminated PGMA were lower compared to PEI25k with the exception of the polymers with molecular weights in the region of 30 kDa. Moreover, the amino PGMA/DNA complexes formed at low N/P ratios, and the increased charge ratio and synergistic effect of hydrogen bonding in the system contributed towards increased stability of the complexes thus preventing nuclease degradation.[490] The transfection efficiency of the methylethylamine modified linear and star-shaped PGMA/DNA complexes and 4-amino-1-butanol modified linear PGMA/DNA complexes were also described to be higher in comparison to PEI25k.[487] One of the most common oligoamines used to functionalise PGMA, to construct gene carriers is ethanolamine. A biocleavable, star-shaped, EA-functionalised PGMA with abundant secondary amine and non-ionic hydroxyl groups, was reported to possess good DNA condensation properties, low cytotoxicity and efficient gene delivery ability.[491] Furthermore, the use of f-PGMA functionalised with pentaethylenehexamine (PEHA) has been investigated previously by Wei *et al*. for gene delivery applications and its cytotoxicity and transfection efficiency performance were studied, alongside other oligoamines.[492] They reported transfection efficiency comparable to that of branched PEI with optimal efficiency occurring at N/P 5:1, but with lower cytotoxicity than branched PEI. Acid-base titrations conducted by the same group confirmed the buffering capacity approached that of branched PEI. Diethylenetriamine (DETA) has also been used for post-modification of PGMA to analyse its potential in effective DNA delivery.[493] Compared to all the other derivatives employed in the study, DETA gave higher transfection efficiency though not as high as PEI.

As previously discussed (Chapter 1.1.3), transfection is a multi-stage complex process where many of the processes are hindered. The polymer/DNA complexes must have sufficient positive charge for intracellular uptake. Following endocytosis, the complexes must resist acidification in the endosomal and lysosomal compartments. Thus endosomal buffering and escape must occur with complexes remaining stable in order to avoid DNA degradation via

enzymes. Once the complex is released into the cytoplasm, it must diffuse through the intracellular space and cross the nuclear membrane; unpackaging of the DNA/polymer complex must also occur before or after entry into nucleus. However their ability to dissociate is dependent on the stability of the complex formation. The structure and morphology of the cationic polymer influence DNA binding and condensation; the number of cationic groups strongly impacts the polymer-DNA interaction. The complexes must also be sufficiently close to the nucleus for transcription and translation to occur. Hence the surface chemistry of the polymer brush plays a crucial role in overcoming these barriers. It has been proposed by several scientists that methods to improve one or several of these stages include varying the type of positive charge whether through a primary, secondary, tertiary or even quaternary amine, as well as the density of the charge. Compared to PEI, PDMAEMA has a lower charge density as the molecular weight of one repeat unit containing one charge is higher. The charge density is thus an important factor affecting the gene delivery efficiency.

Also, to improve DNA release, it is useful to develop a charge-shifting process as the ability to reverse the charge can then facilitate the release of DNA and simultaneously improve endocytic exit.

Functionalisation of polymers has been shown to be an efficient strategy to target and enhance uptake of particles and gene delivery vectors thus transfection efficiency hence the potential of allyl derivatives were explored for this purpose. These allyl-functionalised polymers can also be further functionalised by thiolene chemistry.[494] The two polymers that were explored for functionalisation were PDMAEMA and PGMA as both can be synthesised easily and could be functionalised using accessible, mild and efficient chemistry.

The present work therefore synthesised PGMA-brush functionalised silica nanoparticles via ATRP and functionalised it with oligoamines (Allylamine (AA), DETA or PEHA) by ring-opening nucleophilic substitution. The resulting polyglycerol-like polymer brushes had both hydroxyl and amine moieties. The H-bonding interactions contributed by the hydroxyl groups in the neighbouring atoms of the amine groups of the derivatised PGMA can contribute towards stabilising the DNA/polymer complexes via enhanced co-operative interactions.[495] AA, DETA and PEHA are useful comparisons as the effect of varying the type of amines in gene transfection could be observed.

Hydrophobic modification of PDMAEMA could also be a route to improve the efficacy of transfection as the hydrophobic chains interact with the lipophilic cell membrane to improve cellular uptake.[197] DNA/polymer complex dissociation is also believed to be enhanced as a

result of the hydrophobic interactions compared to that of the dissociation occurring as a result of the ionic interactions between the polymer and the DNA. Thus, post-polymerisation modification of SiO_2-g-PDMAEMA with alkyl halides; methyl iodide,[462, 496, 497], allyl iodide and ethyl iodoacetate could potentially improve the transfection efficiency and the cytotoxicity of the system. Quaternization with these alkyl halides results in quaternary ammonium groups with permanent negative charges as opposed to the comparatively weak negative charge on the PDMAEMA alone.

In order to analyse any improvement to the DNA condensation and hence transfection ability of the aminated PGMA and derivatised PDMAEMA, the prepared systems were first characterised by NMR, ATR-FTIR and Zetasizer (particle size and zeta potential), then their DNA interaction capability was characterised via Zetasizer, followed by transfection assays using optimised conditions obtained for PDMAEMA.

4.2 Experimental methods

4.2.1 Synthesis and functionalisation of PGMA

4.2.1.1 Materials

Dichloromethane (DCM, Fisher Chemical), methanol (Sigma-Aldrich), Glycidyl Methacrylate (GMA, Sigma-Aldrich), free polyglycidyl methacrylate (f-PGMA, synthesised by Burcu Colak), DMF (VWR Chemicals), Et_3N (Sigma-Aldrich), diethyl ether (DEE, VWR Chemicals), THF (VWR Chemicals), deuterium oxide (Sigma-Aldrich), deuterated chloroform (Cambridge Isotope Laboratories, Inc.), allylamine (Sigma-Aldrich), diethylamine (Sigma-Aldrich), deionised water with resistivity of 18.2 MΩ·cm (Millipore) and silicon wafers (100 mm diameter, ⟨100⟩ orientation, polished on one side/reverse etched) (Compart Technology Ltd) were used as received.

4.2.1.2 Synthesis of f-PGMA

Free PGMA (Figure 69) was synthesised by Burcu Colak, by reacting a degassed solution of methanol, water, GMA, bipyridine, copper (II) bromide and coper (I) chloride with a degassed initiator solution containing PEG initiator (Figure 68), methanol and water, for 30 min at RT.

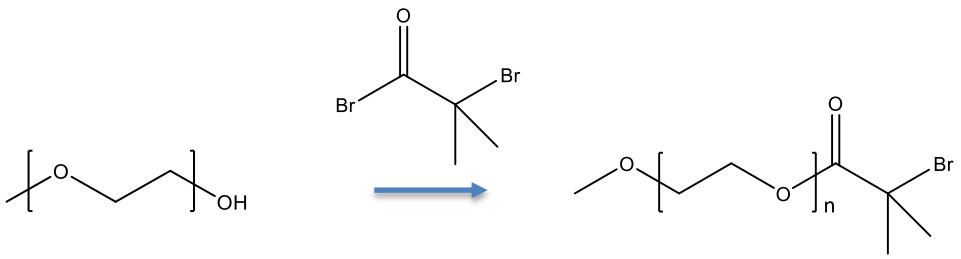

Figure 68: Synthesis of Free ATRP Initiator - PEG

A series of solvents including acetone, methanol and THF were added to the reaction mixture, which was then concentrated and precipitated in cold diethyl ether (DEE), dissolved in THF and precipitated again. The resulting polymer was dissolved in THF again then passed through a flash column to remove the catalyst. It was again precipitated in DEE before filtering and drying.

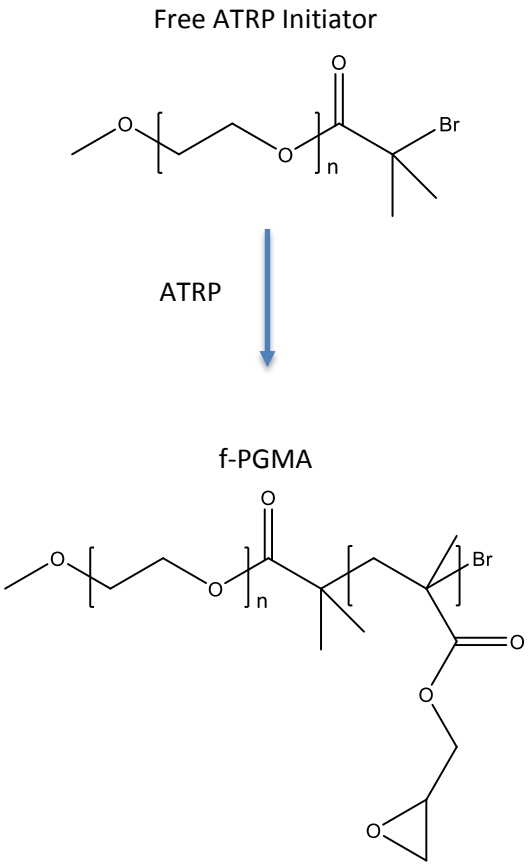

Figure 69: Synthesis of f-PGMA via ATRP.

As PGMA can be chemically modified due to the presence of the epoxide groups, this particular study, focused on the ring-opening reaction of the epoxide group by amines.

4.2.1.3 Functionalisation of f-PGMA with amines

A solution of f-PGMA (85 mg) in DMF (1.25 mL) was combined with a solution of amine (10 M); allylamine (450 µL) or diethylamine (12.5 mL), Et_3N (25% with respect to the amine) (209 µL) in DMF (1.25 mL). The mixture was left to react at 70°C overnight. Due to the low boiling temperature of diethylamine, the reaction with this particular amine was carried out such that the THF, f-PGMA, Et_3N and diethylamine were all added directly into one vial, with the diethylamine being added last. The resulting diethylamine solution containing THF was left to react at 50°C overnight. The THF was then removed by rotary evaporation and the remaining

solution was precipitated, centrifuged and dried lightly. The resulting polymers were dissolved in D_2O (1 mL) and deuterated chloroform (50 µL for allylamine) for NMR analysis.

4.2.1.4 Growth of PGMA brush on silicon wafers – kinetics study

A polymerisation mixture containing GMA (20.84 g, 147 mmol), bpy (564 mg, 3.6 mmol), $CuBr_2$ (15.6 mg, 70 µmol) and methanol/water (4/1 v/v, 20 mL) was stirred and bubbled under argon for 20 min. Cu (I) Cl (146 mg, 1.5 mmol) was added to the mixture and was bubbled for 5 min, sonicated for 2 min and then left to bubble again for a further 5 min under argon.

Initiator-coated silicon substrates were placed in a polymerisation tubes and degassed through 3 vacuum/argon cycles. The polymerisation mixture (4 mL) was added to each polymerisation tube, and left to react for 15 to 110 min. The reactions were quenched by the addition of deionised water. The wafers were removed and washed with deionised water, methanol and DCM before drying under a stream of nitrogen.

4.2.1.5 Growth of PGMA brush on silica nanoparticles

A monomer solution containing GMA (20.84 g, 147 mmol), bpy (564 mg, 3.6 mmol), $CuBr_2$ (15.6 mg, 70 µmol), methanol/water (4/1 v/v, 10 mL) and Cu (I) Cl (146 mg, 1.5 mmol) was prepared according to protocol in the previous section (the solvent was halved so that the final monomer concentration after combining with the particle solution would be the same as for the growth of brushes from silicon substrates).

The initiator-coated silica nanoparticles were sonicated to obtain a homogenous dispersion. Deionised water (800 µL), ethanol (100 µL) and initiator-coated silica nanoparticles (100 µL) were added to a polymerisation tube which was submerged into an ice box (to avoid evaporation of the solvent) and left to bubble under argon for 15 min. The monomer/catalyst mixture (1 mL) was injected into the tube, which was taken out of the ice box and left under argon but without bubbling. The reaction was left for 60 min and was stopped by adding DCM (1 mL) and deionised water (9 mL). The mixture was centrifuged and redispersed thrice in DCM, finally redispersed in 2 mL DMF and refrigerated.

4.2.1.6 Functionalisation of PGMA nanoparticles

Similar to the functionalisation of f-PGMA, PGMA-g-SiO_2 nanoparticles (2.8 mg/ mL, 5 mL) in a solution of 10 mL DMF was mixed with a solution of allylamine (100 mmol, 3.74 mL) or diethylene triamine (100 mmol, 5.4 mL) or pentaethylene hexamine (100 mmol , 12.23 mL) also containing, Et_3N (25mol% with respect to amine, 1.74 mL) in 10 mL DMF. The resulting reaction mixtures were incubated at 70°C in oil baths, overnight. The dispersions were then centrifuged and resuspended in deionised water (5 mL).

4.2.2 Functionalisation of PDMAEMA

4.2.2.1 Materials

Methyl iodide (CH_3I, Sigma-Aldrich), allyl iodide (Sigma-Aldrich), ethyl iodoacetate (Sigma-Aldrich), acetonitrile (ACN, HPLC Gradient grade, Fisher Chemical), Dimethyl sulfoxide (DMSO, Sigma-Aldrich), deionised water with resistivity of 18.2 MΩ·cm obtained using Milli-Q Integral 3 System from Millipore.

4.2.2.2 Functionalisation of f-PDMAEMA

Ethyl iodoacetate (3.77 mL, 0.0319 mmol) was added to a solution of f-PDMAEMA (1000 mg) in acetonitrile (5 mL) and stirred at room temperature for 24 h. The mixture was precipitated in DEE over 3 cycles and dried before dissolving in D_2O (1 mL) for NMR analysis.

4.2.2.3 Functionalisation of PDMAEMA nanoparticles

6 mL of PDMAEMA-g-SiO_2 nanoparticles prepared in three batches (5.4 mg/mL, 3.6 mg/mL and 3.9 mg/mL) following the procedure in Chapter 2.2.4 were incubated with an alkyl iodide solution of methyl iodide (0.032 mmol, 990 µL), allyl iodide (0.032 mmol, 1.455 mL) or ethyl iodoacetate (0.032 mmol, 1.89 mL) respectively, in acetonitrile (1 mL) at room temperature and gently shaken overnight on a 3D lab application shaker. The particle dispersion was washed with acetonitrile and deionised water sequentially via 3 centrifugation (4000 rpm for 15 min)/redispersion cycles and finally dispersed in 6 mL deionised water, with the exception

of allyl iodide-functionalised brush particles which were dispersed in DMSO due to the lack of stability of these particles in water.

4.2.3 DNA interaction study

Similar to the particle size and surface charge characterisation method described in Chapter 2.2.6, a solution containing amine-functionalised PDMAEMA-g-SiO_2 nanoparticles (4.6 mg/mL PDMAEMA-g-SiO_2-f-ethyl iodoacetate nanoparticles, 2.2 mg/mL PDMAEMA-g-SiO_2-f-methyl iodide nanoparticles and 2.4 mg/mL PDMAEMA-g-SiO_2-f-allyl iodide nanoparticles) at N/P ratios 1:1, 5:1, and 20:1, in 1 mL 150 mM NaCl was added to a solution containing 1 mL 150 mM NaCl and 20 µg EGFP (0.375 µg/µL) such that the final DNA concentration of 10 µg/mL was used. The combined solution was incubated at room temperature for 15-30 min to allow binding. The hydrodynamic diameter and the zeta potential of the resulting complexes as well as the particles before complexation were measured.

4.2.4 Transfection assay

Transfection experiments were conducted using optimised conditions from Chapter 3.2.3.2. HaCaTs were seeded at a density of 25k on collagen-coated 24 well-plates. Transfection efficiency was tested for the different amine-functionalised PDMAEMA-g-SiO_2 nanoparticles for N/P ratios 3:1, 5:1, 7:1 and 10:1. Reporter gene assay was performed the day after transfection, using DAPI to localise cell nuclei via epifluorescence microscope (Leica DMI4000B Epifluorescent).

4.2.5 Characterisation

Ellipsometry, NMR spectroscopy, FTIR spectroscopy, TGA, zeta potential measurements, particle sizing and DNA interaction experiments were carried out as described in Chapter 2.2.5.

4.3 Results and discussion

4.3.1 PGMA brush growth

Well-defined PGMA brushes can be prepared by ATRP at ambient temperature.[481, 482] As ATRP polymerises the monomer through the methacrylate group, the resultant polymer brush has pendant epoxide groups. The pendant epoxide ring can be opened and introduced to a range of functionalities via successive reactions with nucleophiles thus making PGMA a versatile polymer.

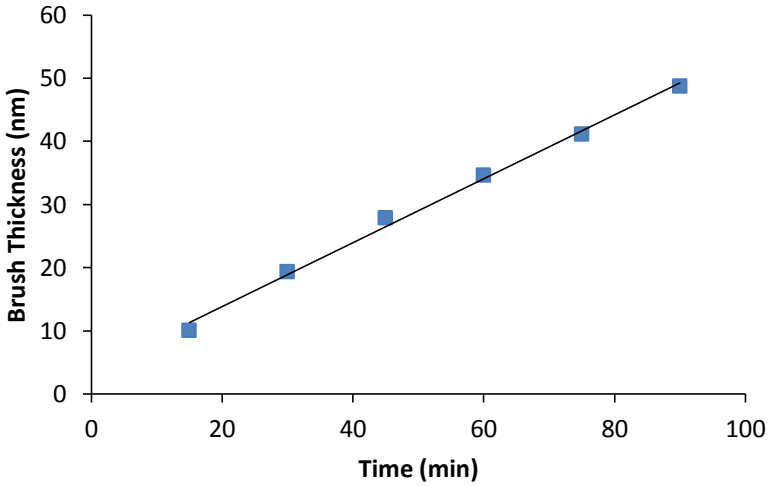

Figure 70: The change in PGMA brush thickness as a function of time as determined by ellipsometry. Values represent mean ± SE, n = 3.

Control of the PGMA brush growth on silane initiator-coated silicon surfaces was determined via ellipsometric measurements at different time points. The brush thickness of interest for this study (30 nm) was achieved at approximately 60 min. The plot of brush thickness with time exhibited a linear behaviour which confirms a truly living radical polymerisation and hence a controlled polymerisation (Figure 70).

4.3.1.1 Free polymer functionalisation

As PGMA can be chemically modified via epoxide side-chains, we first studied the ring-opening reaction of the epoxide by allylamine (Figure 71). Free PGMA was dissolved in

dimethylformamide (DMF), then triethylamine and the allylamine was added to this solution and heated at 70°C for 24 h. The functionalised PGMA was then precipitated in diethylether.

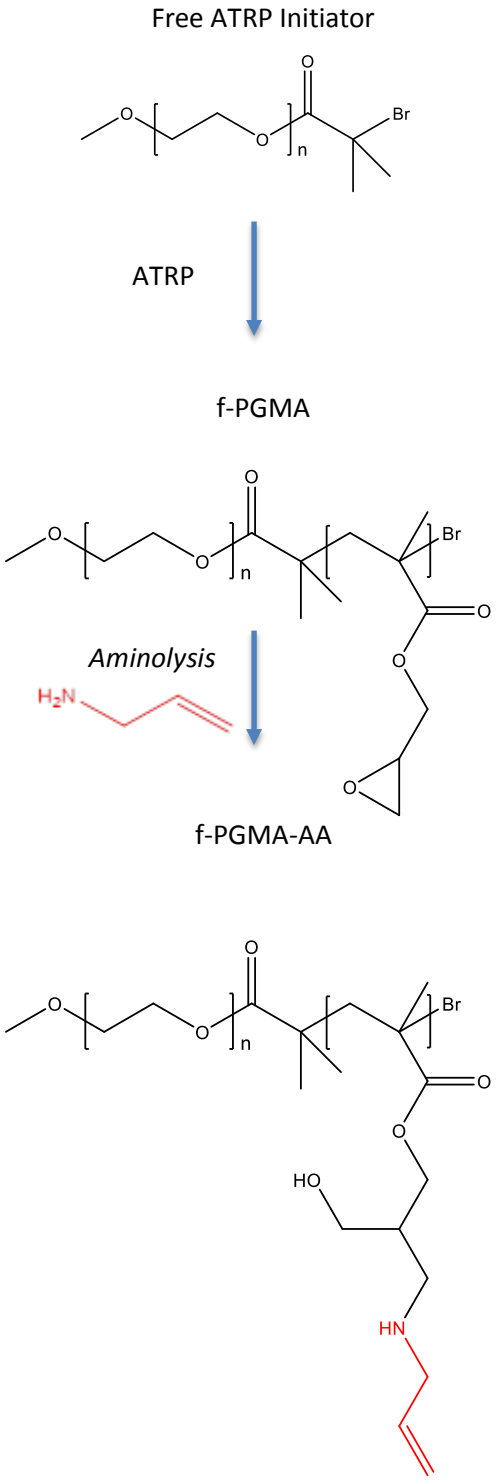

Figure 71: Synthesis of f-PGMA-AA via ATRP and aminolysis.

4.3.1.1.1 NMR

The structure of f-PGMA was characterised by ^{1}H NMR spectroscopy, as shown in Figure 72. The chemical shifts at 0.96, 1.12 and 1.21 ppm belonging to the protons of the methyl of PGMA were split into three peaks; isotactic, heterotactic and syndiotactic triads, respectively.[481, 498] The peak between 1.92 – 1.97 ppm belonged to the methylene protons in the backbone of the PGMA whilst the peaks at 3.83 and 4.32 ppm belonged to the methylene protons of the –O-$\underline{CH_2}$- side groups, adjacent to the oxygen moieties of the ester linkages, at position (c) due to the space isomerisation of the epoxy group.[486, 499, 500] The proton resonances for the epoxide ring, -CH_2-$\underline{CH}$(O)-CH_2 methylidyne and CH-CH(O)-$\underline{CH_2}$ methylene, were attributed to the chemical shifts at 3.25 ppm and 2.66 and 2.86 ppm, respectively.[501] There were two resonances for the protons labelled (e) in Figure 72 (bottom) as they were in different chemical environments (due to the lack of free rotation of the C-C bond of the epoxide).

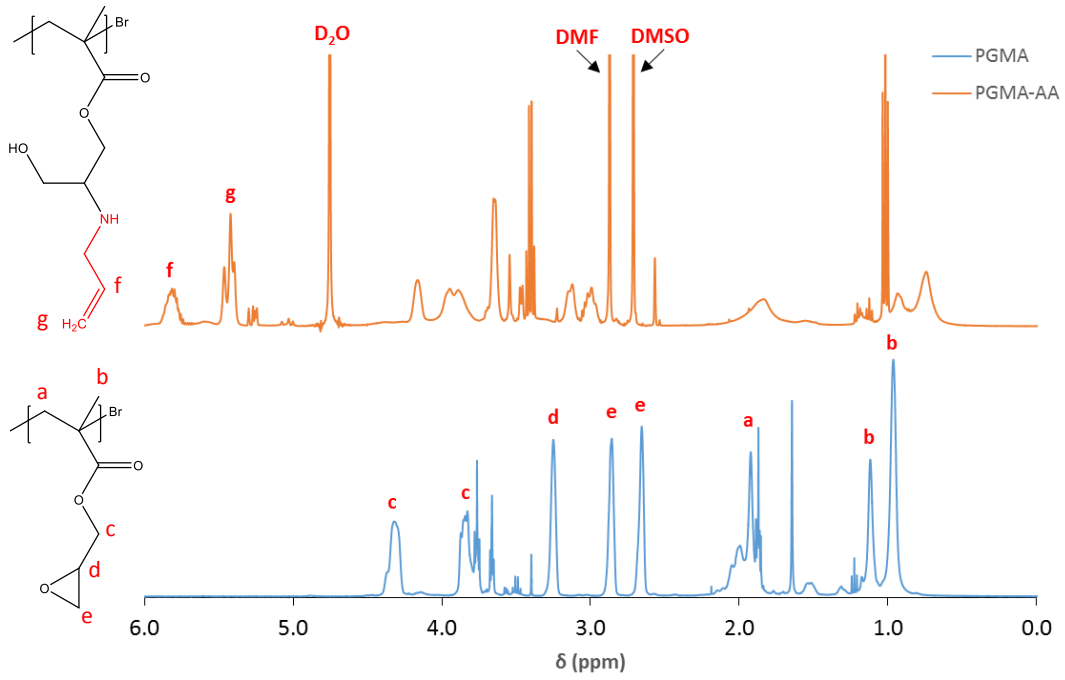

Figure 72: ^{1}H NMR spectra of PGMA and PGMA functionalised with allylamine, dissolved in $CDCl_3$ and D_2O, respectively. Data acquired by Burcu Colak and Reya Shamsah.

The ratio of peak areas of c, d and e is approximately 2:1:2 which suggests that the epoxy groups in the PGMA remained intact throughout the polymerisations of glycidyl methacrylate. [498, 499]

Following the ring-opening reaction of PGMA with allylamine, peak d associated with the epoxy groups of PGMA and peaks e of the methylidyne and methylene groups disappeared whilst two new solvent peaks, attributed to DMF and DMSO,[502] is seen for PGMA-AA. The characteristic signals for the methylene adjacent to the epoxy group at 3.83 and 4.32 ppm disappeared and were replaced by a new, broad peak at 3.88 - 3.94 ppm as a result of the space isomerisation of the epoxy group disappearing,[499, 500, 503] suggesting a quantitative opening of the epoxide rings. Peaks also appeared at 5.81 and 5.42 ppm, corresponding to the olefinic protons. Peaks attributable to the methylene protons connecting to amines appeared between 2.57 - 3.12 ppm. Broad peaks were also seen to form at 0.75 and 1.84 ppm, corresponding to protons in the methacrylate backbones.

4.3.1.1.2 FTIR

The IR spectra in Figure 73 represents the absorbance peaks for f-PGMA and derivatised f-PGMA-allylamine. The characteristic absorption band for the epoxide ring of f-PGMA appeared at 1240 cm^{-1}, whilst the bands for the carbonyl group (O-C=O) were present at 1722 cm^{-1}.[498] The bands at 900 and 837 cm^{-1} were attributed to the epoxide groups present in f-PGMA[482] which disappeared in the aminated PGMA.

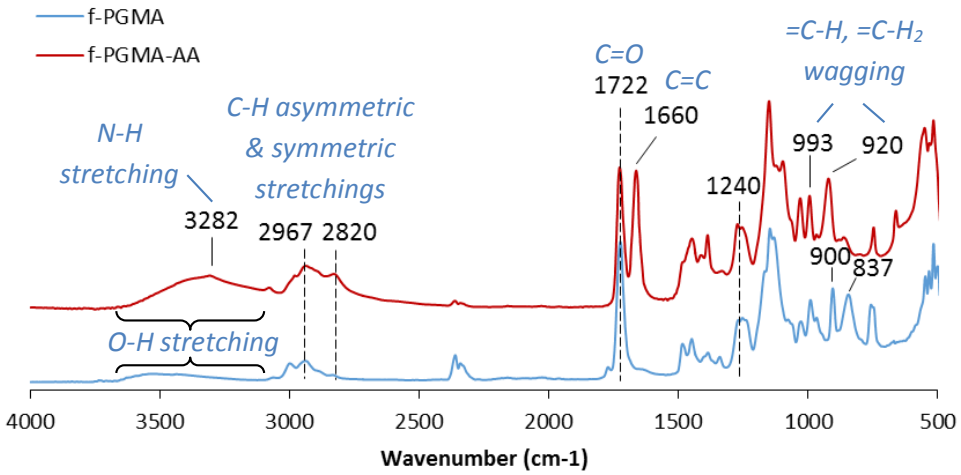

Figure 73: IR Spectra of f-PGMA and f-PGMA functionalised with allylamine.

In addition, the presence of C=C stretching at 1660 cm^{-1} and increase in the intensity of the C-H anti-symmetric and symmetric stretchings at 2967 cm^{-1} and 2820 cm^{-1}, respectively, were observed, consistently with the expected structure and confirming the successful ring-opening

reaction. The peaks at 920 and 993 cm^{-1} were ascribed to =C-H and =C-H_2 wagging, whilst the broad peak between 3100 and 3700 cm^{-1} belonged to O-H stretching and the overlapping stretching peak present at 3282 cm^{-1} was attributed to N-H stretching.[504] Hence, FTIR confirmed the effective functionalisation of f-PGMA with allylamine.

4.3.1.2 SiO_2-g-PGMA functionalisation

Following the successful functionalisation of f-PGMA with allylamine, confirmed via FTIR and NMR spectroscopy, two additional amines (DETA and PEHA) were chosen to functionalise PGMA brushes grown on silica nanoparticles. These modifiers contain between three and seven nitrogen atoms per molecule, respectively. These oligoamines were selected for their similarities to ethylenimine, potential to buffer at endosomal pH when polymerised and promising gene delivery properties with f-PGMA systems. The functionalisation of PGMA brushes with allylamine was also expored as the alkene moiety may be subsequently used for further biofunctionalisation via thiol-ene coupling (for example with cysteine peptides).

As with the functionalisation of f-PGMA, a solution of PGMA brush grafted on silica nanoparticles was mixed with a solution containing the amine of interest in triethylamine and DMF, and left to react at 70°C overnight. The PGMA brush was functionalised with a large excess of the different amine species as shown in Figure 74. The excess oligoamines of the derivatised SiO_2-g-PGMA were then removed by six centrifugation and redispersion cycles and finally resuspended in deionised water before using for DNA interaction and transfection studies.

It was found that the allylamine derivatised PGMA was not forming stable suspensions at near neutral pH, like the other amines. Lowering the pH to acidic conditions (below pH 5) did not improve the dispersion of the colloids. Hence full characterisation could not be performed for allylamine functionalised brushes. This may be due to cross-linking side reactions occurring at the allyl groups, as was sometimes observed for allylamine-functionalised f-PGMA samples. Therefore, only DETA and PEHA derivatised PGMA were used for DNA condensation and transfection studies.

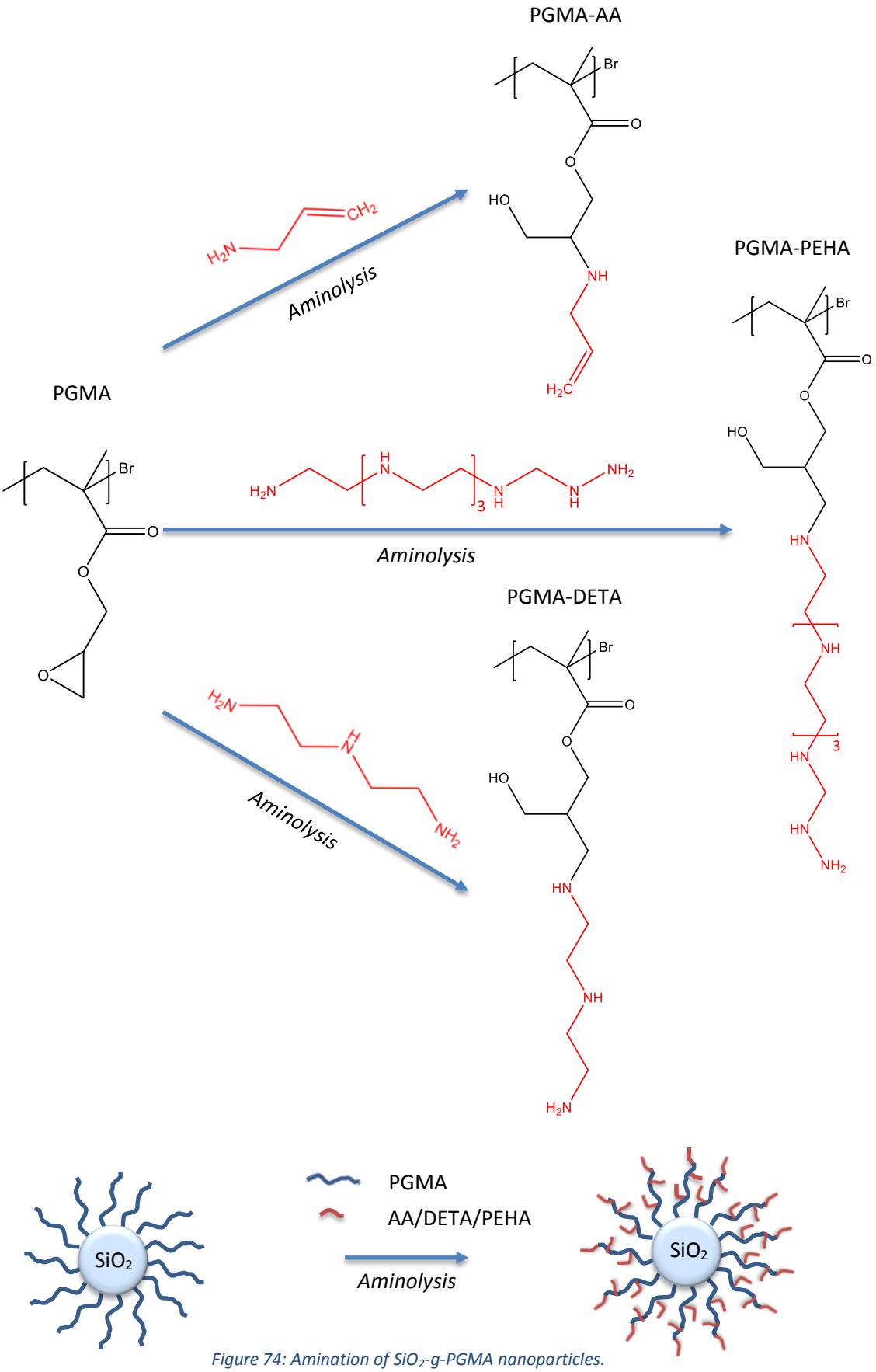

Figure 74: Amination of SiO_2-g-PGMA nanoparticles.

4.3.1.2.1 FTIR

IR spectra of PGMA and PGMA functionalised with AA, DETA and PEHA are shown in Figure 75. A prerequisite for successful post-polymerisation based on GMA grafted onto silica surface is preservation of the reactive epoxide groups during ATRP. The absorption peaks observed at 1268 and 1724 cm^{-1} were attributed to the epoxide ring and ester carbonyl groups (O-C=O) of PGMA, respectively,[498] thus confirming the successful polymerisation of the GMA monomer onto the silica nanoparticles.

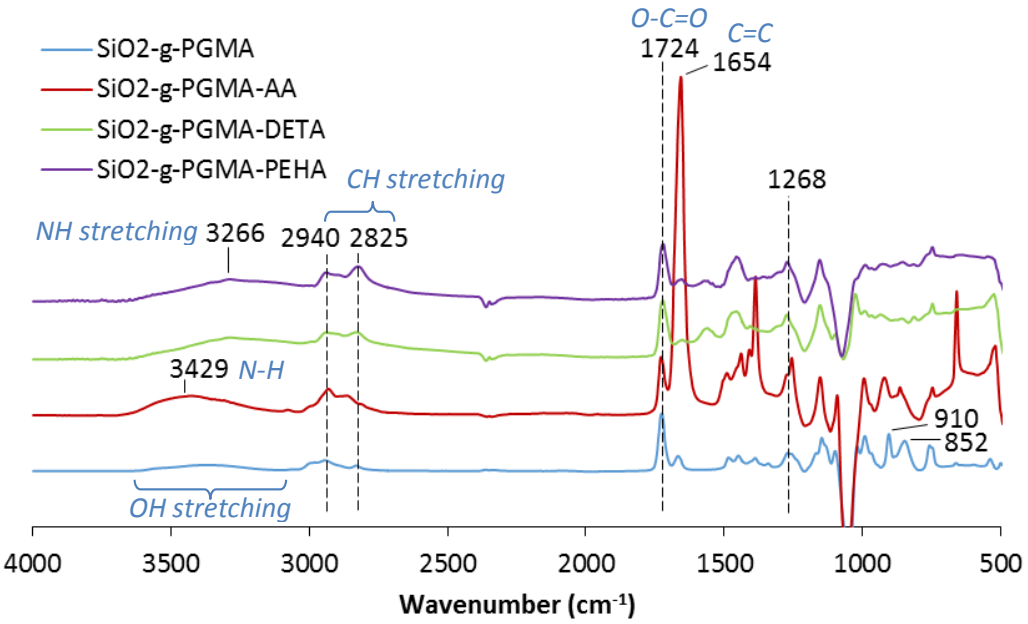

Figure 75: IR spectra of SiO_2-g-PGMA-oligoamines.

The strong absorption peak of the epoxide ring at 1268 cm^{-1} should weaken significantly upon functionalisation but is only clearly observed with SiO_2-g-PGMA-AA, possibly because of the smaller size of the amine which facilitates diffusion and infiltration into the PGMA brushes. Upon amination with DETA, the strong vibrational band at 1724 cm^{-1} is weakened but not substantially which suggests that unlike PGMA, functionalisation is not quantitative. Absorption band at 3429 cm^{-1} of SiO_2-g-PGMA-AA was attributed to the –NH bonds whilst the broad peak in the same region is attributed to O-H stretching of hydroxyl groups. A new band appeared at 1654 cm^{-1} which is attributed to C=C stretching.

The NH stretching around 3266 cm^{-1} appears to show a clearer change upon functionalisation of PGMA. The C-H stretching from the aliphatic backbone of PGMA chains could also be clearly

seen at ≈ 2940 and 2825 cm^{-1}, which increased in intensity upon functionalisation.[505] The nucleophilic reaction of the oligoamines with the epoxy group was further confirmed by the absence of the epoxide bands at 910 and 852 cm^{-1}, although overlap with other bands make it difficult to fully quantify the extent of this change. Additional O-H and N-H stretching bands appeared at 3266 cm^{-1} which also suggested the incorporation of AA, DETA and PEHA into the polymer brush by epoxide ring-opening and the formation of hydrogen bonds.[486] The shift in the position of this band and the appearance of features confirm the presence of both O-H and N-H bonds.[500]

4.3.1.2.2 Particle Size & Zeta Potential

Figure 77 compares the hydrodynamic diameters and the surface charge as indicated by the zeta potential of PGMA and SiO_2-g-PGMA-DETA and SiO_2-g-PGMA-PEHA however it is difficult to accurately compare the zeta potentials of all the functionalised nanoparticles against PGMA as the latter could not be stable resuspended in deionised water hence was redispersed in DMF. It was not possible to characterise the size of SiO_2-g-PGMA-AA particles due to the partial cross-linking of these colloids in the post-functionalisation step, resulting in an aggregated suspension in deionised water (or any solvent tested) (Figure 76).

During amination, once the epoxide ring-opens to a β-amino alcohol, this secondary amine can open a second epoxide thus forming inter and intra-chain bonds and cross-links.[482] This leads to the generation of large aggregates, in particular in the case of SiO_2-g-PGMA-AA.

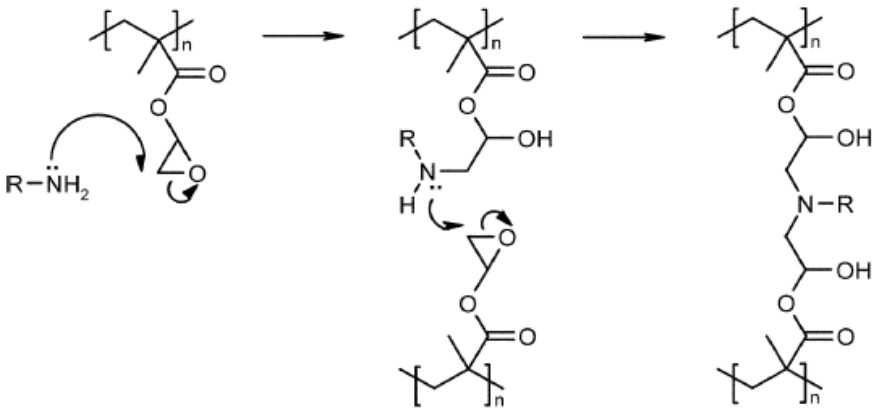

Figure 76: Possible mechanism for the cross-linking of PGMA brush chains by a primary amine.[482]

DETA and PEHA also displayed similar behaviours, but to a lower extent and formed stable colloidal suspensions, although particle aggregation was evident from light scattering experiments (Figure 77) and SEM (Figure 78). The micrographs indicated clear aggregation for DETA and PEHA compared to previous brush grafted nanoparticles.

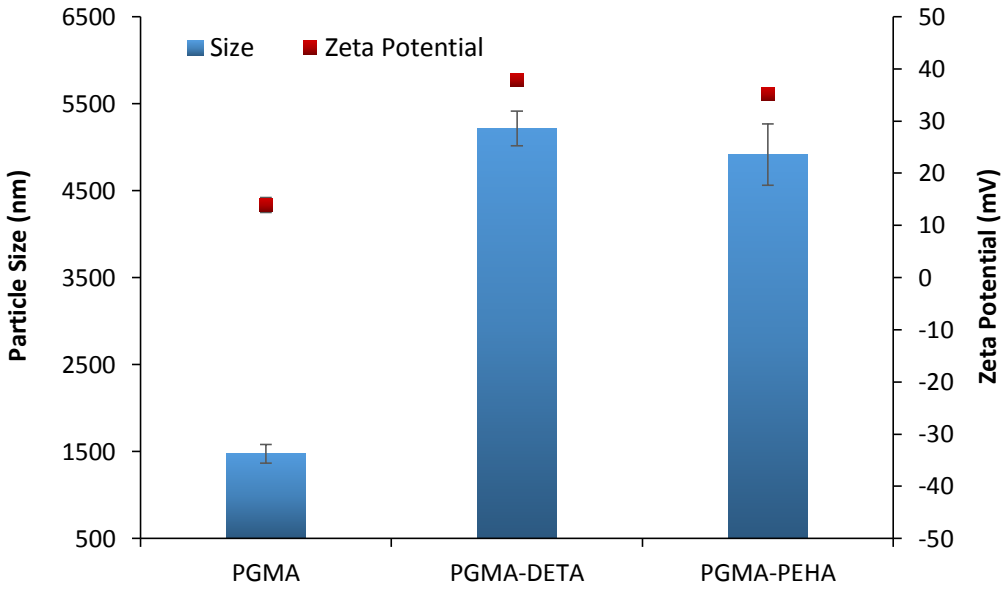

Figure 77: Hydrodynamic diameter and zeta potential of SiO_2-g-PGMA and its functionalised forms, in deionised water except for PGMA which was in DMF. Values represent mean ± SE, n ≥ 3.

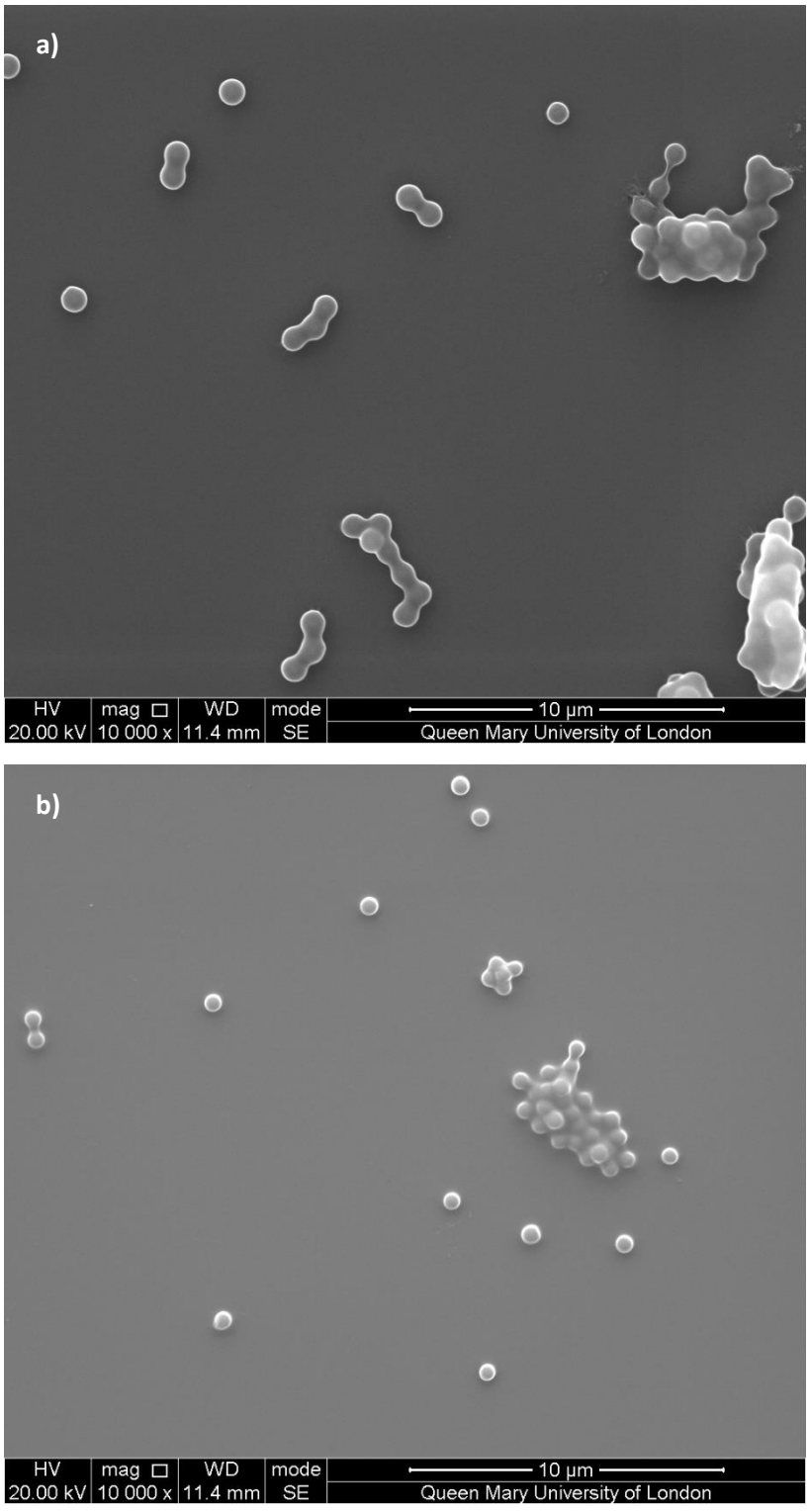

Figure 78: SEM micrographs displaying aggregation for a) SiO_2-g-PGMA-DETA, and b) SiO_2-g-PGMA-PEHA nanoparticles, at magnification 10,000x.

4.3.1.2.3 Interaction with DNA

The hydrodynamic diameter of SiO_2-g-PGMA was observed to be 1470 nm (SE = 110 nm) which is considerably higher compared to SiO_2-g-PDMAEMA which had an average hydrodynamic diameter of 830 nm (SE = 20 nm). This increased particle size of PGMA-functionalised colloids could be due to the hydrophobic nature of the brush which may form aggregates in solution. Partial cross-linking may also occur which in turn can also give rise to aggregates. The size of the error bars suggests that the generation of PGMA must be improved. Derivatisation of the epoxide side-chain of PGMA also gave a large increase, almost three-fold, in particle size for SiO_2-g-PGMA-DETA and SiO_2-g-PGMA-PEHA. It is also clear that upon functionalising with DETA and PEHA, the zeta potential increased notably to 37.9 (SE = 0.3 mV) and 35.1 mV (SE = 0.2 mV), respectively, confirming the formation of a strongly charged cationic polymer brush suitable for condensing DNA.

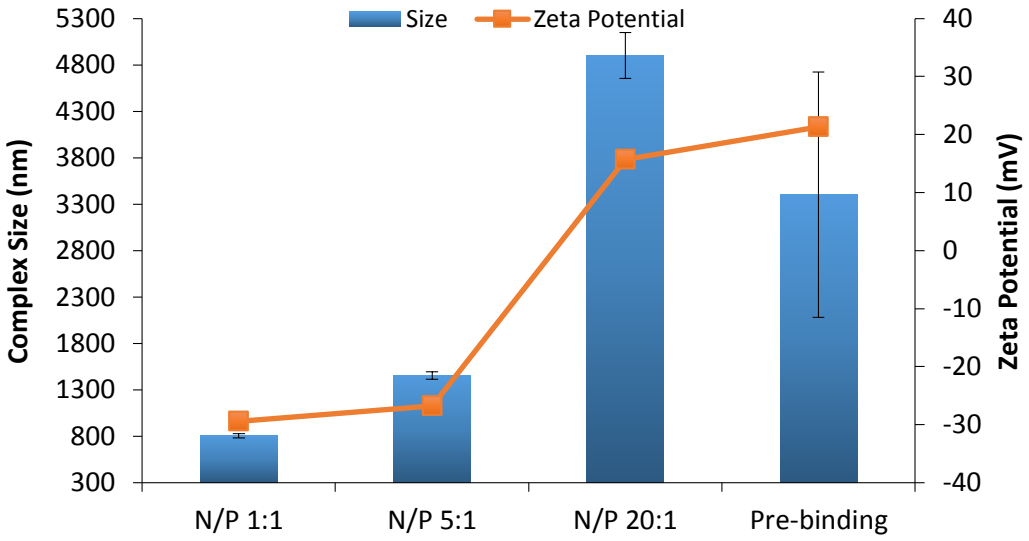

Figure 79: DNA interaction study with SiO_2-g-PGMA-DETA, in 150 mM NaCl. Values respresent mean ± SE, n ≥ 9.

For a successful gene delivery system, it is essential that the DNA is condensed by polycation into nanoparticles of a sufficiently small size as well as sufficient cationic charge as these factors play an important role in modulating cellular uptake. The condensation capability of polymeric gene delivery vectors is therefore of high importance. The condensation capability of the derivatised PGMA; SiO_2-g-PGMA-DETA (Figure 79) and SiO_2-g-PGMA-PEHA (Figure 80), was analysed through a DNA interaction study where the hydrodynamic diameter and the

indicative surface charge of the polymer/DNA complexes were measured as a function of N/P ratio.

The hydrodynamic diameter of SiO_2-g-PGMA-DETA particles/aggregates was significantly reduced upon complexation with DNA at N/P 1:1 and N/P 5:1, thus indicating efficient condensation of DNA by the SiO_2-g-PGMA-DETA. The pre-binding size was, on average, as large as 3400 nm (SE = 1320 nm) with a large error and PDI. It was reduced by almost four-fold following complexation with DNA for 15 min. This is an encouraging result for employing SiO_2-g-PGMA-DETA as a gene delivery vector. The extent of the collapse, however, is not expected. Compared to the collapse of PDMAEMA brushes when exposed to a similar amount of DNA (1.3-fold at N/P 1:1), this collapse implies extensive swelling of DETA-functionalised brushes and dehydration upon DNA interaction. This observation does not support the hypothesis that SiO_2-g-PGMA-DETA particles are aggregated, since the size of the collapsed particles would barely accommodate two particles. However, the extent of swelling measured for these particles prior to DNA interaction seems aberrant, if one assumes that particles were not aggregated. The expected particle size based on a five-fold swelling ratio is approximately 800 nm which is very close to the particle size achieved for N/P 1:1. At N/P 5:1, the complex size increases by about 650 nm from N/P 1:1. This increase can be attributed to partial coverage of DNA and collapse of the polymer brush. At N/P 20:1, there is a considerably lower amount of DNA and phosphates compared to the amount of cations in the polymer brush. The brushes are not condensing enough DNA to collapse significantly and potentially further interact with other particles via exposed DNA chains at their surface, as was observed for PDMAEMA at high N/P ratios. The slight increase in particle size after DNA complexation suggest increased level of aggregation but this remains marginal considering that it corresponds to only 1.4-fold compared to the uncomplexed SiO_2-g-PGMA-DETA particles.

In terms of the zeta potential, a charge reversal occurs as expected at N/P 1:1 due to the formation of a negative shell caused by saturation of the polymer brush with DNA. The zeta potential increases only slightly but still remains strongly negative for N/P 5:1 at -26.8 mV (SE = 1.1 mV) despite the presence of more positively-charged particles to the amount of negatively-charged DNA. PDMAEMA was observed to return to a positive value of 18.5 mV (SE = 1.2 mV) at the same N/P ratio. The negative potential measured for SiO_2-g-PGMA-DETA particles at this N/P ratio is consistent with the still relatively collapsed size of the particles, compared to uncomplexed colloids. This may suggest a complete lack of infiltration of DNA within the brush, perhaps as a result of crosslinks within the brush. Such crosslinking and lack of infiltration is not compatible with the large brush swelling and collapse measured prior and

after DNA interaction. The zeta potential returns to a positive value (15.7 mV, SE = 0.5 mV) at N/P 20:1, as a result of the excess cationic particles in comparison to the concentration of DNA. This aligns with what was observed with PDMAEMA. The positive charge is crucial for allowing electrostatic interaction with negatively charged cell surfaces and facilitate cellular uptake.

With SiO_2-g-PGMA-PEHA, similar trends were observed for both the size and the zeta potential. The hydrodynamic diameter was, however, significantly higher, by 1650 nm, for the pre-binding size whilst the complex sizes were larger for N/P 5:1 and N/P 20:1 compared to SiO_2-g-PGMA-DETA. The zeta potential also differed for the polymer/DNA complex at N/P 5:1. It was observed to be much higher than what was recorded for SiO_2-g-PGMA-DETA, increasing by 19.8 mV though it still remained negative.

Hence, increasing the number of nitrogen atoms in the modified PGMA side chains did not have a significant effect on the general behaviour of colloids during DNA condensation, except at N/P 5:1. This may reflect slight differences in the swelling (and potentially crosslinking) of DETA and PEHA functionalised PGMA brushes.

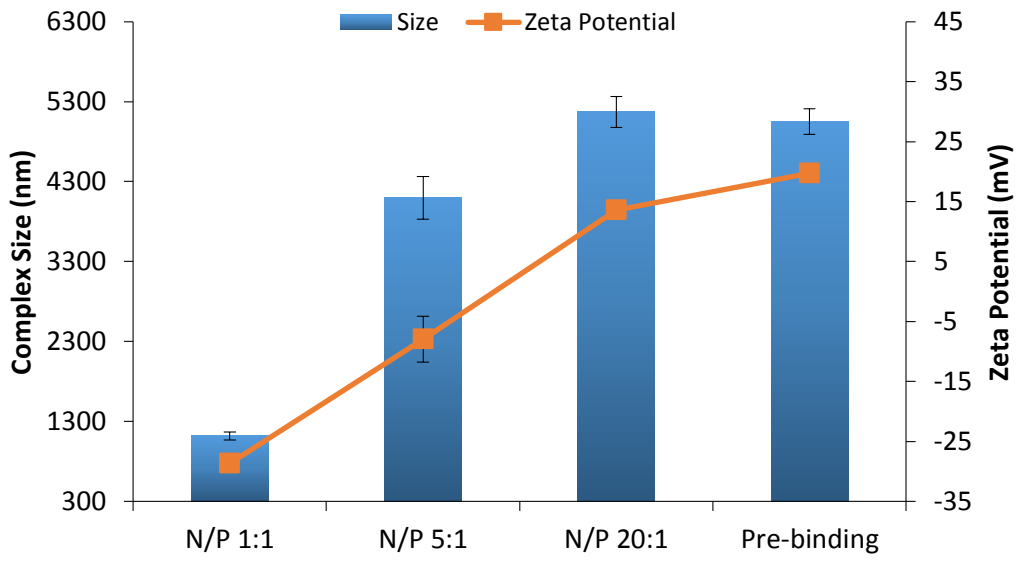

Figure 80: DNA interaction study with SiO_2-g-PGMA-PEHA, in 150 mM NaCl. Values represent mean ± SE, n ≥ 9.

4.3.1.2.4 Transfection Assay

Aminated PGMA brushes are believed to have the potential to deliver genes efficiently. Ethanolamine and methylethylamine functionalised f-PGMA for gene delivery has been reported in recent years,[489, 491, 499, 506] however other amine species have not been investigated extensively. To this end, the current study used three different amines (allylamine (AA), DETA and PEHA) to study their potential in cellular transfection.

It was found that, although transfection efficiency of the positive control jetPEI® was 19% (SE = 3.3 %) and the condensation capability of the aminated PGMA appeared to be encouraging, no transfection was observed for both, SiO_2-g-PGMA-DETA and SiO_2-g-PGMA-PEHA at N/P ratios 3:1, 5:1, 7:1 and 10:1 (Figure 81). Transfection could not be carried out with SiO_2-g-PGMA-AA due to the lack of stability of these colloids.

Although chemistry of these systems is favourable, it is possible that the cells are not uptaking these complexes due to aggregation or simply the large size of the complexes (>2000 nm) which may reduce endocytosis or the fate of complexes once in the cytosol. Other contributing factors may include the molecular weight of the aminated PGMA and the length of the PGMA backbone. DETA is known to have an odd number of repeating amino units[493] which may affect its interaction with DNA and size of complexes, and thus its transfection potential. Further modification by quaternization of the tertiary amine groups of amino PGMAs with an alkyl halide, as reported by Liang *et al.*,[506] could be an approach to improve the transfection efficiency but the complete lack of performance of these materials is not encouraging. Higher N/P ratios should possibly be investigated despite the potential toxicity issues from the positive charges.

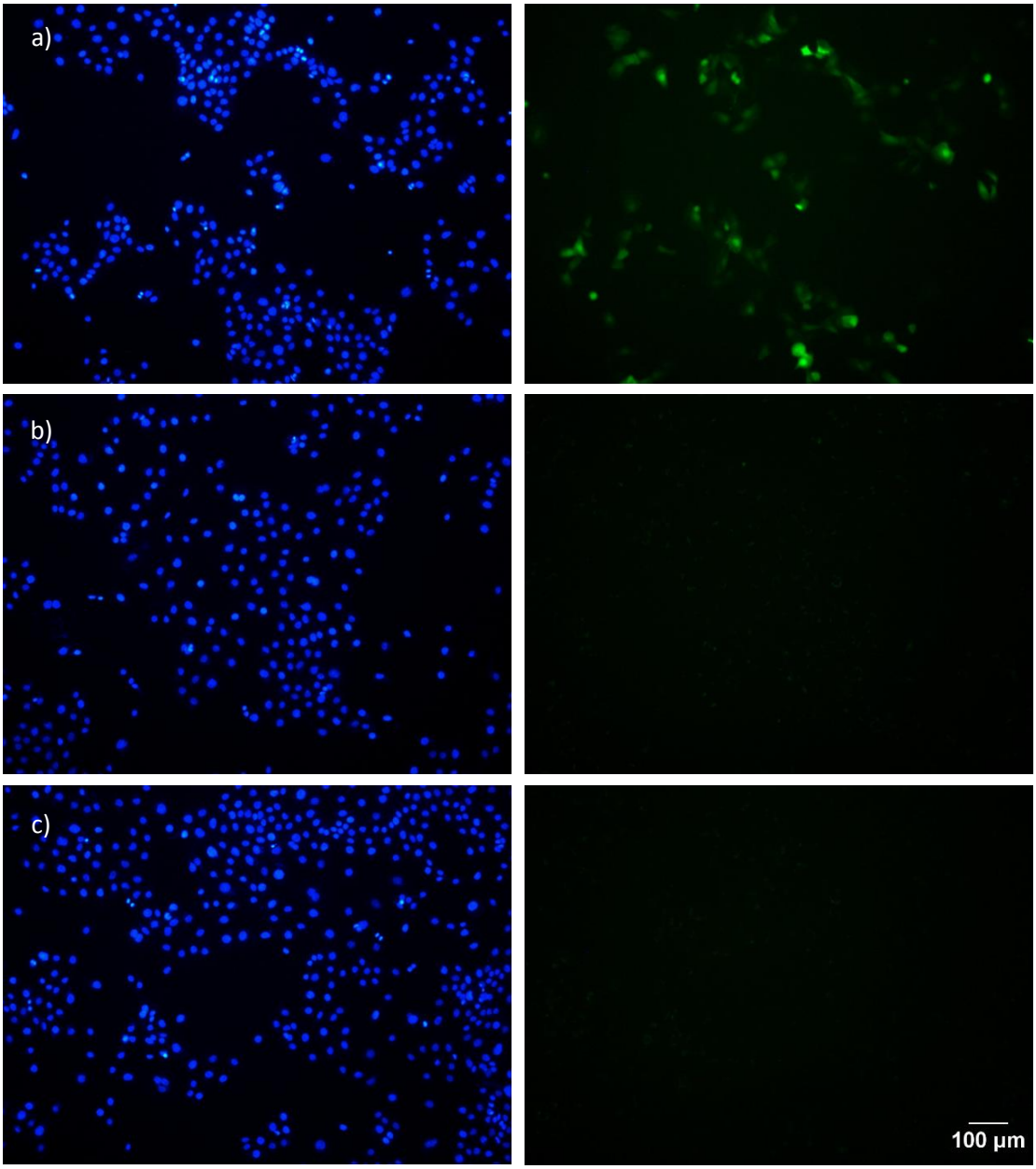

Figure 81: Fluorescence images of a) jetPEI®, b) SiO_2-g-PGMA-DETA and c) SiO_2-g-PGMA-PEHA transfections at N/P ratio 5:1, with HaCaTs, where blue is the nucleus, and green represents EGFP expression in cells

4.3.2 SiO_2-g-PDMAEMA functionalisation

Having systematically studied the potential of SiO_2-g-PDMAEMA for its DNA condensation ability, pH buffering capacity, cytotoxicity and gene transfection efficiency, tuning of its chemistry was of interest the design of improved gene delivery systems.

Hydrophobic modification of cationic polymers is one of the approaches taken to improve the gene delivery efficacy. The hydrophobic interaction within the amphiphilic cationic polymer derivatives and the enhanced cellular uptake resulting from the hydrophobic chains interacting with the lipophilic cell membrane contribute towards improving the gene delivery efficiency. Moreover, the hydrophobic interactions are believed to facilitate DNA/polymer dissociation better than the dissociation occurring from the ionic interactions between the cationic polymer and the anionic DNA. These advantageous traits of the hydrophobic units may lead to a higher transfection efficiency than cationic polymeric systems which rely solely on the ionic interactions. In this regard, SiO_2-g-PDMAEMA was functionalised with alkyl halides; methyl iodide, allyl iodide and ethyl iodoacetate, in an attempt to improve the transfection efficiency and the cytotoxicity of the system (Figure 82).

The initial weak polyelectrolyte PDMAEMA is converted to its strong polyelectrolyte analogue PMETAI upon quaternization with methyl iodide. Similarly, quaternization with allyl iodide and ethyl iodoacetate leads to the formation of quaternary ammonium groups which present permanent cationic charges in contrast with PDMAEMA brushes.

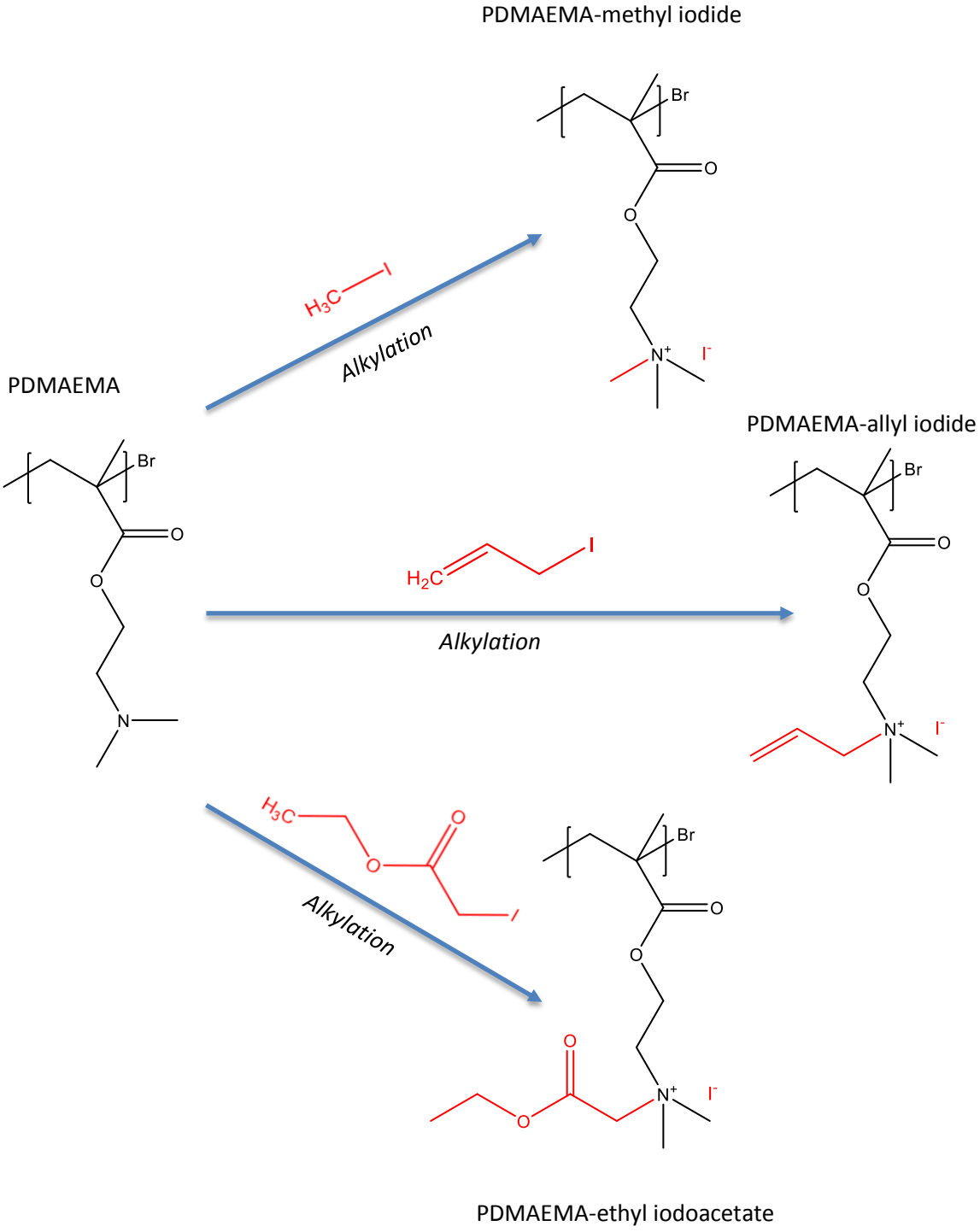

Figure 82: Alkylation of PDMAEMA with alkyl halides.

4.3.2.1 Characterisation

H^1 NMR spectra were obtained for the f-PDMAEMA and its derivatives to determine whether the functionalisation was successful (Figure 83). The peaks of the methyl and methylene group of PDMAEMA, at 2.29 and 2.7 ppm[386] disappeared with the introduction of the quaternary ammonium groups as expected. The D_2O solvent peaks appeared at 4.70 ppm.

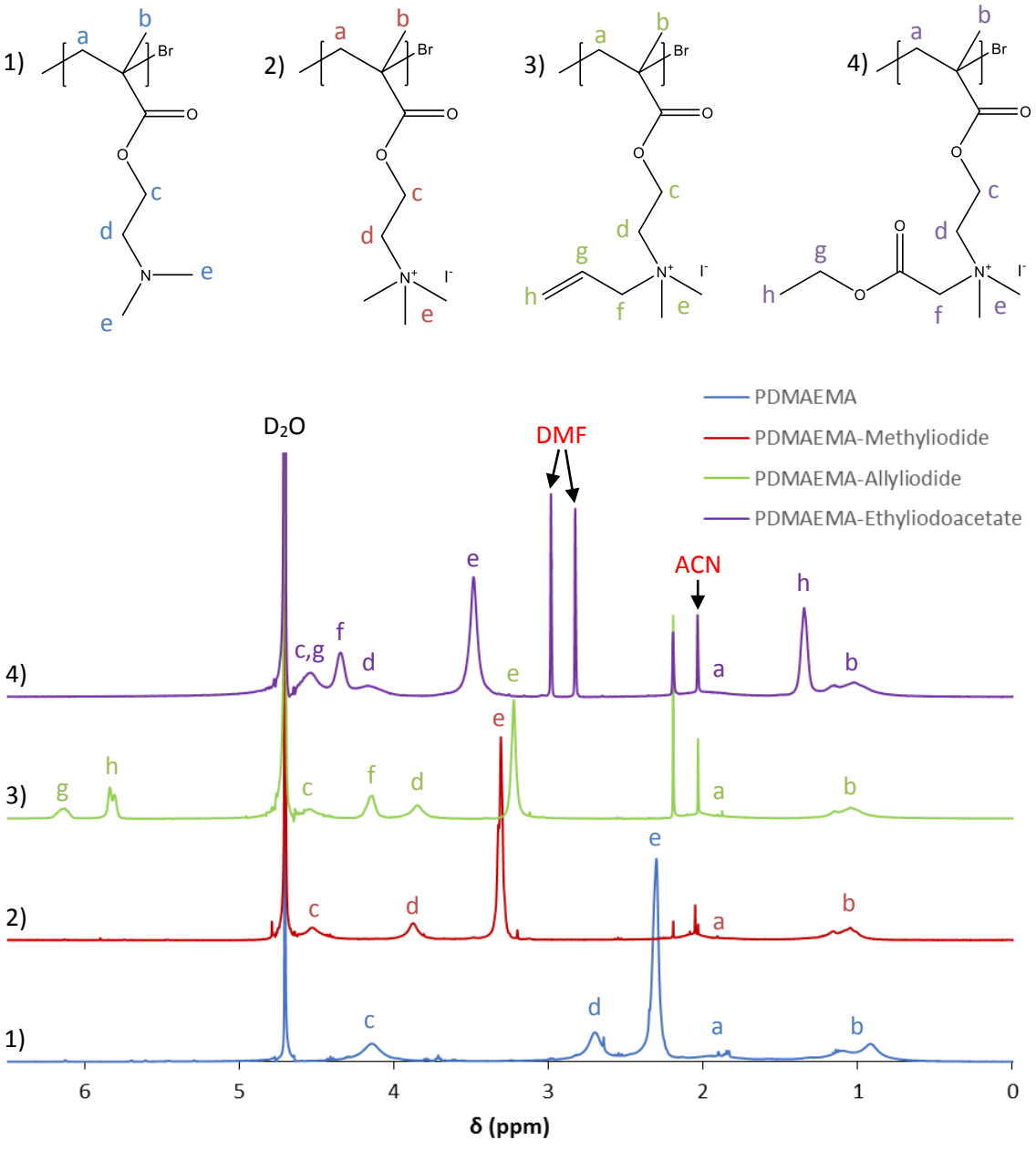

Figure 83: ^1H NMR spectra of 1) f- PDMAEMA and derivatised PDMAEMA; 2) PDMAEMA-methyl iodide, 3) PDMAEMA-allyl iodide, 4) PDMAEMA-ethyl iodoacetate, dissolved in D_2O

The peaks for the protons in the methyl of the main polymer chain appeared in all the free polymers around 1.05 - 1.16 ppm and 1.95 – 2.03 ppm, consistent with the fact that the polymer backbone remains unaffected by the functionalisation. The methylene group adjacent to the carboxylate group also appeared at 4.1 ppm, 3.87 ppm, 4.14 ppm and 4.17 ppm for free polymers 1-4, respectively.[507] Polymer 4 displayed an additional peak in this region, corresponding to the methylene of the ethyl ester adjacent to the carboxylate. Distinctive peaks, corresponding to the methylene adjacent to the ammonium were observed for polymer 2-4 in the region of 3.22 - 4.34 ppm. Finally, clear olefinic peaks are observe at 5.82 and 6.13 ppm for polymer 3, confirming the functionalisation with allyl group. Hence NMR clearly confirmed the efficient and quantitative functionalisation of PDMAEMA in mild conditions.

FTIR

The IR spectra of PDMAEMA grafted brushes on silica nanoparticles and its derivatives were obtained to confirm the functional groups (Figure 84).

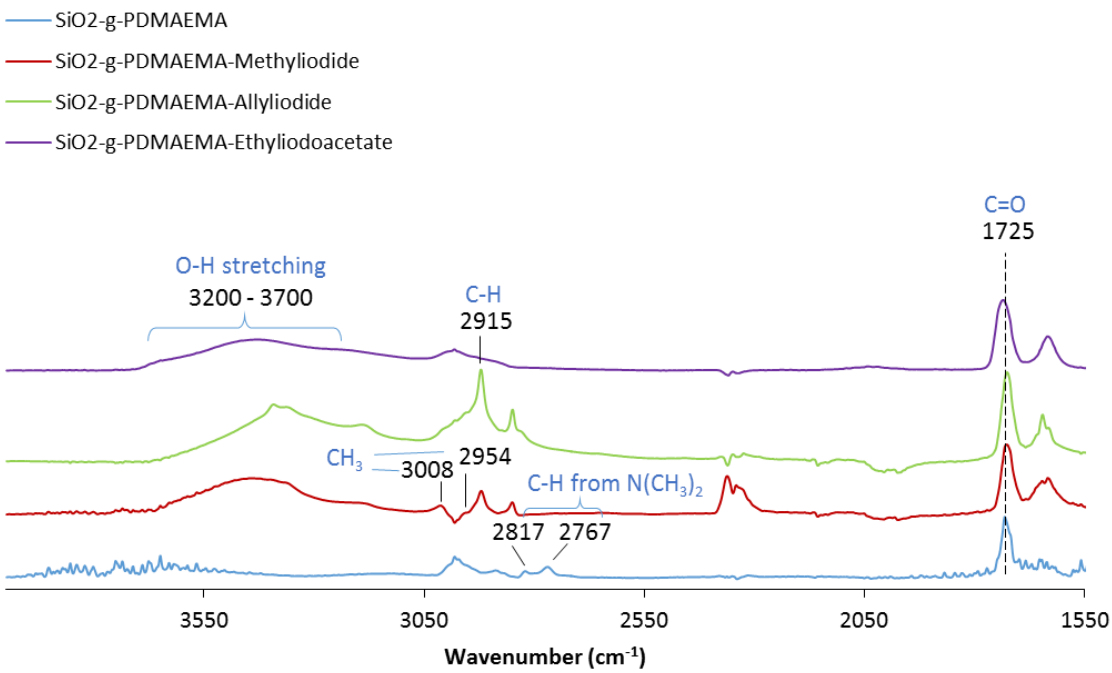

Figure 84: IR spectra of SiO_2-g-PDMAEMA and derivatised SiO_2-g-PDMAEMA nanoparticles.

The absorbance bands for all nanoparticles at 1725 cm^{-1} were attributed to the C=O bonds of the PDMAEMA whilst the bands at 2700 - 3000 cm^{-1} were from $–CH_2$ and α-CH_3 groups. The stretching vibrations at 2767 and 2817 cm^{-1} indicated the presence of the C-H bond of the $–N(CH_3)_2$ group of PDMAEMA [508] and disappeared upon functionalisation indicating full conversion of the amine and thus confirming high levels of functionalisation. The broad band between 3200 and 3700 cm^{-1} was the O-H stretching associated with water molecules that were absorbed by the more hydrophilic alkylated PDMAEMA brush. The methyl iodide functionalisation of PDMAEMA was confirmed by the bands present at 2954 and 3008 cm^{-1} which are attributed to the quaternary ammonium methyl groups.[509] Meanwhile the band at 2915 cm^{-1} for SiO_2-g-PDMAEMA-allyl iodide was observed to be more intense with increasing size of the monomer and thus an increase in the number of C-H groups. The additional ester in SiO_2-g-PDMAEMA-ethyl iodoacetate was evidenced by the slight shift of the carbonyl stretch to the left compared to the other alkylated PDMAEMA around 1725 cm^{-1}.

Particle Size & Zeta Potential

The hydrodynamic diameter and the zeta potential of the PDMAEMA brush grafted on silica nanoparticles and its derivatives were obtained prior to DNA interaction studies (Figure 85). The hydrodynamic diameter of the functionalised PDMAEMA-coated nanoparticles was seen to increase compared to unfunctionalised PDMAEMA-grafted silica nanoparticles, with the exception of the PDMAEMA decorated with allyl iodide. The lower hydrodynamic diameter of the PDMAEMA-allyl iodide indicates the collapse of this brush, in these conditions, perhaps as a result of the increased hydrophobicity conferred by the allyl group. This is also reflected by the low stability of these colloids, which typically sedimented rapidly after sonication.

The surface charge of the functionalised PDMAEMA particles, as indicated by the zeta potential values, also became more positive compared to PDMAEMA alone, reaching as high as 45.8 mV (SE = 0.4 mV) for PDMAEMA-ethyliodoacetate. The increased brush swelling measured for methyl and ethylacetate derivatives also reflects the increase in charge density of these brushes compared to PDMAEMA, as a result of the stronger associated osmotic pressure.

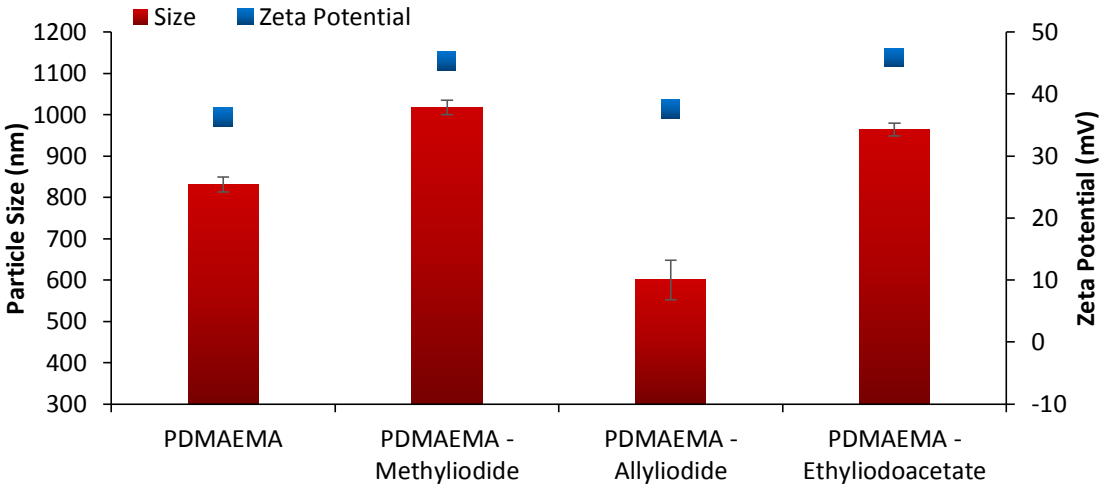

Figure 85: The hydrodynamic diameter and zeta potential of SiO_2-g-PDMAEMA and its derivatives, as measured in deionised water. Values represent mean ± SE, n ≥ 3.

A further study was performed with SiO_2-g-PDMAEMA-ethyliodoacetate to determine its stability over time in relevant pH conditions (pH 5, 7, and 9) due to the presence of the degradable ester on its side chain which impacts the charge shifting efficiency of ethyl acetate (Figure 86). The ethyl iodoacetate functionalised particles remained relatively stable for 7 days, in terms of both, the particle size and he zeta potential, at pH 5 and 7. However, degradation was observed for pH 9 after several days as the particle size was seen to reduce by 232 nm by the end of the 7th day, whilst the zeta potential decreased by almost three-fold to 13.6 mV (SE = 0.2 mV).

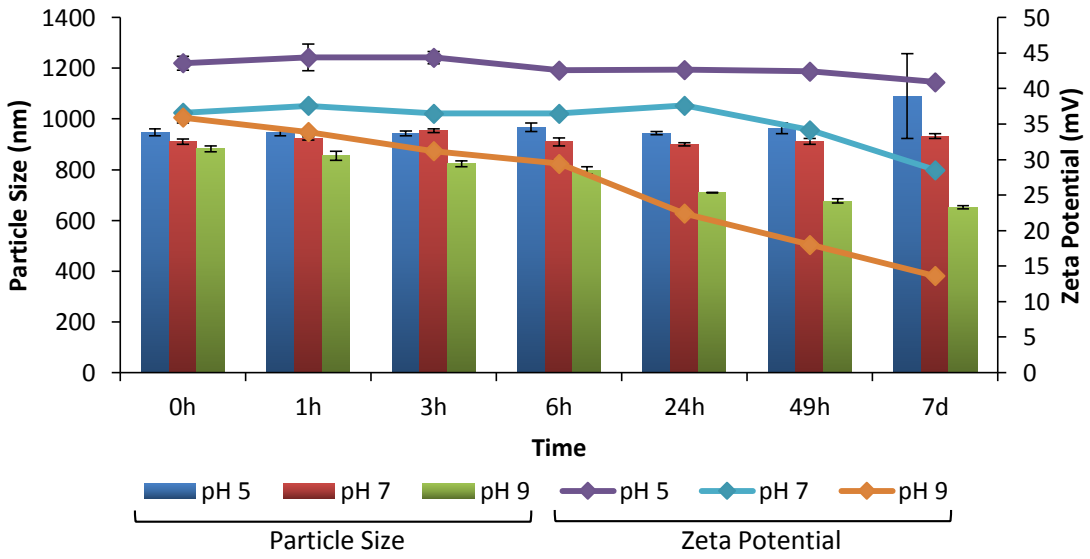

Figure 86: Degradation study of SiO2-g-PDMAEMA-ethyliodoacetate, at pH 5, 7 and 9 over 7 days. Values represent mean ± SE, n = 3.

4.3.2.2 Interaction with DNA

Alongside electrostatic interactions, hydrophobic forces may also contribute towards the formation of complexes between DNA and the hydrophobised SiO_2-g-PDMAEMA nanoparticles, as hydrophobic groups can give rise to co-operative binding of DNA.[197] The contribution of these forces in DNA condensation was analysed through the size and zeta potential measurements of each of the functionalised PDMAEMA nanoparticles (Figure 87). The size of the resulting complexes for the PDMAEMA derivatives (methyl iodide, allyl iodide and ethyl iodoacetate) reduced at N/P 1:1 by 100 nm, 170 nm and 130 nm, respectively. This confirmed the occurrence of DNA condensation by both electrostatic and possibly hydrophobic interactions. The strength of these interactions could be further tested by SPR, which provides further information on the dynamics of surface binding. The collapse of these brushes is attributed to the balancing of positive charges within the brush by the anionic phosphates of DNA molecules. This was also associated with a charge reversal, as for PDMAEMA (see Chapter 2.3.10.3, Figure 48), with negative values reaching between -30 and -32 mV.

At N/P 5:1, the size of complexes increased for all the PDMAEMA derivatives. For PDMAEMA-methyl iodide and PDMAEMA-ethyl iodoacetate the zeta potential also increases and returns to strongly positive values (28.1 mV (SE = 0.1 mV) and 17.1 mV (SE = 1.1 mV), respectively). These positive charges promote brush swelling which is reflected by the increase in the size as the number of cationic charges dominates the amount of DNA present. The increase compared to particles prior to complexation indicates a modest level of aggregation. This is, however, not true for PDMAEMA-allyl iodide – the zeta potential remains strongly negative at -21.6 mV (SE = 7.7 mV). This is perhaps consistent with the higher hydrophobicity of these brushes (and their collapse compared to PDMAEMA, before complexation) and may indicate that DNA molecules are prevented from infiltrating these brushes, as a result. Hence, smaller amounts of DNA would be expected to cover the surface of these particles and reverse the apparent surface charge.

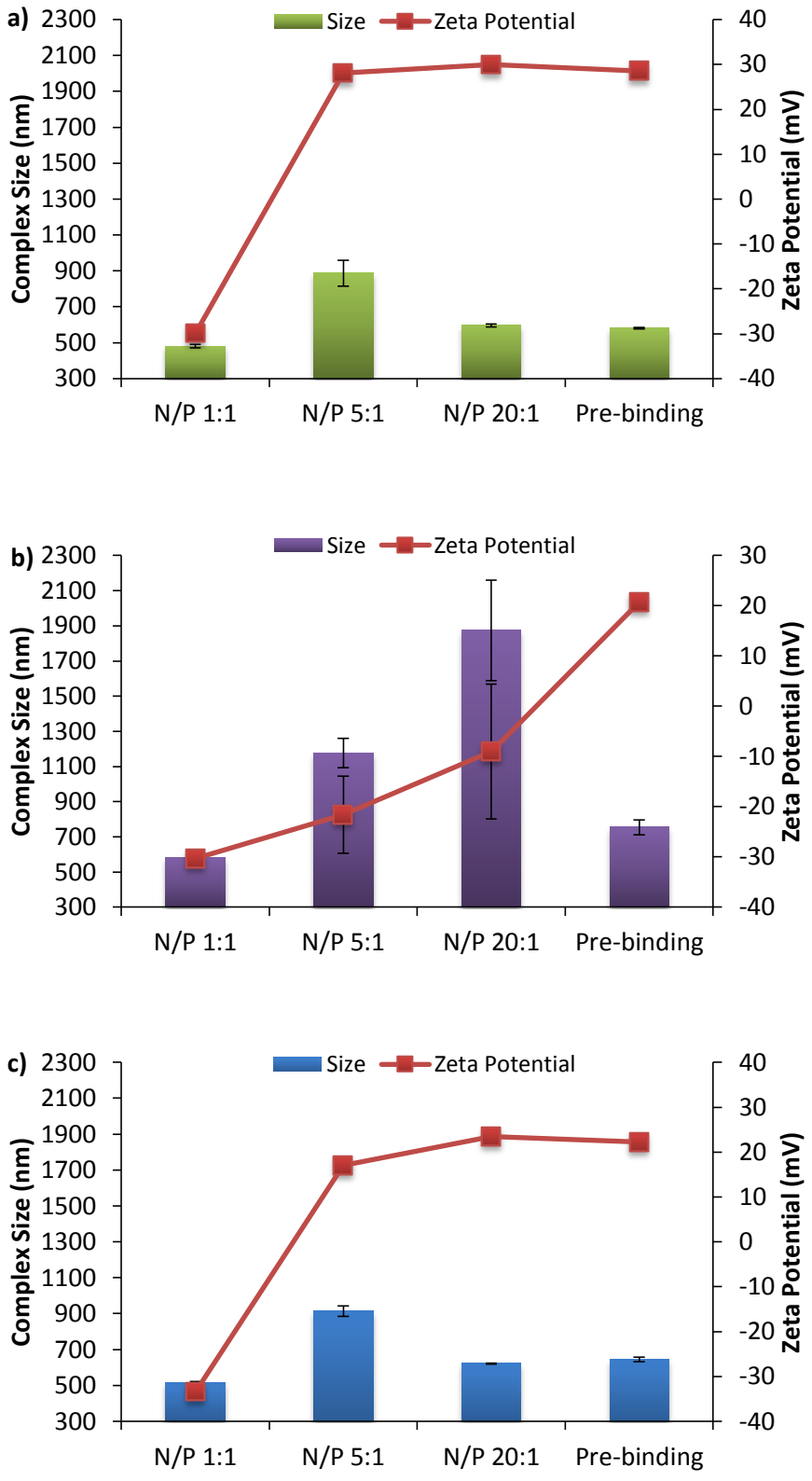

Figure 87: DNA Interaction study using a fixed DNA concentration of 10 µg/mL, with a) PDMAEMA-methyl iodide, b) PDMAEMA-allyl iodide and c) PDMAEMA-ethyl iodoacetate, as a function of N/P ratio, in 150 mM NaCl. Values represent mean ± SE, n ≥ 9.

At N/P ratios of 20:1, the size of complex is seen to decrease again for PDMAEMA-methyl iodide and PDMAEMA-ethyl iodoacetate whilst it increased for PDMAEMA-allyl iodide. The decrease in the size could be caused by decreased number of DNA molecules able to crosslink and aggregate particles, therefore restoring particle sizes and surface potentials close to those of particles prior to complexation. Particles coated with PDMAEMA-allyl iodide brushes did not follow this trend and their size increased further compared to uncomplexed particles, whereas their surface potential remained negative (although less so than at an N/P of 5:1). This may still indicate that the amount of DNA molecules available was sufficient to coat the surface of particles. The increase in particle size may indicate some level of aggregation and potentially the incomplete adsorption of DNA molecules at the surface of particles, with segments of DNA extending away and contributing to increase the particle size.

4.3.2.3 Transfection Assay

Transfection efficiency are not presented for PDMAEMA-methyl iodide and PDMAEMA-allyl iodide as they did not display any transfection. This is possibly due to the methylation of the polycations, which has been reported to give higher toxicity.[462] PDMAEMA-ethyl iodoacetate, on the other hand, showed low levels of transfection, as presented in Figure 88. The transfection efficiency was seen to increase with increasing N/P ratio; the highest transfection efficiency was observed at N/P 10:1 though near 1% which is significantly lower than the highest transfection of SiO_2-g-PDMAEMA at N/P 5:1 (9%, SE = 3%), whilst the positive control (JetPEI®) displayed 16% (SE = 1%) efficiency.

The difference in transfection observed between the tertiary groups and the quaternary groups could be due to the lack of buffering capacity of the quaternized PDMAEMA, which may not allow endosomal escape via a proton sponge effect, as is possibly the case with PDMAEMA. The buffering capacity of the cationic polymer brush is essential not only to protect the DNA from degradation when transported to the lysosome but also to allow lysosomal swelling and rupture as a result of protonation. This process allows the complexes to escape into the cytoplasm.[507] Hence quaternisation process may have weakened the buffering capacity of the derivatised PDMAEMA inside the lysosome which in turn restricts DNA release and results in the loss of transfection efficiency.

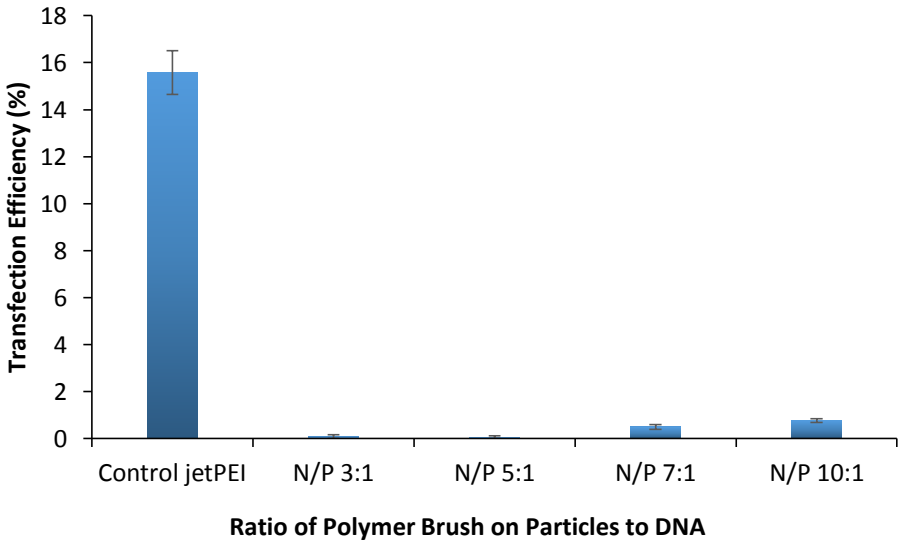

Figure 88: Transfection efficiency of SiO_2-g-PDMAEMA-ethyliodoacetate, using a fixed DNA concentration of 1 µg/mL, with HaCaT cell line (25k). Values represent mean ± SE, n = 3.

The absence of transfection for PDMAEMA-methyl iodide and PDMAEMA-allyl iodide may perhaps be expected due to their permanent charges whilst PDMAEMA-ethyl iodoacetate has charge-shifting properties. The ethyl ester can indeed cleave hydrolytically, resulting in the formation of an acid residue that typically is deprotonated at neutral pH and confers a neutral zwitterionic to the methacrylate repeat unit. Hence charge shifting, if triggered at the right pH and time point, may provide a simple method to control DNA release. However, ethyl esters typically hydrolyse slowly at pH 5-7, leading to poor charge shifting efficiency and may explain the lack of transfection efficiency compared to PDMAEMA brushes. The results from the degradation study of PDMAEMA-ethyliodoacetate indicated that the particle size and the zeta potential remained relatively stable for pH 5 and 7 over 7 days.

With PDMAEMA-ethyliodoacetate, at N/P 3:1 and lower, even lower transfection levels were observed, as the surface potential gradually decreased, together with attractive forces with cell membranes. Therefore, polymer/DNA complexes formed as a result cannot enter the cell easily. Although the increase in the cationic surface charges following quaternization increases affinity for negatively charged cell surfaces, at N/P 5:1 or above, the excess positive charges from the uncomplexed nanoparticles are possibly undesirable as it may prevent cellular association and internalisation due to the increased cytotoxicity. The quaternary amines of the polymer brush may cause cell death by disrupting the cell membranes and allowing the release of the intracellular contents. Another possibility for the lower transfection efficiency,

as mentioned earlier, is the weakened buffering capacity of the complexes as a result of the quaternization, which may restrict the polymer/DNA complexes from escaping the endosome via lysosomal swelling and rupture.[462, 507]

The increasing cationic charges of the polymer brush also impacts its interaction with the DNA. Strong interactions between the positively charged units of the polymer and DNA results in irreversible complexation thus DNA dissociation cannot occur in order to achieve transfection.

4.4 Summary

As PDMAEMA-g-SiO_2 nanoparticles produced moderate transfection efficiencies, the chemistry of the polymer brush coating the silica nanoparticle was tailored, such that the potential of the tuned new cationic system, in the form of PGMA functionalised with allylamine, diethylenetriamine and pentaethylenehexamine, and PDMAEMA modified with methyliodide, allyliodide and ethyliodoacetate were investigated. Each of the oligoamines and alkyl halides modifying the PGMA and PDMAEMA, respectively, were expected to have a beneficiary affect in gene transfection due to their contribution in stabilising the polymer/DNA complexes with the former and the formation of strong polyelectrolyte/ permanent cationic charge with the latter.

However, although the syntheses and functionalisations were conducted successfully with the exception of PGMA-allylamine due to crosslinking, the remaining PGMA-oligoamines and the PDMAEMA-alkylhalides did not successfully transfect cells. Although the DNA interaction studies were encouraging where clear DNA condensation was observed for PGMA functionalised with DETA or PEHA, there was an absence of transfection for both. This is attributed to the large size or aggregation as observed via Zetasizer. Amongst the alkyl halides, PDMAEMA post-modified with ethyliodoacetate was the only system to give any transfection though very low as this alkyl halide is charge-shifting whilst others had permanent charge which may have resulted in high cytotoxicity, and hence no transfection could take place, in addition to the lack of buffering capacity as a result of the quaternization. Having acquired some knowledge of the effect of tuning the chemistry, further optimisation could lead to improved gene delivery efficiency.

5 Conclusions and future directions

5.1 Conclusions

From the literature, it is clear that polymer brushes are useful in various applications. In the present study, cationic polymer brushes were investigated for their potential in gene delivery. The grafting from approach enabled a controlled polymerisation where the brush thickness and chemical composition of the brush could be altered easily. The flexibility of the brushes allowed functionalisation post-polymerisation.

A tailorable non-viral gene delivery system was thus developed with a silica core and a shell of cationic PDMAEMA brushes. The responsive nature of these nanoparticles were determined as a function of pH and pure PDMAEMA brushes were seen to be highly protonated at low pH, exhibiting large hydrodynamic diameters as a result of the interparticle repulsions, and became hydrophobic at high pH. A notable collapse in the zeta potential was observed between pH 7 and 9 near the pK_a of PDMAEMA.

The cationic nature of the brushes enabled electrostatic interaction with and subsequent condensation of DNA into compact complexes in 150 mM NaCl as shown by SPR, DLS, ELS and in situ ellipsometry. The brushes were seen to collapse to an extent thus suggesting that condensation of DNA is occurring. The compacted complex could then be taken up by the cell. The process is further facilitated by the overall cationic surface charge of the polymer/DNA complex at the appropriate N/P ratios which promotes the association of the complex with the anionic cell membrane.

Cellular interaction with the brush surfaces were then studied and lower cell viability was seen over time and with higher composition of PDMAEMA as a result of the positive charges of the cationic brush perturbing the anionic cell membrane. The presence of DNA shielded the positive charges of the brush to an extent thus presenting higher cell viability than direct cell-brush interactions.

The gene expression efficiency observed in the study, particularly for f-PDMAEMA was poor compared to what has been reported in the literature. This could be attributed to the type of assay used to quantify the efficiency. The EGFP-based assay used in the current study, however, gives a more accurate value of the transfection efficiency as it accounts for every transfected cell as opposed to the value derived from the intensity of the expression as measured by the more commonly used luciferase assay which can be misleading.

PDMAEMA-grafted nanoparticles displayed better transfection efficiency than f-PDMAEMA when using the EGFP assay. This could be attributed to the lower amount, if any, of residual copper catalyst present with the polymer brush-grafted nanoparticles compared to free polymer. The cell viability at the most efficient N/P ratio was above 65 %. Several aspects of the transfection assay including cell type, cell seeding density, transfection medium and plasmid batch type could be optimised such that the final transfection assay used HaCaT cell line at 25k seeding density using KSFM as transfection medium and an EGFP batch pre-tested with the control, jetPEI®. The highest transfection level attained for PDMAEMA-grafted nanoparticles was just below 10%. Although this transfection efficiency is low compared to the control, jetPEI® itself only displayed just above 25% transfection efficiency compared to above 80% reported by PolyPlus transfection. Hence further tuning of the chemistry and architecture of the system is necessary. The low levels of transfection are most likely due to the barriers faced by the polymer/DNA complex during intracellular routing. The endosomal escape of PDMAEMA/DNA complexes and subsequent routing through the cytosol may be hindered by a number of factors including enzymatic degradation, early dissociation of complexes resulting in loss of DNA along the transport route to the nucleus and the complexes that do overcome the barriers not reaching the transcriptional machinery. Cellular uptake could not be characterised efficiently as it was difficult to differentiate between cellular binding and uptake as well as the poor emission from the fluorophores.

5.2 Future directions

Further modifications of the non-viral vector system is required in order to improve the transfection efficiency. The present study has elucidated that particle size could be largely impacting this efficiency hence tailoring the system with a smaller core size may be a pathway to gaining better transfection efficiency as aggregation has been generally observed during

most of the characterisations. Changing the size however will impact the other parameters and therefore careful tuning of the system is required. There is likely to be heterogeneous populations of nanoparticles in any sample, and the size, PDI and charge of nanoparticles usually depend on the hydration state and type of measurement technique used.

The molecular weight of PDMAEMA is another factor that could be adjusted to achieve better transfection levels. 25 kDa PDMAEMA does not give comparable transfection to 25 kDa PEI as the number of primary amines in PDMAEMA is lower therefore adjusting the molecular weight may aid the optimisation of the non-viral vector system.

It must also be taken into consideration that non-viral vector efficiency varies in different cell lines, passage number, cell cycles and growth media. The effect of the type of medium used for polymer/DNA complex formation was briefly investigated. The preliminary results indicated that PBS gives higher number of transfected cells than 150 mM NaCl or 10 mM HBS hence it would be useful to perform an in-depth analysis of the ionic strength. Further characterisation with PBS in terms of the swelling and charge behaviour of PDMAEMA-grafted nanoparticles, DNA-brush interaction studies, cytotoxicity assays and transfection assays at a range of N/P ratios would be beneficial.

Furthermore, the pH responsive nature of PDMAEMA could be utilised by varying the pH of the media to control its complexation behaviour as well as transfection by favourably tuning the charge density of the resultant polyanion complex to promote cellular uptake, endosomal escape and DNA release whilst also reducing the cytotoxicity.

The electrostatic interaction between PDMAEMA and DNA can also be examined to obtain information on the strength of the interaction which may shed light on the dissociation abilities of the complexes and subsequent DNA release when in the cytosol. It would be worth also noting whether small molecules from the medium play a role in dissociation of DNA from the complex.

As discussed in Chapter 3, DNA delivery is affected by both endosomal escape and destabilisation of the complexes thus strategies aiming to release DNA earlier from the endosome could improve transfection efficiencies. It would be also useful to perform 3D imaging using CLSM to further monitor the localisation of the complexes and live imaging using the same microscopy method to acquire information on the possible route taken by these complexes.

Developing targeted systems by conjugating ligands such as antibodies, peptides, proteins, growth factors and other small molecules to these nanoparticles can give direct delivery to cancer cells or intracellular organelles including the nucleus (using nuclear localisation factors), whilst avoiding any undesirable side effects.

The current system could also employ quantum dots or labelled particles with more robustly fluorescent particles as they can be more easily detected, thus allowing quantification of the cellular uptake. Simultaneous labelling of DNA would also allow to determine DNA-brush dynamics in the cytosol.

6 Appendices

6.1 Appendix 1

Calculation of Copolymer composition via NMR

The ratio of PDMAEMA to POEGMA in the copolymer brushes were calculated using two methods. It is encouraging that both methods give comparable values.

Method 1

For 25% PDMAEMA and 75% POEGMA:

Integration area for methoxy (-O-CH_3) group present in POEGMA at 3.35 ppm = 0.38

Number of protons = 3

$$\text{Ratio of methoxy group} = \frac{0.38}{3} = 0.126$$

Integration area for methylene (N-CH_2-) group present in PDMAEMA at 2.7 ppm = 0.11

Number of protons = 2

$$\text{Ratio of methylene group} = \frac{0.11}{2} = 0.055$$

$$\text{Ratio of PDMAEMA in copolymer} = \frac{0.055}{0.126 + 0.055} \times 100 = 30.39\%$$

$$\text{Ratio of POEGMA in copolymer} = \frac{0.126}{0.126 + 0.055} \times 100 = 69.61\%$$

Method 2

For 25% PDMAEMA and 75% POEGMA which is 1:3,

Integration area for methoxy (-O-CH_3) group present in POEGMA at 3.35 ppm = 0.38

Number of protons = 3

Integration area for methylene (N-CH_2-) group present in PDMAEMA at 2.7 ppm = 0.11

Number of protons = 2

$$\text{Ratio of POEGMA in copolymer } = \left(\frac{0.38}{3}\right) \div \left(\frac{0.11}{2}\right) = 2.3$$

Hence the ratio of PDMAEMA to POEGMA is 1:2.3

$$\frac{1}{3.3} \times 100 = 30.22\%\ PDMAEMA$$

$$\frac{2.3}{3.3} \times 100 = 69.78\%\ POEGMA$$

7 References

[1] Brown, A. A., Khan, N. S., Steinbock, L., and Huck, W. T. S., 'Synthesis of Oligo(Ethylene Glycol) Methacrylate Polymer Brushes', *European Polymer Journal,* 41 (2005), 1757-65.

[2] Tan, K. Y., Gautrot, J. E., and Huck, W. T. S., 'Formation of Pickering Emulsions Using Ion-Specific Responsive Colloids', *Langmuir,* 27 (2011), 1251-59.

[3] Azzaroni, O., 'Polymer Brushes Here, There, and Everywhere: Recent Advances in Their Practical Applications and Emerging Opportunities in Multiple Research Fields', *Journal of Polymer Science Part A: Polymer Chemistry,* 50 (2012), 3225-58.

[4] Kim, T. K., and Eberwine, J. H., 'Mammalian Cell Transfection: The Present and the Future', *Analytical and Bioanalytical Chemistry,* 397 (2010), 3173-78.

[5] Durocher, Y., Perret, S., and Kamen, A., 'High-Level and High-Throughput Recombinant Protein Production by Transient Transfection of Suspension-Growing Human 293-Ebna1 Cells', *Nucleic Acids Research,* 30 (2002), e9-e9.

[6] Glover, D. J., Lipps, H. J., and Jans, D. A., 'Towards Safe, Non-Viral Therapeutic Gene Expression in Humans', *Nat Rev Genet,* 6 (2005), 299-310.

[7] von der Leyen, H. E., Gibbons, G. H., Morishita, R., Lewis, N. P., Zhang, L., Nakajima, M., Kaneda, Y., Cooke, J. P., and Dzau, V. J., 'Gene Therapy Inhibiting Neointimal Vascular Lesion: In Vivo Transfer of Endothelial Cell Nitric Oxide Synthase Gene', *Proc Natl Acad Sci U S A,* 92 (1995), 1137-41.

[8] Losordo, D. W., Vale, P. R., Symes, J. F., Dunnington, C. H., Esakof, D. D., Maysky, M., Ashare, A. B., Lathi, K., and Isner, J. M., 'Gene Therapy for Myocardial Angiogenesis: Initial Clinical Results with Direct Myocardial Injection of Phvegf165 as Sole Therapy for Myocardial Ischemia', *Circulation,* 98 (1998), 2800-4.

[9] Tomita, T., Takeuchi, E., Tomita, N., Morishita, R., Kaneko, M., Yamamoto, K., Nakase, T., Seki, H., Kato, K., Kaneda, Y., and Ochi, T., 'Suppressed Severity of Collagen-Induced Arthritis by in Vivo Transfection of Nuclear Factor Kappab Decoy Oligodeoxynucleotides as a Gene Therapy', *Arthritis Rheum,* 42 (1999), 2532-42.

[10] Herweijer, H., and Wolff, J. A., 'Progress and Prospects: Naked DNA Gene Transfer and Therapy', *Gene Ther,* 10 (2003), 453-8.

[11] Karra, D., and Dahm, R., 'Transfection Techniques for Neuronal Cells', *The Journal of Neuroscience,* 30 (2010), 6171-77.

[12] Takahashi, K., and Yamanaka, S., 'Induction of Pluripotent Stem Cells from Mouse Embryonic and Adult Fibroblast Cultures by Defined Factors', *Cell,* 126 (2006), 663-76.

[13] Woltjen, K., Michael, I. P., Mohseni, P., Desai, R., Mileikovsky, M., Hamalainen, R., Cowling, R., Wang, W., Liu, P., Gertsenstein, M., Kaji, K., Sung, H.-K., and Nagy, A., 'Piggybac Transposition Reprograms Fibroblasts to Induced Pluripotent Stem Cells', *Nature,* 458 (2009), 766-70.

[14] van de Wetering, M., Oving, I., Muncan, V., Pon Fong, M. T., Brantjes, H., van Leenen, D., Holstege, F. C., Brummelkamp, T. R., Agami, R., and Clevers, H., 'Specific Inhibition of Gene Expression Using a Stably Integrated, Inducible Small-Interfering-Rna Vector', *EMBO Rep,* 4 (2003), 609-15.

[15] Hay, D. C., Sutherland, L., Clark, J., and Burdon, T., 'Oct-4 Knockdown Induces Similar Patterns of Endoderm and Trophoblast Differentiation Markers in Human and Mouse Embryonic Stem Cells', *Stem Cells,* 22 (2004), 225-35.

[16] Nguyen, D. N., Green, J. J., Chan, J. M., Langer, R., and Anderson, D. G., 'Polymeric Materials for Gene Delivery and DNA Vaccination', *Advanced Materials,* 21 (2009), 847-67.

[17] Chamberlain, J. S., 'Gene Therapy of Muscular Dystrophy', *Human Molecular Genetics,* 11 (2002), 2355-62.

[18] van Deutekom, J. C., and van Ommen, G. J., 'Advances in Duchenne Muscular Dystrophy Gene Therapy', *Nat Rev Genet,* 4 (2003), 774-83.

[19] Lee, Tim W R., Matthews, David A., and Blair, G E., 'Novel Molecular Approaches to Cystic Fibrosis Gene Therapy', *Biochemical Journal,* 387 (2005), 1-15.

[20] Walsh, C. E., 'Gene Therapy Progress and Prospects: Gene Therapy for the Hemophilias', *Gene Ther,* 10 (2003), 999-1003.

[21] Asai, J., Takenaka, H., Kusano, K. F., Ii, M., Luedemann, C., Curry, C., Eaton, E., Iwakura, A., Tsutsumi, Y., Hamada, H., Kishimoto, S., Thorne, T., Kishore, R., and Losordo, D. W., 'Topical Sonic Hedgehog Gene Therapy Accelerates Wound Healing in Diabetes by Enhancing Endothelial Progenitor Cell-Mediated Microvascular Remodeling', *Circulation,* 113 (2006), 2413-24.

[22] Branski, L. K., Gauglitz, G. G., Herndon, D. N., and Jeschke, M. G., 'A Review of Gene and Stem Cell Therapy in Cutaneous Wound Healing', *Burns,* 35 (2009), 171-80.

[23] Taniyama, Y., Morishita, R., Aoki, M., Nakagami, H., Yamamoto, K., Yamazaki, K., Matsumoto, K., Nakamura, T., Kaneda, Y., and Ogihara, T., 'Therapeutic Angiogenesis Induced by Human Hepatocyte Growth Factor Gene in Rat and Rabbit Hindlimb Ischemia Models: Preclinical Study for Treatment of Peripheral Arterial Disease', *Gene Ther,* 8 (2001), 181-9.

[24] Ouma, G. O., Jonas, R. A., Usman, M. H., and Mohler, E. R., 3rd, 'Targets and Delivery Methods for Therapeutic Angiogenesis in Peripheral Artery Disease', *Vasc Med,* 17 (2012), 174-92.

[25] Nabel, E. G., 'Gene Therapy for Cardiovascular Disease', *Circulation,* 91 (1995), 541-48.

[26] Meyerson, S. L., Skelly, C. L., Curi, M. A., and Schwartz, L. B., 'Gene Therapy for Cardiovascular Disease', *Seminars in Cardiothoracic and Vascular Anesthesia,* 4 (2000), 289-300.

[27] Tuszynski, M. H., Thal, L., Pay, M., Salmon, D. P., U, H. S., Bakay, R., Patel, P., Blesch, A., Vahlsing, H. L., Ho, G., Tong, G., Potkin, S. G., Fallon, J., Hansen, L., Mufson, E. J., Kordower, J. H., Gall, C., and Conner, J., 'A Phase 1 Clinical Trial of Nerve Growth Factor Gene Therapy for Alzheimer Disease', *Nat Med,* 11 (2005), 551-5.

[28] Smith, R. A., Miller, T. M., Yamanaka, K., Monia, B. P., Condon, T. P., Hung, G., Lobsiger, C. S., Ward, C. M., McAlonis-Downes, M., Wei, H., Wancewicz, E. V., Bennett, C. F., and Cleveland, D. W., 'Antisense Oligonucleotide Therapy for Neurodegenerative Disease', *J Clin Invest,* 116 (2006), 2290-6.

[29] Robbins, P. D., Evans, C. H., and Chernajovsky, Y., 'Gene Therapy for Arthritis', *Gene Ther,* 10 (2003), 902-11.

[30] Roth, J. A., and Cristiano, R. J., 'Gene Therapy for Cancer: What Have We Done and Where Are We Going?', *J Natl Cancer Inst,* 89 (1997), 21-39.

[31] Johnson, L. A., Morgan, R. A., Dudley, M. E., Cassard, L., Yang, J. C., Hughes, M. S., Kammula, U. S., Royal, R. E., Sherry, R. M., Wunderlich, J. R., Lee, C. C., Restifo, N. P., Schwarz, S. L., Cogdill, A. P., Bishop, R. J., Kim, H., Brewer, C. C., Rudy, S. F., VanWaes, C., Davis, J. L., Mathur, A., Ripley, R. T., Nathan, D. A., Laurencot, C. M., and Rosenberg, S. A., 'Gene Therapy with Human and Mouse T-Cell Receptors Mediates Cancer Regression and Targets Normal Tissues Expressing Cognate Antigen', *Blood,* 114 (2009), 535-46.

[32] Miller, A. D., 'Human Gene Therapy Comes of Age', *Nature,* 357 (1992), 455-60.
[33] Mulligan, R. C., 'The Basic Science of Gene Therapy', *Science,* 260 (1993), 926-32.
[34] Cavazzana-Calvo, M., Hacein-Bey, S., de Saint Basile, G., Gross, F., Yvon, E., Nusbaum, P., Selz, F., Hue, C., Certain, S., Casanova, J. L., Bousso, P., Deist, F. L., and Fischer, A., 'Gene Therapy of Human Severe Combined Immunodeficiency (Scid)-X1 Disease', *Science,* 288 (2000), 669-72.
[35] Luo, D., and Saltzman, W. M., 'Synthetic DNA Delivery Systems', *Nat Biotech,* 18 (2000), 33-37.
[36] Kay, M. A., Glorioso, J. C., and Naldini, L., 'Viral Vectors for Gene Therapy: The Art of Turning Infectious Agents into Vehicles of Therapeutics', *Nat Med,* 7 (2001), 33-40.
[37] Thomas, C. E., Ehrhardt, A., and Kay, M. A., 'Progress and Problems with the Use of Viral Vectors for Gene Therapy', *Nat Rev Genet,* 4 (2003), 346-58.
[38] Pack, D. W., Hoffman, A. S., Pun, S., and Stayton, P. S., 'Design and Development of Polymers for Gene Delivery', *Nat Rev Drug Discov,* 4 (2005), 581-93.
[39] Basarkar, A., and Singh, J., 'Nanoparticulate Systems for Polynucleotide Delivery', *International Journal of Nanomedicine,* 2 (2007), 353-60.
[40] Thomas, M., and Klibanov, A. M., 'Non-Viral Gene Therapy: Polycation-Mediated DNA Delivery', *Appl Microbiol Biotechnol,* 62 (2003), 27-34.
[41] Mintzer, M. A., and Simanek, E. E., 'Nonviral Vectors for Gene Delivery', *Chem Rev,* 109 (2009), 259-302.
[42] Graham, F. L., and van der Eb, A. J., 'A New Technique for the Assay of Infectivity of Human Adenovirus 5 DNA', *Virology,* 52 (1973), 456-67.
[43] Jordan, M., Schallhorn, A., and Wurm, F. M., 'Transfecting Mammalian Cells: Optimization of Critical Parameters Affecting Calcium-Phosphate Precipitate Formation', *Nucleic Acids Research,* 24 (1996), 596-601.
[44] Yoshimura, K., Rosenfeld, M. A., Seth, P., and Crystal, R. G., 'Adenovirus-Mediated Augmentation of Cell Transfection with Unmodified Plasmid Vectors', *J Biol Chem,* 268 (1993), 2300-3.
[45] Boviatsis, E. J., Chase, M., Wei, M. X., Tamiya, T., Hurford, R. K., Jr., Kowall, N. W., Tepper, R. I., Breakefield, X. O., and Chiocca, E. A., 'Gene Transfer into Experimental Brain Tumors Mediated by Adenovirus, Herpes Simplex Virus, and Retrovirus Vectors', *Hum Gene Ther,* 5 (1994), 183-91.
[46] Kanegae, Y., Lee, G., Sato, Y., Tanaka, M., Nakai, M., Sakaki, T., Sugano, S., and Saito, I., 'Efficient Gene Activation in Mammalian Cells by Using Recombinant Adenovirus Expressing Site-Specific Cre Recombinase', *Nucleic Acids Research,* 23 (1995), 3816-21.
[47] Verma, I. M., and Somia, N., 'Gene Therapy -- Promises, Problems and Prospects', *Nature,* 389 (1997), 239-42.
[48] Nemerow, G. R., and Stewart, P. L., 'Role of Alpha(V) Integrins in Adenovirus Cell Entry and Gene Delivery', *Microbiol Mol Biol Rev,* 63 (1999), 725-34.
[49] Lin, M. T., Pulkkinen, L., Uitto, J., and Yoon, K., 'The Gene Gun: Current Applications in Cutaneous Gene Therapy', *Int J Dermatol,* 39 (2000), 161-70.
[50] Walther, W., and Stein, U., 'Viral Vectors for Gene Transfer: A Review of Their Use in the Treatment of Human Diseases', *Drugs,* 60 (2000), 249-71.
[51] Podsakoff, G., Wong, K. K., and Chatterjee, S., 'Efficient Gene Transfer into Nondividing Cells by Adeno-Associated Virus-Based Vectors', *Journal of Virology,* 68 (1994), 5656-66.
[52] Kaplitt, M. G., Leone, P., Samulski, R. J., Xiao, X., Pfaff, D. W., O'Malley, K. L., and During, M. J., 'Long-Term Gene Expression and Phenotypic Correction Using Adeno-Associated Virus Vectors in the Mammalian Brain', *Nat Genet,* 8 (1994), 148-54.
[53] Miller, J. L., Donahue, R. E., Sellers, S. E., Samulski, R. J., Young, N. S., and Nienhuis, A. W., 'Recombinant Adeno-Associated Virus (Raav)-Mediated Expression of a Human

Gamma-Globin Gene in Human Progenitor-Derived Erythroid Cells', *Proceedings of the National Academy of Sciences of the United States of America,* 91 (1994), 10183-87.

[54] Davidson, B. L., Stein, C. S., Heth, J. A., Martins, I., Kotin, R. M., Derksen, T. A., Zabner, J., Ghodsi, A., and Chiorini, J. A., 'Recombinant Adeno-Associated Virus Type 2, 4, and 5 Vectors: Transduction of Variant Cell Types and Regions in the Mammalian Central Nervous System', *Proc Natl Acad Sci U S A,* 97 (2000), 3428-32.

[55] Vasileva, A., and Jessberger, R., 'Precise Hit: Adeno-Associated Virus in Gene Targeting', *Nat Rev Microbiol,* 3 (2005), 837-47.

[56] Vile, R. G., and Hart, I. R., 'Use of Tissue-Specific Expression of the Herpes Simplex Virus Thymidine Kinase Gene to Inhibit Growth of Established Murine Melanomas Following Direct Intratumoral Injection of DNA', *Cancer Res,* 53 (1993), 3860-4.

[57] Stavropoulos, T. A., and Strathdee, C. A., 'An Enhanced Packaging System for Helper-Dependent Herpes Simplex Virus Vectors', *Journal of Virology,* 72 (1998), 7137-43.

[58] Palmer, J. A., Branston, R. H., Lilley, C. E., Robinson, M. J., Groutsi, F., Smith, J., Latchman, D. S., and Coffin, R. S., 'Development and Optimization of Herpes Simplex Virus Vectors for Multiple Long-Term Gene Delivery to the Peripheral Nervous System', *Journal of Virology,* 74 (2000), 5604-18.

[59] Paulus, W., Baur, I., Boyce, F. M., Breakefield, X. O., and Reeves, S. A., 'Self-Contained, Tetracycline-Regulated Retroviral Vector System for Gene Delivery to Mammalian Cells', *J Virol,* 70 (1996), 62-7.

[60] Hanenberg, H., Xiao, X. L., Dilloo, D., Hashino, K., Kato, I., and Williams, D. A., 'Colocalization of Retrovirus and Target Cells on Specific Fibronectin Fragments Increases Genetic Transduction of Mammalian Cells', *Nat Med,* 2 (1996), 876-82.

[61] Swift, S., Lorens, J., Achacoso, P., and Nolan, G. P., 'Rapid Production of Retroviruses for Efficient Gene Delivery to Mammalian Cells Using 293t Cell-Based Systems', *Curr Protoc Immunol,* Chapter 10 (2001), Unit 10.17C.

[62] Hacein-Bey-Abina, S., Le Deist, F., Carlier, F., Bouneaud, C., Hue, C., De Villartay, J. P., Thrasher, A. J., Wulffraat, N., Sorensen, R., Dupuis-Girod, S., Fischer, A., Davies, E. G., Kuis, W., Leiva, L., and Cavazzana-Calvo, M., 'Sustained Correction of X-Linked Severe Combined Immunodeficiency by Ex Vivo Gene Therapy', *N Engl J Med,* 346 (2002), 1185-93.

[63] Roesler, J., Brenner, S., Bukovsky, A. A., Whiting-Theobald, N., Dull, T., Kelly, M., Civin, C. I., and Malech, H. L., *Third-Generation, Self-Inactivating Gp91phoxlentivector Corrects the Oxidase Defect in Nod/Scid Mouse–Repopulating Peripheral Blood–Mobilized Cd34+ Cells from Patients with X-Linked Chronic Granulomatous Disease*. Vol. 100 (2002), pp. 4381-90.

[64] Woods, N. B., Muessig, A., Schmidt, M., Flygare, J., Olsson, K., Salmon, P., Trono, D., von Kalle, C., and Karlsson, S., 'Lentiviral Vector Transduction of Nod/Scid Repopulating Cells Results in Multiple Vector Integrations Per Transduced Cell: Risk of Insertional Mutagenesis', *Blood,* 101 (2003), 1284-9.

[65] Moss, B., 'Genetically Engineered Poxviruses for Recombinant Gene Expression, Vaccination, and Safety', *Proc Natl Acad Sci U S A,* 93 (1996), 11341-8.

[66] Derby, M. L., Sena-Esteves, M., Breakefield, X. O., and Corey, D. P., 'Gene Transfer into the Mammalian Inner Ear Using Hsv-1 and Vaccinia Virus Vectors', *Hear Res,* 134 (1999), 1-8.

[67] Gnant, M. F., Noll, L. A., Irvine, K. R., Puhlmann, M., Terrill, R. E., Alexander, H. R., Jr., and Bartlett, D. L., 'Tumor-Specific Gene Delivery Using Recombinant Vaccinia Virus in a Rabbit Model of Liver Metastases', *J Natl Cancer Inst,* 91 (1999), 1744-50.

[68] Lundstrom, K., Schweitzer, C., Rotmann, D., Hermann, D., Schneider, E. M., and Ehrengruber, M. U., 'Semliki Forest Virus Vectors: Efficient Vehicles for in Vitro and in Vivo Gene Delivery', *FEBS Lett,* 504 (2001), 99-103.

[69] Tseng, J. C., Levin, B., Hurtado, A., Yee, H., Perez de Castro, I., Jimenez, M., Shamamian, P., Jin, R., Novick, R. P., Pellicer, A., and Meruelo, D., 'Systemic Tumor Targeting and Killing by Sindbis Viral Vectors', *Nat Biotechnol,* 22 (2004), 70-7.

[70] Lundstrom, K., 'Biology and Application of Alphaviruses in Gene Therapy', *Gene Ther,* 12 Suppl 1 (2005), S92-7.

[71] Chen, C., and Okayama, H., 'High-Efficiency Transformation of Mammalian Cells by Plasmid DNA', *Mol Cell Biol,* 7 (1987), 2745-52.

[72] Batard, P., Jordan, M., and Wurm, F., 'Transfer of High Copy Number Plasmid into Mammalian Cells by Calcium Phosphate Transfection', *Gene,* 270 (2001), 61-8.

[73] Roy, I., Mitra, S., Maitra, A., and Mozumdar, S., 'Calcium Phosphate Nanoparticles as Novel Non-Viral Vectors for Targeted Gene Delivery', *Int J Pharm,* 250 (2003), 25-33.

[74] Olton, D., Li, J., Wilson, M. E., Rogers, T., Close, J., Huang, L., Kumta, P. N., and Sfeir, C., 'Nanostructured Calcium Phosphates (Nanocaps) for Non-Viral Gene Delivery: Influence of the Synthesis Parameters on Transfection Efficiency', *Biomaterials,* 28 (2007), 1267-79.

[75] Behr, J. P., Demeneix, B., Loeffler, J. P., and Perez-Mutul, J., 'Efficient Gene Transfer into Mammalian Primary Endocrine Cells with Lipopolyamine-Coated DNA', *Proceedings of the National Academy of Sciences of the United States of America,* 86 (1989), 6982-86.

[76] Felgner, J. H., Kumar, R., Sridhar, C. N., Wheeler, C. J., Tsai, Y. J., Border, R., Ramsey, P., Martin, M., and Felgner, P. L., 'Enhanced Gene Delivery and Mechanism Studies with a Novel Series of Cationic Lipid Formulations', *J Biol Chem,* 269 (1994), 2550-61.

[77] Holmen, S. L., Vanbrocklin, M. W., Eversole, R. R., Stapleton, S. R., and Ginsberg, L. C., 'Efficient Lipid-Mediated Transfection of DNA into Primary Rat Hepatocytes', *In Vitro Cell Dev Biol Anim,* 31 (1995), 347-51.

[78] Lewis, J. G., Lin, K. Y., Kothavale, A., Flanagan, W. M., Matteucci, M. D., DePrince, R. B., Mook, R. A., Hendren, R. W., and Wagner, R. W., 'A Serum-Resistant Cytofectin for Cellular Delivery of Antisense Oligodeoxynucleotides and Plasmid DNA', *Proceedings of the National Academy of Sciences,* 93 (1996), 3176-81.

[79] Ross, P. C., and Hui, S. W., 'Lipoplex Size Is a Major Determinant of in Vitro Lipofection Efficiency', *Gene Ther,* 6 (1999), 651-9.

[80] Pedroso de Lima, M. C., Simoes, S., Pires, P., Faneca, H., and Duzgunes, N., 'Cationic Lipid-DNA Complexes in Gene Delivery: From Biophysics to Biological Applications', *Adv Drug Deliv Rev,* 47 (2001), 277-94.

[81] Pelisek, J., Gaedtke, L., DeRouchey, J., Walker, G. F., Nikol, S., and Wagner, E., 'Optimized Lipopolyplex Formulations for Gene Transfer to Human Colon Carcinoma Cells under in Vitro Conditions', *J Gene Med,* 8 (2006), 186-97.

[82] Balazs, D. A., and Godbey, W., 'Liposomes for Use in Gene Delivery', *J Drug Deliv,* 2011 (2011), 326497.

[83] Bordier, B., Perala-Heape, M., Degols, G., Lebleu, B., Litvak, S., Sarih-Cottin, L., and Hélène, C., 'Sequence-Specific Inhibition of Human Immunodeficiency Virus (Hiv) Reverse Transcription by Antisense Oligonucleotides: Comparative Study in Cell-Free Assays and in Hiv-Infected Cells', *Proceedings of the National Academy of Sciences of the United States of America,* 92 (1995), 9383-87.

[84] Boussif, O., Lezoualc'h, F., Zanta, M. A., Mergny, M. D., Scherman, D., Demeneix, B., and Behr, J. P., 'A Versatile Vector for Gene and Oligonucleotide Transfer into Cells in Culture and in Vivo: Polyethylenimine', *Proc Natl Acad Sci U S A,* 92 (1995), 7297-301.

[85] Wagner, E., Ogris, M., and Zauner, W., 'Polylysine-Based Transfection Systems Utilizing Receptor-Mediated Delivery', *Adv Drug Deliv Rev,* 30 (1998), 97-113.

[86] Guang Liu, W., and De Yao, K., 'Chitosan and Its Derivatives--a Promising Non-Viral Vector for Gene Transfection', *J Control Release,* 83 (2002), 1-11.

[87] Radu, D. R., Lai, C.-Y., Jeftinija, K., Rowe, E. W., Jeftinija, S., and Lin, V. S. Y., 'A Polyamidoamine Dendrimer-Capped Mesoporous Silica Nanosphere-Based Gene Transfection Reagent', *Journal of the American Chemical Society,* 126 (2004), 13216-17.

[88] Morris, M. C., Vidal, P., Chaloin, L., Heitz, F., and Divita, G., 'A New Peptide Vector for Efficient Delivery of Oligonucleotides into Mammalian Cells', *Nucleic Acids Research,* 25 (1997), 2730-36.

[89] Simeoni, F., Morris, M. C., Heitz, F., and Divita, G., 'Insight into the Mechanism of the Peptide-Based Gene Delivery System Mpg: Implications for Delivery of Sirna into Mammalian Cells', *Nucleic Acids Res,* 31 (2003), 2717-24.

[90] Veldhoen, S., Laufer, S. D., and Restle, T., 'Recent Developments in Peptide-Based Nucleic Acid Delivery', *Int J Mol Sci,* 9 (2008), 1276-320.

[91] Margus, H., Padari, K., and Pooga, M., 'Cell-Penetrating Peptides as Versatile Vehicles for Oligonucleotide Delivery', *Mol Ther,* 20 (2012), 525-33.

[92] Kneuer, C., Sameti, M., Bakowsky, U., Schiestel, T., Schirra, H., Schmidt, H., and Lehr, C. M., 'A Nonviral DNA Delivery System Based on Surface Modified Silica-Nanoparticles Can Efficiently Transfect Cells in Vitro', *Bioconjug Chem,* 11 (2000), 926-32.

[93] Sandhu, K. K., McIntosh, C. M., Simard, J. M., Smith, S. W., and Rotello, V. M., 'Gold Nanoparticle-Mediated Transfection of Mammalian Cells', *Bioconjugate Chemistry,* 13 (2002), 3-6.

[94] Singh, R., Pantarotto, D., McCarthy, D., Chaloin, O., Hoebeke, J., Partidos, C. D., Briand, J. P., Prato, M., Bianco, A., and Kostarelos, K., 'Binding and Condensation of Plasmid DNA onto Functionalized Carbon Nanotubes: Toward the Construction of Nanotube-Based Gene Delivery Vectors', *J Am Chem Soc,* 127 (2005), 4388-96.

[95] Bharali, D. J., Klejbor, I., Stachowiak, E. K., Dutta, P., Roy, I., Kaur, N., Bergey, E. J., Prasad, P. N., and Stachowiak, M. K., 'Organically Modified Silica Nanoparticles: A Nonviral Vector for in Vivo Gene Delivery and Expression in the Brain', *Proceedings of the National Academy of Sciences of the United States of America,* 102 (2005), 11539-44.

[96] Chithrani, B. D., Ghazani, A. A., and Chan, W. C. W., 'Determining the Size and Shape Dependence of Gold Nanoparticle Uptake into Mammalian Cells', *Nano Letters,* 6 (2006), 662-68.

[97] Duan, H., and Nie, S., 'Cell-Penetrating Quantum Dots Based on Multivalent and Endosome-Disrupting Surface Coatings', *J Am Chem Soc,* 129 (2007), 3333-8.

[98] Ghosh, P., Han, G., De, M., Kim, C. K., and Rotello, V. M., 'Gold Nanoparticles in Delivery Applications', *Advanced Drug Delivery Reviews,* 60 (2008), 1307-15.

[99] Capecchi, M. R., 'High Efficiency Transformation by Direct Microinjection of DNA into Cultured Mammalian Cells', *Cell,* 22 (1980), 479-88.

[100] Mehier-Humbert, S., and Guy, R. H., 'Physical Methods for Gene Transfer: Improving the Kinetics of Gene Delivery into Cells', *Adv Drug Deliv Rev,* 57 (2005), 733-53.

[101] Yang, N. S., Burkholder, J., Roberts, B., Martinell, B., and McCabe, D., 'In Vivo and in Vitro Gene Transfer to Mammalian Somatic Cells by Particle Bombardment', *Proceedings of the National Academy of Sciences of the United States of America,* 87 (1990), 9568-72.

[102] Mahvi, D. M., Sondel, P. M., Yang, N. S., Albertini, M. R., Schiller, J. H., Hank, J., Heiner, J., Gan, J., Swain, W., and Logrono, R., 'Phase I/Ib Study of Immunization with Autologous Tumor Cells Transfected with the Gm-Csf Gene by Particle-Mediated Transfer in Patients with Melanoma or Sarcoma', *Hum Gene Ther,* 8 (1997), 875-91.

[103] Larregina, A. T., Watkins, S. C., Erdos, G., Spencer, L. A., Storkus, W. J., Beer Stolz, D., and Falo, L. D., Jr., 'Direct Transfection and Activation of Human Cutaneous Dendritic Cells', *Gene Ther,* 8 (2001), 608-17.

[104] Chu, G., Hayakawa, H., and Berg, P., 'Electroporation for the Efficient Transfection of Mammalian Cells with DNA', *Nucleic Acids Research,* 15 (1987), 1311-26.
[105] Washbourne, P., and McAllister, A. K., 'Techniques for Gene Transfer into Neurons', *Curr Opin Neurobiol,* 12 (2002), 566-73.
[106] Miller, D. L., Pislaru, S. V., and Greenleaf, J. E., 'Sonoporation: Mechanical DNA Delivery by Ultrasonic Cavitation', *Somat Cell Mol Genet,* 27 (2002), 115-34.
[107] Tsunoda, S., Mazda, O., Oda, Y., Iida, Y., Akabame, S., Kishida, T., Shin-Ya, M., Asada, H., Gojo, S., Imanishi, J., Matsubara, H., and Yoshikawa, T., 'Sonoporation Using Microbubble Br14 Promotes Pdna/Sirna Transduction to Murine Heart', *Biochem Biophys Res Commun,* 336 (2005), 118-27.
[108] Sheyn, D., Kimelman-Bleich, N., Pelled, G., Zilberman, Y., Gazit, D., and Gazit, Z., 'Ultrasound-Based Nonviral Gene Delivery Induces Bone Formation in Vivo', *Gene Ther,* 15 (2008), 257-66.
[109] Shirahata, Y., Ohkohchi, N., Itagak, H., and Satomi, S., 'New Technique for Gene Transfection Using Laser Irradiation', *J Investig Med,* 49 (2001), 184-90.
[110] Zeira, E., Manevitch, A., Khatchatouriants, A., Pappo, O., Hyam, E., Darash-Yahana, M., Tavor, E., Honigman, A., Lewis, A., and Galun, E., 'Femtosecond Infrared Laser-an Efficient and Safe in Vivo Gene Delivery System for Prolonged Expression', *Mol Ther,* 8 (2003), 342-50.
[111] Sagi, S., Knoll, T., Trojan, L., Schaaf, A., Alken, P., and Michel, M. S., 'Gene Delivery into Prostate Cancer Cells by Holmium Laser Application', *Prostate Cancer Prostatic Dis,* 6 (2003), 127-30.
[112] Waleed, M., Hwang, S. U., Kim, J. D., Shabbir, I., Shin, S. M., and Lee, Y. G., 'Single-Cell Optoporation and Transfection Using Femtosecond Laser and Optical Tweezers', *Biomed Opt Express,* 4 (2013), 1533-47.
[113] Scherer, F., Anton, M., Schillinger, U., Henke, J., Bergemann, C., Kruger, A., Gansbacher, B., and Plank, C., 'Magnetofection: Enhancing and Targeting Gene Delivery by Magnetic Force in Vitro and in Vivo', *Gene Ther,* 9 (2002), 102-9.
[114] Dobson, J., 'Gene Therapy Progress and Prospects: Magnetic Nanoparticle-Based Gene Delivery', *Gene Ther,* 13 (2006), 283-7.
[115] McBain, S. C., Griesenbach, U., Xenariou, S., Keramane, A., Batich, C. D., Alton, E. W., and Dobson, J., 'Magnetic Nanoparticles as Gene Delivery Agents: Enhanced Transfection in the Presence of Oscillating Magnet Arrays', *Nanotechnology,* 19 (2008), 405102.
[116] Prosen, L., Prijic, S., Music, B., Lavrencak, J., Cemazar, M., and Sersa, G., 'Magnetofection: A Reproducible Method for Gene Delivery to Melanoma Cells', *BioMed research international,* 2013 (2013).
[117] Yin, H., Kanasty, R. L., Eltoukhy, A. A., Vegas, A. J., Dorkin, J. R., and Anderson, D. G., 'Non-Viral Vectors for Gene-Based Therapy', *Nat Rev Genet,* 15 (2014), 541-55.
[118] Lukacs, G. L., Haggie, P., Seksek, O., Lechardeur, D., Freedman, N., and Verkman, A. S., 'Size-Dependent DNA Mobility in Cytoplasm and Nucleus', *J Biol Chem,* 275 (2000), 1625-9.
[119] Bloomfield, V. A., 'DNA Condensation by Multivalent Cations', *Biopolymers,* 44 (1997), 269-82.
[120] Abdelhady, H. G., Allen, S., Davies, M. C., Roberts, C. J., Tendler, S. J. B., and Williams, P. M., 'Direct Real-Time Molecular Scale Visualisation of the Degradation of Condensed DNA Complexes Exposed to Dnase I', *Nucleic Acids Research,* 31 (2003), 4001-05.
[121] Lai, E., and van Zanten, J. H., 'Monitoring DNA/Poly-L-Lysine Polyplex Formation with Time-Resolved Multiangle Laser Light Scattering', *Biophys J,* 80 (2001), 864-73.
[122] Sieczkarski, S. B., and Whittaker, G. R., 'Dissecting Virus Entry Via Endocytosis', *J Gen Virol,* 83 (2002), 1535-45.

[123] Mislick, K. A., and Baldeschwieler, J. D., 'Evidence for the Role of Proteoglycans in Cation-Mediated Gene Transfer', *Proceedings of the National Academy of Sciences of the United States of America,* 93 (1996), 12349-54.

[124] Belting, M., and Petersson, P., 'Protective Role for Proteoglycans against Cationic Lipid Cytotoxicity Allowing Optimal Transfection Efficiency in Vitro', *Biochem J,* 342 (Pt 2) (1999), 281-6.

[125] Ruponen, M., Honkakoski, P., Tammi, M., and Urtti, A., 'Cell-Surface Glycosaminoglycans Inhibit Cation-Mediated Gene Transfer', *J Gene Med,* 6 (2004), 405-14.

[126] Kopatz, I., Remy, J. S., and Behr, J. P., 'A Model for Non-Viral Gene Delivery: Through Syndecan Adhesion Molecules and Powered by Actin', *J Gene Med,* 6 (2004), 769-76.

[127] Goncalves, C., Mennesson, E., Fuchs, R., Gorvel, J. P., Midoux, P., and Pichon, C., 'Macropinocytosis of Polyplexes and Recycling of Plasmid Via the Clathrin-Dependent Pathway Impair the Transfection Efficiency of Human Hepatocarcinoma Cells', *Mol Ther,* 10 (2004), 373-85.

[128] Khalil, I. A., Kogure, K., Akita, H., and Harashima, H., 'Uptake Pathways and Subsequent Intracellular Trafficking in Nonviral Gene Delivery', *Pharmacol Rev,* 58 (2006), 32-45.

[129] Cho, Y. W., Kim, J. D., and Park, K., 'Polycation Gene Delivery Systems: Escape from Endosomes to Cytosol', *J Pharm Pharmacol,* 55 (2003), 721-34.

[130] Kukowska-Latallo, J. F., Bielinska, A. U., Johnson, J., Spindler, R., Tomalia, D. A., and Baker, J. R., 'Efficient Transfer of Genetic Material into Mammalian Cells Using Starburst Polyamidoamine Dendrimers', *Proceedings of the National Academy of Sciences of the United States of America,* 93 (1996), 4897-902.

[131] Behr, J.-P., 'The Proton Sponge: A Trick to Enter Cells the Viruses Did Not Exploit', *CHIMIA International Journal for Chemistry,* 51 (1997), 34-36.

[132] Sonawane, N. D., Szoka, F. C., Jr., and Verkman, A. S., 'Chloride Accumulation and Swelling in Endosomes Enhances DNA Transfer by Polyamine-DNA Polyplexes', *J Biol Chem,* 278 (2003), 44826-31.

[133] Erbacher, P., Roche, A. C., Monsigny, M., and Midoux, P., 'Putative Role of Chloroquine in Gene Transfer into a Human Hepatoma Cell Line by DNA/Lactosylated Polylysine Complexes', *Exp Cell Res,* 225 (1996), 186-94.

[134] Wagner, E., Zatloukal, K., Cotten, M., Kirlappos, H., Mechtler, K., Curiel, D. T., and Birnstiel, M. L., 'Coupling of Adenovirus to Transferrin-Polylysine/DNA Complexes Greatly Enhances Receptor-Mediated Gene Delivery and Expression of Transfected Genes', *Proc Natl Acad Sci U S A,* 89 (1992), 6099-103.

[135] Lee, H., Jeong, J. H., and Park, T. G., 'A New Gene Delivery Formulation of Polyethylenimine/DNA Complexes Coated with Peg Conjugated Fusogenic Peptide', *J Control Release,* 76 (2001), 183-92.

[136] Bonner, W. M., 'Protein Migration into Nuclei. I. Frog Oocyte Nuclei in Vivo Accumulate Microinjected Histones, Allow Entry to Small Proteins, and Exclude Large Proteins', *J Cell Biol,* 64 (1975), 421-30.

[137] Dowty, M. E., Williams, P., Zhang, G., Hagstrom, J. E., and Wolff, J. A., 'Plasmid DNA Entry into Postmitotic Nuclei of Primary Rat Myotubes', *Proceedings of the National Academy of Sciences of the United States of America,* 92 (1995), 4572-76.

[138] Coonrod, A., Li, F. Q., and Horwitz, M., 'On the Mechanism of DNA Transfection: Efficient Gene Transfer without Viruses', *Gene Ther,* 4 (1997), 1313-21.

[139] Subramanian, A., Ranganathan, P., and Diamond, S. L., 'Nuclear Targeting Peptide Scaffolds for Lipofection of Nondividing Mammalian Cells', *Nat Biotechnol,* 17 (1999), 873-7.

[140] Brunner, S., Sauer, T., Carotta, S., Cotten, M., Saltik, M., and Wagner, E., 'Cell Cycle Dependence of Gene Transfer by Lipoplex, Polyplex and Recombinant Adenovirus', *Gene Ther,* 7 (2000), 401-7.

[141] Pouton, C. W., and Seymour, L. W., 'Key Issues in Non-Viral Gene Delivery', *Adv Drug Deliv Rev,* 46 (2001), 187-203.
[142] Chan, C. K., and Jans, D. A., 'Enhancement of Polylysine-Mediated Transferrinfection by Nuclear Localization Sequences: Polylysine Does Not Function as a Nuclear Localization Sequence', *Hum Gene Ther,* 10 (1999), 1695-702.
[143] Erbacher, P., Roche, A. C., Monsigny, M., and Midoux, P., 'The Reduction of the Positive Charges of Polylysine by Partial Gluconoylation Increases the Transfection Efficiency of Polylysine/DNA Complexes', *Biochim Biophys Acta,* 1324 (1997), 27-36.
[144] Schaffer, D. V., Fidelman, N. A., Dan, N., and Lauffenburger, D. A., 'Vector Unpacking as a Potential Barrier for Receptor-Mediated Polyplex Gene Delivery', *Biotechnol Bioeng,* 67 (2000), 598-606.
[145] Ogris, M., Brunner, S., Schuller, S., Kircheis, R., and Wagner, E., 'Pegylated DNA/Transferrin-Pei Complexes: Reduced Interaction with Blood Components, Extended Circulation in Blood and Potential for Systemic Gene Delivery', *Gene Ther,* 6 (1999), 595-605.
[146] Kichler, A., Chillon, M., Leborgne, C., Danos, O., and Frisch, B. t., 'Intranasal Gene Delivery with a Polyethylenimine–Peg Conjugate', *Journal of Controlled Release,* 81 (2002), 379-88.
[147] Howcroft, T. K., Kirshner, S. L., and Singer, D. S., 'Measure of Transient Transfection Efficiency Using Beta-Galactosidase Protein', *Anal Biochem,* 244 (1997), 22-7.
[148] Tseng, W. C., Haselton, F. R., and Giorgio, T. D., 'Transfection by Cationic Liposomes Using Simultaneous Single Cell Measurements of Plasmid Delivery and Transgene Expression', *J Biol Chem,* 272 (1997), 25641-7.
[149] Elsabahy, M., and Wooley, K. L., 'Design of Polymeric Nanoparticles for Biomedical Delivery Applications', *Chem Soc Rev,* 41 (2012), 2545-61.
[150] Al-Dosari, M. S., and Gao, X., 'Nonviral Gene Delivery: Principle, Limitations, and Recent Progress', *The AAPS Journal,* 11 (2009), 671-81.
[151] Olins, D. E., Olins, A. L., and Von Hippel, P. H., 'Model Nucleoprotein Complexes: Studies on the Interaction of Cationic Homopolypeptides with DNA', *J Mol Biol,* 24 (1967), 157-76.
[152] Choi, Y. H., Liu, F., Kim, J. S., Choi, Y. K., Park, J. S., and Kim, S. W., 'Polyethylene Glycol-Grafted Poly-L-Lysine as Polymeric Gene Carrier', *J Control Release,* 54 (1998), 39-48.
[153] Toncheva, V., Wolfert, M. A., Dash, P. R., Oupicky, D., Ulbrich, K., Seymour, L. W., and Schacht, E. H., 'Novel Vectors for Gene Delivery Formed by Self-Assembly of DNA with Poly(L-Lysine) Grafted with Hydrophilic Polymers', *Biochim Biophys Acta,* 1380 (1998), 354-68.
[154] Alexis, F., Pridgen, E., Molnar, L. K., and Farokhzad, O. C., 'Factors Affecting the Clearance and Biodistribution of Polymeric Nanoparticles', *Mol Pharm,* 5 (2008), 505-15.
[155] Wu, G. Y., and Wu, C. H., 'Receptor-Mediated in Vitro Gene Transformation by a Soluble DNA Carrier System', *J Biol Chem,* 262 (1987), 4429-32.
[156] Cotten, M., Wagner, E., Zatloukal, K., Phillips, S., Curiel, D. T., and Birnstiel, M. L., 'High-Efficiency Receptor-Mediated Delivery of Small and Large (48 Kilobase Gene Constructs Using the Endosome-Disruption Activity of Defective or Chemically Inactivated Adenovirus Particles', *Proc Natl Acad Sci U S A,* 89 (1992), 6094-8.
[157] Cotten, M., Wagner, E., and Birnstiel, M. L., 'Receptor-Mediated Transport of DNA into Eukaryotic Cells', *Methods Enzymol,* 217 (1993), 618-44.
[158] Klink, D. T., Chao, S., Glick, M. C., and Scanlin, T. F., 'Nuclear Translocation of Lactosylated Poly-L-Lysine/Cdna Complex in Cystic Fibrosis Airway Epithelial Cells', *Mol Ther,* 3 (2001), 831-41.
[159] Konstan, M. W., Davis, P. B., Wagener, J. S., Hilliard, K. A., Stern, R. C., Milgram, L. J., Kowalczyk, T. H., Hyatt, S. L., Fink, T. L., Gedeon, C. R., Oette, S. M., Payne, J. M.,

Muhammad, O., Ziady, A. G., Moen, R. C., and Cooper, M. J., 'Compacted DNA Nanoparticles Administered to the Nasal Mucosa of Cystic Fibrosis Subjects Are Safe and Demonstrate Partial to Complete Cystic Fibrosis Transmembrane Regulator Reconstitution', *Hum Gene Ther,* 15 (2004), 1255-69.

[160] De Smedt, S. C., Demeester, J., and Hennink, W. E., 'Cationic Polymer Based Gene Delivery Systems', *Pharm Res,* 17 (2000), 113-26.

[161] Abdallah, B., Hassan, A., Benoist, C., Goula, D., Behr, J. P., and Demeneix, B. A., 'A Powerful Nonviral Vector for in Vivo Gene Transfer into the Adult Mammalian Brain: Polyethylenimine', *Hum Gene Ther,* 7 (1996), 1947-54.

[162] Boletta, A., Benigni, A., Lutz, J., Remuzzi, G., Soria, M. R., and Monaco, L., 'Nonviral Gene Delivery to the Rat Kidney with Polyethylenimine', *Hum Gene Ther,* 8 (1997), 1243-51.

[163] Goula, D., Benoist, C., Mantero, S., Merlo, G., Levi, G., and Demeneix, B. A., 'Polyethylenimine-Based Intravenous Delivery of Transgenes to Mouse Lung', *Gene Ther,* 5 (1998), 1291-5.

[164] Coll, J. L., Chollet, P., Brambilla, E., Desplanques, D., Behr, J. P., and Favrot, M., 'In Vivo Delivery to Tumors of DNA Complexed with Linear Polyethylenimine', *Hum Gene Ther,* 10 (1999), 1659-66.

[165] Kircheis, R., Wightman, L., and Wagner, E., 'Design and Gene Delivery Activity of Modified Polyethylenimines', *Adv Drug Deliv Rev,* 53 (2001), 341-58.

[166] Zanta, M. A., Boussif, O., Adib, A., and Behr, J. P., 'In Vitro Gene Delivery to Hepatocytes with Galactosylated Polyethylenimine', *Bioconjug Chem,* 8 (1997), 839-44.

[167] Godbey, W. T., Wu, K. K., and Mikos, A. G., 'Size Matters: Molecular Weight Affects the Efficiency of Poly(Ethylenimine) as a Gene Delivery Vehicle', *J Biomed Mater Res,* 45 (1999), 268-75.

[168] Wightman, L., Kircheis, R., Rossler, V., Carotta, S., Ruzicka, R., Kursa, M., and Wagner, E., 'Different Behavior of Branched and Linear Polyethylenimine for Gene Delivery in Vitro and in Vivo', *J Gene Med,* 3 (2001), 362-72.

[169] Kievit, F. M., Veiseh, O., Bhattarai, N., Fang, C., Gunn, J. W., Lee, D., Ellenbogen, R. G., Olson, J. M., and Zhang, M., 'Pei-Peg-Chitosan Copolymer Coated Iron Oxide Nanoparticles for Safe Gene Delivery: Synthesis, Complexation, and Transfection', *Advanced functional materials,* 19 (2009), 2244-51.

[170] Moghimi, S. M., Symonds, P., Murray, J. C., Hunter, A. C., Debska, G., and Szewczyk, A., 'A Two-Stage Poly(Ethylenimine)-Mediated Cytotoxicity: Implications for Gene Transfer/Therapy', *Mol Ther,* 11 (2005), 990-95.

[171] Hong, S., Leroueil, P. R., Janus, E. K., Peters, J. L., Kober, M.-M., Islam, M. T., Orr, B. G., Baker, J. R., and Banaszak Holl, M. M., 'Interaction of Polycationic Polymers with Supported Lipid Bilayers and Cells: Nanoscale Hole Formation and Enhanced Membrane Permeability', *Bioconjugate Chemistry,* 17 (2006), 728-34.

[172] Lv, H., Zhang, S., Wang, B., Cui, S., and Yan, J., 'Toxicity of Cationic Lipids and Cationic Polymers in Gene Delivery', *J Control Release,* 114 (2006), 100-9.

[173] Nguyen, H. K., Lemieux, P., Vinogradov, S. V., Gebhart, C. L., Guerin, N., Paradis, G., Bronich, T. K., Alakhov, V. Y., and Kabanov, A. V., 'Evaluation of Polyether-Polyethyleneimine Graft Copolymers as Gene Transfer Agents', *Gene Ther,* 7 (2000), 126-38.

[174] Petersen, H., Fechner, P. M., Martin, A. L., Kunath, K., Stolnik, S., Roberts, C. J., Fischer, D., Davies, M. C., and Kissel, T., 'Polyethylenimine-Graft-Poly(Ethylene Glycol) Copolymers: Influence of Copolymer Block Structure on DNA Complexation and Biological Activities as Gene Delivery System', *Bioconjug Chem,* 13 (2002), 845-54.

[175] Thomas, M., and Klibanov, A. M., 'Enhancing Polyethylenimine's Delivery of Plasmid DNA into Mammalian Cells', *Proc Natl Acad Sci U S A,* 99 (2002), 14640-5.

[176] Breunig, M., Lungwitz, U., Liebl, R., and Goepferich, A., 'Breaking up the Correlation between Efficacy and Toxicity for Nonviral Gene Delivery', *Proceedings of the National Academy of Sciences of the United States of America,* 104 (2007), 14454-59.

[177] Van Vliet, L. D., Chapman, M. R., Avenier, F., Kitson, C. Z., and Hollfelder, F., 'Relating Chemical and Biological Diversity Space: A Tunable System for Efficient Gene Transfection', *Chembiochem,* 9 (2008), 1960-7.

[178] Fortune, J. A., Novobrantseva, T. I., and Klibanov, A. M., 'Highly Effective Gene Transfection in Vivo by Alkylated Polyethylenimine', *Journal of drug delivery,* 2011 (2011).

[179] Thomas, M., Lu, J. J., Ge, Q., Zhang, C., Chen, J., and Klibanov, A. M., 'Full Deacylation of Polyethylenimine Dramatically Boosts Its Gene Delivery Efficiency and Specificity to Mouse Lung', *Proceedings of the National Academy of Sciences of the United States of America,* 102 (2005), 5679-84.

[180] Gabrielson, N. P., and Pack, D. W., 'Acetylation of Polyethylenimine Enhances Gene Delivery Via Weakened Polymer/DNA Interactions', *Biomacromolecules,* 7 (2006), 2427-35.

[181] Cherng, J. Y., van de Wetering, P., Talsma, H., Crommelin, D. J., and Hennink, W. E., 'Effect of Size and Serum Proteins on Transfection Efficiency of Poly ((2-Dimethylamino)Ethyl Methacrylate)-Plasmid Nanoparticles', *Pharm Res,* 13 (1996), 1038-42.

[182] van de Wetering, P., Cherng, J.-Y., Talsma, H., and Hennink, W. E., 'Relation between Transfection Efficiency and Cytotoxicity of Poly(2-(Dimethylamino)Ethyl Methacrylate)/Plasmid Complexes', *Journal of Controlled Release,* 49 (1997), 59-69.

[183] van de Wetering, P., Moret, E. E., Schuurmans-Nieuwenbroek, N. M., van Steenbergen, M. J., and Hennink, W. E., 'Structure-Activity Relationships of Water-Soluble Cationic Methacrylate/Methacrylamide Polymers for Nonviral Gene Delivery', *Bioconjugate chemistry,* 10 (1999), 589-97.

[184] Verbaan, F. J., Oussoren, C., van Dam, I. M., Takakura, Y., Hashida, M., Crommelin, D. J., Hennink, W. E., and Storm, G., 'The Fate of Poly(2-Dimethyl Amino Ethyl)Methacrylate-Based Polyplexes after Intravenous Administration', *Int J Pharm,* 214 (2001), 99-101.

[185] Funhoff, A. M., van Nostrum, C. F., Koning, G. A., Schuurmans-Nieuwenbroek, N. M., Crommelin, D. J., and Hennink, W. E., 'Endosomal Escape of Polymeric Gene Delivery Complexes Is Not Always Enhanced by Polymers Buffering at Low Ph', *Biomacromolecules,* 5 (2004), 32-9.

[186] Dubruel, P., Christiaens, B., Rosseneu, M., Vandekerckhove, J., Grooten, J., Goossens, V., and Schacht, E., 'Buffering Properties of Cationic Polymethacrylates Are Not the Only Key to Successful Gene Delivery', *Biomacromolecules,* 5 (2004), 379-88.

[187] Schallon, A., Synatschke, C. V., Jérôme, V., Müller, A. H. E., and Freitag, R., 'Nanoparticulate Nonviral Agent for the Effective Delivery of Pdna and Sirna to Differentiated Cells and Primary Human T Lymphocytes', *Biomacromolecules,* 13 (2012), 3463-74.

[188] van de Wetering, P., Cherng, J. Y., Talsma, H., Crommelin, D. J., and Hennink, W. E., '2-(Dimethylamino)Ethyl Methacrylate Based (Co)Polymers as Gene Transfer Agents', *J Control Release,* 53 (1998), 145-53.

[189] van de Wetering, P., Schuurmans-Nieuwenbroek, N. M., van Steenbergen, M. J., Crommelin, D. J., and Hennink, W. E., 'Copolymers of 2-(Dimethylamino)Ethyl Methacrylate with Ethoxytriethylene Glycol Methacrylate or N-Vinyl-Pyrrolidone as Gene Transfer Agents', *J Control Release,* 64 (2000), 193-203.

[190] Samsonova, O., Pfeiffer, C., Hellmund, M., Merkel, O. M., and Kissel, T., 'Low Molecular Weight Pdmaema-Block-Phema Block-Copolymers Synthesized Via Raft-Polymerization: Potential Non-Viral Gene Delivery Agents?', *Polymers,* 3 (2011), 693.

[191] Verbaan, F. J., Oussoren, C., Snel, C. J., Crommelin, D. J., Hennink, W. E., and Storm, G., 'Steric Stabilization of Poly(2-(Dimethylamino)Ethyl Methacrylate)-Based Polyplexes Mediates Prolonged Circulation and Tumor Targeting in Mice', *J Gene Med,* 6 (2004), 64-75.

[192] Tan, J. F., Too, H. P., Hatton, T. A., and Tam, K. C., 'Aggregation Behavior and Thermodynamics of Binding between Poly(Ethylene Oxide)-Block-Poly(2-(Diethylamino)Ethyl Methacrylate) and Plasmid DNA', *Langmuir,* 22 (2006), 3744-50.

[193] Mastrobattista, E., Kapel, R. H., Eggenhuisen, M. H., Roholl, P. J., Crommelin, D. J., Hennink, W. E., and Storm, G., 'Lipid-Coated Polyplexes for Targeted Gene Delivery to Ovarian Carcinoma Cells', *Cancer Gene Ther,* 8 (2001), 405-13.

[194] van Steenis, J. H., van Maarseveen, E. M., Verbaan, F. J., Verrijk, R., Crommelin, D. J., Storm, G., and Hennink, W. E., 'Preparation and Characterization of Folate-Targeted Peg-Coated Pdmaema-Based Polyplexes', *J Control Release,* 87 (2003), 167-76.

[195] Uchida, H., Miyata, K., Oba, M., Ishii, T., Suma, T., Itaka, K., Nishiyama, N., and Kataoka, K., 'Odd-Even Effect of Repeating Aminoethylene Units in the Side Chain of N-Substituted Polyaspartamides on Gene Transfection Profiles', *J Am Chem Soc,* 133 (2011), 15524-32.

[196] Anderson, D. G., Lynn, D. M., and Langer, R., 'Semi-Automated Synthesis and Screening of a Large Library of Degradable Cationic Polymers for Gene Delivery', *Angew Chem Int Ed Engl,* 42 (2003), 3153-8.

[197] Liu, Z., Zhang, Z., Zhou, C., and Jiao, Y., 'Hydrophobic Modifications of Cationic Polymers for Gene Delivery', *Progress in Polymer Science,* 35 (2010), 1144-62.

[198] Piest, M., and Engbersen, J. F., 'Effects of Charge Density and Hydrophobicity of Poly(Amido Amine)S for Non-Viral Gene Delivery', *J Control Release,* 148 (2010), 83-90.

[199] Sun, J.-T., Hong, C.-Y., and Pan, C.-Y., 'Fabrication of Pdeaema-Coated Mesoporous Silica Nanoparticles and Ph-Responsive Controlled Release', *The Journal of Physical Chemistry C,* 114 (2010), 12481-86.

[200] Cheng, Y., A, C. S., Meyers, J. D., Panagopoulos, I., Fei, B., and Burda, C., 'Highly Efficient Drug Delivery with Gold Nanoparticle Vectors for in Vivo Photodynamic Therapy of Cancer', *J Am Chem Soc,* 130 (2008), 10643-7.

[201] Freese, C., Gibson, M. I., Klok, H. A., Unger, R. E., and Kirkpatrick, C. J., 'Size- and Coating-Dependent Uptake of Polymer-Coated Gold Nanoparticles in Primary Human Dermal Microvascular Endothelial Cells', *Biomacromolecules,* 13 (2012), 1533-43.

[202] Liu, R., Liao, P., Liu, J., and Feng, P., 'Responsive Polymer-Coated Mesoporous Silica as a Ph-Sensitive Nanocarrier for Controlled Release', *Langmuir,* 27 (2011), 3095-9.

[203] Sahoo, B., Devi, K. S., Banerjee, R., Maiti, T. K., Pramanik, P., and Dhara, D., 'Thermal and Ph Responsive Polymer-Tethered Multifunctional Magnetic Nanoparticles for Targeted Delivery of Anticancer Drug', *ACS Appl Mater Interfaces,* 5 (2013), 3884-93.

[204] Teixeira, F., Popa, A. M., Guimond, S., Hegemann, D., and Rossi, R. M., 'Synthesis of Poly(Oligo(Ethylene Glycol)Methacrylate)-Functionalized Membranes for Thermally Controlled Drug Delivery', *Journal of Applied Polymer Science,* 129 (2013), 636-43.

[205] Liu, G., Cai, M., Zhou, F., and Liu, W., 'Charged Polymer Brushes-Grafted Hollow Silica Nanoparticles as a Novel Promising Material for Simultaneous Joint Lubrication and Treatment', *The Journal of Physical Chemistry B,* 118 (2014), 4920-31.

[206] Ohno, K., Akashi, T., Tsujii, Y., Yamamoto, M., and Tabata, Y., 'Blood Clearance and Biodistribution of Polymer Brush-Afforded Silica Particles Prepared by Surface-Initiated Living Radical Polymerization', *Biomacromolecules,* 13 (2012), 927-36.

[207] Zhang, G., Jia, X., Liu, Z., Hu, J., Ma, Z., and Zhou, F., 'Protein Resistance and Ph-Responsive Controlled Release from the Modification of Single-Walled Carbon Nanotubes with a Double Polymer Layer', *Macromolecular Bioscience,* 13 (2013), 1259-66.

[208] Jia, X., Zhang, G., Li, W., Sheng, W., and Li, C., 'Tuning the Low Critical Solution Temperature of Polymer Brushes Grafted on Single-Walled Carbon Nanotubes and Temperature Dependent Loading and Release Properties', *Journal of Polymer Science Part A: Polymer Chemistry,* 52 (2014), 1807-14.

[209] Chen, L., Peng, Z., Zeng, Z., She, Y., Wei, J., and Chen, Y., 'Hairy Polymeric Nanocapsules with Ph-Responsive Shell and Thermoresponsive Brushes: Tunable Permeability for Controlled Release of Water-Soluble Drugs', *Journal of Polymer Science Part A: Polymer Chemistry,* 52 (2014), 2202-16.

[210] Claesson, P. M., Christenson, H. K., Berg, J. M., and Neuman, R. D., 'Interactions between Mica Surfaces in the Presence of Carbohydrates', *Journal of Colloid and Interface Science,* 172 (1995), 415-24.

[211] Wang, Y. X., Robertson, J. L., Spillman, W. B., Jr., and Claus, R. O., 'Effects of the Chemical Structure and the Surface Properties of Polymeric Biomaterials on Their Biocompatibility', *Pharm Res,* 21 (2004), 1362-73.

[212] Becker, A. L., Henzler, K., Welsch, N., Ballauff, M., and Borisov, O., 'Proteins and Polyelectrolytes: A Charged Relationship', *Current Opinion in Colloid & Interface Science,* 17 (2012), 90-96.

[213] Sakata, S., Inoue, Y., and Ishihara, K., 'Quantitative Evaluation of Interaction Force between Functional Groups in Protein and Polymer Brush Surfaces', *Langmuir,* 30 (2014), 2745-51.

[214] Halperin, A., Fragneto, G., Schollier, A., and Sferrazza, M., 'Primary Versus Ternary Adsorption of Proteins onto Peg Brushes', *Langmuir,* 23 (2007), 10603-17.

[215] de Vos, W. M., Biesheuvel, P. M., de Keizer, A., Kleijn, J. M., and Cohen Stuart, M. A., 'Adsorption of the Protein Bovine Serum Albumin in a Planar Poly(Acrylic Acid) Brush Layer as Measured by Optical Reflectometry', *Langmuir,* 24 (2008), 6575-84.

[216] Wang, S., Chen, K., Kayitmazer, A. B., Li, L., and Guo, X., 'Tunable Adsorption of Bovine Serum Albumin by Annealed Cationic Spherical Polyelectrolyte Brushes', *Colloids Surf B Biointerfaces,* 107 (2013), 251-6.

[217] Wang, S., Chen, K., Li, L., and Guo, X., 'Binding between Proteins and Cationic Spherical Polyelectrolyte Brushes: Effect of Ph, Ionic Strength, and Stoichiometry', *Biomacromolecules,* 14 (2013), 818-27.

[218] Wittemann, A., and Ballauff, M., 'Interaction of Proteins with Linear Polyelectrolytes and Spherical Polyelectrolyte Brushes in Aqueous Solution', *Physical Chemistry Chemical Physics,* 8 (2006), 5269-75.

[219] Leermakers, F. A. M., Ballauff, M., and Borisov, O. V., 'On the Mechanism of Uptake of Globular Proteins by Polyelectrolyte Brushes: A Two-Gradient Self-Consistent Field Analysis', *Langmuir,* 23 (2007), 3937-46.

[220] Biesheuvel, P. M., and Wittemann, A., 'A Modified Box Model Including Charge Regulation for Protein Adsorption in a Spherical Polyelectrolyte Brush', *J Phys Chem B,* 109 (2005), 4209-14.

[221] Henzler, K., Haupt, B., Lauterbach, K., Wittemann, A., Borisov, O., and Ballauff, M., 'Adsorption of Beta-Lactoglobulin on Spherical Polyelectrolyte Brushes: Direct Proof of Counterion Release by Isothermal Titration Calorimetry', *J Am Chem Soc,* 132 (2010), 3159-63.

[222] Becker, A. L., Welsch, N., Schneider, C., and Ballauff, M., 'Adsorption of Rnase a on Cationic Polyelectrolyte Brushes: A Study by Isothermal Titration Calorimetry', *Biomacromolecules,* 12 (2011), 3936-44.

[223] Hollmann, O., Gutberlet, T., and Czeslik, C., 'Structure and Protein Binding Capacity of a Planar Paa Brush', *Langmuir,* 23 (2007), 1347-53.

[224] Hollmann, O., Steitz, R., and Czeslik, C., 'Structure and Dynamics of Alpha-Lactalbumin Adsorbed at a Charged Brush Interface', *Phys Chem Chem Phys,* 10 (2008), 1448-56.

[225] Henzler, K., Wittemann, A., Breininger, E., Ballauff, M., and Rosenfeldt, S., 'Adsorption of Bovine Hemoglobin onto Spherical Polyelectrolyte Brushes Monitored by Small-Angle X-Ray Scattering and Fourier Transform Infrared Spectroscopy', *Biomacromolecules,* 8 (2007), 3674-81.

[226] Henzler, K., Haupt, B., Rosenfeldt, S., Harnau, L., Narayanan, T., and Ballauff, M., 'Interaction Strength between Proteins and Polyelectrolyte Brushes: A Small Angle X-Ray Scattering Study', *Phys Chem Chem Phys,* 13 (2011), 17599-605.

[227] Henzler, K., Rosenfeldt, S., Wittemann, A., Harnau, L., Finet, S., Narayanan, T., and Ballauff, M., 'Directed Motion of Proteins Along Tethered Polyelectrolytes', *Phys Rev Lett,* 100 (2008), 158301.

[228] Tan, K. Y., Lin, H., Ramstedt, M., Watt, F. M., Huck, W. T., and Gautrot, J. E., 'Decoupling Geometrical and Chemical Cues Directing Epidermal Stem Cell Fate on Polymer Brush-Based Cell Micro-Patterns', *Integr Biol (Camb),* 5 (2013), 899-910.

[229] Rzhepishevska, O., Hakobyan, S., Ruhal, R., Gautrot, J., Barbero, D., and Ramstedt, M., 'The Surface Charge of Anti-Bacterial Coatings Alters Motility and Biofilm Architecture', *Biomaterials Science,* 1 (2013), 589-602.

[230] Ayres, N., Holt, D. J., Jones, C. F., Corum, L. E., and Grainger, D. W., 'Polymer Brushes Containing Sulfonated Sugar Repeat Units: Synthesis, Characterization and in Vitro Testing of Blood Coagulation Activation', *J Polym Sci A Polym Chem,* 46 (2008), 7713-24.

[231] Kumar, S., Tong, X., Dory, Y. L., Lepage, M., and Zhao, Y., 'A Co2-Switchable Polymer Brush for Reversible Capture and Release of Proteins', *Chem Commun (Camb),* 49 (2013), 90-2.

[232] Lei, H., Wang, M., Tang, Z., Luan, Y., Liu, W., Song, B., and Chen, H., 'Control of Lysozyme Adsorption by Ph on Surfaces Modified with Polyampholyte Brushes', *Langmuir,* 30 (2014), 501-08.

[233] Halperin, A., and Kröger, M., 'Collapse of Thermoresponsive Brushes and the Tuning of Protein Adsorption', *Macromolecules,* 44 (2011), 6986-7005.

[234] Yin, Z., Zhang, J., Jiang, L.-P., and Zhu, J.-J., 'Thermosensitive Behavior of Poly(N-Isopropylacrylamide) and Release of Incorporated Hemoglobin', *The Journal of Physical Chemistry C,* 113 (2009), 16104-09.

[235] Burkert, S., Bittrich, E., Kuntzsch, M., Muller, M., Eichhorn, K. J., Bellmann, C., Uhlmann, P., and Stamm, M., 'Protein Resistance of Pnipaam Brushes: Application to Switchable Protein Adsorption', *Langmuir,* 26 (2010), 1786-95.

[236] Xue, C., Yonet-Tanyeri, N., Brouette, N., Sferrazza, M., Braun, P. V., and Leckband, D. E., 'Protein Adsorption on Poly(N-Isopropylacrylamide) Brushes: Dependence on Grafting Density and Chain Collapse', *Langmuir : the ACS journal of surfaces and colloids,* 27 (2011), 8810-18.

[237] Choi, S., Choi, B. C., Xue, C., and Leckband, D., 'Protein Adsorption Mechanisms Determine the Efficiency of Thermally Controlled Cell Adhesion on Poly(N-Isopropyl Acrylamide) Brushes', *Biomacromolecules,* 14 (2013), 92-100.

[238] Kusumo, A., Bombalski, L., Lin, Q., Matyjaszewski, K., Schneider, J. W., and Tilton, R. D., 'High Capacity, Charge-Selective Protein Uptake by Polyelectrolyte Brushes', *Langmuir,* 23 (2007), 4448-54.

[239] Yu, F., Tang, X., and Pei, M., 'Facile Synthesis of Pdmaema-Coated Hollow Mesoporous Silica Nanoparticles and Their Ph-Responsive Controlled Release', *Microporous and Mesoporous Materials,* 173 (2013), 64-69.

[240] Patil, S. D., Rhodes, D. G., and Burgess, D. J., 'DNA-Based Therapeutics and DNA Delivery Systems: A Comprehensive Review', *Aaps j,* 7 (2005), E61-77.

[241] Zhang, P., Yang, J., Li, W., Wang, W., Liu, C., Griffith, M., and Liu, W., 'Cationic Polymer Brush Grafted-Nanodiamond Via Atom Transfer Radical Polymerization for Enhanced Gene Delivery and Bioimaging', *Journal of Materials Chemistry,* 21 (2011), 7755-64.

[242] Sato, A., Choi, S. W., Hirai, M., Yamayoshi, A., Moriyama, R., Yamano, T., Takagi, M., Kano, A., Shimamoto, A., and Maruyama, A., 'Polymer Brush-Stabilized Polyplex for a Sirna Carrier with Long Circulatory Half-Life', *J Control Release,* 122 (2007), 209-16.

[243] Maruyama, A., Ishihara, T., Kim, J. S., Kim, S. W., and Akaike, T., 'Nanoparticle DNA Carrier with Poly(L-Lysine) Grafted Polysaccharide Copolymer and Poly(D,L-Lactic Acid)', *Bioconjug Chem,* 8 (1997), 735-42.

[244] Störkle, D., Duschner, S., Heimann, N., Maskos, M., and Schmidt, M., 'Complex Formation of DNA with Oppositely Charged Polyelectrolytes of Different Chain Topology: Cylindrical Brushes and Dendrimers', *Macromolecules,* 40 (2007), 7998-8006.

[245] Jiang, X., Lok, M. C., and Hennink, W. E., 'Degradable-Brushed Phema-Pdmaema Synthesized Via Atrp and Click Chemistry for Gene Delivery', *Bioconjug Chem,* 18 (2007), 2077-84.

[246] Layman, J. M., Ramirez, S. M., Green, M. D., and Long, T. E., 'Influence of Polycation Molecular Weight on Poly(2-Dimethylaminoethyl Methacrylate)-Mediated DNA Delivery in Vitro', *Biomacromolecules,* 10 (2009), 1244-52.

[247] Majewski, A. P., Stahlschmidt, U., Jérôme, V., Freitag, R., Müller, A. H. E., and Schmalz, H., 'Pdmaema-Grafted Core–Shell–Corona Particles for Nonviral Gene Delivery and Magnetic Cell Separation', *Biomacromolecules,* 14 (2013), 3081-90.

[248] Synatschke, C. V., Schallon, A., Jérôme, V., Freitag, R., and Müller, A. H. E., 'Influence of Polymer Architecture and Molecular Weight of Poly(2-(Dimethylamino)Ethyl Methacrylate) Polycations on Transfection Efficiency and Cell Viability in Gene Delivery', *Biomacromolecules,* 12 (2011), 4247-55.

[249] Ohno, K., Mori, C., Akashi, T., Yoshida, S., Tago, Y., Tsujii, Y., and Tabata, Y., 'Fabrication of Contrast Agents for Magnetic Resonance Imaging from Polymer-Brush-Afforded Iron Oxide Magnetic Nanoparticles Prepared by Surface-Initiated Living Radical Polymerization', *Biomacromolecules,* 14 (2013), 3453-62.

[250] Yan, P., Zhao, N., Hu, H., Lin, X., Liu, F., and Xu, F. J., 'A Facile Strategy to Functionalize Gold Nanorods with Polycation Brushes for Biomedical Applications', *Acta Biomater,* 10 (2014), 3786-94.

[251] Mishra, S., Webster, P., and Davis, M. E., 'Pegylation Significantly Affects Cellular Uptake and Intracellular Trafficking of Non-Viral Gene Delivery Particles', *Eur J Cell Biol,* 83 (2004), 97-111.

[252] Schaffer, D. V., Neve, R. L., and Lauffenburger, D. A., 'Use of the Green Fluorescent Protein as a Quantitative Reporter of Epidermal Growth Factor Receptor-Mediated Gene Delivery', *Tissue Engineering,* 3 (1997), 53-63.

[253] Kircheis, R., Kichler, A., Wallner, G., Kursa, M., Ogris, M., Felzmann, T., Buchberger, M., and Wagner, E., 'Coupling of Cell-Binding Ligands to Polyethylenimine for Targeted Gene Delivery', *Gene Ther,* 4 (1997), 409-18.

[254] Harbottle, R. P., Cooper, R. G., Hart, S. L., Ladhoff, A., McKay, T., Knight, A. M., Wagner, E., Miller, A. D., and Coutelle, C., 'An Rgd-Oligolysine Peptide: A Prototype Construct for Integrin-Mediated Gene Delivery', *Hum Gene Ther,* 9 (1998), 1037-47.

[255] Ruhe, J., *Polymer Brushes: On the Way to Tailor-Made Surfaces*. ed. by R. C. Advincula, Brittain, W. J., Caster, K. C., Ruhe, J., *Polymer Brushes* (Federal Republic of Germany: Wiley-VCH, 2004).

[256] Jeon, N. L., Choi, I. S., Whitesides, G. M., Kim, N. Y., Laibinis, P. E., Harada, Y., Finnie, K. R., Girolami, G. S., and Nuzzo, R. G., 'Patterned Polymer Growth on Silicon Surfaces Using Microcontact Printing and Surface-Initiated Polymerization', *Applied Physics Letters,* 75 (1999), 4201-03.

[257] Weck, M., Jackiw, J. J., Rossi, R. R., Weiss, P. S., and Grubbs, R. H., 'Ring-Opening Metathesis Polymerization from Surfaces', *Journal of the American Chemical Society,* 121 (1999), 4088-89.

[258] Matyjaszewski, K., Miller, P. J., Shukla, N., Immaraporn, B., Gelman, A., Luokala, B. B., Siclovan, T. M., Kickelbick, G., Vallant, T., Hoffmann, H., and Pakula, T., 'Polymers at Interfaces: Using Atom Transfer Radical Polymerization in the Controlled Growth of Homopolymers and Block Copolymers from Silicon Surfaces in the Absence of Untethered Sacrificial Initiator', *Macromolecules,* 32 (1999), 8716-24.

[259] Pyun, J., Kowalewski, T., and Matyjaszewski, K., 'Synthesis of Polymer Brushes Using Atom Transfer Radical Polymerization', *Macromolecular Rapid Communications,* 24 (2003), 1043-59.

[260] Siegwart, D. J., Oh, J. K., and Matyjaszewski, K., 'Atrp in the Design of Functional Materials for Biomedical Applications', *Progress in polymer science,* 37 (2012), 18-37.

[261] Baum, M., and Brittain, W. J., 'Synthesis of Polymer Brushes on Silicate Substrates Via Reversible Addition Fragmentation Chain Transfer Technique', *Macromolecules,* 35 (2002), 610-15.

[262] Moad, G., Rizzardo, E., and Thang, S. H., 'Radical Addition–Fragmentation Chemistry in Polymer Synthesis', *Polymer,* 49 (2008), 1079-131.

[263] Husseman, M., Malmström, E. E., McNamara, M., Mate, M., Mecerreyes, D., Benoit, D. G., Hedrick, J. L., Mansky, P., Huang, E., and Russell, T. P., 'Controlled Synthesis of Polymer Brushes by "Living" Free Radical Polymerization Techniques', *Macromolecules,* 32 (1999), 1424-31.

[264] Sciannamea, V., Jérôme, R., and Detrembleur, C., 'In-Situ Nitroxide-Mediated Radical Polymerization (Nmp) Processes: Their Understanding and Optimization', *Chemical reviews,* 108 (2008), 1104-26.

[265] Edmondson, S., Osborne, V. L., and Huck, W. T., 'Polymer Brushes Via Surface-Initiated Polymerizations', *Chemical society reviews,* 33 (2004), 14-22.

[266] Brittain, W. J., and Minko, S., 'A Structural Definition of Polymer Brushes', *Journal of Polymer Science Part A: Polymer Chemistry,* 45 (2007), 3505-12.

[267] Ayres, N., 'Polymer Brushes: Applications in Biomaterials and Nanotechnology', *Polymer Chemistry,* 1 (2010), 769-77.

[268] Feng, W., Chen, R., Brash, J. L., and Zhu, S., 'Surface-Initiated Atom Transfer Radical Polymerization of Oligo (Ethylene Glycol) Methacrylate: Effect of Solvent on Graft Density', *Macromolecular rapid communications,* 26 (2005), 1383-88.

[269] Ohno, K., Morinaga, T., Koh, K., Tsujii, Y., and Fukuda, T., 'Synthesis of Monodisperse Silica Particles Coated with Well-Defined, High-Density Polymer Brushes by Surface-Initiated Atom Transfer Radical Polymerization', *Macromolecules,* 38 (2005), 2137-42.

[270] Ma, H., Li, D., Sheng, X., Zhao, B., and Chilkoti, A., 'Protein-Resistant Polymer Coatings on Silicon Oxide by Surface-Initiated Atom Transfer Radical Polymerization', *Langmuir,* 22 (2006), 3751-6.

[271] Estillore, N. C., Park, J. Y., and Advincula, R. C., 'Langmuir–Schaefer (Ls) Macroinitiator Film Control on the Grafting of a Thermosensitive Polymer Brush Via Surface Initiated-Atrp', *Macromolecules,* 43 (2010), 6588-98.

[272] White, M. A., Johnson, J. A., Koberstein, J. T., and Turro, N. J., 'Toward the Syntheses of Universal Ligands for Metal Oxide Surfaces: Controlling Surface Functionality through Click Chemistry', *Journal of the American Chemical Society,* 128 (2006), 11356-57.

[273] Wang, X., Ye, Q., Gao, T., Liu, J., and Zhou, F., 'Self-Assembly of Catecholic Macroinitiator on Various Substrates and Surface-Initiated Polymerization', *Langmuir,* 28 (2012), 2574-81.

[274] Bedair, T. M., Cho, Y., Kim, T. J., Kim, Y. D., Park, B. J., Joung, Y. K., and Han, D. K., 'Reinforcement of Interfacial Adhesion of a Coated Polymer Layer on a Cobalt-Chromium Surface for Drug-Eluting Stents', *Langmuir,* 30 (2014), 8020-8.

[275] Zeng, L., Wang, H., Fu, G., Jiang, J., and Zhang, X., 'A New Approach for Synthesis of the Comb-Shaped Poly (Epsilon-Caprolactone) Brushes on the Surface of Nano-

Hydroxyapatite by Combination of Atrp and Rop', *J Colloid Interface Sci,* 352 (2010), 36-42.

[276] Steenackers, M., Gigler, A. M., Zhang, N., Deubel, F., Seifert, M., Hess, L. H., Lim, C. H. Y. X., Loh, K. P., Garrido, J. A., and Jordan, R., 'Polymer Brushes on Graphene', *Journal of the American Chemical Society,* 133 (2011), 10490-98.

[277] Badri, A., Whittaker, M. R., and Zetterlund, P. B., 'Modification of Graphene/Graphene Oxide with Polymer Brushes Using Controlled/Living Radical Polymerization', *Journal of Polymer Science Part A: Polymer Chemistry,* 50 (2012), 2981-92.

[278] Majoinen, J., Walther, A., McKee, J. R., Kontturi, E., Aseyev, V., Malho, J. M., Ruokolainen, J., and Ikkala, O., 'Polyelectrolyte Brushes Grafted from Cellulose Nanocrystals Using Cu-Mediated Surface-Initiated Controlled Radical Polymerization', *Biomacromolecules,* 12 (2011), 2997-3006.

[279] Yameen, B., Khan, H. U., Knoll, W., Förch, R., and Jonas, U., 'Surface Initiated Polymerization on Pulsed Plasma Deposited Polyallylamine: A Polymer Substrate-Independent Strategy to Soft Surfaces with Polymer Brushes', *Macromolecular Rapid Communications,* 32 (2011), 1735-40.

[280] Coad, B. R., Lu, Y., and Meagher, L., 'A Substrate-Independent Method for Surface Grafting Polymer Layers by Atom Transfer Radical Polymerization: Reduction of Protein Adsorption', *Acta Biomaterialia,* 8 (2012), 608-18.

[281] Ameringer, T., Ercole, F., Tsang, K., Coad, B., Hou, X., Rodda, A., Nisbet, D., Thissen, H., Evans, R., Meagher, L., and Forsythe, J., 'Surface Grafting of Electrospun Fibers Using Atrp and Raft for the Control of Biointerfacial Interactions', *Biointerphases,* 8 (2013), 1-11.

[282] Hucknall, A., Simnick, A. J., Hill, R. T., Chilkoti, A., Garcia, A., Johannes, M. S., Clark, R. L., Zauscher, S., and Ratner, B. D., 'Versatile Synthesis and Micropatterning of Nonfouling Polymer Brushes on the Wafer Scale', *Biointerphases,* 4 (2009), FA50-FA57.

[283] Telford, A. M., Neto, C., and Meagher, L., 'Robust Grafting of Peg-Methacrylate Brushes from Polymeric Coatings', *Polymer,* 54 (2013), 5490-98.

[284] Gonçalves, S., Leirós, A., Van Kooten, T., Dourado, F., and Rodrigues, L. R., 'Physicochemical and Biological Evaluation of Poly (Ethylene Glycol) Methacrylate Grafted onto Poly (Dimethyl Siloxane) Surfaces for Prosthetic Devices', *Colloids and Surfaces B: Biointerfaces,* 109 (2013), 228-35.

[285] Bozukova, D., Pagnoulle, C., De Pauw-Gillet, M.-C., Ruth, N., Jérôme, R., and Jérôme, C., 'Imparting Antifouling Properties of Poly (2-Hydroxyethyl Methacrylate) Hydrogels by Grafting Poly (Oligoethylene Glycol Methyl Ether Acrylate)', *Langmuir,* 24 (2008), 6649-58.

[286] Barbey, R., Lavanant, L., Paripovic, D., Schüwer, N., Sugnaux, C., Tugulu, S., and Klok, H.-A., 'Polymer Brushes Via Surface-Initiated Controlled Radical Polymerization: Synthesis, Characterization, Properties, and Applications', *Chemical reviews,* 109 (2009), 5437-527.

[287] Murata, H., Koepsel, R. R., Matyjaszewski, K., and Russell, A. J., 'Permanent, Non-Leaching Antibacterial Surface--2: How High Density Cationic Surfaces Kill Bacterial Cells', *Biomaterials,* 28 (2007), 4870-9.

[288] Odian, G., *Principles of Polymerization* (John Wiley & Sons, 2004).

[289] Matyjaszewski, K., and Xia, J., 'Atom Transfer Radical Polymerization', *Chemical Reviews,* 101 (2001), 2921-90.

[290] Wink, T., Van Zuilen, S., Bult, A., and Van Bennekom, W., 'Self-Assembled Monolayers for Biosensors', *Analyst,* 122 (1997), 43R-50R.

[291] Marx, K. A., 'Quartz Crystal Microbalance: A Useful Tool for Studying Thin Polymer Films and Complex Biomolecular Systems at the Solution-Surface Interface', *Biomacromolecules,* 4 (2003), 1099-120.

[292] Lutolf, M., and Hubbell, J., 'Synthetic Biomaterials as Instructive Extracellular Microenvironments for Morphogenesis in Tissue Engineering', *Nature biotechnology,* 23 (2005), 47-55.

[293] Wilson, C. J., Clegg, R. E., Leavesley, D. I., and Pearcy, M. J., 'Mediation of Biomaterial-Cell Interactions by Adsorbed Proteins: A Review', *Tissue engineering,* 11 (2005), 1-18.

[294] Schierholz, J. M., and Beuth, J., 'Implant Infections: A Haven for Opportunistic Bacteria', *J Hosp Infect,* 49 (2001), 87-93.

[295] Lichter, J. A., Van Vliet, K. J., and Rubner, M. F., 'Design of Antibacterial Surfaces and Interfaces: Polyelectrolyte Multilayers as a Multifunctional Platform', *Macromolecules,* 42 (2009), 8573-86.

[296] Lego, B., Skene, W. G., and Giasson, S., 'Swelling Study of Responsive Polyelectrolyte Brushes Grafted from Mica Substrates: Effect of Ph, Salt, and Grafting Density', *Macromolecules,* 43 (2010), 4384-93.

[297] Schüwer, N., and Klok, H.-A., 'Tuning the Ph Sensitivity of Poly (Methacrylic Acid) Brushes', *Langmuir,* 27 (2011), 4789-96.

[298] Sanjuan, S., Perrin, P., Pantoustier, N., and Tran, Y., 'Synthesis and Swelling Behavior of Ph-Responsive Polybase Brushes', *Langmuir,* 23 (2007), 5769-78.

[299] Fielding, L. A., Edmondson, S., and Armes, S. P., 'Synthesis of Ph-Responsive Tertiary Amine Methacrylate Polymer Brushes and Their Response to Acidic Vapour', *Journal of Materials Chemistry,* 21 (2011), 11773-80.

[300] Willott, J. D., Murdoch, T. J., Humphreys, B. A., Edmondson, S., Webber, G. B., and Wanless, E. J., 'Critical Salt Effects in the Swelling Behavior of a Weak Polybasic Brush', *Langmuir,* 30 (2014), 1827-36.

[301] Li, D., He, Q., Cui, Y., and Li, J., 'Fabrication of Ph-Responsive Nanocomposites of Gold Nanoparticles/Poly (4-Vinylpyridine)', *Chemistry of materials,* 19 (2007), 412-17.

[302] Abraham, S., So, A., and Unsworth, L. D., 'Poly(Carboxybetaine Methacrylamide)-Modified Nanoparticles: A Model System for Studying the Effect of Chain Chemistry on Film Properties, Adsorbed Protein Conformation, and Clot Formation Kinetics', *Biomacromolecules,* 12 (2011), 3567-80.

[303] Mi, L., Bernards, M. T., Cheng, G., Yu, Q., and Jiang, S., 'Ph Responsive Properties of Non-Fouling Mixed-Charge Polymer Brushes Based on Quaternary Amine and Carboxylic Acid Monomers', *Biomaterials,* 31 (2010), 2919-25.

[304] Jonas, A. M., Glinel, K., Oren, R., Nysten, B., and Huck, W. T., 'Thermo-Responsive Polymer Brushes with Tunable Collapse Temperatures in the Physiological Range', *Macromolecules,* 40 (2007), 4403-05.

[305] Ishida, N., and Biggs, S., 'Effect of Grafting Density on Phase Transition Behavior for Poly(N-Isopropylacryamide) Brushes in Aqueous Solutions Studied by Afm and Qcm-D', *Macromolecules,* 43 (2010), 7269-76.

[306] Cheng, N., Brown, A. A., Azzaroni, O., and Huck, W. T. S., 'Thickness-Dependent Properties of Polyzwitterionic Brushes', *Macromolecules,* 41 (2008), 6317-21.

[307] Lutz, J.-F., Akdemir, Ö., and Hoth, A., 'Point by Point Comparison of Two Thermosensitive Polymers Exhibiting a Similar Lcst: Is the Age of Poly(Nipam) Over?', *Journal of the American Chemical Society,* 128 (2006), 13046-47.

[308] Azzaroni, O., Brown, A. A., and Huck, W. T., 'Ucst Wetting Transitions of Polyzwitterionic Brushes Driven by Self-Association', *Angew Chem Int Ed Engl,* 45 (2006), 1770-4.

[309] Krishnamoorthy, M., Hakobyan, S., Ramstedt, M., and Gautrot, J. E., 'Surface-Initiated Polymer Brushes in the Biomedical Field: Applications in Membrane Science, Biosensing, Cell Culture, Regenerative Medicine and Antibacterial Coatings', *Chemical Reviews,* 114 (2014), 10976-1026.

[310] Petrie, T. A., Raynor, J. E., Reyes, C. D., Burns, K. L., Collard, D. M., and García, A. J., 'The Effect of Integrin-Specific Bioactive Coatings on Tissue Healing and Implant Osseointegration', *Biomaterials,* 29 (2008), 2849-57.

[311] Ren, X., Wu, Y., Cheng, Y., Ma, H., and Wei, S., 'Fibronectin and Bone Morphogenetic Protein-2-Decorated Poly(Oegma-R-Hema) Brushes Promote Osseointegration of Titanium Surfaces', *Langmuir,* 27 (2011), 12069-73.

[312] Fan, X., Lin, L., and Messersmith, P. B., 'Cell Fouling Resistance of Polymer Brushes Grafted from Ti Substrates by Surface-Initiated Polymerization: Effect of Ethylene Glycol Side Chain Length', *Biomacromolecules,* 7 (2006), 2443-48.

[313] Bhat, R. R., Chaney, B. N., Rowley, J., Liebmann-Vinson, A., and Genzer, J., 'Tailoring Cell Adhesion Using Surface-Grafted Polymer Gradient Assemblies', *Advanced Materials,* 17 (2005), 2802-07.

[314] Mei, Y., Wu, T., Xu, C., Langenbach, K. J., Elliott, J. T., Vogt, B. D., Beers, K. L., Amis, E. J., and Washburn, N. R., 'Tuning Cell Adhesion on Gradient Poly (2-Hydroxyethyl Methacrylate)-Grafted Surfaces', *Langmuir,* 21 (2005), 12309-14.

[315] Du, H., Chandaroy, P., and Hui, S. W., 'Grafted Poly-(Ethylene Glycol) on Lipid Surfaces Inhibits Protein Adsorption and Cell Adhesion', *Biochimica et Biophysica Acta (BBA) - Biomembranes,* 1326 (1997), 236-48.

[316] Sofia, S. J., Premnath, V., and Merrill, E. W., 'Poly(Ethylene Oxide) Grafted to Silicon Surfaces: Grafting Density and Protein Adsorption', *Macromolecules,* 31 (1998), 5059-70.

[317] Patrucco, E., Ouasti, S., Vo, C. D., De Leonardis, P., Pollicino, A., Armes, S. P., Scandola, M., and Tirelli, N., 'Surface-Initiated Atrp Modification of Tissue Culture Substrates: Poly(Glycerol Monomethacrylate) as an Antifouling Surface', *Biomacromolecules,* 10 (2009), 3130-40.

[318] Jiang, H., Wang, X. B., Li, C. Y., Li, J. S., Xu, F. J., Mao, C., Yang, W. T., and Shen, J., 'Improvement of Hemocompatibility of Polycaprolactone Film Surfaces with Zwitterionic Polymer Brushes', *Langmuir,* 27 (2011), 11575-81.

[319] Wang, X., Miao, J., Zhao, H., Mao, C., Chen, X., and Shen, J., 'Fabrication of Nonbiofouling Metal Stent and in Vitro Studies on Its Hemocompatibility', *J Biomater Appl,* 29 (2013), 14-25.

[320] Villa-Diaz, L. G., Nandivada, H., Ding, J., Nogueira-de-Souza, N. C., Krebsbach, P. H., O'Shea, K. S., Lahann, J., and Smith, G. D., 'Synthetic Polymer Coatings for Long-Term Growth of Human Embryonic Stem Cells', *Nat Biotechnol,* 28 (2010), 581-3.

[321] Sin, M.-C., Sun, Y.-M., and Chang, Y., 'Zwitterionic-Based Stainless Steel with Well-Defined Polysulfobetaine Brushes for General Bioadhesive Control', *ACS Applied Materials & Interfaces,* 6 (2014), 861-73.

[322] Wang, X., Gan, H., Zhang, M., and Sun, T., 'Modulating Cell Behaviors on Chiral Polymer Brush Films with Different Hydrophobic Side Groups', *Langmuir,* 28 (2012), 2791-8.

[323] Shi, X., Wang, Y., Li, D., Yuan, L., Zhou, F., Wang, Y., Song, B., Wu, Z., Chen, H., and Brash, J. L., 'Cell Adhesion on a Poegma-Modified Topographical Surface', *Langmuir,* 28 (2012), 17011-8.

[324] Ivanov, A. E., Eccles, J., Panahi, H. A., Kumar, A., Kuzimenkova, M. V., Nilsson, L., Bergenstahl, B., Long, N., Phillips, G. J., Mikhalovsky, S. V., Galaev, I. Y., and Mattiasson, B., 'Boronate-Containing Polymer Brushes: Characterization, Interaction with Saccharides and Mammalian Cancer Cells', *J Biomed Mater Res A,* 88 (2009), 213-25.

[325] Ivanov, A. E., Kumar, A., Nilsang, S., Aguilar, M. R., Mikhalovska, L. I., Savina, I. N., Nilsson, L., Scheblykin, I. G., Kuzimenkova, M. V., and Galaev, I. Y., 'Evaluation of Boronate-Containing Polymer Brushes and Gels as Substrates for Carbohydrate-Mediated Adhesion and Cultivation of Animal Cells', *Colloids Surf B Biointerfaces,* 75 (2010), 510-9.

[326] da Silva, R. M., Mano, J. F., and Reis, R. L., 'Smart Thermoresponsive Coatings and Surfaces for Tissue Engineering: Switching Cell-Material Boundaries', *Trends Biotechnol,* 25 (2007), 577-83.

[327] Nagase, K., Kobayashi, J., and Okano, T., 'Temperature-Responsive Intelligent Interfaces for Biomolecular Separation and Cell Sheet Engineering', *J R Soc Interface,* 6 Suppl 3 (2009), S293-309.

[328] Cooperstein, M. A., and Canavan, H. E., 'Biological Cell Detachment from Poly (N-Isopropyl Acrylamide) and Its Applications', *Langmuir,* 26 (2009), 7695-707.

[329] Yu, Q., Zhang, Y., Chen, H., Zhou, F., Wu, Z., Huang, H., and Brash, J. L., 'Protein Adsorption and Cell Adhesion/Detachment Behavior on Dual-Responsive Silicon Surfaces Modified with Poly(N-Isopropylacrylamide)-Block-Polystyrene Copolymer', *Langmuir,* 26 (2010), 8582-8.

[330] Okano, M. N. T., and Winnik, F. M., 'Poly (N Isopropylacrylamide)-Based Smart Surfaces for Cell Sheet Tissue Engineering', *Material Matters,* 5 (2010), 56.

[331] Vihola, H., Laukkanen, A., Valtola, L., Tenhu, H., and Hirvonen, J., 'Cytotoxicity of Thermosensitive Polymers Poly(N-Isopropylacrylamide), Poly(N-Vinylcaprolactam) and Amphiphilically Modified Poly(N-Vinylcaprolactam)', *Biomaterials,* 26 (2005), 3055-64.

[332] Cunliffe, D., de las Heras Alarcón, C., Peters, V., Smith, J. R., and Alexander, C., 'Thermoresponsive Surface-Grafted Poly(N−Isopropylacrylamide) Copolymers: Effect of Phase Transitions on Protein and Bacterial Attachment', *Langmuir,* 19 (2003), 2888-99.

[333] Xu, F. J., Zhong, S. P., Yung, L. Y. L., Kang, E. T., and Neoh, K. G., 'Surface-Active and Stimuli-Responsive Polymer−Si(100) Hybrids from Surface-Initiated Atom Transfer Radical Polymerization for Control of Cell Adhesion', *Biomacromolecules,* 5 (2004), 2392-403.

[334] Ernst, O., Lieske, A., Jager, M., Lankenau, A., and Duschl, C., 'Control of Cell Detachment in a Microfluidic Device Using a Thermo-Responsive Copolymer on a Gold Substrate', *Lab on a Chip,* 7 (2007), 1322-29.

[335] Rzaev, Z. M. O., Dinçer, S., and Pişkin, E., 'Functional Copolymers of N-Isopropylacrylamide for Bioengineering Applications', *Progress in Polymer Science,* 32 (2007), 534-95.

[336] Zhang, C., Vernier, P. T., Wu, Y. H., Yang, W., and Thompson, M. E., 'Surface Chemical Immobilization of Parylene C with Thermosensitive Block Copolymer Brushes Based on N-Isopropylacrylamide and N-Tert-Butylacrylamide: Synthesis, Characterization, and Cell Adhesion/Detachment', *J Biomed Mater Res B Appl Biomater,* 100 (2012), 217-29.

[337] Kong, B., Choi, J. S., Jeon, S., and Choi, I. S., 'The Control of Cell Adhesion and Detachment on Thin Films of Thermoresponsive Poly[(N-Isopropylacrylamide)-R-((3-(Methacryloylamino)Propyl)-Dimethyl(3-Sulfopro Pyl)Ammonium Hydroxide)]', *Biomaterials,* 30 (2009), 5514-22.

[338] Nagase, K., Hatakeyama, Y., Shimizu, T., Matsuura, K., Yamato, M., Takeda, N., and Okano, T., 'Hydrophobized Thermoresponsive Copolymer Brushes for Cell Separation by Multistep Temperature Change', *Biomacromolecules,* 14 (2013), 3423-33.

[339] Idota, N., Ebara, M., Kotsuchibashi, Y., Narain, R., and Aoyagi, T., 'Novel Temperature-Responsive Polymer Brushes with Carbohydrate Residues Facilitate Selective Adhesion and Collection of Hepatocytes', *Science and Technology of Advanced Materials,* 13 (2012), 064206.

[340] Chernyy, S., Jensen, B. E., Shimizu, K., Ceccato, M., Pedersen, S. U., Zelikin, A. N., Daasbjerg, K., and Iruthayaraj, J., 'Surface Grafted Glycopolymer Brushes to Enhance Selective Adhesion of Hepg2 Cells', *J Colloid Interface Sci,* 404 (2013), 207-14.

[341] Lutz, J.-F., 'Thermo-Switchable Materials Prepared Using the Oegma-Platform', *Advanced Materials,* 23 (2011), 2237-43.
[342] Porsch, C., Hansson, S., Nordgren, N., and Malmström, E., 'Thermo-Responsive Cellulose-Based Architectures: Tailoring Lcst Using Poly(Ethylene Glycol) Methacrylates', *Polymer Chemistry,* 2 (2011), 1114.
[343] Uhlig, K., Boysen, B., Lankenau, A., Jaeger, M., Wischerhoff, E., Lutz, J.-F., Laschewsky, A., and Duschl, C., 'On the Influence of the Architecture of Poly(Ethylene Glycol)-Based Thermoresponsive Polymers on Cell Adhesion', *Biomicrofluidics,* 6 (2012), 024129.
[344] Yang, W. J., Neoh, K.-G., Kang, E.-T., Lee, S. S. C., Teo, S. L.-M., and Rittschof, D., 'Functional Polymer Brushes Via Surface-Initiated Atom Transfer Radical Graft Polymerization for Combating Marine Biofouling', *Biofouling,* 28 (2012), 895-912.
[345] Yu, Q., Cho, J., Shivapooja, P., Ista, L. K., and López, G. P., 'Nanopatterned Smart Polymer Surfaces for Controlled Attachment, Killing, and Release of Bacteria', *ACS Applied Materials & Interfaces,* 5 (2013), 9295-304.
[346] Kakizawa, Y., and Kataoka, K., 'Block Copolymer Micelles for Delivery of Gene and Related Compounds', *Advanced drug delivery reviews,* 54 (2002), 203-22.
[347] Murthy, N., Campbell, J., Fausto, N., Hoffman, A. S., and Stayton, P. S., 'Design and Synthesis of Ph-Responsive Polymeric Carriers That Target Uptake and Enhance the Intracellular Delivery of Oligonucleotides', *Journal of Controlled Release,* 89 (2003), 365-74.
[348] Fischer, D., Li, Y., Ahlemeyer, B., Krieglstein, J., and Kissel, T., 'In Vitro Cytotoxicity Testing of Polycations: Influence of Polymer Structure on Cell Viability and Hemolysis', *Biomaterials,* 24 (2003), 1121-31.
[349] Ghosh, P. S., Kim, C. K., Han, G., Forbes, N. S., and Rotello, V. M., 'Efficient Gene Delivery Vectors by Tuning the Surface Charge Density of Amino Acid-Functionalized Gold Nanoparticles', *ACS Nano,* 2 (2008), 2213-8.
[350] Putnam, D., Zelikin, A. N., Izumrudov, V. A., and Langer, R., 'Polyhistidine–Peg:DNA Nanocomposites for Gene Delivery', *Biomaterials,* 24 (2003), 4425-33.
[351] Langer, R., and Tirrell, D. A., 'Designing Materials for Biology and Medicine', *Nature,* 428 (2004), 487-92.
[352] Rana, S., Yeh, Y. C., and Rotello, V. M., 'Engineering the Nanoparticle-Protein Interface: Applications and Possibilities', *Curr Opin Chem Biol,* 14 (2010), 828-34.
[353] Yuan, L., Yu, Q., Li, D., and Chen, H., 'Surface Modification to Control Protein/Surface Interactions', *Macromol Biosci,* 11 (2011), 1031-40.
[354] Li, X., Wang, M., Wang, L., Shi, X., Xu, Y., Song, B., and Chen, H., 'Block Copolymer Modified Surfaces for Conjugation of Biomacromolecules with Control of Quantity and Activity', *Langmuir,* 29 (2013), 1122-8.
[355] Lee, M., and Kim, S. W., 'Polyethylene Glycol-Conjugated Copolymers for Plasmid DNA Delivery', *Pharmaceutical Research,* 22 (2005), 1-10.
[356] Gautrot, J. E., Huck, W. T., Welch, M., and Ramstedt, M., 'Protein-Resistant Nta-Functionalized Polymer Brushes for Selective and Stable Immobilization of Histidine-Tagged Proteins', *ACS Appl Mater Interfaces,* 2 (2010), 193-202.
[357] Li, Y., Liu, T., Zhang, G., Ge, Z., and Liu, S., 'Tumor-Targeted Redox-Responsive Nonviral Gene Delivery Nanocarriers Based on Neutral-Cationic Brush Block Copolymers', *Macromol Rapid Commun,* 35 (2014), 466-73.
[358] Wisniewski, N., and Reichert, M., 'Methods for Reducing Biosensor Membrane Biofouling', *Colloids and Surfaces B: Biointerfaces,* 18 (2000), 197-219.
[359] Piehler, J., Brecht, A., Valiokas, R., Liedberg, B., and Gauglitz, G., 'A High-Density Poly(Ethylene Glycol) Polymer Brush for Immobilization on Glass-Type Surfaces', *Biosens Bioelectron,* 15 (2000), 473-81.
[360] Charles, P. T., Stubbs, V. R., Soto, C. M., Martin, B. D., White, B. J., and Taitt, C. R., 'Reduction of Non-Specific Protein Adsorption Using Poly(Ethylene) Glycol (Peg)

Modified Polyacrylate Hydrogels in Immunoassays for Staphylococcal Enterotoxin B Detection', *Sensors (Basel),* 9 (2009), 645-55.

[361] Hu, W., Liu, Y., Lu, Z., and Li, C. M., 'Poly[Oligo(Ethylene Glycol) Methacrylate-Co-Glycidyl Methacrylate] Brush Substrate for Sensitive Surface Plasmon Resonance Imaging Protein Arrays', *Advanced Functional Materials,* 20 (2010), 3497-503.

[362] Deshpande, M. C., Davies, M. C., Garnett, M. C., Williams, P. M., Armitage, D., Bailey, L., Vamvakaki, M., Armes, S. P., and Stolnik, S., 'The Effect of Poly(Ethylene Glycol) Molecular Architecture on Cellular Interaction and Uptake of DNA Complexes', *J Control Release,* 97 (2004), 143-56.

[363] Üzgün, S., Akdemir, O. z. r., Hasenpusch, G. n., Maucksch, C., Golas, M. M., Sander, B., Stark, H., Imker, R., Lutz, J.-F., and Rudolph, C., 'Characterization of Tailor-Made Copolymers of Oligo (Ethylene Glycol) Methyl Ether Methacrylate and N, N-Dimethylaminoethyl Methacrylate as Nonviral Gene Transfer Agents: Influence of Macromolecular Structure on Gene Vector Particle Properties and Transfection Efficiency', *Biomacromolecules,* 11 (2009), 39-50.

[364] Venkataraman, S., Ong, W. L., Ong, Z. Y., Joachim Loo, S. C., Ee, P. L., and Yang, Y. Y., 'The Role of Peg Architecture and Molecular Weight in the Gene Transfection Performance of Pegylated Poly(Dimethylaminoethyl Methacrylate) Based Cationic Polymers', *Biomaterials,* 32 (2011), 2369-78.

[365] Rungsardthong, U., Deshpande, M., Bailey, L., Vamvakaki, M., Armes, S. P., Garnett, M. C., and Stolnik, S., 'Copolymers of Amine Methacrylate with Poly (Ethylene Glycol) as Vectors for Gene Therapy', *Journal of controlled release,* 73 (2001), 359-80.

[366] Verbaan, F. J., Klein Klouwenberg, P., van Steenis, J. H., Snel, C. J., Boerman, O., Hennink, W. E., and Storm, G., 'Application of Poly(2-(Dimethylamino)Ethyl Methacrylate)-Based Polyplexes for Gene Transfer into Human Ovarian Carcinoma Cells', *Int J Pharm,* 304 (2005), 185-92.

[367] van der Aa, M. A., Huth, U. S., Hafele, S. Y., Schubert, R., Oosting, R. S., Mastrobattista, E., Hennink, W. E., Peschka-Suss, R., Koning, G. A., and Crommelin, D. J., 'Cellular Uptake of Cationic Polymer-DNA Complexes Via Caveolae Plays a Pivotal Role in Gene Transfection in Cos-7 Cells', *Pharm Res,* 24 (2007), 1590-8.

[368] Zhu, C., Jung, S., Luo, S., Meng, F., Zhu, X., Park, T. G., and Zhong, Z., 'Co-Delivery of Sirna and Paclitaxel into Cancer Cells by Biodegradable Cationic Micelles Based on Pdmaema-Pcl-Pdmaema Triblock Copolymers', *Biomaterials,* 31 (2010), 2408-16.

[369] Mathew, A., Cao, H., Collin, E., Wang, W., and Pandit, A., 'Hyperbranched Pegmethacrylate Linear Pdmaema Block Copolymer as an Efficient Non-Viral Gene Delivery Vector', *Int J Pharm,* 434 (2012), 99-105.

[370] Yu, S., Chen, J., Dong, R., Su, Y., Ji, B., Zhou, Y., Zhu, X., and Yan, D., 'Enhanced Gene Transfection Efficiency of Pdmaema by Incorporating Hydrophobic Hyperbranched Polymer Cores: Effect of Degree of Branching', *Polymer Chemistry,* 3 (2012), 3324.

[371] Dou, X. B., Hu, Y., Zhao, N. N., and Xu, F. J., 'Different Types of Degradable Vectors from Low-Molecular-Weight Polycation-Functionalized Poly(Aspartic Acid) for Efficient Gene Delivery', *Biomaterials,* 35 (2014), 3015-26.

[372] Lee, H., Son, S. H., Sharma, R., and Won, Y.-Y., 'A Discussion of the Ph-Dependent Protonation Behaviors of Poly (2-(Dimethylamino) Ethyl Methacrylate)(Pdmaema) and Poly (Ethylenimine-Ran-2-Ethyl-2-Oxazoline)(P (Ei-R-Eoz))', *The Journal of Physical Chemistry B,* 115 (2011), 844-60.

[373] Agarwal, S., Zhang, Y., Maji, S., and Greiner, A., 'Pdmaema Based Gene Delivery Materials', *Materials Today,* 15 (2012), 388-93.

[374] Lim, D. W., Yeom, Y. I., and Park, T. G., 'Poly (Dmaema-Nvp)-B-Peg-Galactose as Gene Delivery Vector for Hepatocytes', *Bioconjugate chemistry,* 11 (2000), 688-95.

[375] Luten, J., van Nostrum, C. F., De Smedt, S. C., and Hennink, W. E., 'Biodegradable Polymers as Non-Viral Carriers for Plasmid DNA Delivery', *J Control Release,* 126 (2008), 97-110.

[376] Jones, R. A., Poniris, M. H., and Wilson, M. R., 'Pdmaema Is Internalised by Endocytosis but Does Not Physically Disrupt Endosomes', *J Control Release,* 96 (2004), 379-91.

[377] Mahltig, B., Gohy, J.-F., Antoun, S., Jérôme, R., and Stamm, M., 'Adsorption and Structure Formation of the Weak Polyelectrolytic Diblock Copolymer, Pvp-B-Pdmaema', *Colloid and Polymer Science,* 280 (2002), 495-502.

[378] Plamper, F. A., Schmalz, A., Penott-Chang, E., Drechsler, M., Jusufi, A., Ballauff, M., and Müller, A. H., 'Synthesis and Characterization of Star-Shaped Poly (N, N-Dimethylaminoethyl Methacrylate) and Its Quaternized Ammonium Salts', *Macromolecules,* 40 (2007), 5689-97.

[379] Titaux, G. A., Contreras-García, A., and Bucio, E., 'Surface Modification by Γ-Ray-Induced Grafting of Pdmaema/Pegmema onto Pe Films', *Radiation Physics and Chemistry,* 78 (2009), 485-88.

[380] Zhang, M., Liu, L., Wu, C., Fu, G., Zhao, H., and He, B., 'Synthesis, Characterization and Application of Well-Defined Environmentally Responsive Polymer Brushes on the Surface of Colloid Particles', *Polymer,* 48 (2007), 1989-97.

[381] Shen, Y., Qi, L., Wei, X., Zhang, R., and Mao, L., 'Preparation of Well-Defined Environmentally Responsive Polymer Brushes on Monolithic Surface by Two-Step Atom Transfer Radical Polymerization Method for Hplc', *Polymer,* 52 (2011), 3725-31.

[382] Chen, J., Xiao, P., Gu, J., Han, D., Zhang, J., Sun, A., Wang, W., and Chen, T., 'A Smart Hybrid System of Au Nanoparticle Immobilized Pdmaema Brushes for Thermally Adjustable Catalysis', *Chem Commun (Camb),* 50 (2014), 1212-4.

[383] Dong, Z., Wei, H., Mao, J., Wang, D., Yang, M., Bo, S., and Ji, X., 'Synthesis and Responsive Behavior of Poly(N,N-Dimethylaminoethyl Methacrylate) Brushes Grafted on Silica Nanoparticles and Their Quaternized Derivatives', *Polymer,* 53 (2012), 2074-84.

[384] Rauch, S., Uhlmann, P., and Eichhorn, K.-J., 'In Situ Spectroscopic Ellipsometry of Ph-Responsive Polymer Brushes on Gold Substrates', *Analytical and bioanalytical chemistry,* 405 (2013), 9061-69.

[385] Willott, J. D., Humphreys, B. A., Murdoch, T. J., Edmondson, S., Webber, G. B., and Wanless, E. J., 'Hydrophobic Effects within the Dynamic Ph-Response of Polybasic Tertiary Amine Methacrylate Brushes', *Physical Chemistry Chemical Physics,* 17 (2015), 3880-90.

[386] Xu, Y., Bolisetty, S., Drechsler, M., Fang, B., Yuan, J., Ballauff, M., and Müller, A. H. E., 'Ph and Salt Responsive Poly(N,N-Dimethylaminoethyl Methacrylate) Cylindrical Brushes and Their Quaternized Derivatives', *Polymer,* 49 (2008), 3957-64.

[387] Houbenov, N., Minko, S., and Stamm, M., 'Mixed Polyelectrolyte Brush from Oppositely Charged Polymers for Switching of Surface Charge and Composition in Aqueous Environment', *Macromolecules,* 36 (2003), 5897-901.

[388] Tokarev, I., Tokareva, I., and Minko, S., 'Optical Nanosensor Platform Operating in near-Physiological Ph Range Via Polymer-Brush-Mediated Plasmon Coupling', *ACS applied materials & interfaces,* 3 (2011), 143-46.

[389] Chen, J.-K., and Bai, B.-J., 'Diagnosis of Breast Cancer Recurrence after Surgery by Using Poly(2-Dimethylaminoethyl Methacrylate) Brushes as a Medium on Silicon Surface', *Sensors and Actuators B: Chemical,* 160 (2011), 1011-19.

[390] Zhou, F., Shu, W., Welland, M. E., and Huck, W. T., 'Highly Reversible and Multi-Stage Cantilever Actuation Driven by Polyelectrolyte Brushes', *Journal of the American Chemical Society,* 128 (2006), 5326-27.

[391] Lo Nostro, P., and Ninham, B. W., 'Hofmeister Phenomena: An Update on Ion Specificity in Biology', *Chem Rev,* 112 (2012), 2286-322.

[392] Aoki, H., Kitamura, M., and Ito, S., 'Nanosecond Dynamics of Poly (Methyl Methacrylate) Brushes in Solvents Studied by Fluorescence Depolarization Method', *Macromolecules,* 41 (2008), 285-87.

[393] Baines, F., Dionisio, S., Billingham, N., and Armes, S., 'Use of Block Copolymer Stabilizers for the Dispersion Polymerization of Styrene in Alcoholic Media', *Macromolecules,* 29 (1996), 3096-102.

[394] Xu, C., Wu, T., Drain, C. M., Batteas, J. D., Fasolka, M. J., and Beers, K. L., 'Effect of Block Length on Solvent Response of Block Copolymer Brushes: Combinatorial Study with Block Copolymer Brush Gradients', *Macromolecules,* 39 (2006), 3359-64.

[395] Fukumori, K., Akiyama, Y., Kumashiro, Y., Kobayashi, J., Yamato, M., Sakai, K., and Okano, T., 'Characterization of Ultra-Thin Temperature-Responsive Polymer Layer and Its Polymer Thickness Dependency on Cell Attachment/Detachment Properties', *Macromol Biosci,* 10 (2010), 1117-29.

[396] Mizutani, A., Kikuchi, A., Yamato, M., Kanazawa, H., and Okano, T., 'Preparation of Thermoresponsive Polymer Brush Surfaces and Their Interaction with Cells', *Biomaterials,* 29 (2008), 2073-81.

[397] Zhu, X., Yan, C., Winnik, F., and Leckband, D., 'End-Grafted Low-Molecular-Weight Pnipam Does Not Collapse above the Lcst', *Langmuir,* 23 (2007), 162-69.

[398] Idota, N., Kikuchi, A., Kobayashi, J., Sakai, K., and Okano, T., 'Modulation of Graft Architectures for Enhancing Hydrophobic Interaction of Biomolecules with Thermoresponsive Polymer-Grafted Surfaces', *Colloids and Surfaces B: Biointerfaces,* 99 (2012), 95-101.

[399] Tamura, A., Kobayashi, J., Yamato, M., and Okano, T., 'Thermally Responsive Microcarriers with Optimal Poly (N-Isopropylacrylamide) Grafted Density for Facilitating Cell Adhesion/Detachment in Suspension Culture', *Acta biomaterialia,* 8 (2012), 3904-13.

[400] Plunkett, K. N., Zhu, X., Moore, J. S., and Leckband, D. E., 'Pnipam Chain Collapse Depends on the Molecular Weight and Grafting Density', *Langmuir,* 22 (2006), 4259-66.

[401] Cho, S. H., Jhon, M. S., Yuk, S. H., and Lee, H. B., 'Temperature-Induced Phase Transition of Poly(N,N-Dimethylaminoethyl Methacrylate-Co-Acrylamide)', *Journal of Polymer Science Part B: Polymer Physics,* 35 (1997), 595-98.

[402] Plamper, F. A., Ruppel, M., Schmalz, A., Borisov, O., Ballauff, M., and Müller, A. H. E., 'Tuning the Thermoresponsive Properties of Weak Polyelectrolytes: Aqueous Solutions of Star-Shaped and Linear Poly(N,N-Dimethylaminoethyl Methacrylate)', *Macromolecules,* 40 (2007), 8361-66.

[403] Zhou, W., Liu, H., Ye, H., Cui, H., Wang, R., Li, J., and Zhang, X., 'Synthesis and Adsorption Behaviors of Poly(2-(Dimethylamino)Ethyl Methacrylate) Brushes on Silica Particles by Surface-Initiated Atom Transfer Radical Polymerization', *Powder Technology,* 249 (2013), 1-6.

[404] Han, X., Zhang, X., Zhu, H., Yin, Q., Liu, H., and Hu, Y., 'Effect of Composition of Pdmaema-B-Paa Block Copolymers on Their Ph- and Temperature-Responsive Behaviors', *Langmuir,* 29 (2013), 1024-34.

[405] Nagase, K., Kobayashi, J., Kikuchi, A., Akiyama, Y., Kanazawa, H., and Okano, T., 'High Stability of Thermoresponsive Polymer-Brush-Grafted Silica Beads as Chromatography Matrices', *ACS Appl Mater Interfaces,* 4 (2012), 1998-2008.

[406] Ha, S. W., Camalier, C. E., Weitzmann, M. N., Beck, G. R., Jr., and Lee, J. K., 'Long-Term Monitoring of the Physicochemical Properties of Silica-Based Nanoparticles on the Rate of Endocytosis and Exocytosis and Consequences of Cell Division', *Soft Mater,* 11 (2013), 195-203.

[407] Wang, X. S., and Armes, S. P., 'Facile Atom Transfer Radical Polymerization of Methoxy-Capped Oligo(Ethylene Glycol) Methacrylate in Aqueous Media at Ambient Temperature', *Macromolecules,* 33 (2000), 6640-47.
[408] Gonçalves, D., and Irene, E. A., 'Fundamentals and Applications of Spectroscopic Ellipsometry', *Química Nova,* 25 (2002), 794-800.
[409] Griffiths, P. R., and De Haseth, J. A., *Fourier Transform Infrared Spectrometry*. Vol. 171 (John Wiley & Sons, 2007).
[410] Duckett, S., and Gilbert, B. C., *Foundations of Spectroscopy* (Oxford: Oxford University Press, 2000).
[411] Moore, C., 'Gel Permeation Chromatography', in *Characterization of Macromolecular Structure: Proceedings of a Conference, April 5-7, 1967* (National Academies, 1968), p. 273.
[412] Goldstein, J., Newbury, D. E., Echlin, P., Joy, D. C., Romig Jr, A. D., Lyman, C. E., Fiori, C., and Lifshin, E., *Scanning Electron Microscopy and X-Ray Microanalysis: A Text for Biologists, Materials Scientists, and Geologists* (Springer Science & Business Media, 2012).
[413] Haines, P. J., *Principles of Thermal Analysis and Calorimetry* (Royal society of chemistry, 2002).
[414] Li, C., and Benicewicz, B. C., 'Synthesis of Well-Defined Polymer Brushes Grafted onto Silica Nanoparticles Via Surface Reversible Addition-Fragmentation Chain Transfer Polymerization', *Macromolecules,* 38 (2005), 5929-36.
[415] Attard, P., Antelmi, D., and Larson, I., 'Comparison of the Zeta Potential with the Diffuse Layer Potential from Charge Titration', *Langmuir,* 16 (2000), 1542-52.
[416] Zhou, G., Ma, C., and Zhang, G., 'Synthesis of Polyurethane-G-Poly(Ethylene Glycol) Copolymers by Macroiniferter and Their Protein Resistance', *Polymer Chemistry,* 2 (2011), 1409-14.
[417] Jin, L., Deng, Y., Hu, J., and Wang, C., 'Preparation and Characterization of Core–Shell Polymer Particles with Protonizable Shells Prepared by Oxyanionic Polymerization', *Journal of Polymer Science Part A: Polymer Chemistry,* 42 (2004), 6081-88.
[418] Yang, Y., Wang, J., Zhang, J., Liu, J., Yang, X., and Zhao, H., 'Exfoliated Graphite Oxide Decorated by Pdmaema Chains and Polymer Particles', *Langmuir,* 25 (2009), 11808-14.
[419] Bomfim João, A. S., Mincheva, R., Beigbeder, A., Persenaire, O., and Dubois, P., '(Quaternized/Betainized) Amino-Based Amphiphilic Block Copolymers: Quantitative Composition Characterization Via Ftir and Thermogravimetry', in *e-Polymers* (2009), p. 421.
[420] Du, Z., Sun, X., Tai, X., Wang, G., and Liu, X., 'Synthesis of Hybrid Silica Nanoparticles Grafted with Thermoresponsive Poly(Ethylene Glycol) Methyl Ether Methacrylate Via Aget-Atrp', *RSC Adv.,* 5 (2015), 17194-201.
[421] Li, C., Zhang, Y., Peng, J., Wu, H., Li, J., and Zhai, M., 'Adsorption of Cr(Vi) Using Cellulose Microsphere-Based Adsorbent Prepared by Radiation-Induced Grafting', *Radiation Physics and Chemistry,* 81 (2012), 967-70.
[422] Zhou, L., Yuan, W., Yuan, J., and Hong, X., 'Preparation of Double-Responsive Sio2-G-Pdmaema Nanoparticles Via Atrp', *Materials Letters,* 62 (2008), 1372-75.
[423] Yang, C., Li, H., Goh, S. H., and Li, J., 'Cationic Star Polymers Consisting of Alpha-Cyclodextrin Core and Oligoethylenimine Arms as Nonviral Gene Delivery Vectors', *Biomaterials,* 28 (2007), 3245-54.
[424] Gao, B., Chen, Y., and Zhang, Z., 'Preparation of Functional Composite Grafted Particles Pdmaema/Sio2 and Preliminarily Study on Functionality', *Applied Surface Science,* 257 (2010), 254-60.
[425] Xu, G., Zhang, J., and Song, G., 'Effect of Complexation on the Zeta Potential of Silica Powder', *Powder technology,* 134 (2003), 218-22.

[426] Shin, Y., Lee, D., Lee, K., Ahn, K. H., and Kim, B., 'Surface Properties of Silica Nanoparticles Modified with Polymers for Polymer Nanocomposite Applications', *Journal of Industrial and Engineering Chemistry,* 14 (2008), 515-19.

[427] Lee, H., Son, S. H., Sharma, R., and Won, Y. Y., 'A Discussion of the Ph-Dependent Protonation Behaviors of Poly(2-(Dimethylamino)Ethyl Methacrylate) (Pdmaema) and Poly(Ethylenimine-Ran-2-Ethyl-2-Oxazoline) (P(Ei-R-Eoz))', *J Phys Chem B,* 115 (2011), 844-60.

[428] Hartley, P., and Scales, P., 'Electrostatic Properties of Polyelectrolyte Modified Surfaces Studied by Direct Force Measurement', *Langmuir,* 14 (1998), 6948-55.

[429] Liang, Y., Hilal, N., Langston, P., and Starov, V., 'Interaction Forces between Colloidal Particles in Liquid: Theory and Experiment', *Advances in colloid and interface science,* 134 (2007), 151-66.

[430] Drescher, D. G., Ramakrishnan, N. A., and Drescher, M. J., 'Surface Plasmon Resonance (Spr) Analysis of Binding Interactions of Proteins in Inner-Ear Sensory Epithelia', *Methods Mol Biol,* 493 (2009), 323-43.

[431] Cheesman, B. T., Smith, E. G., Murdoch, T. J., Guibert, C., Webber, G. B., Edmondson, S., and Wanless, E. J., 'Polyelectrolyte Brush Ph-Response at the Silica–Aqueous Solution Interface: A Kinetic and Equilibrium Investigation', *Physical Chemistry Chemical Physics,* 15 (2013), 14502-10.

[432] Vijayanathan, V., Thomas, T., and Thomas, T., 'DNA Nanoparticles and Development of DNA Delivery Vehicles for Gene Therapy', *Biochemistry,* 41 (2002), 14085-94.

[433] Arigita, C., Zuidam, N. J., Crommelin, D. J., and Hennink, W. E., 'Association and Dissociation Characteristics of Polymer/DNA Complexes Used for Gene Delivery', *Pharmaceutical research,* 16 (1999), 1534-41.

[434] Ahmed, M., Deng, Z., Liu, S., Lafrenie, R., Kumar, A., and Narain, R., 'Cationic Glyconanoparticles: Their Complexation with DNA, Cellular Uptake, and Transfection Efficiencies', *Bioconjugate chemistry,* 20 (2009), 2169-76.

[435] Jeong, J. H., Kim, S. H., Christensen, L. V., Feijen, J., and Kim, S. W., 'Reducible Poly(Amido Ethylenimine)-Based Gene Delivery System for Improved Nucleus Trafficking of Plasmid DNA', *Bioconjugate chemistry,* 21 (2010), 296-301.

[436] Zhang, W., Cheng, Q., Guo, S., Lin, D., Huang, P., Liu, J., Wei, T., Deng, L., Liang, Z., Liang, X. J., and Dong, A., 'Gene Transfection Efficacy and Biocompatibility of Polycation/DNA Complexes Coated with Enzyme Degradable Pegylated Hyaluronic Acid', *Biomaterials,* 34 (2013), 6495-503.

[437] Daghestani, H. N., and Day, B. W., 'Theory and Applications of Surface Plasmon Resonance, Resonant Mirror, Resonant Waveguide Grating, and Dual Polarization Interferometry Biosensors', *Sensors (Basel),* 10 (2010), 9630-46.

[438] Homola, J., Yee, S. S., and Gauglitz, G., 'Surface Plasmon Resonance Sensors: Review', *Sensors and Actuators B: Chemical,* 54 (1999), 3-15.

[439] Wink, T., de Beer, J., Hennink, W. E., Bult, A., and van Bennekom, W. P., 'Interaction between Plasmid DNA and Cationic Polymers Studied by Surface Plasmon Resonance Spectrometry', *Analytical Chemistry,* 71 (1999), 801-05.

[440] Ramakrishnan, A., and Sadana, A., 'A Kinetic Study of Analyte-Receptor Binding and Dissociation for Biosensor Applications: A Fractal Analysis for Two Different DNA Systems', *Biosystems,* 66 (2002), 165-77.

[441] Liedberg, B., Lundström, I., and Stenberg, E., 'Principles of Biosensing with an Extended Coupling Matrix and Surface Plasmon Resonance', *Sensors and Actuators B: Chemical,* 11 (1993), 63-72.

[442] Howard, K. A., Dash, P. R., Read, M. L., Ward, K., Tomkins, L. M., Nazarova, O., Ulbrich, K., and Seymour, L. W., 'Influence of Hydrophilicity of Cationic Polymers on the Biophysical Properties of Polyelectrolyte Complexes Formed by Self-Assembly with DNA', *Biochimica et Biophysica Acta (BBA)-General Subjects,* 1475 (2000), 245-55.

[443] Cantor, C., 'Biophysical Chemistry: Part Ii'techniques for the Study of Biological Structure and Function'', *Biochemical Education,* 9 (1981), 4.

[444] Baumann, C. G., Smith, S. B., Bloomfield, V. A., and Bustamante, C., 'Ionic Effects on the Elasticity of Single DNA Molecules', *Proceedings of the National Academy of Sciences,* 94 (1997), 6185-90.

[445] Gottenbos, B., van der Mei, H. C., Klatter, F., Grijpma, D. W., Feijen, J., Nieuwenhuis, P., and Busscher, H. J., 'Positively Charged Biomaterials Exert Antimicrobial Effects on Gram-Negative Bacilli in Rats', *Biomaterials,* 24 (2003), 2707-10.

[446] Croisier, F., and Jérôme, C., 'Chitosan-Based Biomaterials for Tissue Engineering', *European Polymer Journal,* 49 (2013), 780-92.

[447] Kenausis, G. L., Vörös, J., Elbert, D. L., Huang, N., Hofer, R., Ruiz-Taylor, L., Textor, M., Hubbell, J. A., and Spencer, N. D., 'Poly(L-Lysine)-G-Poly(Ethylene Glycol) Layers on Metal Oxide Surfaces: Attachment Mechanism and Effects of Polymer Architecture on Resistance to Protein Adsorption†', *The Journal of Physical Chemistry B,* 104 (2000), 3298-309.

[448] Grainger, D. W., 'All Charged up About Implanted Biomaterials', *Nat Biotechnol,* 31 (2013), 507-9.

[449] Hans, M., and Lowman, A., 'Biodegradable Nanoparticles for Drug Delivery and Targeting', *Current Opinion in Solid State and Materials Science,* 6 (2002), 319-27.

[450] He, X. L., Nie, P. P., Sun, Y. K., Wang, Y., Dong, Y. Y., and Chen, L., 'Immobilization of Galactose Ligands on Thermoresponsive Culture Surface and Its Influence on Cell Adhesion/Detachment', *J Colloid Interface Sci,* 350 (2010), 471-9.

[451] Cheng, G., Xue, H., Zhang, Z., Chen, S., and Jiang, S., 'A Switchable Biocompatible Polymer Surface with Self-Sterilizing and Nonfouling Capabilities', *Angew Chem Int Ed Engl,* 47 (2008), 8831-4.

[452] Zdyrko, B., Klep, V., Li, X., Kang, Q., Minko, S., Wen, X., and Luzinov, I., 'Polymer Brushes as Active Nanolayers for Tunable Bacteria Adhesion', *Materials Science and Engineering: C,* 29 (2009), 680-84.

[453] Lee, H. S., Yee, M. Q., Eckmann, Y. Y., Hickok, N. J., Eckmann, D. M., and Composto, R. J., 'Reversible Swelling of Chitosan and Quaternary Ammonium Modified Chitosan Brush Layers: Effect of Ph and Counter Anion Size and Functionality', *J Mater Chem,* 22 (2012), 19605-16.

[454] Terada, A., Okuyama, K., Nishikawa, M., Tsuneda, S., and Hosomi, M., 'The Effect of Surface Charge Property on Escherichia Coli Initial Adhesion and Subsequent Biofilm Formation', *Biotechnol Bioeng,* 109 (2012), 1745-54.

[455] Yang, W. J., Cai, T., Neoh, K. G., Kang, E. T., Dickinson, G. H., Teo, S. L., and Rittschof, D., 'Biomimetic Anchors for Antifouling and Antibacterial Polymer Brushes on Stainless Steel', *Langmuir,* 27 (2011), 7065-76.

[456] Ye, Q., Gao, T., Wan, F., Yu, B., Pei, X., Zhou, F., and Xue, Q., 'Grafting Poly (Ionic Liquid) Brushes for Anti-Bacterial and Anti-Biofouling Applications', *Journal of Materials Chemistry,* 22 (2012), 13123-31.

[457] Dong, R., Molloy, R. P., Lindau, M., and Ober, C. K., 'Direct Synthesis of Quaternized Polymer Brushes and Their Application for Guiding Neuronal Growth', *Biomacromolecules,* 11 (2010), 2027-32.

[458] Yao, F., Fu, G., Zhao, J., Kang, E., and Neoh, K., 'Antibacterial Effect of Surface-Functionalized Polypropylene Hollow Fiber Membrane from Surface-Initiated Atom Transfer Radical Polymerization', *Journal of Membrane Science,* 319 (2008), 149-57.

[459] Sui, Y., Gao, X., Wang, Z., and Gao, C., 'Antifouling and Antibacterial Improvement of Surface-Functionalized Poly(Vinylidene Fluoride) Membrane Prepared Via Dihydroxyphenylalanine-Initiated Atom Transfer Radical Graft Polymerizations', *Journal of Membrane Science,* 394-395 (2012), 107-19.

[460] Stephens, P., Grenard, P., Aeschlimann, P., Langley, M., Blain, E., Errington, R., Kipling, D., Thomas, D., and Aeschlimann, D., 'Crosslinking and G-Protein Functions of Transglutaminase 2 Contribute Differentially to Fibroblast Wound Healing Responses', *J Cell Sci,* 117 (2004), 3389-403.

[461] Barbe, C., Bartlett, J., Kong, L., Finnie, K., Lin, H. Q., Larkin, M., Calleja, S., Bush, A., and Calleja, G., 'Silica Particles: A Novel Drug-Delivery System', *Advanced materials,* 16 (2004), 1959-66.

[462] Kean, T., Roth, S., and Thanou, M., 'Trimethylated Chitosans as Non-Viral Gene Delivery Vectors: Cytotoxicity and Transfection Efficiency', *J Control Release,* 103 (2005), 643-53.

[463] Ferruti, P., Knobloch, S., Ranucci, E., Duncan, R., and Gianasi, E., 'A Novel Modification of Poly(L-Lysine) Leading to a Soluble Cationic Polymer with Reduced Toxicity and with Potential as a Transfection Agent', *Macromolecular Chemistry and Physics,* 199 (1998), 2565-75.

[464] Parhamifar, L., Larsen, A. K., Hunter, A. C., Andresen, T. L., and Moghimi, S. M., 'Polycation Cytotoxicity: A Delicate Matter for Nucleic Acid Therapy—Focus on Polyethylenimine', *Soft Matter,* 6 (2010), 4001.

[465] Reschel, T., Konak, C., Oupicky, D., Seymour, L. W., and Ulbrich, K., 'Physical Properties and in Vitro Transfection Efficiency of Gene Delivery Vectors Based on Complexes of DNA with Synthetic Polycations', *J Control Release,* 81 (2002), 201-17.

[466] Schallon, A., Jérôme, V., Walther, A., Synatschke, C. V., Müller, A. H. E., and Freitag, R., 'Performance of Three Pdmaema-Based Polycation Architectures as Gene Delivery Agents in Comparison to Linear and Branched Pei', *Reactive and Functional Polymers,* 70 (2010), 1-10.

[467] Yamano, S., Dai, J., and Moursi, A. M., 'Comparison of Transfection Efficiency of Nonviral Gene Transfer Reagents', *Mol Biotechnol,* 46 (2010), 287-300.

[468] Lechardeur, D., Verkman, A. S., and Lukacs, G. L., 'Intracellular Routing of Plasmid DNA During Non-Viral Gene Transfer', *Adv Drug Deliv Rev,* 57 (2005), 755-67.

[469] Hufnagel, H., Hakim, P., Lima, A., and Hollfelder, F., 'Fluid Phase Endocytosis Contributes to Transfection of DNA by Pei-25', *Mol Ther,* 17 (2009), 1411-7.

[470] El-Sayed, A., and Harashima, H., 'Endocytosis of Gene Delivery Vectors: From Clathrin-Dependent to Lipid Raft-Mediated Endocytosis', *Mol Ther,* 21 (2013), 1118-30.

[471] Hu, L., Mao, Z., and Gao, C., 'Colloidal Particles for Cellular Uptake and Delivery', *Journal of Materials Chemistry,* 19 (2009), 3108.

[472] Davis, M. E., 'Non-Viral Gene Delivery Systems', *Current opinion in biotechnology,* 13 (2002), 128-31.

[473] Moore, M. N., 'Do Nanoparticles Present Ecotoxicological Risks for the Health of the Aquatic Environment?', *Environ Int,* 32 (2006), 967-76.

[474] Grigsby, C. L., and Leong, K. W., 'Balancing Protection and Release of DNA: Tools to Address a Bottleneck of Non-Viral Gene Delivery', *J R Soc Interface,* 7 Suppl 1 (2010), S67-82.

[475] Janes, K. A., Calvo, P., and Alonso, M. J., 'Polysaccharide Colloidal Particles as Delivery Systems for Macromolecules', *Advanced Drug Delivery Reviews,* 47 (2001), 83-97.

[476] Mao, Z., Ma, L., Jiang, Y., Yan, M., Gao, C., and Shen, J., 'N,N,N-Trimethylchitosan Chloride as a Gene Vector: Synthesis and Application', *Macromol Biosci,* 7 (2007), 855-63.

[477] Luo, D., Han, E., Belcheva, N., and Saltzman, W. M., 'A Self-Assembled, Modular DNA Delivery System Mediated by Silica Nanoparticles', *J Control Release,* 95 (2004), 333-41.

[478] Dawson, G. F., and Halbert, G. W., 'The in Vitro Cell Association of Invasin Coated Polylactide-Co-Glycolide Nanoparticles', *Pharmaceutical research,* 17 (2000), 1420-25.

[479] Hauck, T. S., Ghazani, A. A., and Chan, W. C., 'Assessing the Effect of Surface Chemistry on Gold Nanorod Uptake, Toxicity, and Gene Expression in Mammalian Cells', *Small,* 4 (2008), 153-9.

[480] Luo, D., and Saltzman, W. M., 'Enhancement of Transfection by Physical Concentration of DNA at the Cell Surface', *Nature biotechnology,* 18 (2000), 893-95.

[481] Krishnan, R., and Srinivasan, K., 'Controlled/"Living" Radical Polymerization of Glycidyl Methacrylate at Ambient Temperature', *Macromolecules,* 36 (2003), 1769-71.

[482] Edmondson, S., and Huck, W. T. S., 'Controlled Growth and Subsequent Chemical Modification of Poly(Glycidyl Methacrylate) Brushes on Silicon Wafers', *Journal of Materials Chemistry,* 14 (2004), 730.

[483] Tsyalkovsky, V., Klep, V., Ramaratnam, K., Lupitskyy, R., Minko, S., and Luzinov, I., 'Fluorescent Reactive Core–Shell Composite Nanoparticles with a High Surface Concentration of Epoxy Functionalities', *Chemistry of Materials,* 20 (2008), 317-25.

[484] Rittich, B., Španová, A., and Horák, D., 'Functionalised Magnetic Microspheres with Hydrophilic Properties for Molecular Diagnostic Applications', *Food Research International,* 42 (2009), 493-98.

[485] Bernand-Mantel, D., Chehimi, M. M., Millot, M. C., and Carbonnier, B., 'Protein-Functionalized Ultrathin Glycidyl Methacrylate Polymer Grafts on Gold for the Development of Optical Biosensors : An Spr Investigation', *Surface and Interface Analysis,* 42 (2010), 1035-40.

[486] Ma, M., Li, F., Chen, F. J., Cheng, S. X., and Zhuo, R. X., 'Poly(Ethylene Glycol)-Block-Poly(Glycidyl Methacrylate) with Oligoamine Side Chains as Efficient Gene Vectors', *Macromol Biosci,* 10 (2010), 183-91.

[487] Gao, H., Lu, X., Ma, Y., Yang, Y., Li, J., Wu, G., Wang, Y., Fan, Y., and Ma, J., 'Amino Poly(Glycerol Methacrylate)S for Oligonucleic Acid Delivery with Enhanced Transfection Efficiency and Low Cytotoxicity', *Soft Matter,* 7 (2011), 9239.

[488] Li, F., Ma, M., Yuan, Z.-F., Huang, J.-Y., and Zhuo, R.-X., 'Novel Poly (Glycidyl Methacrylate-B-Propylene Oxide-B-Glycidyl Methacrylate) Derivatives with Low Cytotoxicity and Efficient Gene Delivery', *Journal of Bioactive and Compatible Polymers* (2011), 0883911511410461.

[489] Dou, X. B., Chai, M. Y., Zhu, Y., Yang, W. T., and Xu, F. J., 'Aminated Poly(Glycidyl Methacrylate)S for Constructing Efficient Gene Carriers', *ACS Appl Mater Interfaces,* 5 (2013), 3212-8.

[490] Prevette, L. E., Kodger, T. E., Reineke, T. M., and Lynch, M. L., 'Deciphering the Role of Hydrogen Bonding in Enhancing Pdna-Polycation Interactions', *Langmuir,* 23 (2007), 9773-84.

[491] Hu, Y., Zhu, Y., Yang, W. T., and Xu, F. J., 'New Star-Shaped Carriers Composed of Beta-Cyclodextrin Cores and Disulfide-Linked Poly(Glycidyl Methacrylate) Derivative Arms with Plentiful Flanking Secondary Amine and Hydroxyl Groups for Highly Efficient Gene Delivery', *ACS Appl Mater Interfaces,* 5 (2013), 703-12.

[492] Wei, H., Pahang, J. A., and Pun, S. H., 'Optimization of Brush-Like Cationic Copolymers for Nonviral Gene Delivery', *Biomacromolecules,* 14 (2013), 275-84.

[493] Li, C., Yang, Y.-W., Liang, Z.-x., Wu, G.-l., and Gao, H., 'Post-Modification of Poly(Glycidyl Methacrylate)S with Alkyl Amine and Isothiocyanate for Effective Pdna Delivery', *Polymer Chemistry,* 4 (2013), 4366.

[494] Tan, K. Y., Ramstedt, M., Colak, B., Huck, W. T. S., and Gautrot, J. E., 'Study of Thiol-Ene Chemistry on Polymer Brushes and Application to Surface Patterning and Protein Adsorption', *Polymer Chemistry,* 7 (2016), 979-90.

[495] Gao, H., Elsabahy, M., Giger, E. V., Li, D., Prud'homme, R. E., and Leroux, J.-C., 'Aminated Linear and Star-Shape Poly(Glycerol Methacrylate)S: Synthesis and Self-Assembling Properties', *Biomacromolecules,* 11 (2010), 889-95.

[496] Tack, F., Bakker, A., Maes, S., Dekeyser, N., Bruining, M., Elissen-Roman, C., Janicot, M., Brewster, M., Janssen, H. M., and De Waal, B., 'Modified Poly (Propylene Imine) Dendrimers as Effective Transfection Agents for Catalytic DNA Enzymes (Dnazymes)', *Journal of drug targeting,* 14 (2006), 69-86.

[497] Mao, Z., Ma, L., Yan, J., Yan, M., Gao, C., and Shen, J., 'The Gene Transfection Efficiency of Thermoresponsive N,N,N-Trimethyl Chitosan Chloride-G-Poly(N-Isopropylacrylamide) Copolymer', *Biomaterials,* 28 (2007), 4488-500.

[498] Li, G., Zhu, X., Zhu, J., Cheng, Z., and Zhang, W., 'Homogeneous Reverse Atom Transfer Radical Polymerization of Glycidyl Methacrylate and Ring-Opening Reaction of the Pendant Oxirane Ring', *Polymer,* 46 (2005), 12716-21.

[499] Xu, F. J., Zhu, Y., Chai, M. Y., and Liu, F. S., 'Comparison of Ethanolamine/Ethylenediamine-Functionalized Poly(Glycidyl Methacrylate) for Efficient Gene Delivery', *Acta Biomater,* 7 (2011), 3131-40.

[500] Wang, L., Yang, Y.-W., Zhu, M., Qiu, G., Wu, G., and Gao, H., 'B-Cyclodextrin-Conjugated Amino Poly(Glycerol Methacrylate)S for Efficient Insulin Delivery', *RSC Advances,* 4 (2014), 6478.

[501] Yang, X. C., Niu, Y. L., Zhao, N. N., Mao, C., and Xu, F. J., 'A Biocleavable Pullulan-Based Vector Via Atrp for Liver Cell-Targeting Gene Delivery', *Biomaterials,* 35 (2014), 3873-84.

[502] Gottlieb, H. E., Kotlyar, V., and Nudelman, A., 'Nmr Chemical Shifts of Common Laboratory Solvents as Trace Impurities', *The Journal of Organic Chemistry,* 62 (1997), 7512-15.

[503] Yang, X. C., Chai, M. Y., Zhu, Y., Yang, W. T., and Xu, F. J., 'Facilitation of Gene Transfection with Well-Defined Degradable Comb-Shaped Poly(Glycidyl Methacrylate) Derivative Vectors', *Bioconjug Chem,* 23 (2012), 618-26.

[504] Jiang, X., Qu, W., Pan, D., Ren, Y., Williford, J. M., Cui, H., Luijten, E., and Mao, H. Q., 'Plasmid-Templated Shape Control of Condensed DNA-Block Copolymer Nanoparticles', *Adv Mater,* 25 (2013), 227-32.

[505] Bui, T. N., Verhage, J. J., and Irgum, K., 'Tris(Hydroxymethyl)Aminomethane-Functionalized Silica Particles and Their Application for Hydrophilic Interaction Chromatography', *J Sep Sci,* 33 (2010), 2965-76.

[506] Liang, Z., Wu, X., Yang, Y.-W., Li, C., Wu, G., and Gao, H., 'Quaternized Amino Poly(Glycerol-Methacrylate)S for Enhanced Pdna Delivery', *Polymer Chemistry,* 4 (2013), 3514.

[507] Wang, Z. H., Li, W. B., Ma, J., Tang, G. P., Yang, W. T., and Xu, F. J., 'Functionalized Nonionic Dextran Backbones by Atom Transfer Radical Polymerization for Efficient Gene Delivery', *Macromolecules,* 44 (2011), 230-39.

[508] Özçam, A. E., Roskov, K. E., Spontak, R. J., and Genzer, J., 'Generation of Functional Pet Microfibers through Surface-Initiated Polymerization', *Journal of Materials Chemistry,* 22 (2012), 5855.

[509] Sanjuan, S., and Tran, Y., 'Synthesis of Random Polyampholyte Brushes by Atom Transfer Radical Polymerization', *Journal of Polymer Science Part A: Polymer Chemistry,* 46 (2008), 4305-19.